UNIVERSITÀ
DEGLI STUDI
DI PADOVA

Sede Amministrativa: Università degli Studi di Padova

Dipartimento Territorio e Sistemi Agro-Forestali

DOCTORAL COURSE LAND ENVIRONMENT RESOURCES AND HEALTH

XXX° CYCLE

Hydrological-hydraulic modelling of the bench terraces in hilly and mountain areas

Director of the School: Ch.mo Prof. Davide Matteo Pettenella

Supervisor: Ch.mo Prof. Vincenzo D'Agostino

PhD student: Chiara Perlotto

ABSTRACT

Terrace building have been expanded in the 19th century because of the increased demographic pressure and the need to crop additional areas at steeper slopes. Terraces are also important to regulate the hydrological behavior of the hillslope. Bench terraces, reducing the terrain slope and the length of the overland flow, quantitatively control the runoff flow velocity, facilitating the drainage and thus leading to a reduction of soil erosion. The study of the hydrologic-hydraulic function of terraced slopes is essential in order to evaluate their possible use to cooperate for flood-risk mitigation also preserving the landscape value.

Few studies in literature are available on rainfall-runoff transformation and flood risk mitigation in terrace areas. Then, research results in this field are still scarce.

The goal of this work is to improve knowledge on hydrological processes affecting a terraced slope and their effect on flood control. Specific researches objectives are:

- Studing the the reduction of peak runoff at the toe of a hillslope and the delay in the passage of peak flow, which are provided by sequence of dry-stone walls under different space arrangements along the hillslope;
- Understanding the rainfall-runoff separation mechanism and the superficial and subsurface flow propagation in case of terraced slopes.

In order to reach the above objectives the hydrological response of a bench terrace was investigated by using a research approache based on modelling and experimental activities.

In the first part of the thesis the The FLO-2D model is used to analyse the runoff propagation mechanism of a terraced slope (sequence of dry-stone walls) by varying number and spacing of terraces and assuming two hydrological soil setting scenarios in terms of antecedent moisture conditions within the Soil Conservation Service-Curve Number method. The model analysis shows that the majority of runoff modifications at the outlet of a terraced system result from topographical modifications rather than local variations of the infiltration capacity at the dry-stone wall zone. Repeated modelling applications show that, given a quite-typical scenario of a 20°-sloped hillslope and a reference intense rainstorm, the peak discharge reduction at the hillslope outlet depends on the percentage of the area managed with terraces. The reduction can be calculated with a logarithmic-type function (for example, an increase of terraced area from 10% to 30% might bring to runoff peak reduction of almost 45%). This information can help determine where terrace additions are more effective in terms of hydrological benefit.

The second part of the thesis focus on an experimental/modelling research that aims to better focus the times of the hydrological response, which are determined by a hillslope plot bounded by a dry-stone wall, considering both the overland flow and the groundwater. A physical model, characterized by a quasi-real scale, has been built to reproduce the behavior of a 3%, 6% and 9% outward sloped terrace at bare and vegetated soil condition.The model consists of a steel metal box (1 m large, 3.3 m long, 0.8 m high) containing the hillslope terrain. The terrain is equipped with two piezometers, 9 TDR sensors measuring the volumetric water content, a surface spillway at the head releasing the steady discharge under test, two scales one at the wall base to measure the groundwater discharge and another at the top of the wall to measure the surface runoff. The experiments deal with different initial moisture condition (high and low degree of saturation), and discharges of 19.5, 12.0 and 5.0 l/min. Each experiment has been replicated, conducting a total number of 35 tests.

The volumetric water content analysis produced by the 9 TDR sensors was able to provide a quite satisfactory representation of the soil moisture during the runs. Then, different lag times at the outlet since the inflow initiation were measured both for runoff and groundwater. Moreover, the time of depletion and the piezometer response have been monitored and analyzed, well corroborating the findings on the kinematics of the terrace plot.

Finally, the computation of the specific Curve Number (Soil Conservation Service) of the physical model has revealed values rather large if compared with those reported in the literature. This phenomenon was likely caused by the high values of the inflow discharge, the limited cross-width of the model (1 m), the increasing compactness of the soil owing to the experiment repetition and the confined waterproof box).

The experimental results indicate that terrace soil was highly heterogeneous, including discontinuities and piping systems that facilitated a rapid infiltration and the development of fast subsurface flow. The Groundwater in general is a small part of the total outflow but in case the presence of pipe is important it is coupled with impulsesive infiltration rates.

A conceptual hydrological model was implemented and calibrated based on the experimental data. The model results fit well the measurements even if the groundwater component is not properly modelled. This is due to the activation of important piping systems during some of the tests; the physical proces that describ this located losses were not studied and integrated in the model.

These pioneering experiments have produced some remarkable outcomes on the important role of lag-times (runoff and groundwater) and provided new knowledgement on the

hydrological functioning of bench terraced systems for addressing more efficient management and maintenance issues of this important agricoltural structures.

RIASSUNTO

I sistemi terrazzati si sono diffusi nel diciannovesimo secolo a seguito della crescente pressione demografica e della conseguente necessità di estendere le coltivazioni anche su terreni ad elevata pendenza.

Oltre che dal punto di vista agrario tali sistemi sono importanti ai fini della regolazione della risposta idrogeologica di un versante. Infatti essi riducono la pendenza e la lunghezza dello scorrimento superficiale, controllando quindi quantitativamente la velocità del deflusso superficiale, facilitando il drenaggio e contribuendo in questo modo alla riduzione dei fenomeni erosivi. Lo studio della funzione idrologico-idraulica dei versanti terrazzati è essenziale per valutarne il possibile utilizzo come misure di mitigazione del rischio idraulico capaci anche di preservare il valore paesaggistico dei territori su cui essi insistono.

In letteratura sono disponibili pochi studi inerenti la risposta idrologica di versanti terrazzati; l'avanzamento della ricerca in tale ambito è l'obiettivo principale di questo lavoro. In particolare vengono affrontate le seguenti tematiche:

- la valutazione degli effetti di mitigazione della pericolosità idraulica (riduzione del picco di piena e suo ritardo temporale) a scala di versante indotti dalla presenza di sistemi terrazzati;
- lo studio dei meccanismi di trasformazione afflussi-deflussi e dei processi di propagazione degli stessi in sistemi terrazzati;

Al fine di raggiungere tali obiettivi è stato implementato un approccio integrato basato su attività sperimentali e modellistiche.

Nella prima parte del lavoro è stato utilizzato il modello idraulico FLO-2D per analizzare i processi di propagazione in atto in un versante terrazzato (composto da una sequenza di muri a secco) al variare del numero e della disposizione spaziale dei terrazzi e assumendo due diversi scenari di saturazione del suolo rappresentati da diversi valori di umidità iniziale antecedente l'evento, come previsto dal metodo Soil Conservation Service - Curve Number.

L'analisi modellistica mostra che la riduzione del deflusso alla base del sistema terrazzato dipende maggiormente dalle modifiche topografiche piuttosto che dalle variazioni della capacità di infiltrazione del suolo adiacente il muro. Le simulazioni eseguite su di un versante con una pendenza di 20° e alimentato da un evento di precipitazione intensa, mostrano che il picco di piena alla sezione di chiusura si riduce in funzione della percentuale di area terrazzata. Tale riduzione può essere valutata attraverso una specifica funzione logaritmica (per esempio, al crescere dell'area terrazzata da 10% a 30% la riduzione del picco di piena

può essere quasi del 45%). Questa informazione può aiutare a individuare il corretto inserimento dei terrazzi per una maggiore efficace in termini di benefici idrologici.

La seconda parte del lavoro riguarda lo studio della risposta idrologica di un'unità terrazzata con un muro a secco attraverso attività sperimentali e modellistiche. In particolare è stato costruito un modello fisico a scala reale per riprodurre il comportamento di un terrazzo al variare della sua pendenza (3%, 6% e 9%) e del tipo di copertura del suolo (suolo nodo o inerbito). Il modello consiste in un box metallico (1 metro di larghezza, 3.3 metri di lunghezza e 0.8 m di altezza) che contiene al suo interno un terrazzo composto da un versante delimitato a valle da un muro a secco. Tale versante è stato strumentato con 9 sensori TDR per la misura del contenuto di umidità del suolo, uno sfioratore delle portate liquidi in ingresso al versante a monte dello stesso, due bilance per la misura del deflusso, una posizionata alla base del muro per la misura del deflusso sotterraneo e una in corrispondenza della parte superiore del muro per la misura del deflusso superficiale. Gli esperimenti sono stati caratterizzati da differenti condizioni di umidità iniziale (ad alto e basso grado di saturazione) e da portate liquide in ingresso costanti e pari a 19.5, 12 e 5 l/minuto. Ogni esperimento è stato replicato per un totale di 35 esperimenti eseguiti.

L'esame delle misure dei 9 sensori TDR ha fornito una soddisfacente rappresentazione dell'andamento dell'umidità globale del suolo nel corso di ogni esperimento. Sono stati poi misurati diversi tempi caratteristici della risposta idrologica alla sezione di chiusura sia per il deflusso superficiale che per il deflusso sotterraneo. I risultati ottenuti aiutano a comprendere la cinematica dei processi idrologici che caratterizzano l'unità terrazzata.

E' stato calcolato uno specifico Curve Number (Soil Conservation Service) associato all'unità terrazzata che assume valori piuttosto alti se comparati a quelli riportati in letteratura. Questo comportamento è probabilmente legato alle alte portate in ingresso, alla limitata sezione idraulica (1m), alla crescente compattazione del suolo causata dal susseguirsi delle prove e al fatto che il terrazzo è confinato all'interno di una struttura metallica impermeabile.

Un innovativo modello idrologico è stato implementato e calibrato sui dati sperimentali. I risultati modellistici riproducono in modo soddisfacente le misure soprattutto per quanto riguarda il deflusso superficiale che è la componente prevalente di deflusso. In generale il deflusso sotterraneo non risulta invece essere propriamente simulato in quanto il modello non tiene conto di particolari fenomeni di infiltrazione impulsiva presenti in alcune prove. Infatti, i risultati sperimentali indicano che il suolo all'interno del terrazzo è altamente eterogeneo, con la presenza di discontinuità e sistemi di canali sotterranei che facilitano una rapida

infiltrazione e lo sviluppo di deflusso sub-superficiale impulsivo che va a sommarsi al deflusso profondo (generalmente di modesta entità) alimentato dall'infiltrazione connessa agli strati superficiali del suolo.

La sperimentazione effettuata risulta innovativa e fornisce nuove conoscenze sulla funzione idrologica-idraulica di un sistema terrazzato che possono servire per indirizzare in modo più efficiente la gestione e la manutenzione di queste importanti sistemazioni agrarie.

INDEX

1 RESEARCH BACKGROUND AND JUSTFICATIONS

1.1 Introduction

Terraces cover large areas of the earth and are among the most evident human land signatures on the landscape (Tarolli et al., 2014). They are generally built to retain more water and soil, to reduce both hydrological connectivity and erosion (Lasanta et al., 2001; Cammeraat, 2004; Cots-Folch et al., 2006), to allow machinery and ploughs to work in better conditions, to make human work in the slopes easy and comfortable, and to promote irrigation. Terraces reduce the slope gradient and length, facilitating cultivation on steep slopes. They increase water infiltration in areas with moderate to low soil permeability (Van Wesemael et al., 1998; Yuan et al., 2003), controlling the overland flow (quantity) and velocity (energy), thereby leading to a reduction in soil erosion (Gachene et al., 1997; Wakindiki and Ben-Hur, 2002; Louwagie et al., 2011; Li et al., 2012), with positive effects on agricultural activities. In all Mediterranean basins, terraced landscapes are considered to be among the most important and characteristic anthropological imprints on the relief (Douglas et al., 1994, 1996; Gallart et al., 1994; Dunjo´ et al., 2003; Trischitta, 2005), and they symbolize an important European cultural heritage (Varotto, 2008; Arnaez et al., 2011). During the past centuries, the need for cultivable and well-exposed areas determined the extensive anthropogenic terracing of large parts of hillslopes. Several publications have reported the presence, construction, and soil relationship of ancient terraces in the Americas (e.g., Spencer and Hale, 1961; Donkin, 1979; Healy et al., 1983; Beach and Dunning, 1995; Dunning et al., 1998; Beach et al., 2002). In the arid landscape of south Peru, terrace construction and irrigation techniques used by the Incas continue to be utilized today (Londoño, 2008). In these arid landscapes, pre-Columbian and modern indigenous population developed terraces and irrigation systems to better manage the adverse environment (Williams, 2002). In the Middle East, thousands of dry-stone terrace walls were constructed in the dry valleys by past societies to capture runoff and floodwaters from local rainfall to enable agriculture in the desert (Ore and Bruins, 2012). In Asia, terracing is a widespread agricultural practice. Since ancient times, one can find terraces in different topographic conditions (e.g., hilly, steep slope mountain landscapes) and

used for different crops (e.g., rice, maize, millet, wheat). Examples of these are the new terraces now under construction in the high altitude farmland of Nantou County, Taiwan.

Italy still presents nowadays a great heritage of rural landscapes, built during the millennia and strictly connected to the traditional practices, with the aim to adapt to difficult environmental condition and providing, at the same time, multiple products, services and places of extraordinary beauty (Agnoletti, 2012). Among these, terraces represent a fundamental and extremely characteristic system of landscape organization in the Mediterranean area, which connects traditional knowledge of agricultural and building techniques to a perfect comprehension of the hydrogeological and climatic characteristics of the rural areas in which terraces are inserted. Therefore, they are systems characterized by high aesthetical quality, as well as the ability to model the landscape by integrating with the natural features of their locations (Laureano, 2004).

In Italy, evidences of the first terraced landscapes date back to the Neolithic, but the affirmation of this particular system was mainly during the Middle Age, probably favoured by the diffusion of the monastic orders in the territory, with a consequent systematic exploitation of the lands for agricultural purposes. In the 1700s, Italian agronomists such as Landeschi, Ridolfi and Testaferrata began to learn the art of hill and mountain terracing, earning their recognition as ‘‘Tuscan masters of hill management’’ (Sereni, 1961). Another important period for the spreading of the terracing system was during the XIX century, when the higher demographic pressure led to a noticeable increasing of cultivation practices also in hilly and mountain areas. Several agronomic treatises written in the eighteenth and nineteenth centuries observe that in those times there was a critical situation due to a prevalence of a ‘‘rittochino’’ (slopewise) practice (Greppi, 2007).

During the same period, the need to increase agricultural surfaces induced farmers to till the soil even on steep slopes and hence to engage in impressive terracing works. Terraced areas are found all over Italy, from the Alps to the Apennines and in the interior, both in the hilly and mountainous areas, representing distinguishing elements of the cultural identity of the country, particularly in the rural areas. Contour terraces and regular terraces remained in use until the second post-war period, as long as sharecropping contracts guaranteed their constant maintenance. Thus, terraces became a regular feature of many hill and mountain landscapes in central Italy.

Terracing is a complex system which is continuously in transformation, following population needs, demographic increments, socioeconomic evolution and climate changes. However, terraced landscapes are always based on a simple but essential element: the retaining wall.

The practice of retaining drywalls constitutes a system to model the steep slopes which is fundamental for the Italian territory, where the slopes are continuously subject to landslides and erosion processes. Without drainages or drywalls, a great part of the Italian landscape, whether Alpine, Apenninic or Mediterranean, would not exist (Branduini, 2009).

Since the 1940s, the gradual abandonment of agricultural areas led to the deterioration of these typical elements of the landscape. With the industrialization of agriculture and the depopulation of the countryside since the 1960s, there has been a gradual decline in terrace building and maintenance, as a consequence of the introduction of tractors capable of tilling the soil along the steepest direction of the hillside ('ridging'), which resulted in a reduction of labour costs. Basically, this means the original runoff drainage system is lost. The results consist of an increase in soil erosion due to uncontrolled runoff concentration and slope failures that can be a serious issue for densely populated areas.

In the last few years during intense rainfall events in different regions of Italy, especially in Cinque Terre, several slope failures have been observed , which have caused high damage to the local communities (Agnoletti et al., 2012). Recently, the heavy rains which washed through the Veneto foothills from the 2nd to 3rd of August 2014 generated a flash flood in the Rio Lierza basin (7.5 km^2 wide), causing the death of four people and major damage to the Municipality of Refrontolo (Treviso Province) (Marcadella, 2014). This basin is characterized by an extended portion of land cultivated with sparkling wine by means of terraces of recent construction. The non correct construction of terraces may have contributed to an ineffective action to mitigate flood risk.

The effect of terracing on hydrological processes depend on geology, soil properties (Grove and Rackham, 2003) and on their spacing. Terraces reduce the slope gradient and length, facilitating cultivation on steep slopes. They increase water infiltration in areas with moderate to low soil permeability (Van Wesemael et al., 1998; Yuan et al., 2003), controlling the overland flow (quantity) and velocity (energy), thereby leading to a reduction in soil erosion (Gachene et al., 1997; Wakindiki and Ben-Hur, 2002; Louwagie et al., 2011; Li et al., 2012), with positive effects on agricultural activities.

Few studies are available on the rainfall-runoff transformation in terraced areas and specifically on the quantitative performance of bench-terraces in a flood-risk mitigation framework. In particular, the gaps in the research consist in a lack of quantitative evaluations of: i) the hydrological componentes involved in a flooded terraced slope and ii) the effect of the spatial arrangement of terraces on flood risk reductions. These parameters are critical to define guidelines to proper design a terraced slope or to restore an existing one. For exemple,

it is of primary importance to define a correct runoff coeffient to be applied to the reference rainfall event in order to estimate the reference peak discharge ar different sections along the terrace slope. Moreover, for a correct planimetric planning of the terrace slope, for the dimensioning of the walls and of drainage network it is also important to know other features of the response hydrograph (peak flow, time to peak, surface and subsurface outflow volumes); these will hep to guarantee slope stability and the appropriate level of risk to the sorrounding territories .

The goal of this research is to improve knowledge on hydrological processes affecting a terraced slope and their effect on flood control. Specific researches objectives are:

1. Studying the hydrological response of a terrace in terms of quantification of rainfall vs runoff and propagation timing for the surface and subsurface flow components under different initial soil moisture conditions;
2. Studying the benefit in terms of runoff reduction (the decrease of the flood risk downstream of a terrace slope), which is provided by sequence of dry-stone walls under different space arrangements along the hillslope.

In order to reach the above objectives the hydrological response of bench terraces will be analyzed by laboratory tests and hydrological – hydraulic modeling.

1.2 State of knowledge on the research topic

1.2.1 Terraces classification

A notable work on terrace system classification was authored by Morgan (2005), in which terraces were defined as earth embankments constructed across a slope to intercept surface runoff, convey it to a stable outlet at a non-erosive velocity and shorten the slope length.

A terraced slope is characterized by the following technical characteristics which typical ranges are reported in Table 1.1:

- length of the terraces
- spacing of the terraces
- the location of outlets
- the gradient and dimensions of the terrace channel
- the layout of the terrace system

Technical characteritis	Range
Maximum length	Normal: 250 m (sandy soils) – 400 m (clay soils) Absolute: 400 m (sandy soils) – 450 m (clay soils)
Design slope	First 100 m: 1:1000 Second 100 m: 1:500 Third 100 m: 1:330 Fourth 100 m: 1:250 Constant grade: 1:250
Ground slopes	Diversion terraces: - Usable on slopes up to 7°; on steeper slopes the cost of construction is too great and the spacing too close to allow mechanized farming Retention terraces: - Recommended only on slopes up to 4.5° Bench terraces: - Recommended on slopes of 7-30°

Table 1.1. Design lengths and grades for terrace channels (source: after Hudson,1981).

Terraces can be classified into three main types: diversion (overland-flow interception), retention (water storage) and bench (steep slope cultivation) (Figure 1.1). The primary aim of **diversion terraces** (Figure 1.1b) is to intercept runoff and channel it across the slope to a suitable outlet. They therefore run at a slight grade, usually 1:250, to the contour. There are several varieties of diversion terrace. Diversion terraces are not suitable for agricultural use on ground slopes greater than 7° because of the expense of construction and the close spacing that would be required. Closer spacings are feasible, however, on steeper slopes on road banks, mining spoil and along pipeline corridors. Surprisingly, standard pipeline engineering practice is to grade the channel behind the terrace or berm at a slope of 9° so as to remove surface water as rapidly as possible without the channel overtopping (Marshall & Ruban, 1983). Such a grade is far too steep, particularly since the risk of overtopping is extremely small. In the Tbilisi area of Georgia, sheet and gully erosion occurred on pipeline corridors on slopes of 18–26° as a result of installing channel terraces that were too steep and at spacings that were too wide, and a failure to extend them on to vegetated land beyond the right-of-way (Morgan & Hann, 2003). This example shows that a poorly designed terrace system can actually exacerbate an erosion problem.

Retention terraces (Figure 1.1a) are used where it is necessary to conserve water by storing it on the hillside.They are therefore ungraded or level and generally designed with the capacity to store the runoff volume expected with a ten-year return period without

overtopping. These terraces are normally recommended only for permeable soils on slopes of less than 4.5°.

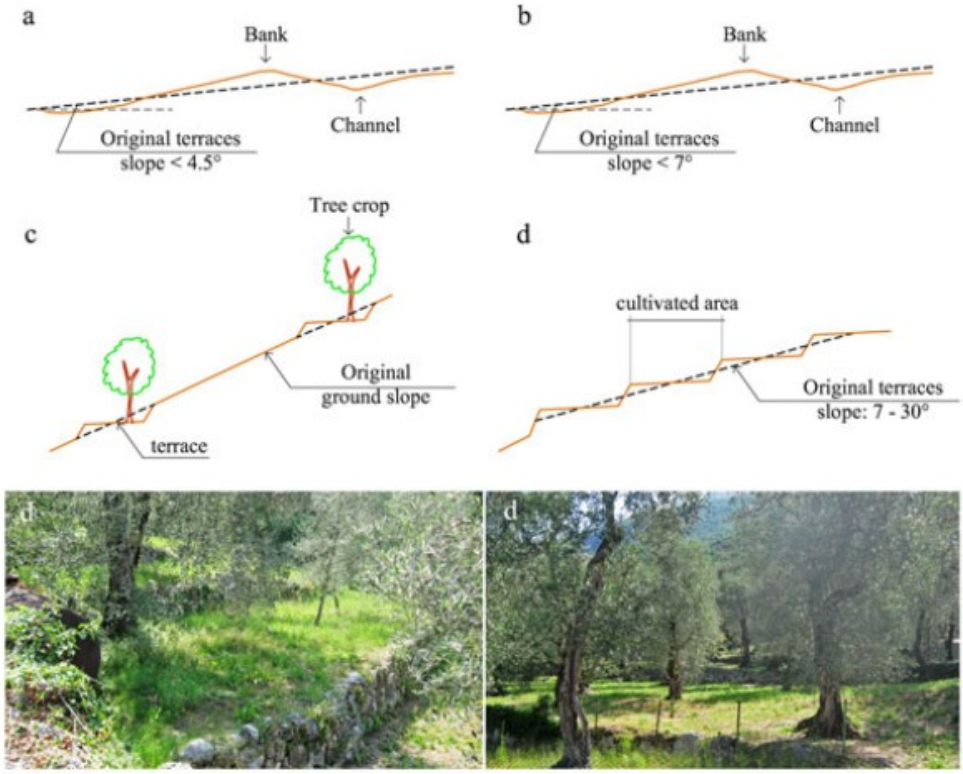

Figure 1.1. Types of terraces (modified from Morgan, 2005): (a) sketch of retention terraces; (b) sketch of diversion terraces; (c) sketch of bench-terraces for treecrop lines; and (d) sketch of bench-terraces for continuously cultivated areas and photographs of the reference bench-terraces considered in this study (Malcesine, Verona, Italy). This figure is available in colour online at wileyonlinelibrary.com/journal/ldr.

Bench terraces (Figure 1.1c-d) consist of a series of alternating shelves and risers are employed where steep slopes, up to 30°, need to be cultivated. The riser is vulnerable to erosion and should be protected by a vegetation cover or faced with stones or concrete. Unprotected risers can be the source of most of the erosion in terraced systems (Critchley & Bruijnzeel, 1995). The basic bench terrace system can be modified according to the nature and value of the crops grown. Two kinds of system are used in Malaysia. Where tree crops are grown, the terraces are widely spaced, the shelves being wide enough for one row of plants, usually rubber or oil palm, and the long, relatively gentle riser banks being planted with grass or a ground creeper; this system is sometimes known as orchard terracing. With more valuable crops such as temperate vegetables grown in the highlands, the shelves are closely spaced and the steeply sloping risers frequently protected with masonry. Level bench terraces are used where water conservation is also a requirement, as in the loess areas of

China (Fang et al., 1981). Bench terraces are unsuitable for shallow soils because their construction can expose infertile subsoil.
In Italy the diversion and retention terraces are not used. Instead, it is common the use of bench terraces for continuously cultivated areas as described in Figure 1.1d. This reaserach is focused on bench terraces which have been used as a conservation measure for over 2000 years in China, Southeast Asia, Mediterranean Europe and the Andes. Although they can reduce erosion substantially compared to unterraced land, their success depends on being well constructed and, equally important, well maintained. In areas of rural depopulation or increased availability of alternative sources of income to agriculture, the labour is often not available to undertake the necessary repairs (Critchley et al., 2001).

1.2.1.1 Dry stone wall

The dry stone wall is a particular type of wall build with stony blocks arranged one by one without using any fastening material. Such walls may be built with different heights, generally depending on the slope steepness, and different widths, also as a function of the parcelling of the territory.
The development of this typology is due to the necessity to create terraced systems with the aim of reducing the slope in the steepest terrains, in order to permit the agricultural practices in such difficult conditions. Dry stone walls are usually built for slopes greater than 20-30%, to have the possibility to work in steep and rough terrains also with mechanical machinery.
Throughout history, dry stone walls have shown many advantages with respect to other forms of barriers or structures. Stone is a very hard wearing material, it lasts for age and it is not affected by decay or fire as, for example, wood materials are. These properties have been the main contributors to the use of stone over the centuries (Post, 2005). The management of steep slopes through the use of dry walls represents, in addiction, a very advantageous technique both from the environmental and the agricultural point of view, as well as a good low-impact choice from the landscape perspective.
The main benefits related to the use of such technique are listed below:

- Reduction of slope steepness
- Formation of a cultivable soil layer
- Creation of a micro-climate favourable to plant roots
- Removal and dislocation of soil heaps
- Removal of gravel from the terrain

- Reduction of the velocity of superficial water
- Reduction of erosion
- Reduction of the pushing forces of the terrain, in case of extreme meteorological events
- Good hydraulic management due to channelling of excess rainwater
- Increase the water infiltration processes upstream of the terrace, guaranteeing plants to be well watered during rainy events
- Low environmental impact and masking of the structure due to greening effects
- Rapid re-building of the interested parts only.

Stone walls can be built in different methods, but the most diffuse technique is constituted by several distinct elements (Figure 1.2), each with its own function:

- Foundation: the base on which the wall is built. Usually it is constituted by bare soil or the parent rock;
- Footings: the stones that make up the bottom layer, usually the largest in the wall. The footings may be partly or entirely below ground, depending on the conditions in which the wall is being built. In some cases, the footings are called foundation stones or collectively referred to as the foundation;
- Cope: the top stones on the wall. There are numerous styles used for copes, but all of these have the function of adding height and capping of the wall in a structurally sound manner;
- Face: this term can refer to the wall collectively or the individual stones and in both cases refers to the side that is visible;
- Face stones: they are the stones that can be seen in the front of a wall. They represent the majority of the volume and the structure of a wall. They are sometimes referred to as “wall-stones”;
- Course: a layer of face stones in the wall. Some walls are built without courses and they are called “random walls”. The courses may be more or less rigid, depending on the type of stone, the building style and the builder itself;

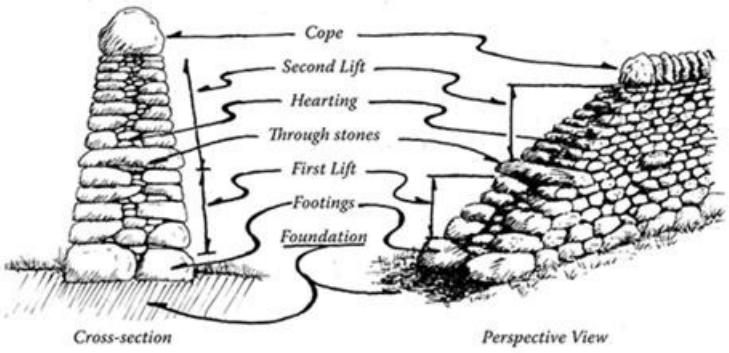

Figure 1.2 Basics components of a dry stone wall (Post, 2005).

- Hearting: small stones used to fill the gaps between the stones in a wall. As the face stones, hearting is scaled, so larger stones are used at the bottom and smaller material is used near the top;
- Pinning: pinning stones are used to hold the face stones in place. They are very similar to hearting, but they are specifically chosen and placed to wedge the face stones in place, where hearting stones are only placed to fill gaps.
- Through stones: stones that extend through the wall, connecting the two sides. They are usually part of boundary walls, much less frequent in retaining walls. They are typically inserted at half of the wall's height and every meter in length, with the purpose to prevent the sides from separating.

1.2.1.2 Terraces design

The parameter to be sized for the terraces is the height difference between two successive risers, as defined in the following V_i (vertical interval) (Figure 1.3). In literature it is possible to find find many empirical formulas that make dependent this size on both the gradient slope and soil erosion. All these vary according to the geographic area of interest and type of crops in case of agricultural practices. In the following a physical approach for the dimension of the terraces is reported as described in Morgan (2005) .

Figure 1.3 Basics components Basics Vertical Interval (Morgan, 2005)

For steady state conditions, the runoff (per unit width) Q at slope length x on a hillside can be expressed as in Figure 1.4:

$$Q = (R - i) \cdot x \cdot cos\,\theta \tag{1.1}$$

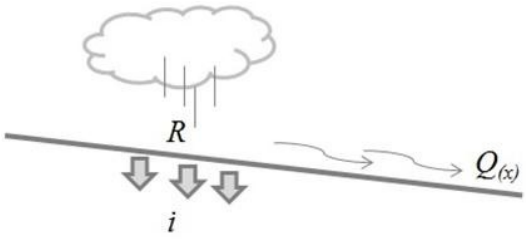

Figure 1.4 Calculation scheme.

where R is the rainfall intensity, i is the infiltration capacity of the soil and θ is the slope angle. The runoff Q can also be espressed using the Manning equation of flow velocity as:

$$Q = \frac{r^{5/3} \cdot \sin^{0.5}\theta}{n} \tag{1.2}$$

where r is the hydraulic radius/depth function of the mean flow velocity v and the Manning's roughness n as it follows:

$$r = \left(\frac{v \cdot n}{\sin^{0.5}\theta} \right)^{1.5} \tag{1.3}$$

Using 1.3 and 1.2 the equation 1.1 becomes:

$$(R - i) \cdot x \cdot cos\,\theta = \left[\left(\frac{v \cdot n}{\sin^{0.5}\theta} \right)^{1.5} \right]^{5/3} \frac{\sin^{0.5}\theta}{n} \tag{1.4}$$

Rearranging for given values of R and i (for example for the 1-hour rainfall with a 10-year return period, and for a preselected value of v_c as the maximum permissible velocity for the soil), the equation 1.4 gives a slope distance $x_{crit,}$ which can be used as the design distance between the terraces downslope:

$$x_{crit} = \frac{\mathrm{v}_c^{5/2} n^{3/2}}{(R-i)\sin^{3/4}\theta \cos\theta} \qquad (1.5)$$

where a value of n = 0.01 might be recommended for bare soil.

For example, if the peak rainfall excess (R - i) on a sandy loam soil is 0.2 mm/s, and the selected value for v_c is 0.75m/s, then for a slope of 3°:

$$x_{crit} = \frac{0.75^{5/2} 0.01^{3/2}}{0.0002 \cdot 0.109421^{3/4} \cdot 0.9886} = 22.55\, m \qquad (1.6)$$

and then the vertical height between two successive risers is:

$$V_i = x_{crit} \sin\theta = 1.18\ m \qquad (1.7)$$

A similar approach was used by Mirtskhoulava (2001) to produce the following formula:

$$x_{crit} = \frac{0.000034_c^{3.32}}{(R-i)\, m^{2.32} \mathrm{s}^{1.16} \mathrm{n}} \qquad (1.8)$$

where m is a coefficient describing the roughness related to the soil particles (m = 1.0 for silts, 1.1 for sands and sandy loams, 1.3 for loamy sands and clay loams and 1.5 for clays), and s = slope (m/m). This method tends to give wider terrace spacings on low-angled slopes and closer spacings on steep slopes. When the two methods were applied to the design of diverter berm spacings on pipeline rights-of-way near Tbilisi, Georgia, they gave very similar results over slopes ranging from 19 to 26° (Morgan et al., 2003).

1.2.2 Terraced hillslope hydrology

Terraces provide flat surfaces and deep loose soils that increase infiltration, limit sediment transport and reduce soil erosion (Arnáez et al., 2015; López-Vicente et al., 2013; Cots-Folch et al., 2006; Lasanta et al., 2001), decrease the hydrological connectivity (Cammeraat, 2004) and thus reduce runoff (Meerkerk et al., 2009; Perlotto & D'Agostino, 2016). Therefore,

understanding the main hydrological processes that determine water flow pathways and runoff generation in terraced landscapes is of paramount importance for a better conceptualization of the functioning of these systems and for proper design and maintenance (Preti et al. 2017).

1.2.2.1 Estimation of runoff and sediment yeald through experiments

Past studies were focused on quantyfing and understanding the runoff and sediment yield by terraces. Most of the authors studied this issues following a field research experimental approach. Li et al. (2014) recently investigated runoff and sediment yield through field experiments based on 20 × 5 m plots on a 21% slope in southern China. Rainfall, runoff and sediment yield from five plots were recorded for 5 years (2001–2005) and which five different types of terraces on sloping red soil were compared. The results showed that the planting of grass on the riser is the most important factor affecting runoff and sediment yield, the next most important factor was the construction of a bund built on the edge of the terrace. Although the terrace bed slope (slope < 5 degrees) does not significantly affect the runoff, it does benefit the soil. A terrace combined with vegetation measures is effective in controlling runoff and soil erosion. Among various terraces, the level terrace (i.e. grass planted on the riser and bunds built on the edge of a bench terrace) is apparently the most beneficial for soil conservation purposes, indicating that this type is an excellent choice for conserving soil and water resources in sloping red soil in Southeastern China. Other authors investigated the erosion problems linked with terraces: Lasanta et al. (2001) describe that the foot of a terrace wall is often affected by erosion, because of the steepness and the sparse vegetation cover; Li et al. (2011) showed that level terraces (Figure 1.1d, with a horizontal tread) exert a positive influence on soil loss in accordance to what was previously considered by the Universal Soil Loss Equation (USLE) (Wischmeier & Smith, 1978).

Earlier investigations in an agricultural Mediterranean catchment in Spain revealed that the terraced topography and low soil permeability significantly modified subsurface flow patterns, inducing frequent saturation of the inner part of the terraces during periods of intense rain. Gallart et al. (1994) argue that the presence of this saturated area could increase the storm overland flow for the same rainfall and antecedent moisture conditions as well as increase the runoff coefficient. Lorents et. al (1992) studied the Cal Parisa basin (36 ha) in Eastern Spanish Pyrenees, where a sub-basin of 17 ha was Instrumented In 1989 in order to study the hydrologlcal response and the sediment dynamics of mountainous areas highly modified by traditional agriculture and now abandoned. The hydrological analysis

demonstrated the for this sub-basin runoff generation is linked to saturation processes instead to Hortonian ones. In spite of the clayey character of the soils, their good structure and thickness, together with the terraced topography, enable high infiltration rates and retention capacities. However, there is field evidence that Hortonian runoff occurs in small areas of the basin where the clayey bedrock outcrops, but the runoff produced in these areas is infiltrated when it reaches the terraced area if this is not saturated enough. An hydro-geomorphologlcal analysis was conducted using GIS and the superposition of the Topographical Index map with the digitized saturated areas map. It appears that in the basin the Topographical Index of these frequently saturated areas ranges from 5.4 to 13.9 with a maximal frequency for a value of 6.7. The distribution of the saturated areas in terms of the Topographical Index is not a normal one, but shows a marked bimodal nature which is even more clear if we divide each relative frequency by the frequency of its corresponding Topographical Index value in the basin, as is illustrated by the test of the probabilistic plot (Figure 1.5). The first peak is formed by anthropic saturated areas having a relatively low Topographical Index, about 7, while the second one is made by the natural saturated areas characterized by aTopographical Index of about 10.

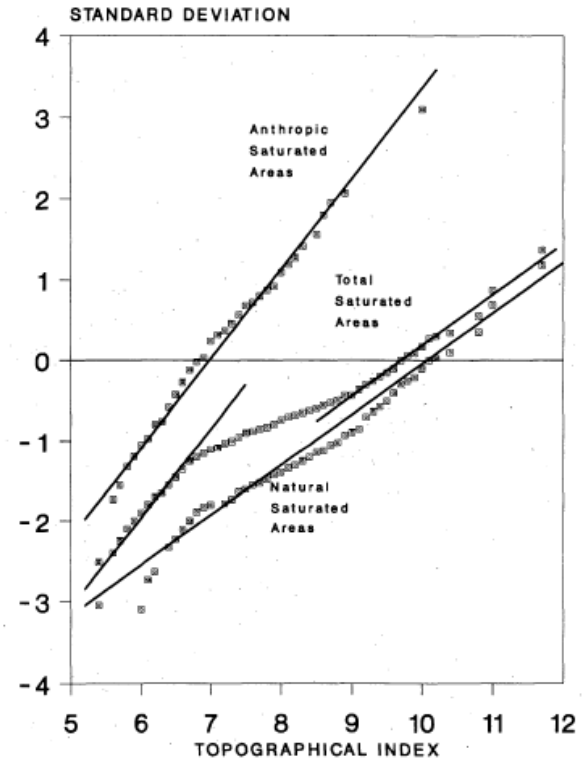

Figure 1.5 Probabilistic plot test for the weighted frequency distribution of classified saturated areas. (Lorents et. al (1992))

On the basis of this bimodal distribution the authors judged that the construction of terraces has promoted a reorganisation of the distribution of the saturated areas, shifting it from a natural one, mainly controlled by the original topography, to a more anthropic one which shows the role of the new terraced topography and its associated artificial drainage net. The results of the study showed the preservative role of the agricultural terraces, characterized by a high water retention capacity and a very low sediment yield, in spite of significant amounts of sediment which are transferred within the basin but do not reach the outlet. During rainy periods the partial saturation of terraces produces important runoff volumes quickly drained by the man made network of ditches, generating sharp runoff peaks. These ditches are shown therefore to be the elements of major hydrologlcal and linear erosion risks. Nowadays the lack of drainage network maintenance, as a result of land abandonment, has caused disorganization which may have some Important hydro-geomorphologlcal and land conservation consequences. The research suggested that modifications produced by terracing enhance a quick response of the basin because of the outcrop of phreatic waters on the inner part of the terraces, and the conveyance of runoff by the net of ditches. On the other hand, however, water retention may have been increased by terracing because of the formation of deeper soils with a more open structure. More research is needed to describe the stockage and movement of the water within the terraces and to understand the behavior of saturated areas throughout the year and during rainfall events.

Lu et al. (2009) suggested that about one-third of the evaporative water losses occur from the terrace riser surface. Thus, the retention of a significant amount of water by the terrace may not have a remarkable influence on saturation and storm runoff to some degree, especially in an arid area. Zhang et al. (2008) indicated that the runoff coefficient from sloping terraces with grasses and trees was only 3% in hilly areas of the Sichuan Basin (southern China). This result was similar to those obtained by Li et al. (2011) (northern Jiangxi Province, centre of hilly red soil lands in southern China). Zhang et al. (2008) noted that lower amounts of runoff were observed on sloping terraces where fruit trees were interplanted with other crops.

Another important contribution derived from field experiments was achieved by Gardner & Gerrard (2003), who measured runoff and soil erosion from plots on outward sloping agricultural terraces (Likhu Khola drainage basin, Middle Hills, Nepal) during both pre-monsoon and monsoon periods. In the study catchments the *bari* terraces slope outwards at between 1 and >10°. The *bari* terraces are rainfed cultivated bench terraces where crops are dependent entirely on the monsoon rains for moisture. The most frequent individual slope angle was approximately 5°.

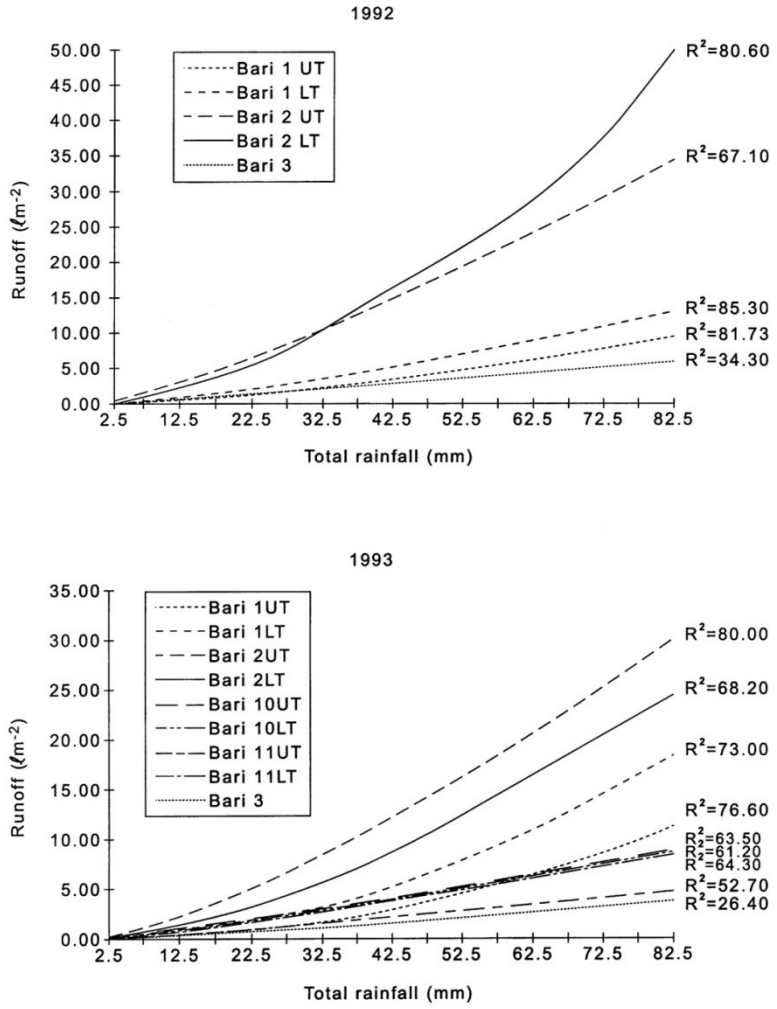

Figure 1.6 Rainfall/Runoff relationships and statistical correlations for 1992 and 1993. (from Gardener and Gerrards (2003). The bari terraces monitored were encoded by a number (1,2,10,11,3) followed by the UT or LT string. UT stands for upper terrace and LT stands for lower terrace

Empirical relationships between total rainfall and runoff allowed comparisons to be made between terraces. The relationships can also be used to produce estimates of total runoff and runoff coefficients over the pre-monsoon and monsoon periods. Rainfall/runoff relationships for all terraces in both 1992 and 1993 are shown in Figure 1.6. The relationships are clearly non-linear and show that runoff is highly variable between the terraces. Runoff coefficients (water running off the plot as a percentage of the total volume of water entering by rainfall) for individual rainfall events varied considerably from less than 5% to over 50%, depending on the nature of the event and the terrace. Much of the interevent variability on each terrace could be accounted for by a combination of total rainfall and a measure of rainfall intensity. Most of the runoff from *bari* land is lost rapidly from the hillslope system. In general, their

data suggested that although the relationships between soil loss and rainfall characteristics were highly variable, runoff and soil loss were considerably reduced when a vegetation cover was present.

1.2.2.2 Rainfall-runoff separation modelling

Few studies focusing on rainfall-runoff separation modelling in terraced slopes are available. An innovative theoretical approach applied to terraces was introduced by Van Dijk and Bruijnzeel (2004). The authors investigated the spatially variable infiltration model (Yu et al., 1997) and proposed an event-based model of rainfall infiltration and surface runoff. In the spatially variable infiltration model (SVI; Yu et al., 1997a) the infiltration-excess rainfall (Q' in mm/hour) is calculated as the difference between the rainfall intensity (R) and the infiltration rate *(I(R))* assuming an exponential trend of maximum infiltration rates, represented by the average maximum infiltration rate (I_m in mm/hour):

$$Q' = R - I(R) = R - I_m\left[1 - \exp\left(\frac{R}{I_m}\right)\right] \qquad (1.9)$$

Theoretically, I_m is reached when the entire area under consideration generates runoff (Yu et al., 1997a).

To avoid the need for high-resolution rainfall intensity data, an exponential depth–rainfall intensity distribution for individual storms was proposed and tested by Van Dijk (2002). It is characterized by storm depth P (mm) and depth-averaged rainfall intensity R (mm/hour), calculated for n time intervals making up a storm as

$$\bar{R} = \frac{\sum_{i=1}^{n}(PR)i}{P} = \frac{\sum_{i=1}^{n}(R^2\Delta t)i}{P} \qquad (1.10)$$

Based on the exponential rainfall distribution, an expression was derived relating storm runoff depth (Q_{tot}) to P, $\bar{R}$ and I_m (see Van Dijk, 2002):

$$Q_{tot} = max\left\{P\left[1 - \frac{I_m}{\bar{R}} ln\left(1 + \frac{\bar{R}}{I_m}\right)\right] - S_I, 0\right\} \qquad (1.11)$$

where S_I (mm) is initial excess infiltration and I_m is the average maximum infiltration rate.

The bench terraces examined are comprised of three segments with contrasting infiltration characteristics (Figure 1.7).

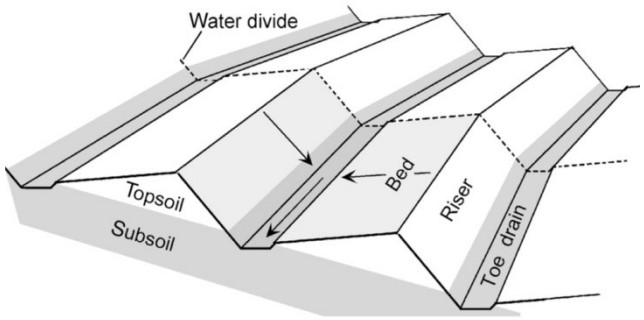

Figure 1.7 General layout of back-sloping bench terraces, the three component sections and their intersection with the subsoil (dark shaded). A hydrologically defined terrace unit is shown lightly shaded (Van DiI Jk and Bruijnzeel, 2004).

The theoretical runoff response from the entire terrace is therefore found by weighting the infiltration characteristics of each segment by its relative area:

$$Q' = \sum_{i=1}^{n} F_{A,i}\left[R - I_{m,i}\left(1 - e^{\frac{R}{I_{m,i}}}\right)\right] \qquad (1.12)$$

where $F_{A,i}$ is the relative area, and $I_{m,i}$ (mm/hour) the maximum average infiltration rate associated with segment *i*. Similarly, overall runoff depth is given by the equation:

$$Q_{tot} = \sum_{i=1}^{n} F_{A,i} max\left\{\left(P\left[1 - \frac{I_{m,i}}{\bar{R}} ln\left(1 + \frac{\bar{R}}{I_{m,i}}\right)\right] - S_{I,i}\right), 0\right\} \qquad (1.13)$$

where $S_{I,i}$ (mm) is the initial additional infiltration on segment *i*. If the resulting distribution of maximum infiltration rates over the entire terrace remains exponential the corresponding spatially averaged value $\tilde{I}_m$ (mm hour^{-1}) is given by:

$$\tilde{I}_m = \sum_{i=1}^{n}(F_A I_m)_i \qquad (1.14)$$

However, in most cases the distribution of infiltration rates of the total area will no longer conforms to an exponential distribution. If Equations 1.9 or 1.11 are used with $\tilde{I}_m$ calculated from Equation 1.14 to predict instantaneous runoff rates or event runoff totals, respectively, the results will be different from those calculated with the corresponding Equations 1.12 and 1.13 for the entire terrace, respectively. This is illustrated in Figure 1.8(a,b) for combinations of relative area and Im for the three segments of a representative bench terrace. Instead of using an $\tilde{I}_m$ value calculated with Equation 1.14, an 'apparent' value may be chosen such that it best fits infiltration rates over the range of observed rainfall intensities (Figure 1.8a,b).
Total runoff depth from the composite area is hence described by (see Equation 1.11):

$$Q_{tot} = max\left\{P\left[1 - \frac{\tilde{I}_m}{\bar{R}} ln\left(1 + \frac{\bar{R}}{\tilde{I}_m}\right)\right] - \tilde{S}_I, 0\right\} + \varepsilon \qquad (1.15)$$

where $\tilde{S}_I$ denotes an 'effective' spatially averaged storage term and ε is the error that is introduced by the approximation.

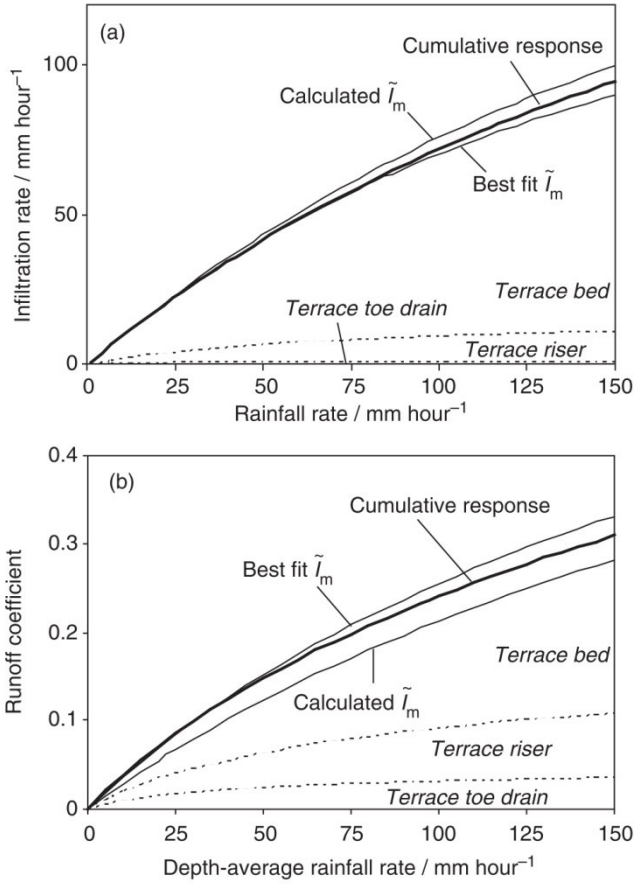

Figure 1.8 The combined response of the three terrace sections expressed as the relationship between (a) rainfall intensity (R) and infiltration rate (I(R);Equation (1.12)) and (b) depth-averaged rainfall intensity ($\bar{R}$) and runoff coefficient (rc; Equation (1.13)). Cumulative contributions by the three sections are shown by dashed lines, whereas solid lines indicate the relationships for the combined response using area-weighted average values of $\tilde{I}_m$. Relative area values of 5, 16 and 79% and Im values of 20, 70 and 200mmhour-1 were used for the central drain, riser and bed, respectively. (Van DiI Jk and Bruijnzeel (2004)).

Van DiI Jk and Bruijnzeel (2004) validated and tested the theory developed in Van Dijk (2002) using a data set of rainfall intensity, runoff depth and runoff rates from small to medium-sized (1–231m^2) erosion plots. These measurements were collected in bench-terraced hillslopes in volcanic upland terrain in West Java, Indonesia. These bench terraces comprise a terrace riser and a terrace bed with a central drain (Figure 1.7). Totals of measured rainfalls and associated surface runoff coefficients have been analyzed for the terrace beds and risers and for the terrace units.

Runoff coefficients associated with bare terrace riser sections (12–28%) were not higher than those for bare terrace beds (16–26%), despite the difference in slope gradient and subsoil exposure. However, runoff from terrace beds with appreciable vegetation cover was generally less than that from bare plots, especially under mixed cropping (0.1–24%). Similarly, runoff from terrace risers with vegetation cover was generally less than half (0.6–13%) that from bare risers, whereas unweeded risers with variable degrees of cover showed intermediate values (8–20%). The storm-based equations were used successfully to model runoff depths and maximum effective runoff rates for individual events. Resulting values for maximum average infiltration rate (I_m) varied between 18 and 443mm/hour and reflected effects of vegetation or mulch cover and soil compaction. The authors concluded that the SVI model and the derived equations provide a robust and accurate method for predicting runoff at the investigated scale.

As reported in Gallart et. al (2009) *"The modelling of Mediterranean mountain areas is often seen as a complex challenge and an unresolved problem for which model improvements are required"*. These authors carried out modelling exercises in the Vallcebre small research basins, located in the Eastern Pyrenees (Latron et al., 2009) in order to both improve the understanding of the hydrological processes and test the adequacy of some models in such Mediterranean mountain conditions. One of these exercises consisted of the analysis of the hydrological role of the agricultural terraces using the TOPMODEL topographic index. This last is defined as ln $(\frac{a}{tanb})$ where a is the local upslope area draining through a certain point per unit contour length and *tanb* is the local slope in radians.

The results showed that the frequently saturated areas had a bi-modal distribution of topographic index values, one mode attributed to the general topography of the basin and the other (with lower values) to the role of terraces. The terraces promoted the formation of saturated areas in drier conditions than those expected by the main topography. Furthermore, the analysis of the response time of these basins demonstrated a delay of flows when compared with the response times expectable for saturated overland flow in basins of similar size (Gallart et al., 2005a).

1.2.2.3 Mechanisms governing the hydrological functioning

Recent studies have reported the close link among terraced land management, soil erosion and instability problems (Brandolini et al., 2016; Al Qudah et al., 2016; Tarolli et al., 2015; Arnáez et al., 2011; see Tarolli et al., 2014 for a comprehensive review), and it is now clear

that the maintenance of terraces represents a primary geo-hydrological hazard mitigation and soil conservation measure (Brandolini et al., 2016; Preti et al., 2013). However, a clear description of terrace subsoil structure and its influence on water circulation is missing. Moreover, only few past studies that we are aware of have tried to explain the mechanisms governing the hydrological functioning of agricultural terraces especially in relation to dry-stone wall instability. A better understanding of the main hydrological processes that govern surface and subsurface water flow pathways and that are responsible for terrace failure and dry-stone wall collapse is essential for appropriate water resource management and rural landscape maintenance in terraced areas. In a recent study Preti et al. (2017) monitored a terrace system in a hilly site of central Italy cultivated with vineyards. They adopted a multidisciplinary approach based on soil analysis, different geophysical techniques, hydrological monitoring, high-resolution grid terrain analysis and field experiments (infiltration and flooding tests). Their results indicate that terrace soil was highly heterogeneous, including discontinuities and piping systems that facilitated a rapid infiltration and the development of fast subsurface flow. Groundwater rise did not occur, as observed in other terraced sites, but infiltrated water accumulated behind dry-stone walls, increasing pore water pressure and inducing wall bulging and instability.

The Department of Earth Sciences, University of Milan, is conducting research on the processes of infiltration and groundwater flows in the soil back-filling of retain dry-stone walls to assess its effects on the deformation of the retaining walls and on the stability of the terraced slopes (Camera, 2011). The research involves analysis geotechnical and hydro-geological, based on a series of field tests and laboratory. The main parameters are hydraulic conductivity, permeability, infiltration rate, density, organic content, and soil moisture. It was implemented a numerical flow model that allows to make estimates of the moisture content of the soil and of the water pressure in the pores. The results are important for analyzing a stress-strain relationship for the stability of the soil-wall. The aim is to analyze the effects of the flow in terms of maximum shear strain and deformation of the wall, in addition to identification of the relative importance of the factors of instability.

In another work Camera (2012) tried to understand and reproduce the dynamics of hydrological terraced slopes with dry-stone walls. He evaluated the influence of temporary groundwater that it may cause instability of the wall. It was chosen the study area in Valtellina, near Tresenda, that it controlling by Debris flow caused 18 deaths in 1983. In 2002 there was another event with no deaths but with interruptions of traffic. One of the causes of risk was the collapse of the drywall after saturation coverage upstream. The authors

emphasized the importance of direct measurements and monitoring activities to develop reliable conceptual models for numerical analysis of groundwater flow and stability in an anthropogenic impacted geological context. Moreover it highlights the importance of field measures to reduce the uncertainty of parameters that are almost impossible to be measured directly. An analysis of the connection between rainfall and the response of groundwater in terms of forming a perched water table indicated that water table formation in this context is related above all to the intensity of the rainfall event, whereas the exhaustion time depends more on the amount of rain that fell in the final part of the event. Once these relationships were known, it was possible to define an intensity duration threshold for the onset of a perched groundwater table. Numerical modeling was then used to determine how a perched groundwater table is formed. The study attempted to reproduce the groundwater hydrographs during different actual rainfall events beginning with the recorded pressure head values from a datalogger installed in the field. The model, once calibrated, returned a good output in terms of both time and height of the maximum level reached by the groundwater table. The model was also validated, and a sensitivity analysis was performed showing that the effect of the variation of isotropic and anisotropic hydraulic conductivity. The aim of the work was to define and understand the conditions and the processes that could lead to a collapse in a terraced slope. Numerical modeling, supported by an intense in situ and laboratory tests and a groundwater monitoring plan, demonstrated to be a good methodology to approach such analysis. In this study the numerical modelling was performed using SEEP/W, which is a finite element numerical modelling code (GEO-SLOPE International Ltd. 2002). SEEP/W enables the modeling of groundwater flows both in saturated and unsaturated zones and allows for the study of steady and transient states. The model was then used as a predictive tool for different rainfalls that were calculated using statistical methods on the basis of fixed return periods (10, 50 and 100 years) and durations (3 and 7 days). The aim was to determine when it is possible to observe the formation of a saturated horizon that could push on the wall and trigger its possible failure. Rainfall intensity was considered to be constant when applied to the model. Figure 1.9 shows the results obtained with a return period of 50 years and a rainfall duration of 3 days. In Figure 1.9a, where the saturated conductivity *ks* was higher than that of the soil, the wall was able to drain water from the perched water table that was present at the contact area between the soil and the bedrock. However, when *ks* was decreased to $1x10^{-6}$ m/s, the wall acted as a barrier to water (Figure 1.9b).

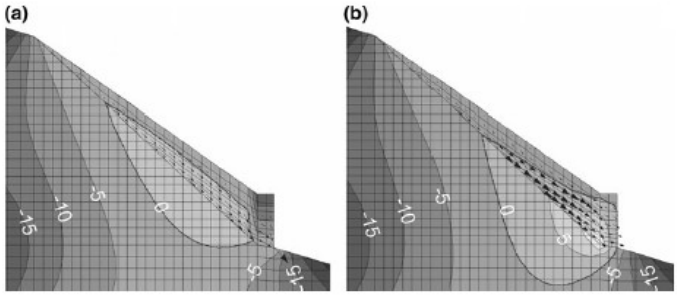

Figure 1.9. Pore water pressure contours (kPa) calculated for rainfall with a return period of 50 years and a duration of 3 days with a) ks of the wall=5x10^{-4}; and b) ks of the wall=1x10^{-6} m/s. The bold lines border the saturated zones. (Camera (2012)).

Considering that the hydraulic conductivity of the wall was greater than that of soil, for any combination of duration and return period, the wall was able to successfully drain the water from its backfill; therefore, no overpressure occurred. When the hydraulic conductivity of the wall was lowered to an order of magnitude less than that of the soil, large high positive pore-water pressures zones developed in the backfill of the wall for rainfall events with return periods of 50 years and even lower. Therefore, the model was able to not only reproduce a real event but also to correctly represent the differing behaviour between well and poorly maintained walls.

Camera et al. (2014) described the role of soil saturation and provided a physical explanation of the mechanisms causing failures of terraced slopes in Northern Italy. Their findings revealed that the formation of a perched groundwater table at the contact between the bedrock and the backfill soil of dry-stone walls, as well as the concomitant saturation of the backfill soil were the determining factors of slope failure. The wall collapse was mainly driven by the overpressure that developed at the base of a wall that was not able to drain efficiently. This explanation was consistent with earlier findings by Crosta et al. (2003), who described the mechanisms of landslide triggering in other terraced areas in Northern Italy. Permeability tests performed by these authors showed a general decrease of hydraulic conductivity with depth in the terrace soil that contributed to the formation of perched groundwater tables and the build-up of positive pore pressures in layers above permeability barriers. An alternative explanation of water movement related to wall instability and slope failure was provided by Arnáez et al. (2015), who stated that ‘when water meets the original soil of the hillside or a more impermeable substrate, it starts to act like subsurface runoff and accumulates behind the stone walls’. This observation stresses the role of lateral subsurface flow and subsequent

water accumulation behind the wall from above, not invoking the rise of groundwater or of perched water table reported by Camera et al. (2014) and Crosta et al. (2003).

Previous studies in a typical terraced vineyard in Tuscany (Central Italy) reported soil erosion and frequent dry-stone wall instability issues (Tarolli et al., 2015; Preti et al., 2013). These works showed that high-resolution digital terrain models (DTMs) derived by terrestrial laser scanner can be valuable tools to assess hydro-geomorphologic problems in terraced landscapes, but no explanation on water circulation processes related to slope and wall failures were provided. So, despite the amount of work on waterrelated phenomena in terraced areas, there is still a lack of knowledge on the main hydrological and hydraulic processes, including surface and subsurface flow pathways, which characterize terraced hillslopes. There is a need of better understanding of water resources with agricultural purposes and more effective maintenance strategies.

1.2.2.4 Terraces influence on peak runoff and hydraulic hazard at watershed scale

Mediterranean slope areas have been intensively used in the last century for cultivation on constructed terraces, retained by stone walls. The effects of agricultural land abandonment are strongly dependent on the relevant modifications on the local slopes and land use induced by the terrace construction.

Few works studied the influence of terraced areas on the hydrological processes at the basis of runoff production and the consequent changes on hydraulic hazard related with the inefficiency of the terraces. Earlier studies (Preti, 2001, 2002) have investigated the increase of hydrogeological risk associated with terrace abandonment. A study of the evolution of land use and terrace maintenance in the Fosso delle Rave basin in Versilia after the flood of 19 June 1996 has yielded interesting data (Ravenna, 2001; Preti et al., 2001). Other studies on areas in the Apuan mountains have highlighted the relationship between the abandonment of terrace areas and landscape dynamics, biodiversity, and the hydrogeological disasters that occurred in the Cardoso area in 1996. Meerkerk et al. (2009) determine the influence of terrace removal on hydrological connectivity and peak discharge in a south-east Spanish basin, using the rational formula applied to the contributing area of concentrated flow to the river.

Vieri et al. (2015) studied the historical influence of terraces on peak runoff and hydraulic hazards at a basin scale. The goal of their work was to assess the influence of terraced areas on runoff production and the hydraulic hazards related to terrace inefficiency. Their study

was carried out in a small catchment in Tuscany (Farnocchia, Italy: the Rave creek basin, 1.4 km^2) that was representative of recently abandoned fruit chestnut areas. After surveying the terraced zones, they conducted simulations of increasing level of abandonment scenarios using a hydrological model. In particular, simulations are run with an hydrological model (Preti et al., 1996; Preti et al., 2011) and different hydrologic response on terraced and not-terraced areas and the consequences on hydraulic hazard caused by the abandonment of the terraced areas were tested. The hydrologic modelling at watershed scale was supported by on-site activities, collected data relevant to the basin characterization. From the model application, it clearly appeared that surface runoff regulation and land conservation strategies, where terraces in abandonment conditions were present, need to be carried out to control the hydrological and geomorphic processes at basin scale. Furthermore, stability analysis on stone walls were carried out to verify the influence of the effectiveness lost of the drainage system behind the walls due to maintenance lacking. Their results revealed that both the concentration time and the peak flows were affected by the presence and maintenance level of bench-terraces. The same study showed that the hillslopes of a catchment where terraces collapse may be responsible for the diminished effectiveness of a terrace drainage system and result in further terrace collapse.

2 PERFORMANCE ASSESSMENT OF BENCH TERRACES THROUGH 2-D MODELLING[1]

2.1 Introduction

The use of dry-stone walls to build bench-terraces has traditionally played a key role in the management of hilly and mountainous agricultural areas. Because the mean gradient is greatly reduced by the presence of bench-terraces, the hydrological response of a terraced slope should result in a reduction of peak runoff at the toe of a hillslope and a delay in the passage of peak flows.

This research investigates the hydrologic-hydraulic behaviour of a hillslope, which is terraced using dry-stone walls, through a mathematical model (FLO-2D) to assess the effectiveness of this ancient technical solution. In fact, the stone walls merit attention for a flood-risk mitigation that is environmentally sound and historically well accepted by both inhabitants and public agencies (e.g. managing conservation sites designated under the Natura 2000 Network).

The methodological section describes the assumptions to apply the mathematical modelling under certain topographical and hydrological 'schemes' of bench-terraces. To this aim, a pilot representative hillslope with different extensions of terraced/no-terraced zones has been considered. The following section presents the model outcomes produced by several simulations of these 'schemes'. The overall advancements in design and arrangement of bench-terraces that maximize their hydrological performance are considered in the Discussion section, and parallels with the literature are included. An overview of the key points achieved through this research study closes the chapeter.

2.2 Method and assumptions for bench-terrace modeling

The study of runoff propagation in a terraced slope is modelled with the FLO-2D (2009) model. FLO-2D is a two-dimensional hydraulic model that works on either erodible or fixed terrains ('floodplain areas'). The model can be used for modelling water flows and non-Newtonian flows through a raster adaptation of the fully dynamic equation. During the

[1] The study described in this chapter has been extracted from Perlotto and D'Agostino (2017)

simulation, the runoff is routed cell by cell according to the energy slope with respect to the eight neighbours and moves from upland terraces as input to downstream terraces. Existing literature highlights several positive applications and verifications of this model, which well performs the flow propagation at steep slopes of the terrain, including terraced areas (Bertolo & Wieczorek, 2005; Li et al., 2005; Quan Luna et al., 2014). Given an input rainstorm event and/or a flood hydrograph, the model can predict the floodplain area, the mean flow velocities and flow depths for each cell in which the topography is discretized. The main model inputs consist of a Digital Terrain Model (DTM) area of simulation (floodplain) and a rainfall event that, after accounting for losses, is routed along the hillslope to produce a flood hydrograph in a selected outlet section. The precipitation losses simulated with FLO-2D include both interception and infiltration. The initial interception is performed prior to simulating the infiltration and is assigned by the user. The user can choose between two different infiltration/effective runoff algorithms: the Green & Ampt (1911) and the Soil Conservation Service-Curve Number (SCS-CN) method (Chow et al., 1988).

When using the Green-Ampt infiltration model, the spatial variability of infiltration is modelled by assigning values of both hydraulic conductivity and soil absorption for each element of the grid.

When the SCS method is used, a different *CN* can be assigned to each floodplain cell, also automatically setting the value of the initial abstraction equal to 20% of the maximum water retention (*S*) according to the standard method. For both methods, the portion of precipitation infiltrated into the soil is lost from the system and does not contribute to the flood hydrograph. This assumption is locally forced for the dry-stone walls because of their draining capacity, but the small portion of involved surface (wall thickness) makes it acceptable on the whole. The SCS-CN method has been adopted in this modelling analysis because of the practical aim of this investigation and its widespread use among researchers and practitioners.

After the runoff is produced on the floodplain cells—and if the water depth is greater than the assigned surface detention limit—the model propagates the flow by applying the full dynamic de Saint-Venant equation in eight cardinal directions. The velocity for each direction is solved, and the water depth in the cell under computation is then updated via mass conservation.

2.2.1 *The pilot test area*

A typical setting of the central-western pre-alpine belt of the Veneto Region, Italy (e.g. the Garda-lake hillslopes of Brenzone or Malcesine in the province of Verona; Figure 1.1d is selected and reproduced as pilot area for the modeling analysis.

As such, a schematic hillslope 'floodplain' (Figure 2.1a) is built with the following characteristics:

• DTM resolution of 10×10 m or 5×5 m, when simulating terraces with the shortest spacing;

• Test area size of 1000 m long in the downslope direction and 500 m wide in the cross-flow direction, being a hillslope of 50 ha, a reliable area considering the reference setting.

• Hillslope inclination angle of 20° (36%), which represents a mean gradient in the reference area similar to many worldwide areas managed with bench-terraces (slope range from 7° up to 30° according to Morgan, 2005). It is worth specifying how the assumption of a lower slope angle (e.g. 10°) would not be a realistic hypothesis for the stone-wall bench-terraces of the reference condition (Figure 1.1d).

• Manning's n roughness is uniformly distributed on the DTM and assigned a value of n = 0.125 in the typical range of the overland flow (Fathi-Moghadam et al., 2011);

• Surface-water detention equal to 1 mm.

Based on a recent regional analysis of precipitation in the Veneto Region (Dipartimento della Protezione Civile, 2008), all simulations are carried out assuming a heavy rainfall event of 100 mm in 1 h (200-year return period), which also corresponds to a flood scenario with medium probability according to the European directive 2007/60/ EC 'on the assessment and management of flood risks'.

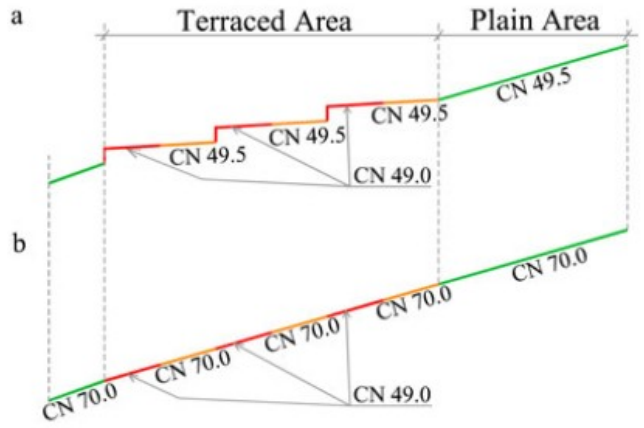

Figure 2.1.(a) Scheme A (Scheme B is similar: CN = 70 instead of CN = 49.5); (b) Scheme C; the plain area length is only indicative.

A basic sketch of the Scheme-A hillslope (Figure 2.1a and Figure 2.3) with dry-stone walls (Figure 2.2) is modelled by varying both the number of dry-stone walls used to manage the hillslope (one to six wall lines, beginning from the toe of the hillslope and incrementally adding one wall line toward the top of the hill) and the spacing (L) between adjacent bench-terraces (10, 20, 30, 50 and 100 m). The combination of both variables determines the proportion of the pilot hillslope that is covered by bench-terraces and produces 30 simulation scenarios. In other words, the modelling series presents a succession of terraces in the downstream portion of the slope and the presence of no-terraced areas in the upstream portion of the slope; these are defined as "terraced areas" and "plain areas", respectively (Figure 2.1a). The terraced area is morphologically modified by the presence of dry-stone walls that are assumed to be 1.5 m high (Figure 2.2), as this often occurs in the geographical area of interest.

As stated earlier, the simulation topography is built starting from the toe of the hillslope (Sec.1, Figure 2.3) and adding the first line of walls. Then the terrain profile behind each wall begins from the wall crest, maintains a constant bench angle of 5° (9%) and ends when the selected spacing (L) is reached. Upstream of the last highest terrace strip of the hillslope profile continues assuming the slope of 20° until the total length of 1000 m (pilot area, Figure 2.3) is covered.

This means each simulation has a different maximum elevation of the top of the hill according to L and number of walls that are selected (Figure 2.1a). In representing this sketch in a raster DTM, the cells containing the dry-stone walls ("wall cells" in Figure 2.2) have been hydrologically differentiated from the other cells ("no-wall cells"). To assess the proper *CN* value for the wall cells, the following assumptions have been formulated for the volume of a single cell (Figure 2.2):

- 90% composed of compacted soil made of clayey sands with a porosity $p = 0.163$ (VSS, 1999);
- 7% composed of gravel backfill of the wall with a porosity $p = 0.350$; and
- 3% composed of the dry stones of the wall with $p = 0.350$.

The volume resulting from the three parts (soil, backfill and wall) is calculated by multiplying the area of each component by the wall height (Table 2.1 and Figure 2.2). Because of the different porosities, the maximum volume of storable subsurface water (Va) is calculated considering a permeable terrain volume (Vs) that corresponds to a soil thickness equal to the wall height. This hypothesis is consistent with bench terrace conditions for

typical agricultural uses when the soil depth is shallow and the wall height is a good proxy of the soil depth (Morgan, 2005). The storable subsurface water can be expressed as follows:

$$V_a = V_s \, p \qquad (2.1)$$

The resulting *Va* volumes from Equation 2.1 are listed in Table 2.1 for a cell of 10×10 m (for the cell size of 5×5 m, the computation is similar).

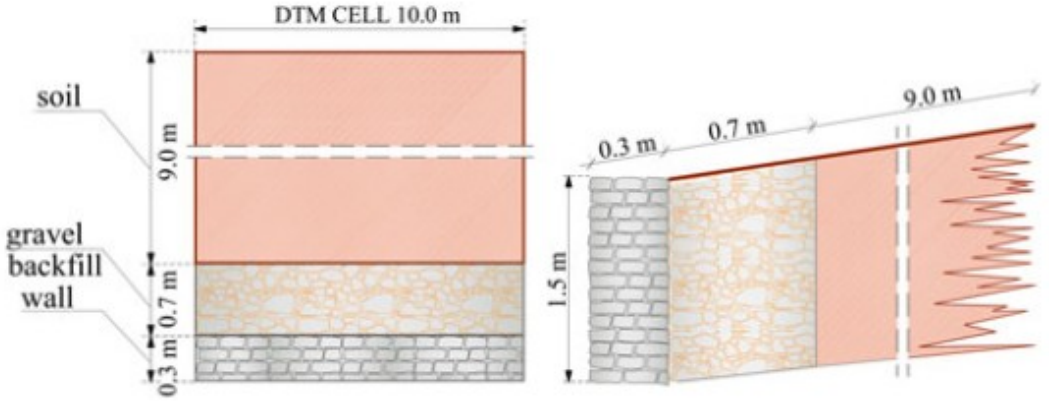

Figure 2.2.Sketch of a "wall cell": plan view (on the left) and lengthwise profile (on the right).

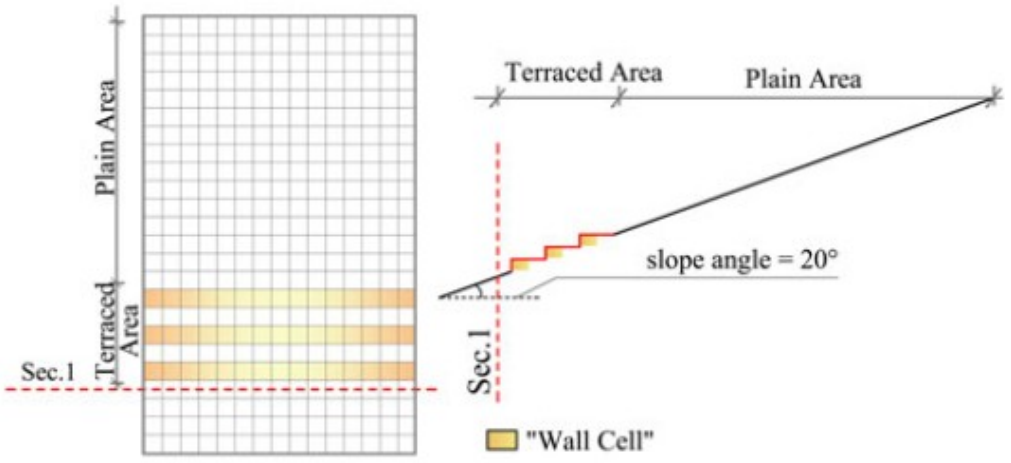

Figure 2.3.Sketch of the modelled terrace slope (pilot area for Scheme A or B); example with three walls, cells of 10 m and L = 20 m (width and length of the hillslope are indicative).

When calculating the *CN* value that matches with the previous assumption, the maximum retention water depth (*S*) within the soil can be assessed under the hypothesis of dry antecedent moisture conditions [antecedent moisture conditions (AMC) group I, Chow et al., 1988] and then approximated as the ratio between *Va* and the cell area (Table 2.1). Based on

this approach, the compacted soil behind the wall assumes a *CN* value of 51, and the gravel backfill and the stone wall both have a *CN* value of 32.6.

	Area (m^2)	**Volume V_s (m^3)**	**Porosity *p* (-)**	**Water volume V_a (m^3)**	***S* (mm)**	***CN***	**Area× *CN*/100**
SOIL	90	135	0.163	22.01	244.5	50.95	45.86
BACKFILL	7	10.5	0.350	3.68	525.0	32.61	2.28
WALL	3	4.50	0.350	1.58	525.0	32.61	0.98
							49.12

Table 2.1. Calculation of the weighted curve number (CN = 49·12) for a 'wall cell' (Figure 2.2) with area equal to 100m^2 (S = maximum retention water depth).

These local *CN* values are then averaged by using the competence areas as weights, thus obtaining a weighted *CN* = 49.1 (49, hereafter) for the "wall cells" (Table 2.1). For the "no-wall cells" (plain area, less compacted soil), it is set to *CN* = 49.5.

To complete the analysis, two schemes have been added to the basic scheme (Scheme A) described earlier.

The first one, Scheme B, assumes that the hillslope prior to a rainfall occurrence of 100 mm in 1 h has been brought into intermediate AMC in such a way that only the "no-wall cells" (plain area) increase their *CN* value from 49.5 to 70.

This assumption corresponds in the SCS-CN method to a switch from the AMC group I to the AMC group II (Chow et al., 1988), whereas the 'wall cells' maintain their original value (*CN* = 49) because of the efficient drainage capacity at their boundary (dry-stone walls and gravel backfill).

Assuming the same topography as Scheme A, Scheme B considers the worsening of the *CN* in the entire surface not adjacent to the dry-stone walls. This is simulated for four scenarios: a fixed number of walls equal to four wall lines and five cases of L spacing between the works: 10, 20, 30, 50 and 100 m.

The second scheme, Scheme C, maintains the hypothesis of maximum differentiation between the *CN* of the wall/ no-wall cells as in Scheme B, but completely obliterates the topographic modifications induced by the bench-terraces and assumes a uniform hillslope angle of 20° (Figure 2.1b). Scheme C is a topographically unrealistic hypothesis and is a reductio ad absurdum. It aims to show the impact of strips of soil with terrace properties (low *CN*) while the terrace topography is obliterated.

This scheme is simulated for eight scenarios: the same five cases of Scheme B (four wall lines and *L* = 10, 20, 30, 50 and 100 m) and three cases with a fixed number of terrace

spacing of L = 100 m and variable terrace numbers from one to three (the case with four walls falls in the previous group).

A final view of the three schemes adopted to model the pilot area can be highlighted as follows (Table 2.2, first four columns, run n. 1–43):

• Scheme A: several topographical combinations of terraced and non-terraced areas (from plain area to almost total managed hillslope) under the hypothesis of a low (group I) AMC (Figure 2.1a, Table 2.2: runs n. 1–30 and run n. 0. A for comparison).

• Scheme B: selection of combinations of the Scheme A (four walls) under the hypothesis of intermediate AMC (group II) for soil and low AMC (group I) for walls (well-draining wall cells) (Table 2.2, runs n. 31–35 and run n. 0.B for comparison);

• Scheme C "topographically unrealistic hypothesis" of a constant slope angle of 20°, and assumption of a "terraced" CN distribution (group II AMC) as implemented in the Scheme B (plus the case with L = 100 m and a number of 1–3 walls) (Figure 2.1b, Table 2.2, runs n. 36–43 and run n. 0.C for comparison).

2.2.2 Indices

To evaluate the benefits of flood reduction produced by the terraces, two numerical indices are defined. Figure 2.3 shows an example in which part of the pilot test area is terraced by inserting three lines of stone walls. Based on Figure 2.3, a percentage ratio of terraced area (A_T%) can be calculated that is termed the 'terracing degree index' (*TDI*). It can be written as

$$TDI = A_{T\%} = \frac{100\ A_T}{A_T + A_F} \qquad (2.2)$$

where: A_T is the area occupied by terraces and A_F is the plain area without terraces. Second, a "lag time index" (*LTI*) can be considered as follows:

$$LTI = \frac{t_{pT} - t_{pWT}}{t_{pWT}} \qquad (2.3)$$

The *LTI* is capable of rating the difference between the time of occurrence of flood peak, from rainfall initiation, when terraces are present (t_{pT}) and without any terraces (t_{pWT}). Both variables t_{pT} and t_{pWT} are evaluated at the outlet indicated as "Sec.1" in Figure 2.3.

Run n.	Scheme	L (m)	n. walls	TDI (%)	Q_{pT} (m^3/s)	t_{pT} (h)	LTI (%)	PRI (%)	Runoff (mm)
0.A	-	-	-	-	0.41*	1.12*	-	-	6.5
1	A	10	1	1.23	0.41	1.20	7.14	0.00	6.5
2	A	10	2	2.47	0.41	1.28	14.29	0.00	6.5
3	A	10	3	3.70	0.41	1.28	14.29	0.00	6.4
4	A	10	4	4.94	0.41	1.28	14.29	0.00	6.4
5	A	10	5	6.17	0.40	1.36	21.43	2.44	6.5
6	A	10	6	7.41	0.40	1.44	28.57	2.44	6.4
7	A	20	1	2.47	0.41	1.44	28.57	0.00	6.4
8	A	20	2	4.94	0.41	1.52	35.71	0.00	6.5
9	A	20	3	7.41	0.41	1.76	57.14	0.00	6.4
10	A	20	4	9.88	0.41	1.92	71.43	0.00	6.4
11	A	20	5	12.35	0.40	1.92	71.43	2.44	6.4
12	A	20	6	14.81	0.40	2.08	85.71	2.44	6.4
13	A	30	1	3.70	0.41	1.68	50.00	0.00	6.4
14	A	30	2	7.41	0.40	1.92	71.43	2.44	6.4
15	A	30	3	11.11	0.38	2.16	92.86	7.32	6.4
16	A	30	4	14.81	0.35	2.32	107.14	14.63	6.3
17	A	30	5	18.52	0.31	2.64	135.71	24.39	6.3
18	A	30	6	22.22	0.27	2.88	157.14	34.15	6.4
19	A	50	1	6.17	0.39	2.00	78.57	4.88	6.4
20	A	50	2	12.35	0.32	2.4	114.29	21.95	6.3
21	A	50	3	18.52	0.24	2.88	157.14	41.46	6.3
22	A	50	4	24.69	0.18	3.60	221.43	56.10	6.2
23	A	50	5	30.86	0.14	4.40	292.86	65.85	5.9
24	A	50	6	37.04	0.14	4.48	300.00	65.85	5.9
25	A	100	1	12.35	0.33	2.48	121.43	19.51	6.4
26	A	100	2	24.69	0.22	3.52	214.29	46.34	6.4
27	A	100	3	37.04	0.15	4.96	342.86	63.41	6.1
28	A	100	4	49.38	0.09	6.48	478.57	78.05	5.5
29	A	100	5	61.73	0.07	8.96	700.00	82.93	4.8
30	A	100	6	74.07	0.05	11.92	964.29	87.80	3.8
0.B/C	-	-	-	-	4.88*	1.04*	-	-	31.5
31	B	10	4	4.94	4.88	1.12	7.69	0.00	31.3
32	B	20	4	9.88	4.73	1.12	7.69	3.07	29.6
33	B	30	4	14.81	4.37	1.20	15.38	10.45	29.6

Run n.	Scheme	L (m)	n. walls	TDI (%)	Q_{pT} (m^3/s)	t_{pT} (h)	LTI (%)	PRI (%)	Runoff (mm)
34	B	50	4	24.69	3.45	1.36	30.77	29.30	29.4
35	B	100	4	49.38	1.29	2.24	115.38	73.57	29.6
36	C	10	4	4.94	4.88	1.04	0.00	0.00	31.0
37	C	20	4	9.88	4.73	1.04	0.00	3.07	30.3
38	C	30	4	14.81	4.69	1.04	0.00	3.89	30.3
39	C	50	4	24.69	4.67	1.12	7.69	4.30	30.0
40	C	100	4	49.38	4.66	1.12	7.69	4.51	29.8
41	C	100	1	12.35	4.80	1.04	0.00	1.64	31.3
42	C	100	2	24.69	4.77	1.04	0.00	2.25	31.0
43	C	100	3	37.04	4.77	1.04	0.00	2.25	30.5

*Table 2.2. Summary of all simulations (runs n.1–30 of Scheme A, runs n. 31–35 runs of Scheme B, runs n. 36–43 of Scheme C). *Indicates that peak discharge and time to peak correspond to the hillslope without any terrace: Qp_{WT}, tp_{WT} . (runs n. 0.A, 0.B, 0.C). LTI, lag time index; PRI, peak reduction index; TDI, terracing degree index.*

Finally, a "peak reduction index" (*PRI*) of the peak discharge (Q) is set via the following position:

$$PRI = \frac{Q_{pWT} - Q_{pT}}{Q_{pWT}} \qquad (2.4)$$

Where: Q_{pT} represents, similar to the *LTI* subscripts, the peak discharge at the hillslope outlet (Figure 2.3, Sec. 1) in the presence of terraces and Q_{pWT} represents the peak discharge in the absence of terraces.

2.3 Results

The results of all simulations (45 runs, Schemes A, B, C) are summarized in Table 2.2, where the model outputs are listed in terms of time to peak (t_{pT}), peak discharges (Q_{pT}) and dimensionless indices (*LTI*, *PRI*) for a given *TDI*. The same table also shows the simulation results without bench-terraces for Scheme A (run n. 0.A: no stepped profile, *CN*= 49·5 for the entire pilot area) and Schemes B and C (run n. 0.B/C: no stepped profile, *CN*= 70 for the entire pilot area). The general pattern of the hydrological responses in a case when the TDI values are effective is plotted in Figure 2.4. The flood hydrograph is shown dealing with four walls and different terrace spacing (Scheme A, run n. 10, 16, 22 and 28 of Table 2.2. In the figure, both the peak attenuation and the peak delay can be dimensionally appreciated when

the area covered by the bench-terraces increases ($A_{T\%}$). When given a fixed number of walls (four in Figure 2.4), a greater spacing between walls indicates a greater extension of the pilot area covered by the bench-terraces.

A summary of the Scheme A simulations (run n. 1–30 of Table 2.2) is illustrated in Figure 2.5a,b, where the *LTI* and the *PRI* indices are, respectively, plotted against the *TDI*.

The two best-fitting functions are plotted in the same figure and show a parabolic and logarithmic trend that can be expressed in the following forms:

$$LTI = k_1\, TDI^{\,2} + k_2\, TDI + k_3 \qquad (2.5)$$

$$PRI = k_4 \ln(TDI) - k_5 \qquad (2.6)$$

The k_i symbols are the constants (written in Figure 2.5a,b) provided by the two least-square regressions (coefficient of determination R^2 equal to 0.99 and 0.93 for *LTI* and *PRI*, respectively).

It is worth noting that although the regression for Equation 2.5 accounts for all "modelling experiments" (30 data), the regression for Equation 2.6 considers only those data (16 data) having a numerically significant *PRI* value greater than 2.5%. This fact occurs when the *TDI*>15% (Table 2.2). When all data fit the k_i coefficient in Equation 2.6, the function does not fit the data very satisfactorily and R^2 reduces to 0.77 because of data flattening in the field of close-to-zero *PRI* values (Figure 2.5b and Table 2.2).

.

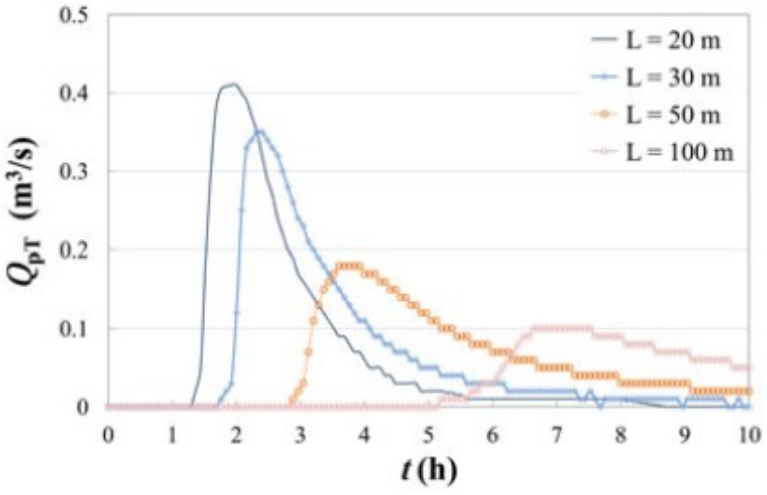

Figure 2.4. Flood hydrographs (t = time; Q_{pT} = water discharge) calculated at the terraced-hillslope outlet: Scheme A, four walls with spacings L = 20, 30, 50 and 100 m.

The direct comparison of the five Scheme-B cases with the corresponding Scheme-A cases (Figure 2.6a) highlights an important *LTI* down-switch (Scheme B) caused by greater runoff depths (higher *CN* value of the no-wall cells), which proportionally speed up the flow propagation through the terraced areas. In this case (fixed wall number), the *TDI* increase depends only on a longer L and the trend is not parabolic as in Equation 2.5 but almost linear. A similar comparison is shown in Figure 2.6b in terms of *PRI* responses, where the patterns of the two Schemes A and B are quite close and *PRI* is obtained through the peak-discharge scaling over the respective no-terrace scenario (0.A and 0.B).

Figure 2.7a,b compares five Scheme-C cases (run n. 36–40, Table 2.2) with the five corresponding Scheme-B cases (run n. 31–35, Table 2.2).

Given the persistency of the same *CN* spatial distribution on the pilot area (*CN*= 70 for plain areas; *CN*= 49 for terraced areas), the plot (Figure 2.7) demonstrates the dominant role of the stepped topography on the flood hydrograph formation. In fact, when *TDI* is close to 50%, the lag times of peak occurrence even double for Scheme B, while they do not vary significantly for the Scheme C (Figure 2.7a). Similarly, when *TDI* increases, the effects on the peak discharges are tangible only for Scheme B (Figure 2.7b). Finally, the runs of Scheme C provide evidence in Table 2.2 (run n. 36-43) of the poor effect on Q_{pT} and t_{pT} (as well as on *LTI* and *PRI*) when the *TDI* is only "virtually" raised (because of *L* variations or larger numbers of walls affecting only the *CN* distribution and not the topography). In the case *TDI* ≅ 50%, *LTI* reaches about 8% (Table 2.2, run n. 39–40), and *PRI* is close to 5%.

2.4 Discussion on results

The coupled hydrological-hydraulic modelling of a simplified hillslope with bench-terraces is scientifically opportune because testing an analogous situation in the reality would be an extremely difficult task. In fact, the monitoring of overland flow responses requires the occurrence of heavy rainstorm events, and the prior installation and long-time functioning of proper instrumentation (e.g. a network of drainage pipes discharging the outflow into a storage basin or receiving channel that is continuously monitored).The test results from Scheme A merit particular attention because the progressive influence of the Terracing Degree Index (*TDI*) on the *LTI* and *PRI* can offer practical outcomes for designers. The benefits of the terraced area results are incrementally consistent until the *TDI* reaches a value equal to 35%; at this level, the time-to-peak increment is amplified by 3.1 times t_{pWT} (Equation 2.5) and the maximum peak-hydrograph index (*PRI*) approximately equals 61%

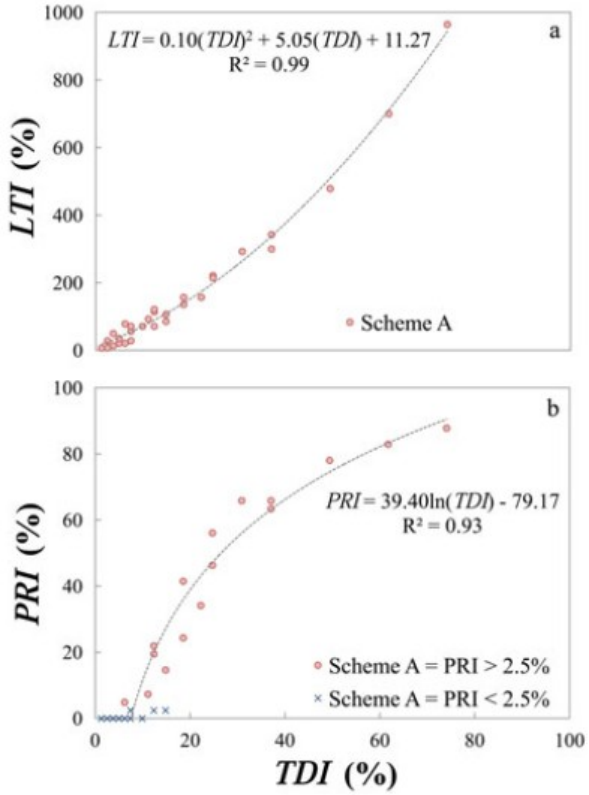

Figure 2.5. (a) Lag time index (LTI) versus terracing degree index (TDI) for Scheme A; (b) peak reduction index (PRI) as function of the TDI for Scheme A.

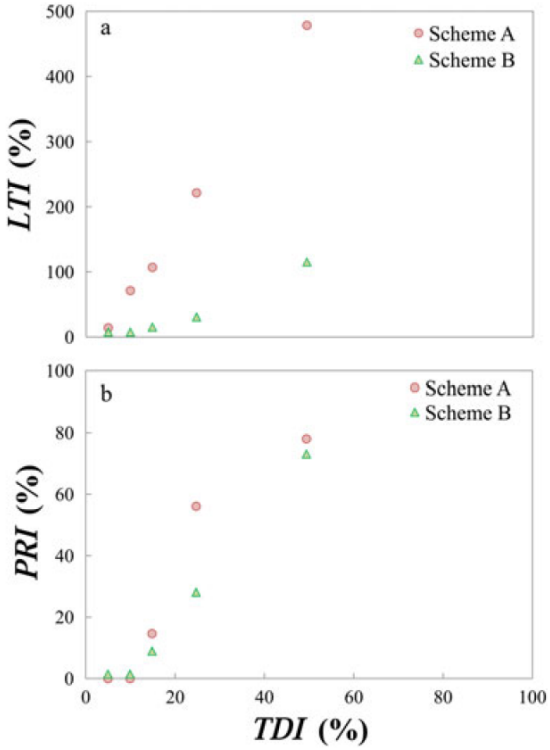

Figure 2.6. (a) Comparison between Schemes A and B in terms of (a) lag time index (LTI) versus terracing degree index (TDI); (b) peak reduction index (PRI) versus TDI.

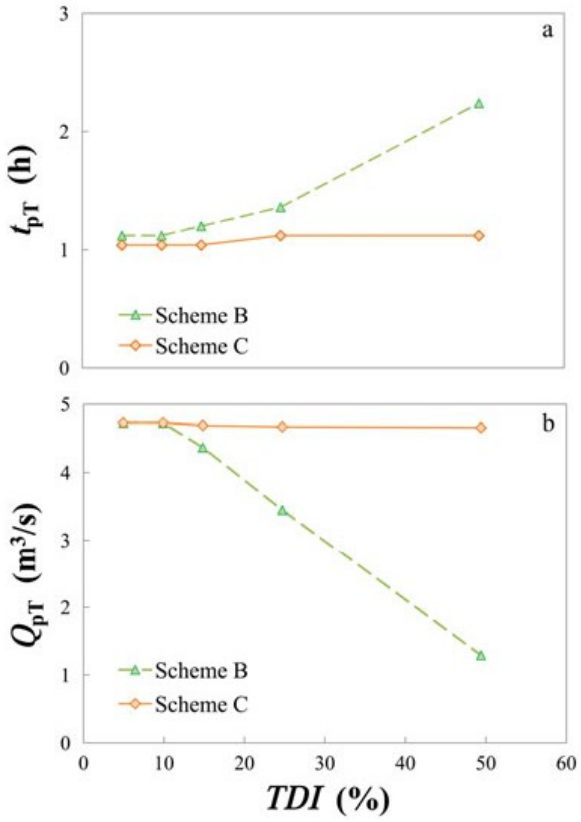

Figure 2.7. Comparison between Scheme B and Scheme C: four walls and different L spacings (run 25–28 and 29–32; main variables listed in Table 2.2); (a) time to peak (tpT) versus terracing degree index (TDI); (b) peak discharge (QpT) versus TDI.

(Equation 2.6). According the quadratic/logarithmic trends (Figure 2.5a,b), doubling the value of the *TDI* to 70% raises the *LTI* to 855% and the *PRI* to 88%.

It is worth observing that the presence of bench-terraces in not always hydrologically effective to reduce the peak discharges at the hillslope outlet. In fact, considering the results from Schemes A and B, a minimum *TDI* threshold of 15% emerges below which the lag-time variation (maximum *LTI*<125% for the Scheme A, and *LTI*<15% for the Scheme B) is not capable to modify the maximum flow rates in comparison with no terraces at all (*PRI*<15% for both Schemes).

It can be noted that simulations with same *TDI* have slightly different *PRI* values (Figure 2.5b). As to physical meaning, the difference derives from the mathematical model characteristics, because the energy line of the flow is always computed joining the centre of pairs of cells.

Within the computational grid, each "wall cell" is followed downstream by the cell at the base of the wall that is located 1.5 m lower. When the current propagates, these two cells

undergo flow velocity increase and travel time decrease because of local energy-line amplification, which, in turn, is caused by the drop from the wall head to the wall base.

Thereby, given a certain *TDI*, the model response indicates that a higher number of terraces would cause a lower *LTI* (the time of concentration is lower) and a lower *PRI* (e.g. for *TDI* = 18.5% in Table 2.2, the combinations of five walls and *L* = 30 m, and that with three walls and *L*=50 m provide *LTI* = 136%, and *PRI* = 24% against *LTI* = 157% and *PRI* = 41%, respectively). Certainly, this behavior needs field verifications under different rain intensities, which could lead to opposite conclusions. The local phenomenon is anyway quite complex, and the flow motion in correspondence to the drop (crest, face, base) might affect, as the modelling envisages, the overall hydrologic response. The results on *LTI* and *PRI*, referring to an unmanaged slope angle of 20° quite typical for bench-terraces with stone wall, represent quali-quantitative indications for decision making in the reality (e.g. building walls or not, choice of terrace spacing), although they can vary by changing the reference storm intensity and steepness of the pilot area. Moreover, if a steeper (e.g. 30°) plain area hillslope had been simulated (given that slope of the treads between adjacent walls does not vary because of cultivation needs), the hydrological benefit of land terracing would result greater, being the *PRI* values obtained through the scaling of peak discharge over a steeper and shorter lag-time system. Viceversa, the simulation of a milder plain area (e.g. 15°), would have provided lower *PRI*, being the gradients of terraced and unmanaged areas more similar. Hydrologic peak discharges per unit of drainage area (see run n. 0.A and run no. 0.B–C, Table 2.2) between 0.8 and 10 $m^3s^{-1}km^{-2}$ are representative of the discharges in the pre-alpine belt of the Veneto Region (Villi & Bacchi, 2001). It is worth noting that when terraced hillslope areas are part of a larger catchment, the benefits of terracing extend beyond local improvements. In fact, thanks to the *TDI* that affects the terraced areas (Figure 2.5a), the final flood hydrograph of the entire basin can greatly benefit from the desynchronization of runoff responses from the terraced zones (e.g. for *TDI* = 25%, the local time-to-peak increment doubles). In addition, this positive hydrological conditioning effect is significant when the *TDI* $\geq$ 50%, providing a *LTI* approximately greater than 500% (Equation 2.5).

Scheme B gives an insight on those hydrologic conditions that become critical during the year. In fact, Gallart et al. (2002) demonstrated that the hydrological response of terraced catchment shows a ‘switching’ behaviour between a dry and a wet season and is markedly driven by the temporal pattern of soil moisture.

The results of Scheme B are realistic because the cultivated area behind the wall — and the wall when well maintained — can significantly reduce the soil memory of the AMC,

particularly if served by secondary subsurface drainages. Camera et al. (2014) (Valtellina, Italy) have also proved that the proper maintenance of stone walls (e.g. initial draining condition active since the rain starts) brings to an unsaturated surface zone behind the wall after 72 h of precipitation (rainfall with 50-year return period). This finding makes our modeling hypothesis (Scheme B) consistent also in terms of *CN* assignation (Figure 2.6a, p.48 in Camera et al., 2014).

The Scheme-B scenarios result in a *TDI* ranging from 4.9% to 49.4% and highlight two additional findings (Figure 2.6a,b): (i) a confirmation of the direct functional linkage between *LTI*/*PRI* and *TDI* and (ii) a demonstration that proper maintenance of stone walls and preparation of a drained terrain (e.g. building an efficient network of ditches and/or subsurface drainage pipes) extending up to the plain area are extremely useful in mitigating repeated rain storm events in a short time interval (e.g. 3–4 days). In fact, if the AMC does not change, then the Scheme-A hillslope remains valid regardless of the antecedent rainstorm pattern. For example, in comparing the Scheme-B run n. 34 (Table 2.2: *TDI* = 24.7%, Q_{pT} = 3.45 m^3s^{-1}) with the corresponding Scheme-A run n. 22 (Table 2.2: *TDI* = 24.7%, Q_{pT} = 0.18 m^3s^{-1}), it is clear that there is a considerable advantage in setting up a subsurface drainage system capable of controlling (at least partially) soil moisture conditions above the terraced area and thus limiting the soil-moisture variation between dry and wet periods (Gallart et al., 2002).

It can be concluded that the hydrological-hydraulic response of a terraced hillslope highlights some contrasting effects. In fact, while Gallart et al. (1994) found that storm runoff could be generated by the contributes of terraces promoting the premature formation of saturated areas (particularly in the upper part of the terrace, Camera et al., 2014), we stressed, in contrast, the important increase of the overland-flow routing times thanks to the stepped terrain profile of bench-terraces. The concentration time increased in our bench-terrace simulations, markedly reducing storm runoff both under dry (Scheme A) and humid (Scheme B) scenarios.

Scheme C originates in a fictitious scenario (no stepped topography) and isolates the LTI and PRI reductions caused only by the *CN* variation between the "wall cells" (low *CN* values) and the plain area (high *CN* values). The result comparison of this Scheme with Scheme B (Figure 2.7) proves clearly how the *LTI* is poorly affected by the only *CN* distribution, and the outward stepped topography drives the overland flow propagation by dramatically lowering the routing times. Therefore, it is not surprising that a "real"' *TDI* of 50% produces a peak discharge of almost one-fourth in comparison with that expected when the terrain is not affected by morphological modifications (Table 2.2 and Figure 2.7b). As a consequence,

when bench-terraces are built for hydrological benefit, maximizing the terrain profile modification is very important; this requires uniformly reducing the slope of the hillslope reach that separates the top of each consolidation wall from the toe of the uphill wall. Our overall findings partially agree with Vieri et al. (2015). They showed through a hydrological modeling study (catchment area of 1.44 km^2) that the concentration time and peak flow values are influenced by the presence and maintenance level of bench-terraces. In their analysis, authors found that a lack of slope stabilization works for the 13% of the basin resulted in an increase of 13% of peak discharges. In our investigative approach, we, similarly, found for a hillslope catchment (0.5 km^2) that the flood hazard at the outlet may dramatically rise when decreasing the terraced area proportion, for example from *PRI* = 66% to *PRI* = 48% passing from a *TDI* = 40% to *TDI* = 25% according to Equation 2.6 of Scheme A. Additional modelling of responses to a severe reference rain storm (100 mm/h lasting 1 h) demonstrates (Scheme C compared with Scheme B) that this hazard can increase more because of the terrain morphology modifications (less terraces) rather than local variations of soil permeability (higher AMC).

3 PHYSICAL AND NUMERICAL MODELING TO ASSESS HYDROLOGICAL PROCESSES IN A BENCH - TERRACE

3.1 Introduction

This research aims to better focus the hydrological response, which is determined by a hillslope plot bounded by a dry-stone wall, considering both the overland flow and the groundwater. A physical model, characterized by a quasi-real scale, has been built to reproduce the behavior of a outward sloped terrace with gradient ranging between 3 to 9 %; bare soil and vegetated soil conditions were analyzed.

The model consists of a steel metal box (1 m large, 3.3 m long, 2 m high) containing the hillslope terrain. The terrain is equipped with two piezometers, 9 TDR sensors measuring the volumetric water content, a surface spillway at the head releasing the steady discharge under test, a scale at the wall base to measure the groundwater discharge and a second scale connected through a pipe system at the wall top to measure the surface runoff component.

The experiments deal with different initial moisture conditions (high/low degree of saturation) applyied to a partially satured soil, and uniform inflow distribution along the width of 1 m using three discharges of 19.5, 12.0 and 5.0 l/min.

A voumetric water content analysis was conducted to rapresent the overall soil moisture behaviour during the runs and its connection with the infiltration processes. Then the characteristisc response times of overland fow and groundwater flow were monitored to understand the kinematics of the terrace plot. Finally, a numerical modeling analysis was conducted to reproduce the hydrological response of the experimental plot.

The following sections describe the experimental and modelling configurations and the relative results. An overview of the key points achieved through this research study closes the chapter.

3.2 Materials and methods

3.2.1 First configuration of the physical model

A physical model of a bench terrace, characterized by a realistic scale, has been installed at the University of Padua (Azienda Agraria). The model is located in the outside area of Experimental farm "Lucio Toniolo" at Legnaro (Padova) (Figure 3.1).

Figure 3.1. The physical model

The model is in real scale (1:1) and it is composed by a rectangular box consisting of three vertical panels in galvanized steel and it is open in one of the two shorter sides. The structure was built by a professional locksmith in order to guarantee the structural safety.
The use of this system can avoid the more complicated work in the field if it is properly built. Therefore, the model was created in order to simulate the same conditions that occur in the field and it was also implemented with all the instruments able to detect all the information during the experiments. In particular, it was thought to represent a terrace affected by a superficial laminar sheet of water flowing on it, that is overland flow.
The container is laid on six foots which permit to have the model lifted (Figure 3.2). The dimensions of the base of the metal container are 1 m width, 3.3 m length and the base is sloped to permit the collection of residual water through a valve. The container is so closed

by two side metal walls and one head metal wall. The walls of the box vary from 1.4 to 1.6 m of height; the tallest wall is also used to locate the instruments and as support for a removable covering. In fact, the set up of the model was completed by a removable roof useful to cover the model from the rain when not used. The free side of the container represents the outlet of the model where a dry stone wall has been built.

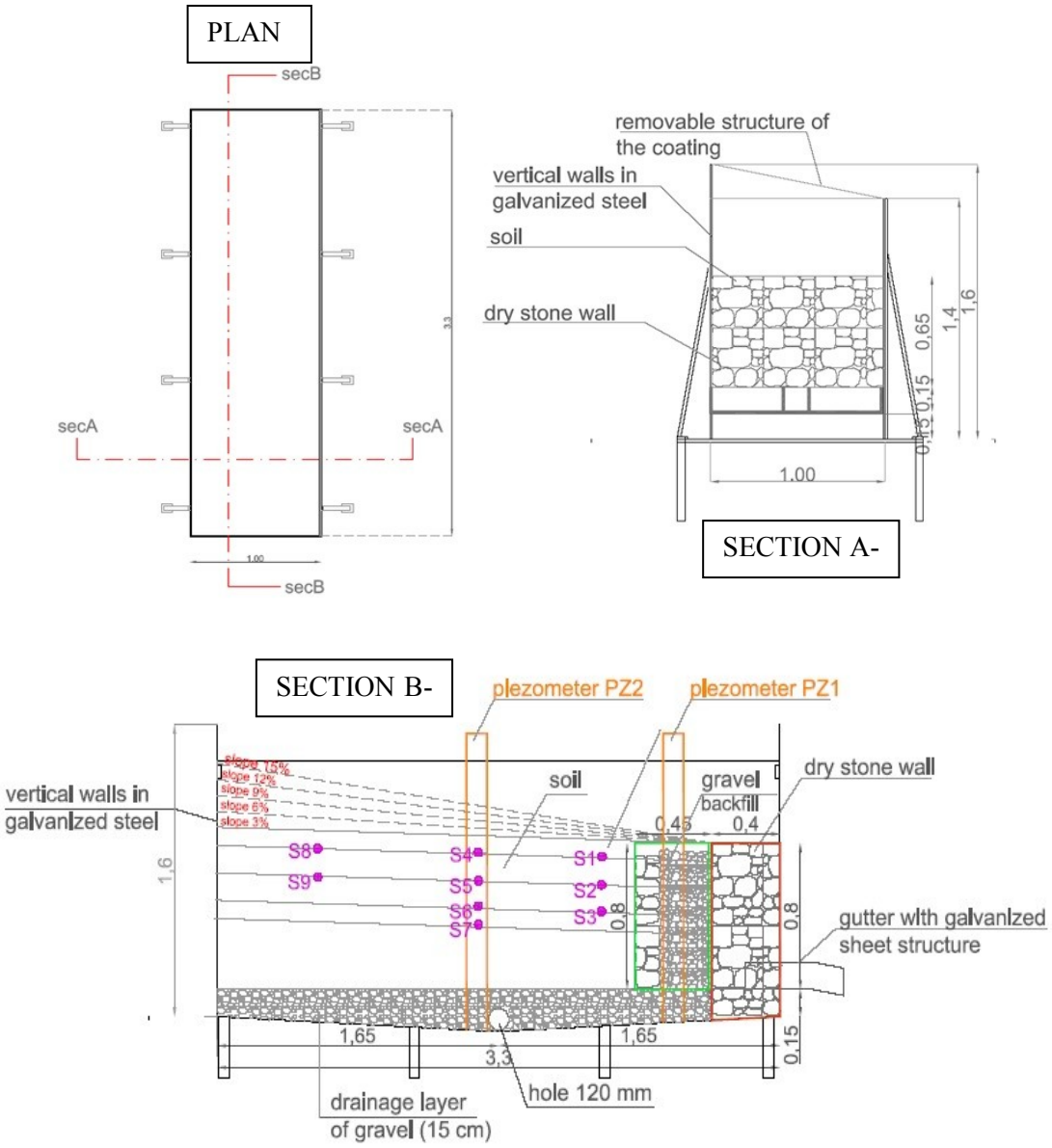

Figure 3.2. Scketch of the first configuration of the experimental model.

On the left side wall (looking downstream), close to the bottom, there is a hole of a 12 cm of diameter capable of emptying the water after the test. In order to protect the box by external meteorological condition a roof has been realized. In the frontal side of the box, before

starting to build the wall, a vertical panel of 15 cm (height) has been fixed to the bottom. Above this panel a particular artifact has been incorporated to the box by fixing it to the lateral panels.This artifact is a small flume, dedicated to the collection of the water exfiltrating from the wall (Figure 3.3); it is 1m wide , 40 cm long and has an height of 15 cm.

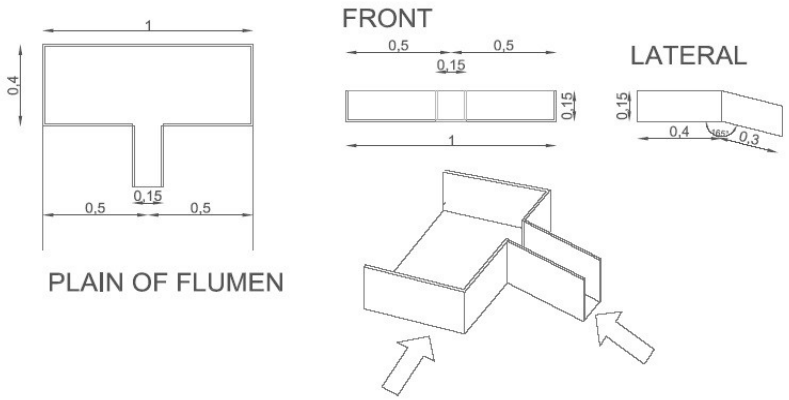

Figure 3.3. Outflow flume

The description of the first configuration of the plot has been reported in detail in Buzzanca (2016) . The box has been completed, transported and positioned at the end of April 2016. Immediately after the installation, some load tests were made by partially filling the box. The aim was to verify the sealing of the junctions. The tests have shown that the box leaked water in some point, therefore the joints were suitably siliconised. Subsequently, a traditional dry-stone wall 1m wide, 80 cm high and 20 cm deep was realized by the workers of the "Forest Service of the Verona Province" (Figure 3.4).

Figure 3.4. Realization of the dry wall

The stones were taken from the Veronese territory as well as the dimensions of the wall are the typical ones for the terraces in that area. The wall was built by placing superposed layers of stones stuck together starting from the bottom of the box. At the same time a drainage layer of gravel (15 cm height) has been laid on the bottom of the box. The stones have been manually cut to allow stable work. The joint between the lateral metal panels and the dry wall has been waterproofed by means of a special sheath.

Once the construction of the wall was finished a geotextile layer has been positioned above the gravel which are positioned in the bed of the box (Figure 3.5). The primary function of the geotextile consists in separating two soils with different textures or two different materials, without limiting the circulation of water between the two layers.

Figure 3.5. Positioning of the geotextile and backfilling of the wall face

A gravel backfill was built upstream the wall (Figure 3.5) and finally the box was filled with soil which was available in the farm. The soil was compacted layer by layer as showed in Figure 3.6. The completed terrace was then equipped with several instruments for monitoring the groundwater levels, the outflows and the water content in the soil.

Figure 3.6. the terraced slope completed

3.2.1.1 The inflow and outflow instruments

In order to simulate the overland flow on the hillslope behind the stone wall, an hydraulic system was created. A plastic tube connected by the hydraulic system of the farm brings

water to the system. Along the pipe a liter counter with a precision of 5% has been installed. The instrument shows on the display the effective flowing discharge expressed in liter per minutes (Figure 3.7). Thanks to this device, the quantity of water which enters in the system is known.

On the uphill part of the terrace, beside the wall, a spillway was set down, characterized by 1 m length and 10 cm of the internal width; the spillway is able to release the 'laminar' water flow on the terrain when totally filled. The instrument has a dedicated conection where the tube bringing water can be linked. When the flow is on, the water is released softly within the the spillway thanks to micro-holes in the last part of the tube. Once completely filled by water, the spillway is able to release a laminar sheet of water that flows along the terrace.

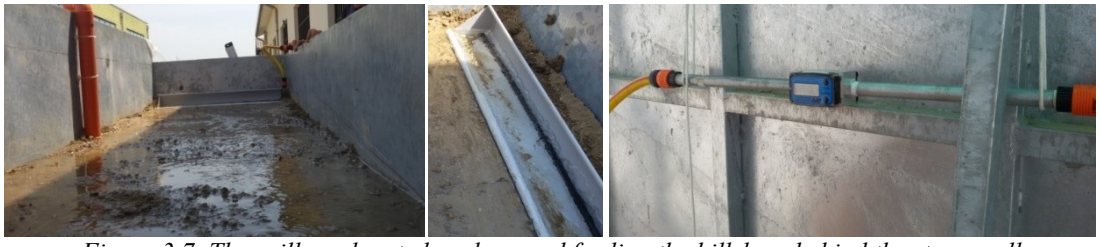

Figure 3.7. The spillway located upslope and feeding the hillslope behind the stone wall

At the outlet of the model it was necessary to set an instrument in order to know the discharge of the water coming out from the system. Below the metal drain pipe a scale has been positioned on which a big tank was present collecting the total runoff (Figure 3.8).

Figure 3.8. Outlet of the model where the water is collected and weighted by the scale

The box of 30 liters capacity has been positioned on the surface of the scale, and during the first experiments it has been manually empty (after collecting 10-15 liters). The scale is able

to record the difference in weight every second, in order to permit the calculation of the outflowing discharge.

3.2.1.2 The piezometers

After the construction of the wall, on one side of the box (on the tallest wall), the installation of the piezometer Dipper-PT has been carried out (Figure 3.9).

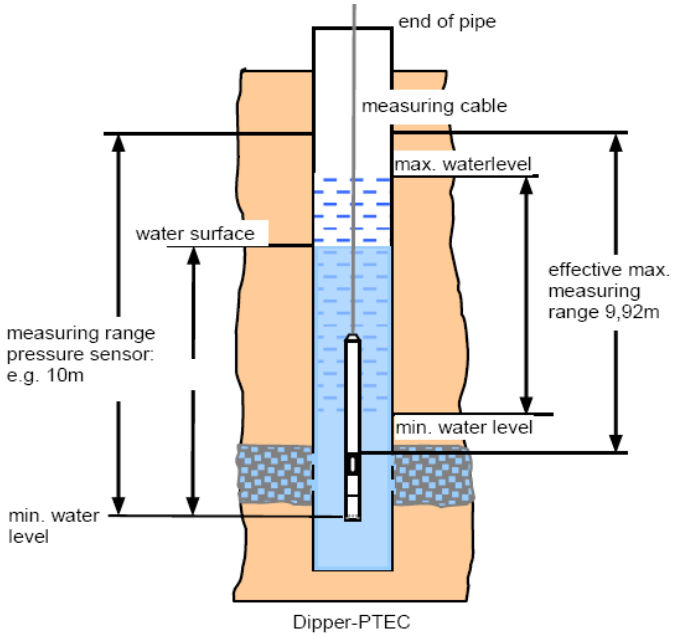

Figure 3.9. Schematic representation of the Dipper-PT piezometer (Seba Hydrometrie)

Two plastic tubes of 8 cm of diameter has been used to locate the instruments. The PVC tubes have been previously drilled (hole of 5 mm) and covered by a fabric that allows the entrance of the water only. Inside the tubes the two instruments have been fixed by screws in order to not permit their movement. Once set, the two tubes with the instruments inside have been installed inside the box in vertical position. The two piezometers were installed with an horizontal spacing of 120 cm; one instrument just upstream the wall and the other in the middle of the length of the container. These instruments are used for digital data recording of water level, water temperature and conductivity in groundwater and surface water. Thanks to the robust ceramics pressure measuring cell, it is possible to measure the water level above the probe (hydrostatic pressure). The combination of the referential pressure sensor and the special measuring cable with integrated air pressure compensation capillary compensates air pressure fluctuations. After the installation of the tubes containing the piezometers, the metal

box has been filled by 200 l of water. This procedure has been realized in order to set the value zero (corresponding with the base of the dry stone wall) at the instrument.
Software SEBAConfig is used for setup, maintenance and data read-out of SEBA data loggers and digital sensors. During the experiments the instruments were set to record the water level every minute by the software. After every tests the recorded data are downloaded on the PC. A file reporting the trend of the piezometer quota according to the time is so created.

3.2.1.3 The soil moisture sensors

In order to control the different moisture of the soil during the experiment, 9 sensors were installed in the terrain. The probes are the 5TM by Decagon Devices company (Figure 3.10). The 5TM are able to measure the water content, electrical conductivity, and temperature of soil. The 5TM sensor uses an electromagnetic field to measure the dielectric permittivity of the surrounding medium. The sensor supplies a 70 MHz oscillating wave to the sensor prongs that charges according to the dielectric of the material. The stored charge is proportional to soil dielectric and soil volumetric water content. The 5TM microprocessor measures the charge and outputs a value of dielectric permittivity from the sensor. The 5TM uses a surface-mounted thermistor to take temperature readings. The thermistor is underneath the sensor overmold, next to one of the prongs, and it reads the temperature of the prong surface. The 5TM outputs temperature in ◦C.

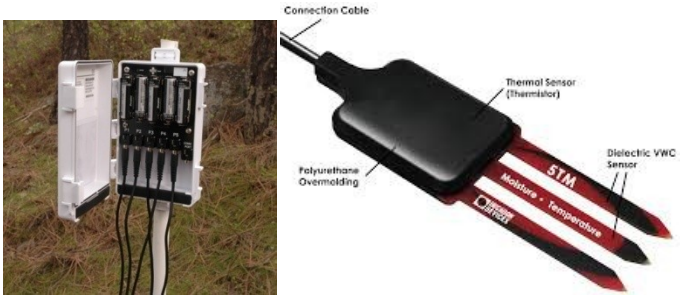

Figure 3.10. Soil moisture probe and data logger station

The 9 sensors are located in three different positions along the length of the slope, at 4 different depths (Figure 3.11). All the probes are situated in the middle of the width of the terrace (50 cm from the lateral walls) in places able to uniformely cover the length of the slope. The sensors 1, 2 and 3 are located in the section A at a distance of 1,10 m from the end of the wall. Sensors 4, 5, 6 and 7 are situated in the same position of the piezometer number 2 (1.75 m upstream of the wall), in the section B. The last three probes, number 8, 9 and 10

are located at a distance of 50 cm from the spillway in the section C. The depth of the sensors are respectively 10, 25, 40 and 50 cm.

The different sensors were installed with an inclination of 45°, that betters their measurement performance. For the installation of the probes a core drill and an instrument that helps to maintain the diagonal were used. The core was so extracted from the soil, the sensor was planted in the soil at the bottom of the hole and then the terrain was located again to cover the hole.

The 5TM sensor comes standard with a five-meter cable. Decagon designed the 5TM to work specifically with the Em50 data logger (five sensor ports). Next, it was necessary to configure the logger port for the 5TM and set the measurement interval. During the analysis, the instruments were set to record the water content and the temperature every minute.

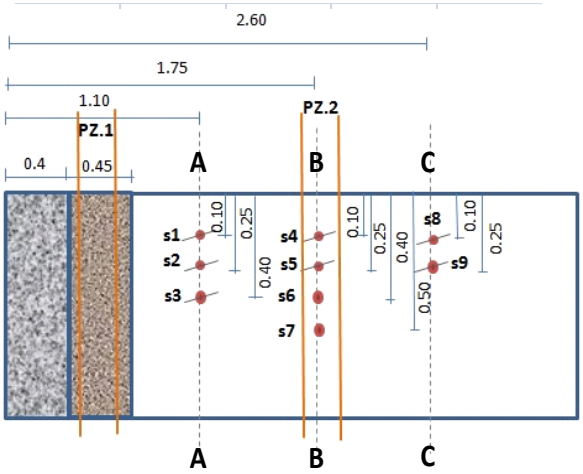

Figure 3.11. Section showing the disposition of the 5TM sensors in the model

The Figure 3.12 shows the calibration fit function between sensor response and real volumetric water content obtained for the type of soil which characterized the plot. The sampled soil has a porosity of 52.1%, an apparent density of 1.268 g/ cm^3 and a dry density of 2.65 g/cm^3. The calibration procedure allowed to find the following mathematical relation that must be used to correct the real observations:

$$real\ soil\ moisture = 0.074\ e^{5.228 \times soil\ moisture\ measured} \qquad (3.1)$$

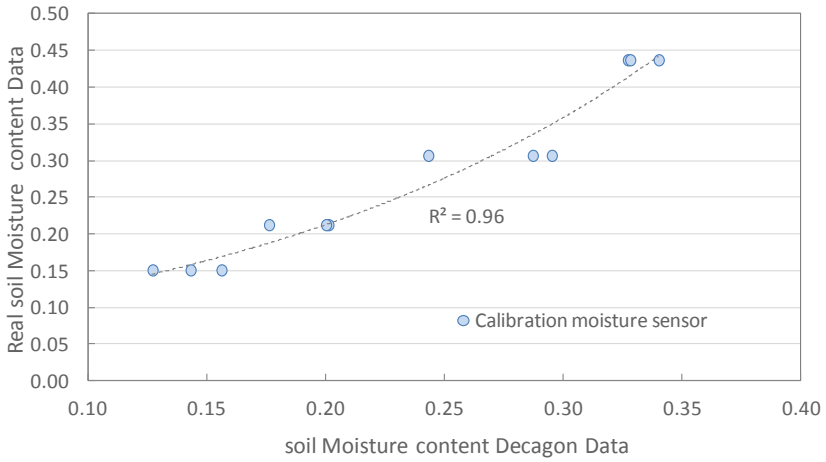

Figure 3.12. Soil moisture calibration curve

3.2.1.4 The characteristics of the terrain inside the model

A first layer of 15 cm of gravel was located at the bottom of the box to help the flow of the water toward the bottom valve. After that, about 9 cubic meter of soil were poured in the metal box. That soil was first worked and moved in order to obtain a soil representing a soil for agronomic purpose. In order to have a better knowledge on the characteristics of the soil, a particle size analysis has been carried out in the laboratory. Three different samples of the soil have been analyzed in order to obtain the subdivision in three different classes according to the size of the particle: sand, silt and the smallest one, clay. The samples gave back the different composition in percentage of the soil in the three categories defined (Table 3.1 and ternary diagram of Figure 3.13).

Sample Name	***Sand > 50 µm***	***Silt 2-50 µm***	***Clay < 2 µm***
1	23.33	58.92	17.74
2	23.98	57.65	18.37
3	23.04	58.46	18.50
Average	23.45	58.35	18.20

Table 3.1. Granulometric analysis of three samples of the soil used

By analyzing the average values of the three samples, the soil used for the experiment shows an high percentage of silt: 58,35%. The smallest particle, clay, corresponds to the 18,20% of the sample, while the sand is about 23,45% of the composition. According to the composition of the particle of the soil, the soil is characterized by different physical and hydraulic

performance and thanks to the ternary diagram, it is possible to identify and named the soil as a silt-loam soil.

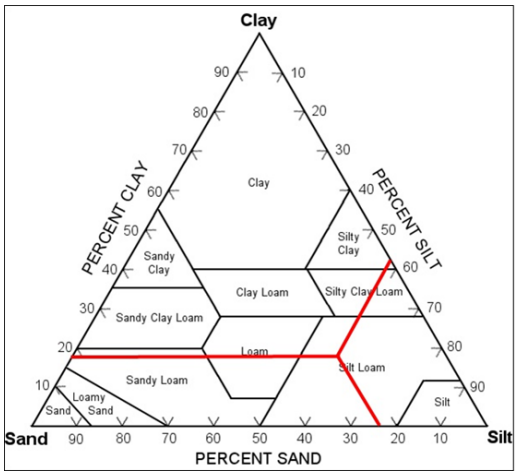

Figure 3.13. Ternary diagram related with the characteristics of the soil used

3.2.1.5 Model setting

For the different experiment the soil was prepared and set to a 3% of slope. After the installation and the setting of the instruments, the system needed to be evaluated according to the response on water releasing. On doing that, a series of different experiments have been carried on in order to test the response and the reliability of the model. Moreover, in this phase it was necessary to analyze the response of the soil at the release of the water by checking the compactness of the soil and the possible erosion. As previously stated, the soil has been tilled in order to simulate a soil for agronomic purpose and to obtain a homogeneity in terms of compaction and surface regularity (that is soil roughness). After the location in the box the soil has been slightly compacted to contain the the potential erosion.

The compaction process has been carry on by positioning small wooden board on the ground and loading it using the weight of the operator (about 70 Kg).

Another problem to take in account was related with the holes created by the installation of TDR sensors. On closing the holes created to locate the sensors, the soil was repositioned using a stick. Anyway this operation left some subsurface holes and a compactness of the soil different from the one already compacted.

The different tests to stabilize and evaluate the response of the system have been conducted simulating a maximum discharge (19.50 l/min) for 30-40 min. Thanks to these tests it was possible to observe the erosion of the soil and the creation of holes above the crown space.

During the first tests it was possible to figure out how the compaction process was not sufficient to reach the right density of the soil in order to avoid erosion and subsidence due to the weight of wet soil.

The first release of water has leaded to an impacting erosion which has brought to the excavation of a rill with a depth of about 5-6 cm. Moreover, the weight of the wet soil has leaded to a natural compaction characterized by a depth decrease of about 7-9 cm in correspondence of the 'irrigation' spillway (top of the hillslope).

In order to set again the model at the right slope (3%) it was necessary to refill the box with additional soil. This process has been done in two steps; after the first test, the model has been re-set on the right slope by replenishing about 120 kg of soil. Another test has further compacted the soil and so it has been necessary to refill the model with other 50 kg of material. After those processes, the soil has reached the right density in order to avoid problem of erosion and collapse.

It was possible to identify another process of the erosion due the water on the soil above and just behind the wall (Figure 3.14). In this area, the system is covered by a shallow layer of the soil. As already described, the wall is composed by stones with big diameter and that leads to the creation of big holes in the adiacent soil. This fact was able to lead to an excavation of the soil and create holes which reach a depth of about 10-12 cm.

The collapse of the soil with the consequent creation of the holes does not permit that the overland flow reaches the wall, leading to a total contribution of the liquid at the subsurface system. The problem developed was so fixed by refilling the holes with soil in order to obtain a more stable layer of soil above this delicate part of the system.

Figure 3.14. Section showing the holes just upstream of the wall in the first preparatory tests

3.2.2 *Second configuration of the plot*

The results with the first plot configuration described in the section 3.3 showed some problems expecially concerning with the surface probes geometrical distribution. Then, the final configuration of the plot (summer 2017) was improved by following the suggestions derived from the initial set of tests.

3.2.2.1 The different distribution of soil moisture sensors

A new distribution of the probes was assumed as described in Figure 3.15. In particular, the sensors were located in three different spots along the length of the slope, at 3 different depths. All the probes are situated in the middle of the width of the terrace (50 cm from the lateral walls) in places able to well cover the length of the slope. The sensors 1, 2 and 3 were located in the section A at a distance of 70 cm from the end of the wall. Sensors 4, 5, 6 were placed at same position of the piezometer number 2, in the section B. The last three probes, number 7, 8 and 9, were located at a distance of 70 cm from the spillway in the section C. The depth of the sensors were respectively 20, 40, and 55 cm. The probe installation has been already described above.

During all the experiments, the instruments were set to record the water content every minute.

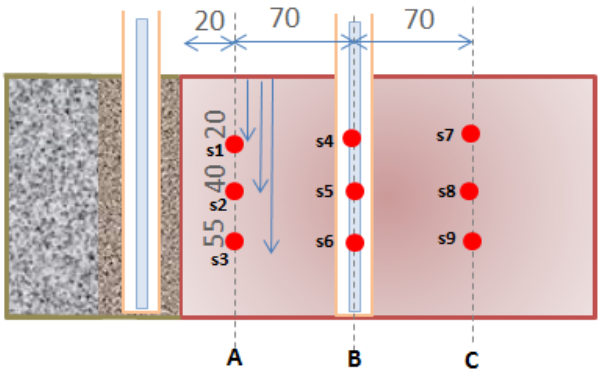

Figure 3.15. Planimetric distribution of soil moisture probes

For the new tests the first calibration of probes has been maintained since the ground horizon was made up of the same type of soil.

3.2.2.2 Integration of the outflow measurement system

In the first configuration of the plot only the total outflow of runoff was measured at the wall bottom. In order to measured the two components of runoff (overland flow and groundwater) two scales were used to measure the outflowing discharges (Figure 3.16).

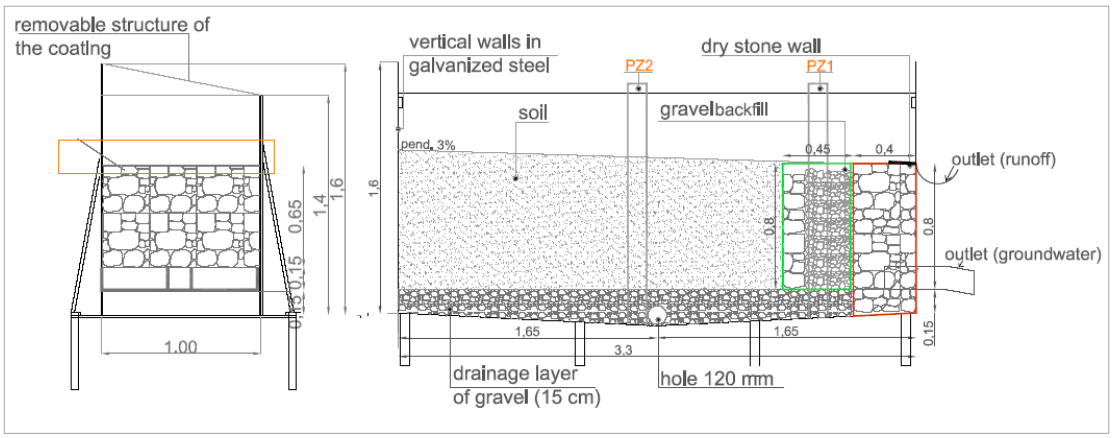

Figure 3.16. Perspective and section of the physical model(second configuration).

In details one scale measured the weight of the surface runoff, which is caught by means of a plastic sheath positioned just upstream the wall. The tube was positioned at the edge of the wall with screws attached to the metal frame of the box. In order to intercept all the surface outflow, a plastic towel was placed above the wall and fastened below the top ground (5 cm longitudinal extension and depth of 3 cm). One side of the towel is placed inside the tube. The water is conveyed into a 80 x 60 cm tank placed above a scale with a maximum capacity of 300 L.

The second scale (the same used in the first plot configuration) was positioned at the outlet of the model and measured the weight of the groundwater flow by means of a metal drainpipe, which collects the subsurface flow during the experiments. As the groundwater is limited in relation to the surface runoff, this scale is now able to wheigt the whole outflow during a test without the necessity of having to empty the tank. This procedure that was required in the first configuration produced spikes in measurement records that were corrected in the post-analysis of the data.

Both scales were initially setup with 1 second frequency acquisition; then, frequency acquisition was set to 2 seconds in order to get smother hydrograms.

3.2.2.3 Model setting in the second configuration

The tests with the second configuration covered different slope gradients: 3, 6 and 9%. In changing the slopes, all the soil moisture probes were removed and the soil was tilled again for a depth of 50 cm; then the instruments have been repositioned and subsequently all the checks and compaction procedures described in the section 3.2.1.5 have been followed.

It has been observed that by increasing the slopes the erosion increases and the check concerning the presence of holes it had to be done after each single test. In general it was difficult to start with a stable configuration and keeping it for several tests. The presence of soil cracks should also be verified, especially after periods of inoperability longer than 1 week.

The final tests realized in the 2017 summer were executed with the terrace cultivated with grass above the 9% slope (Figure 3.17). In particular the type of grass selected had the composition reported in the Table 3.2; this type of grass is characterized by a rapid growth.

Figure 3.17. The terraced slope covered with grass

Composition	***%***
Festuca rubra rubra (Rotschwingel ausl.) Gondolin	42.5
Bromus inermis (Wehrlose Trespe)	1
Festuca arundinacea (Hoher Schwingel-Rohrschwingel) Finelawn	14
Phleum pratense (Lieschgras-Timothe) Tiller	5.5
Lolium perenne (Engl. Raygras) Mathilde	15
Poa pratensis (Wiesenrispe) Balin	5
Dactylis glom. (Knaulgras) früh Amba	6.3
Festuca pratensis (Wiesenschwingel) Senu	2
Lotus corniculatus (Hornschotenklee) Bull	0.5

Composition	***%***
Trifolium hybridum (Schwedenklee) Aurora	1
Trifolium repens (Weissklee) Huia/Haifa	2
Trifolium pratense (Rotklee) Altaswede	1
Medicago sativa (Luzerne) Bella Campagnola	1
Onobrychis sativa (Esparsette) enthülst	1
Vicia sativa (Sommerwicken) Jose/Hanka	1
Vicia villosa (Winterwicken) Villana	1
Sanguisorba minor (Wiesenknopf)	0.1
Plantago lanceolata (Spitzwegerich)	0.1

Table 3.2. Composition of the grass

3.2.3 Data analysis

The model permits to carry out several analysis in different conditions. The instruments installed in the system permits an accurate study of the hydrological behavior that occurs in the terrace during forced flooding event. In particular, the analysis of data focused on:

- Variation of the soil moisture during different stages of the experiment;
- Hydrological response of the system to different events;
- Estimation of soil erosion;
- Determination of a local Curve Number related with the terrace unit under analysis.

The experiments have been conducted with different terrain slopes (3, 6, 9%) and different values and duration of input discharges.

The different input discharges applied were related to the capacity of the hydraulic system of the farm; however they permit to test the model within a reliable ranges of input flow rates.Therefore, for the experiments three different constant input discharges have been used:

- MAXIMUM VALUE; this discharge is equal to the maximum value provided by water-line when the tap is totally open. This value is about 19.5 l/min;
- MEDIUM VALUE of about 12 l/min;
- MINIMUM VALUE; this value is about 5 l/min; this discharge represents the minimum value for the experiments. It has been thought to represents one fourth of the maximum discharge.

The values reported above are indicative of an average value of the different discharges since it was complicated to obtain exactly the same value for every test. During the experiments the input discharge was affected by two particular problems. The first issue was related with the

right opening of the tap in order to obtain the selected discharge. This problem was related when it was necessary to set the discharge at the medium and minimum values, since at the maximum value the tap was totally open. The second factor was related to the different pressure of the aqueduct. It has been noticed that during the experiments the value of the input discharge was subjected to small differences during time. This problem was related to the hydraulic system of the farm but anyway the differences have never been greater than ± 0,20 l/min. Therefore, for the analysis has been taken in account the average value of the discharge, anyway computing precisely the total water volume distributed in each single experiment (real flooding hydrograph).

The study of the behavior of the water on the terrace can be important for different scopes. In agriculture, knowing the water infiltrated permit to know the available water content in the soil and so to avoid to reach the wilting point. Moreover, splitting the water between the surface and subsurface components is important in order to protect the terrace system from damages.

Thanks to devices installed on the model, it was possible to analyze the behavior of a terrace affected by a release of water upslope, identifying the infiltrated water, the surface runoff and relative components at the outlet discharge. Moreover, the time of the hydrological response of the system has been analyzed.

3.2.3.1 The soil water content analysis

The following procedure has been carried on to analyze the recorded data:

- Analysis of the data recorded by every sensors, to be able to recognize the trend of the change in volumetric water content (VWC);
- Analysis of the change in VWC from the beginning to the end of the experiment;
- Computation of an overall value of VWC for the soil and analysis of the change during the experiments.

The study to obtain an overall value of the volumetric water content has been applied by considering the data recorded by the all the probes. To obtain an overall value of the VWC in the soil, a weighted average was calculated according to the different volume of interest of each sensor. Thus, the overall VWC is calculated with the formula:

$$VWC = \frac{\sum V_i * VWC_i}{V} \qquad (3.2)$$

where V_i is the volume of interest of a single sensor, V is the total volume considered (corresponding to 50 cm depth of soil) and VWC_i are described as it follow. For every experiment three overall values are calculated:

- *VWC1*, Volumetric water content 1: it is the overall volumetric water content obtained by the data recorded at the beginning of the experiment;
- *VWC2*, volumetric water content 2: the overall volumetric water content at the closure of the input discharge;
- *VWC3*, volumetric water content 3: it is the overall volumetric water content obtained by the data recorded from the TDR sensors after the end of the experiment.

Each volume of interest has been extracted through a geometric subdivision of the total volume V in equivalent areas associated to each sensors.

3.2.3.2 Discharge measurements and hydrological analysis

3.2.3.2.1 Filtering row data

The hydrographs of the outflow discharges from the wall (runoff and groundwater) were obtained indirectly from the analysis of the recorded cumulative weight curves relative to the volume of water fallen into the buckets located at the bottom of the wall. In detail, the mean discharge in a fixed period of time was obtained from the difference of two consecutive cumulative weights subdivided by the corresponding time interval. For all tests the computational time interval equal to 20 seconds was selected since it has been found – after several verifications - that the flow rates corresponding to lower time intervals were not able to filter the variations of the real intermittent flow response, which is out of the practical interest for the time scale of our hydrological analysis and subsequent modeling.

3.2.3.2.2 Inflow and outflow hydrographs and characteristic times

The following analysis of the time of response of the terrace-unit model has been carried out (Figure 3.18). The figure is representing the hydrological behavior of the terrace during an experiment. The blue line consists of the groundwater passing through the outlet (wall bottom), meanwhile the grey line is representative of the surface runoff just before the jump. In general the hydrographs of surface runoff and groundwater have a trapezoidal shape. According to these pattern, the hydrological analysis will be performed considering the time reported in the figure defined as:

- *T1*, time from the start of the test to the time when runoff (surface/groundwater) reaching the wall (the top of the wall in case of surface runoff and the base of the wall in case of groundwater);
- *T2*, time from the start of the test to the time when the surface runoff reaches the first relative maximum; after this time the slope of the flow curve shows a great decrease.
- *T3*, time from the start of the experiment to the time when the surface runoff reaches the second relative maximum at the begging of the depletion curve;
- *T4*, time from the start of the experiment to the time when the depletion of the outlet discharge is completed;

The same definitions can be applied to the groundwater flow, with the difference that usually the times *T2* and *T3* tend to coincide.

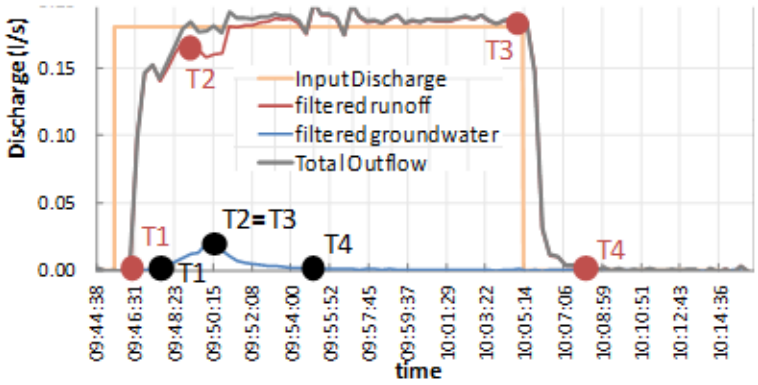

Figure 3.18. Representation of the hydrological response of the model(red: runoff; blue: groundwater)

3.2.3.2.3 Identifying routing times of runoff along the wall

The measured surface runoff is relative to the upper end of the wall. In order to calculate the surface runoff hydrograph at the bottom of the wall the relation between the discharges and the corresponding propagation times along the wall has been studied (Figure 3.19).

In detail, the spillway of input discharges has been moved from its original position up to 30 cm upstream the vertical drop (face of the wall). Then several tests have been executed with different discharges and the time needed to reach the bottom of the wall has been recorded. In this way it was possible to find a mathematical function which relates the routing times of the water along the downstream wall face with discharges.

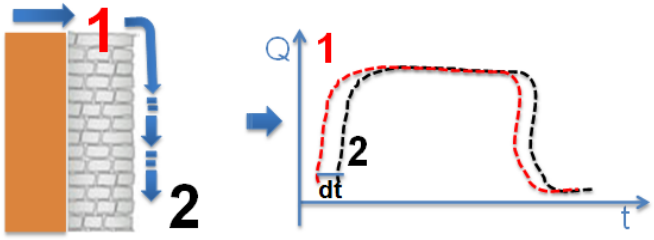

Figure 3.19. Representation of the routing time of runoff along the wall

3.2.3.2.4 Computation of the Curve Number

An important part of the analysis of the system is related with the calculation of a specific curve number representing a terraced hillslope for the specific characteristic of the soil used in the model. The curve number is a parameter for the calculation of the surface runoff with the SCS method (U.S SCS, 1986) (see chapter 2).

Since the terrace system is a particular structure that influences the hydrological behaviour, the need of calculation a specific curve number has raised. In particular, the dry-stone walls are a breaklines across the hillslope and the contribution of the groundwater component can flow out (e.g. exfiltration in the lowest part of the face) and influence the amount of the total surface runoff. Therefore, on calculating the specific curve number for a terraced hillslope, the total amount of the outlet discharge is considered both for high/low initial degree of soil saturation. In order to obtain a comparison with the the *CN* values of the literatures, even a relative curve number associated only to hillslope-runoff has been computed. The computation of the curve number becomes possible since the total discharge (runoff + groundwater) produced is known and it is recorded at the outlet of the model.

Therefore, the **traditional *CN*** is obtained via the manipulated equation for runoff computation that it results as follow:

$$CN = \frac{1}{\left[\left(\frac{Smax}{254}\right)+1\right]^{*1/100}} = \frac{1}{\left[\left(\frac{\frac{P^2}{R_S}-P}{254}\right)+1\right]^{*1/100}} \qquad (3.3)$$

where P is the total volume in input to the system and R_s is the total surface runoff volume and Smax is the potential maximum retention at the start.

whereas the new **terrace area *CN*$_{ta}$** is given by:

$$CN_{ta} = \frac{1}{\left[\left(\frac{Smax}{254}\right)+1\right]^{*1/100}} = \frac{1}{\left[\left(\frac{\frac{P^2}{R_S+R_{gw}}-P}{254}\right)+1\right]^{*1/100}} \quad (3.4)$$

where R_{gw} is is the total groundwater volume.

To carry on the analysis three assumption has been defined:

- The component of the surface runoff R_s and R_{gw} are equal to the cumulated values at the end of experiments (water volumes converted in millimiters of water);
- The initial abstraction (I_a) due to interception of the vegetation and deformation in the soil is equal to zero;
- The total amount of input water surrogates the total precipitation P.

In the case of "initial high degree of saturation" the equation 3.3 and 3.4 rapresent the "wet antecedent moisture content AMCIII". In the case of "initial low degree of saturation" the CN rapresents the "AMCII" conditions. The computation of the curve number has been applied according to the two different methods for all the experiments.

3.3 Results of measurements

3.3.1 Results for the first plot configuration

From September 2016 the tests reported in Table 3.3 were performed based on the first plot configuration. The 3% slope was flooded with three different valuse of discharge (5, 12, 19.5 l/min). Moreover, for each test, a replication of the experiment has been made trying to maintain the same characteristics (piezometer quota and soil moisture) of the first test.

Therefore, a total of 12 experiments has been performed according to the following scheme.

The tests listed in the Table 3.3 are a subset of all the tests performed and in particular those that have passed the setting procedure described in the paragraph 3.2.1.5. All the selected experiments are characterized by a partly satured soil.

The experiments characterized by "high initial degre of saturation" conditions have been conducted by waiting for a maximum of 1 day from the previous test and they are characterized by a initial degree of saturation grater than 75% (range: 75% - 82%) coupled with maximum piezometric levels (water table at the reference quota of 18 cm).

Test n°	*Date*	*Q input (l/min)*	*Flooding time (minutes)*	*Initial degree of saturation*	*Replicated test n°*
7	13/09/2016	20.253	10	High	
8	14/09/2016	12.810	7	Low	
9	14/09/2016	4.990	7	High	
10	19/09/2016	5.323	16	Low	
11	22/09/2016	11.457	7	Low	8
13	12/10/2016	20.253	10	High	7
14	18/10/2016	19.469	23	Low	
15	18/10/2016	5.735	7	High	9
16	26/10/2016	5.299	15	Low	10
17	26/10/2016	11.602	7	High	
18	26/10/2016	12.122	7	High	17
19	02/11/2016	20.179	23	Low	14

Table 3.3. Scheme of the 12 experiments carried out with the first plot configuration

To carry out the experiments under "low initial degre of saturation" with values lower than 75% (72% - 74%) the following assumptions have been taken. For the moisture of the soil, a pause lasting 7 days in natural dry conditions was the standard. Moreover, the piezometer quota needed to be lower than 18 cm in the first test and its replication; in this case the level of the groundwater could be adjusted by the releasing the water from the bottom outlet of the model.

3.3.1.1 Soil moisture analysis

From the analysis of the volumetric water content carried on for the different discharge applied, it is possible to identify a similar behavior in every tests. In every of the six experiments applied, with "low initial degree of saturation", it is possible to identify a precise pattern.

Sensor 1 and 8 are affected by sudden negative shifts due to measurement errors but they show always a general negative trend. The two sensors characterized the most superficial sensors for the section A and C; they show for every analysis negative tendency to a reduction of the volumetric water content. This behavior it is in countertrend of what happens to the other sensors installed in the same section: deepest sensors installed in the same sector shows an increasing tendency.

Moreover the section in the middle shows an important increase of humidity in the sensor number 4 and 5 representing the more superficial probes. In one case the variation for this probe has reached the value of 7.50%. By the way, in this section the difference from the deepest sensors situated at 40 and 50 cm of depth is quite important.

It's worth noting how the deepest sensors of this section, the number 7, does not show important change during the test; the greatest change is equal to 0.55%.

Tests number 19 is representative of experiments with a maximum discharge on "near saturated soil" (Figure 3.20). The section A shows a parallel increase of the sensors 2 and 3 but at the same time a decreasing of the more superficial sensor, the number 1.

In the middle sector the superficial sensors number 4 and 5 shows a similar trend with increasing values water content. By the way, sensor 4 shows a collapse after the end of the analysis as in the previous experiment. Sensor number 6 shows a bizarre behavior with an initial decreasing followed by an increasing, a stable value for three minutes and a successive collapse. After that behavior the data recorded shows a constant little increment during the test. Sensor number 7 after an initial increasing shows no alteration. In the section C, different behavior characterizes the two sensors. An important initial increasing followed by a sharp constant increasing for the sensor 9. Meanwhile the sensor 8 shows a collapse of almost 0.50% at the beginning until it reaches stable conditions.

The analysis of all the tests show similar trends. In particuar it was possible to observe that;

- less deep sensors show abnormal behaviors. The soil is subject to the formation of cracks and the water is channeled into preferential ways and can jump especially the superficial probes
- other abnormal behavior in the rest of the probes may be due to the creation of preferential routes caused by drilling with the drill during the sensors installation.

These observations have been taken into account to improve the distribution of sensors and their installation procedure in the second configuration as described in the section 3.2.2.

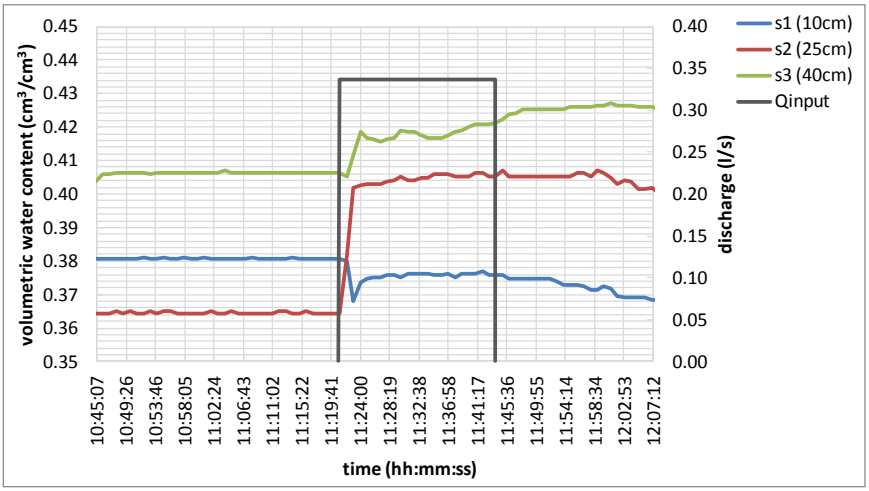

a)

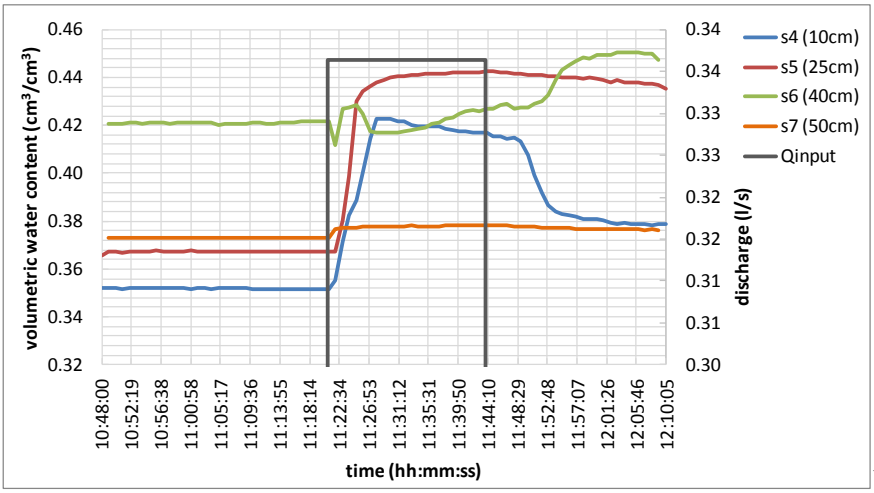

b)

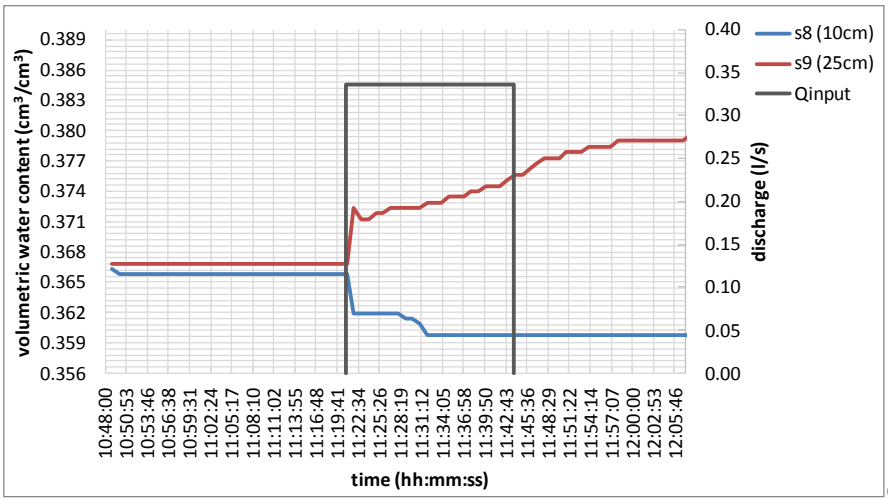

c)

Figure 3.20. Trend of the volumetric water content during the experiment 19 a) section A close to the wall; b) section B in the middle; C) section C the farest from the wall

OVERALL DATA OF VWC

In order to obtain an overall view of the trend of the volumetric water content (VWC) it was necessary to calculate an average volumetric water content representative for all the soil in the model.

The overall volumetric water content for the two experiments characterized by the maximum discharge is represented in the Figure 3.21. Test number 19 is characterized by lower initial VWC rather test number 14, but it shows an higher capacity of absorbing water; at the closing time test 19 has increased its humidity 3.33%, meanwhile test 14 just 1.04%. Even the capacity of getting dryer is expanded in test 19; after the closing time we can calculate a decrease of 0.64% until the stop of data recording rather than 0.156% of test 14.

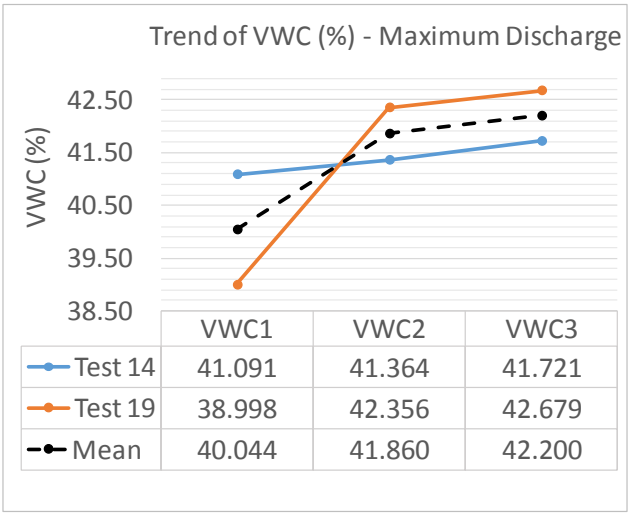

Figure 3.21. Trend of the overall Volumetric Water Content (VWC) for the two test characterized by maximum discharge: test 14 and 19

The overall volumetric water content for the two experiments characterized by the maximum discharge is represented in the Figure 3.22. Test number 19 is characterized by lower initial *VWC* rather test number 14, but it shows an higher capacity of absorbing water; at the closing time test 19 has increased its humidity 3.33%, meanwhile test 14 just 1.04%.

Even the capacity of getting dryer is expanded in test 19; after the closing time we can calculate a decrease of 0.64% until the stop of data recording rather than 0.156% of test 14.

The overall volumetric water content for the two experiments characterized by the maximum discharge is represented in the Figure 3.22. Test number 19 is characterized by lower initial *VWC* rather test number 14, but it shows an higher capacity of absorbing water; at the closing time test 19 has increased its humidity 3.33%, meanwhile test 14 just 1.04%.

Even the capacity of getting dryer is expanded in test 19; after the closing time we can calculate a decrease of 0.64% until the stop of data recording rather than 0.156% of test 14.

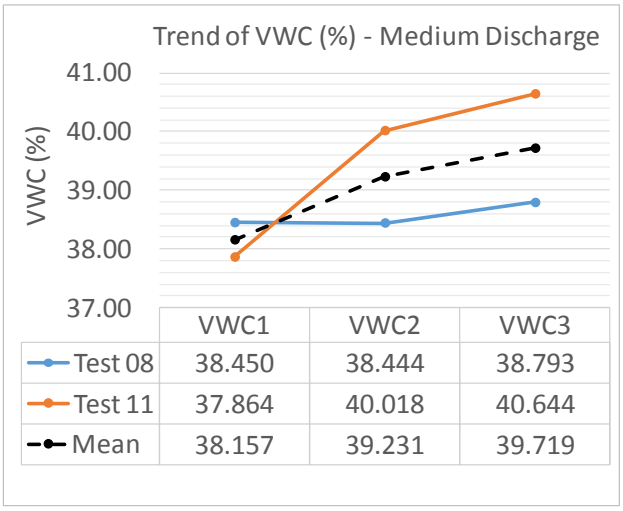

	VWC1	VWC2	VWC3
Test 08	38.450	38.444	38.793
Test 11	37.864	40.018	40.644
Mean	38.157	39.231	39.719

Figure 3.22.Trend of the overall VWC for the two test characterized by medium discharge: test 8 and 11

The experiments for the medium discharge shows a little decrease of *VWC* in test 8 meanwhile an important increase occurs for test 11, respectively 1.75% for test 11 and -0.06% for test number 8. After the closing time an increase of humidity is occurring with the same trend for both the experiments: +0.305% for test 11 and +0.258% for the experiment number 8.

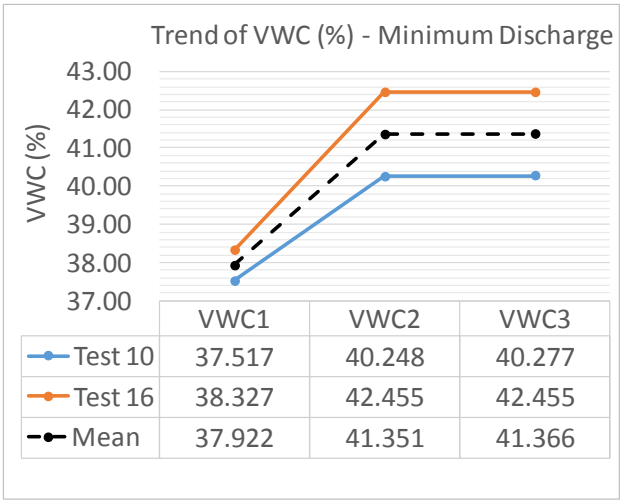

	VWC1	VWC2	VWC3
Test 10	37.517	40.248	40.277
Test 16	38.327	42.455	42.455
Mean	37.922	41.351	41.366

Figure 3.23.Trend of the overall VWC for the two test characterized by minium discharge: test 10 and 16

For the analysis carried out with the minimum discharge, the initial *VWC* is quite similar: 37.28% and 37.57%. By the way test 16 is subjected to a greater increase of moisture in the soil: 3.34% respect of 1.46% for test number 10.

After the closing time, the volumetric water constant continues to increase in the test 10 but a decrease occurs in test 16.

3.3.1.2 Hydrological analysis

For each experiment the corresponding runoff hydrograph was obtained by filtering the raw measures as described in the section 3.2.3.2.1. An example of the visualization of the hydrological response is reported in Figure 3.24. The tests number 19 is representing the experiments with a maximum discharge on "low initial degree of saturation". The experiment lasted 23 minutes for an average input discharge of 19.30 l/minute. The Figure 3.24 shows the filter hydrograpgh of total runoff, the time series of input discharges and piezometric levels.

The total runoff reaches the feet of the wall after 1'27", the discharge increases very fast untill to reach a quite constant value of 0.30 l/s. The runoff start to descrease at the end of forced flooding and goes to zero in 2'25".

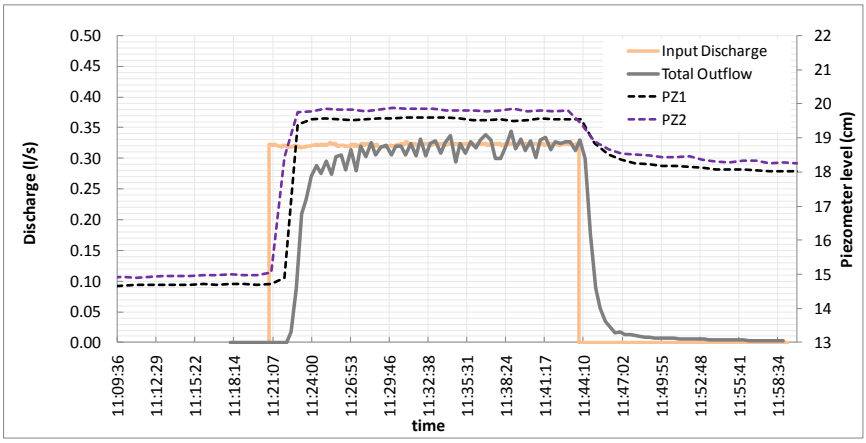

Figure 3.24. Hydrological response for test 19 by the data recorded from the instruments

The piezometric data analysis indicates that in average the water is stored in the bottom of the box for a 3 cm depth (piezometric levels from 15 to 18 cm). Then the groundwater flow starts to exit from the base of the wall; the piezometric level ramains constant until the end of the forced flood wich corresponds in a constant groundwater flow. After the end of the input discharge the piezometric level and the corresponding flow start to decrease.

The Table 3.4 reports the results concerning the verification of the water balance between input and output for all the experimental tests. Each test is characterized by a water volume in

input, a volume in output and a water volume stored in the bottom of the plot; all these volumes were obtained from the recorded flow measurements.

Test n°	***Vol tot inp*** *(l)*	***Vol tot output*** *(l)*	***VWC1*** *(%)*	***VWC2*** *(%)*	***DH*** *(cm)*	***Bottom water storage*** *(l)*	***Terrace water storage*** *(l)*	***Water Balance error***	
								(l)	*%*
7	192.92	170.00	40.73	40.93	-0.51	6.11	2.50	14.32	**7.4**
8	89.66	69.32	38.45	38.44	-2.31	27.40	0.00	-7.06	**-7.9**
9	39.89	32.95	38.96	39.32	0.00	0.00	4.46	2.48	**6.2**
10	85.18	42.41	37.52	40.25	-3.70	43.97	34.08	-35.28	-41.4
11	80.20	49.61	37.86	40.02	-3.20	38.04	26.88	-34.33	-42.8
13	202.53	192.60	39.89	40.57	-0.71	8.47	8.42	-6.96	**-3.4**
14	447.79	405.87	41.09	41.36	-4.40	52.24	3.41	-13.72	**-3.1**
15	40.15	34.45	41.74	41.74	0.00	0.00	0.00	5.70	**14.2**
16	79.49	44.08	38.33	42.46	-3.62	43.02	51.52	-59.12	-74.4
17	81.22	73.40	42.38	42.43	0.00	0.00	0.54	7.28	**9.0**
18	84.86	82.13	42.57	42.50	-0.51	6.11	0.00	-3.38	**-4.0**
19	443.95	374.44	39.00	42.36	-3.84	45.62	41.91	-18.02	**-4.1**

Table 3.4. Water balance from measurement for the first configuration

The volume of water stored in the bottom of the plot is obtained from the following equation:

$$BottomWaterStorage = dH * A * n_g \qquad (3.5)$$

where *dH* is the difference between the initial groundwater level and the threshold level that triggers the groundwater flow, *A* is the horizzontal area of the plot, n_g is the porosity of gravel in the bottom (36%).

The volume of water stored in the terrace is obtained from the following equation:

$$TerraceWaterStorage = (VWC2 - VWC1) * A * H * n_s \qquad (3.6)$$

where *H* is the high of the terrace (0.80 m), n_s is the porosity of the terrace soil (52%), VWC3 and VWC1 are the volumetric water content at the end and at the beginning of the experiment respectively.

The water balance error apply to each test is then given by:

$$WaterBalanceError = VtotInp - VtotOut - BottomWaterStorage - TerraceWaterStorage \qquad (3.7)$$

The errors in the water balance calculation can be related to error in the volumes estimation. In particular:

- the estimation of input volume can be affected by an error in the range +- 5%;
- the estimation of the volume in output could be negative affected by the fact that part of the water was not measured since some losses occured during the experiment. These losses may occurred at the moment in which a filled bucket was changed with another one empthy. Or they may be due to sealing problems of the bottom of the plot that actuallt were observed in particular for greater input discharges or long irrigation periods.
- the volume of water stored in the bottom of the plot is very influenced by the correct estimation of the threshold level that triggers the groundwater flow. This level can vary at each test significantly as it dependes strongly on the current distribution of the gravel and soil material upstream of the otflow artifact which can hinder the release of water. Moreover the estimation of this storage volume can be affected by the porosity value associated to the gravel;
- the volume of water stored in the terrace is influenced by the estimation of the overall water content and by the porosity value associated to the terrace soil.

The Table 3.4 shows the error values in terms of volumes (liters) and percentage (ratio between the error and volume in input). It is possible to notice that the 75% of the tests are associated to an error in the range +-20% (errors highlighted in bold in Table 3.4). The remaining 25% of the tests show errors between -75% and -40%. These tests (n°10, 11 and 16) are associated at the same time with the biggest values of the bottom water storage and the terrace water storage. It is possible that one of these two component has been overestimated due to the problems described above.

3.3.1.3 Computation of the specific Curve Number

The computation of the **terrace area** $\boldsymbol{CN_{ta}}$ has been carried for all the experiments using the equation 3.4.

The table Table 3.5 represents the computation of the special $\boldsymbol{CN_{ta}}$ for the six test characterized by “low initial degree of saturation”. The value of the $\boldsymbol{CN_{ta}}$ ranges from 89.95 (test 10) to 96.85 (test 8) with an average value equal to 93.70.

The Table 3.6 show the calculation of $\boldsymbol{CN_{ta}}$ for the the six experiments characterized by “high initial degree of saturation”. In this case the value of $\boldsymbol{CN_{ta}}$ ranges from 97.12 (test 13) to 99.01 (test 18) with an average value equal to 98.35. Hence, as aspected, the average $\boldsymbol{CN_{ta}}$ in

case of "high initial degree of saturation" is greater than the one corresponding to "low initial degree of saturation".

These results show that the global hydrological response of the plot is very important for both the soil moisture initial conditions. In order to understand better the impact of the various runoff components in the globale hydrological response, it has emerged the need to separate the surface runoff from the groundwater outflow. This activity has been the subject of research conducted with the second configuration of the plot.

Number test	***Total Vol Inp.*** *(l)*	***Total Vol Inp.*** *(mm)*	***Total Vol Out.*** *(l)*	***Total Vol Out.*** *(mm)*	S_{max} *(mm)*	***CN****
19	443.950	147.983	374.440	124.813	27.471	90.240
14	447.790	149.263	405.870	135.290	15.417	94.278
8	89.660	29.887	66.130	22.043	10.634	95.982
11	80.200	26.733	47.270	15.757	18.623	93.169
10	85.180	28.393	40.350	13.450	31.546	88.952
16	79.490	26.497	42.000	14.000	23.651	91.482

Table 3.5. Computation of the "terrace area CN" for low initial degree of saturation
**As reported in 3.2.3.3., in the case of "initial low degree of saturation" the calculated CN rapresents the "AMCII" conditions.*

Number test	***Total Vol Inp.*** *(l)*	***Total Vol Inp.*** *(mm)*	***Total Vol Out.*** *(l)*	***Total Vol Out.*** *(mm)*	S_{max} *(mm)*	***CN*****
7	192.920	64.307	180.140	60.047	4.562	98.236
13	202.530	67.510	182.220	60.740	7.525	97.123
17	81.220	27.073	69.810	23.270	4.425	98.288
18	84.860	28.287	78.170	26.057	2.421	99.056
9	39.890	13.297	31.330	10.443	3.633	98.590
15	40.150	13.383	32.750	10.917	3.024	98.823

Table 3.6. Computation of the "terrace area CN" for high initial degree of saturation.
***As reported in 3.2.3.3. for the case characterized by "initial high degree of saturation" the equation 3.4 rapresents the "wet antecedent moisture content AMCIII".*

3.3.2 Results for the second plot configuration

From June 2017 the tests reported in Table 3.7 were performed. As for the first configuration all the tests deal with partly satured soil. In this case just 2 experiments where characterized by "very low initial degree of saturation" with values lower than 60% (59% for test n°1; 57% for test n°15). To conduct these 2 experiments the following conditions have been taken: 1)

to have stopped the tests for several days since the previous test; 2) presence of very dry atmospheric conditions; moreover, the piezometer quota needed to be lower than 18 cm;

Test n°	***Date***	***Slope*** *(%)*	***Q input*** *(l/min)*	***Flooding time*** *(hour)*	***Soil***	**Initial degre of saturation**
1	28/05/2017	3%	4.91	1.229	Bare soil	Low
2	07/06/2017	3%	5.11	0.126	Bare soil	High
3	07/06/2017	3%	5.61	0.129	Bare soil	High
4	07/06/2017	3%	19.81	0.167	Bare soil	High
5	08/06/2017	3%	8.25	0.121	Bare soil	High
6	08/06/2017	3%	12.38	0.124	Bare soil	High
7	08/06/2017	3%	18.83	0.167	Bare soil	High
8	20/06/2017	6%	5.51	0.776	Bare soil	High
9	21/06/2017	6%	10.82	0.328	Bare soil	High
10	22/06/2017	6%	18.70	0.206	Bare soil	High
11	29/06/2017	6%	5.65	0.716	Bare soil	High
12	03/07/2017	6%	10.61	0.329	Bare soil	High
13	04/07/2017	6%	18.96	0.206	Bare soil	High
14	06/07/2017	6%	19.22	0.218	Bare soil	High
15	11/07/2017	9%	5.78	0.871	Bare soil	Low
16	12/07/2017	9%	5.17	0.637	Bare soil	High
17	12/07/2017	9%	10.36	0.317	Bare soil	High
18	13/07/2017	9%	18.88	0.208	Bare soil	High
19	18/07/2017	9%	10.60	0.344	Bare soil	High
20	19/07/2017	9%	5.17	0.699	Bare soil	High
21	20/07/2017	9%	19.16	0.207	Bare soil	High
22	18/08/2017	9%	20.29	0.628	Grass cover	High
24	18/08/2017	9%	19.30	0.168	Grass cover	High

Table 3.7. List of tests for the second plot configuration

The experiments characterized by "high initial degre of saturation" conditions have been conducted by waiting for a maximum of 1 day from the previous test and they are characterized by a initial degree of saturation grater than 60% (range: 61% - 76%) coupled with maximum piezometric levels (water table close to the reference quota of 18 cm).

The tests 1-7 were executed in a 3% slope, the tests 8-14 in a 6% slope and the tests 15-24 in a 9% slope. For each slope three discharges were used as input to the terrace: a Minimum Input Discharge (around 5.5 l/min for irrigation period in a range of 0.1-0.8 hours); a Mean

Input Discharge (around 12 l/min for irrigation period in a range of 0.12-0.35 hours); a Maximum Input Discharge (around 18 l/min for irrigation period in a range of 0.12-0.2 hours). The tests 22-24 where conducted over a 9% slope cultivated with grass.
It is possible to note from the list that each test characterized by an input discharge and slope has been replicated to have more concrete results.

3.3.2.1 Volumetric water content analysis

After each test the data collected from all the soil moisture sensors were downloaded and elaborated. A typical behavior of soil moisture during a forced irrigation test is showed in Figure 3.25 for the test 9. The sensors positioned close to the wall in section A and in middle of the terrace in section B seem not reacting so much during the tests independently of their depth. Instead, the sensors located close to the upstream spillway in section C show important increases of soil moistures in particular at the mean depth of 40 cm from the ground level (sensor 8). This behavior could be caused by an important infiltration process focused in the upstream part of the terrace.
The Figure 3.26 shows the soil moisture results for all the sensors in case of a mean input discharge in the 6% slope (test 9 and 12). The results are reported in terms of percentage change in *VWC* from the beginning to the end of the experiment. Moreover for each sensor the initial soil moisture is reported. The graph confirms the behavior showed in Figure 3.26 with the sensors located close to the spillway reacting more than the other.
The new setup of sensors used in this configuration seems to give a better representation of the soil moisture trends. In particular, the anomalies characterizing the surface probes of the first setting are no longer present.

OVERALL DATA OF VWC

For each test a overall volumetric water content has been calculated at the beginning of the experiment (*VWC1*), at the closure of the input discharge (*VWC2*) and at the last data recorded from the TDR sensors 1 hour after the end of the forced flooding (*VWC3*).
The Figure 3.27 reports the overall volumetric water content for the tests characterized by "high initial saturation degree" for each combination of slope and input discharge. The results obtained show that in case of a 3% slope the overall soil moisture increases during the experiment only for the medium and maximum input discharge; in case of a 6% slope the overall soil moisture increases for all the input discharges but more for the medium one; in

case of 9% slope the overall soil moisture increases for the Maximum and Minimum input discharges and not for the Medium one.

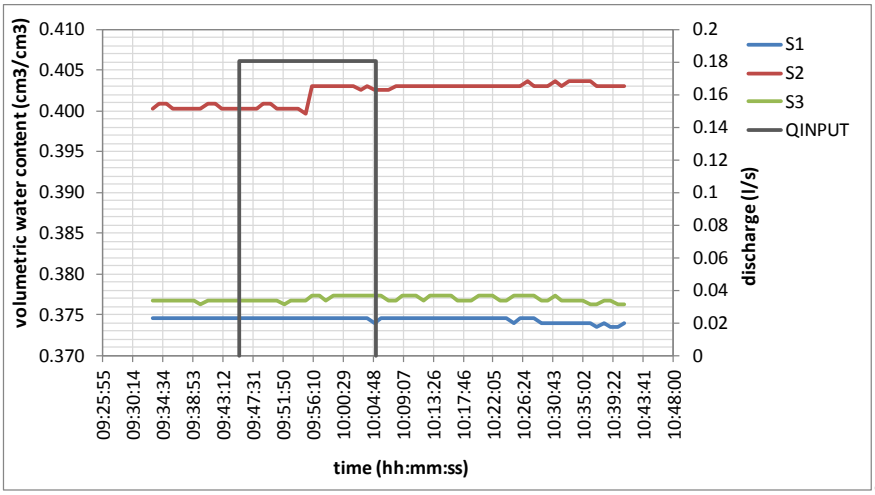

a)

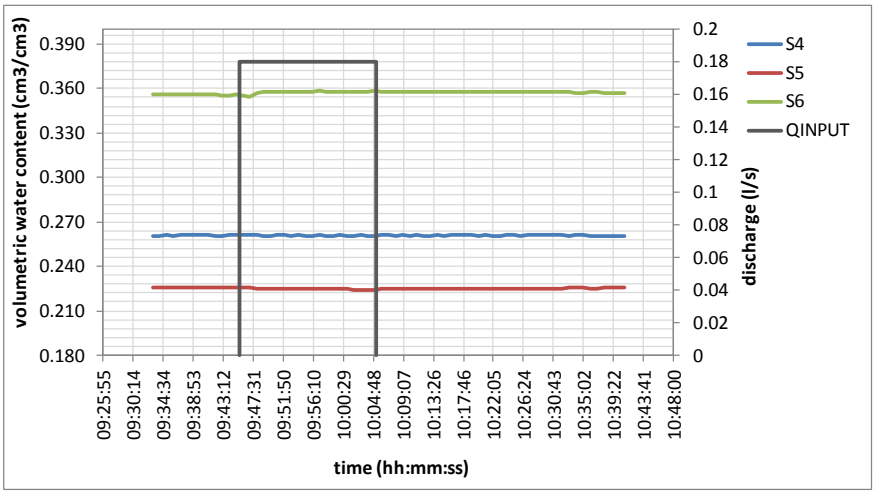

b)

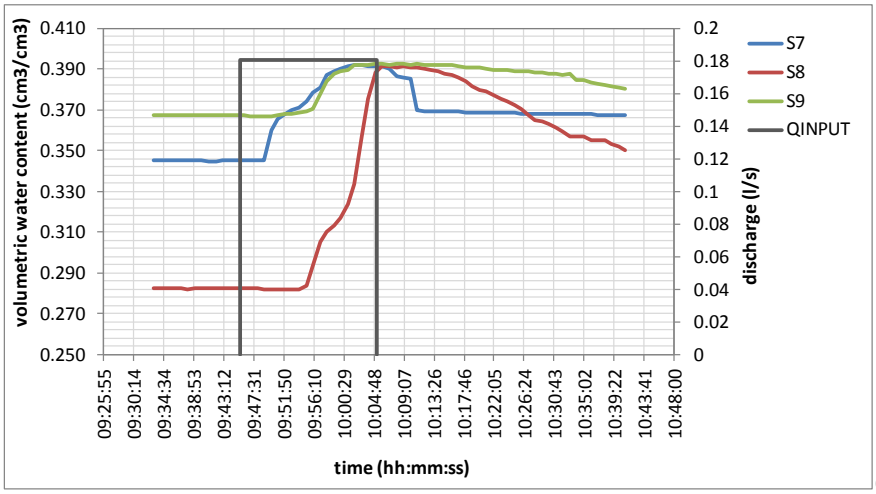

c)

Figure 3.25.Typical behavior of soil moisture sensors (Test 9):a) Section A; b) Section B; c) Section C)

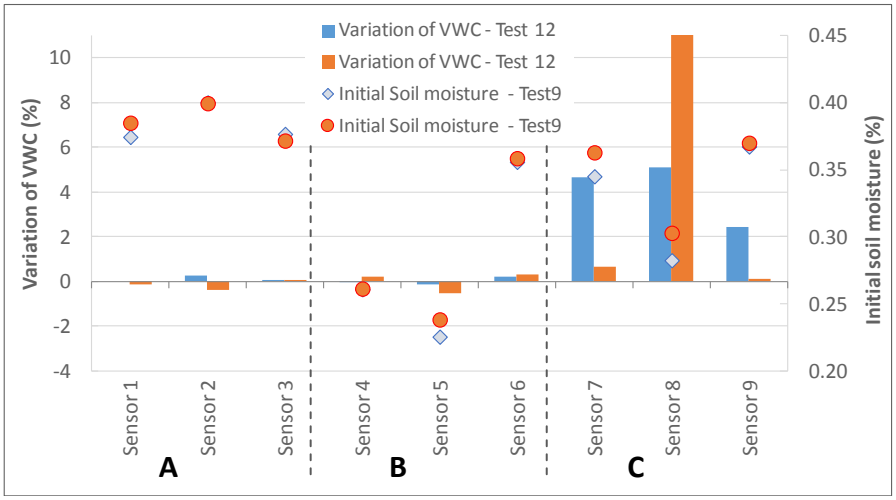

Figure 3.26.Change in VWC from the beginning to the end of the experiment (%) and initial soil moisture for a mean input discharge for the 6% slope

a)

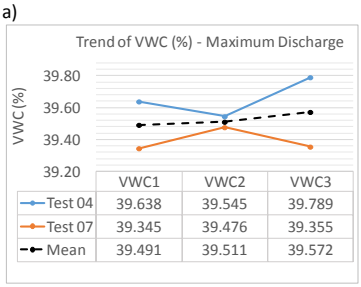

	VWC1	VWC2	VWC3
Test 04	39.638	39.545	39.789
Test 07	39.345	39.476	39.355
Mean	39.491	39.511	39.572

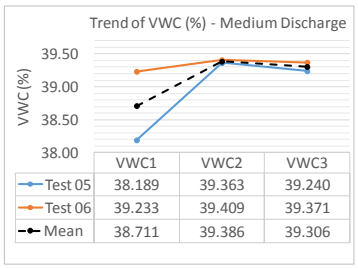

	VWC1	VWC2	VWC3
Test 05	38.189	39.363	39.240
Test 06	39.233	39.409	39.371
Mean	38.711	39.386	39.306

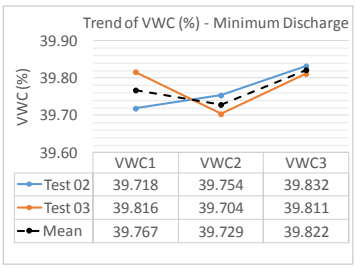

	VWC1	VWC2	VWC3
Test 02	39.718	39.754	39.832
Test 03	39.816	39.704	39.811
Mean	39.767	39.729	39.822

b)

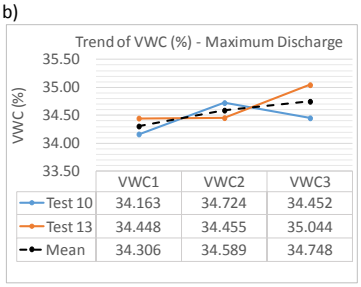

	VWC1	VWC2	VWC3
Test 10	34.163	34.724	34.452
Test 13	34.448	34.455	35.044
Mean	34.306	34.589	34.748

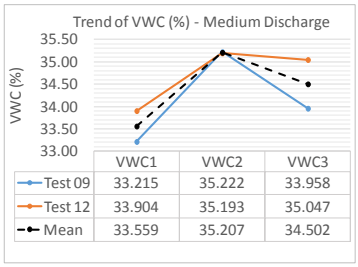

	VWC1	VWC2	VWC3
Test 09	33.215	35.222	33.958
Test 12	33.904	35.193	35.047
Mean	33.559	35.207	34.502

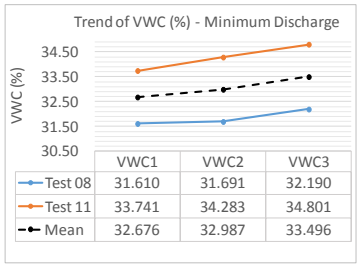

	VWC1	VWC2	VWC3
Test 08	31.610	31.691	32.190
Test 11	33.741	34.283	34.801
Mean	32.676	32.987	33.496

c)

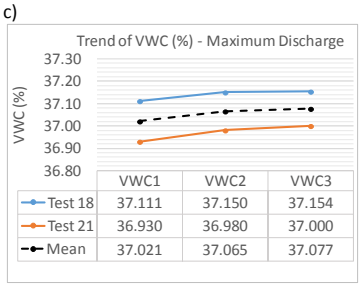

	VWC1	VWC2	VWC3
Test 18	37.111	37.150	37.154
Test 21	36.930	36.980	37.000
Mean	37.021	37.065	37.077

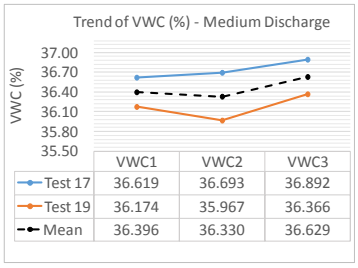

	VWC1	VWC2	VWC3
Test 17	36.619	36.693	36.892
Test 19	36.174	35.967	36.366
Mean	36.396	36.330	36.629

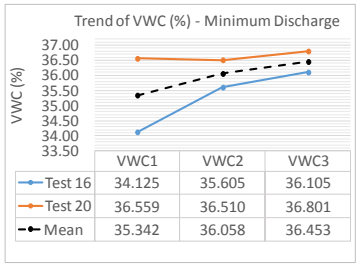

	VWC1	VWC2	VWC3
Test 16	34.125	35.605	36.105
Test 20	36.559	36.510	36.801
Mean	35.342	36.058	36.453

Figure 3.27.*Overall Volumetric Water content for min, mean and max input discharges: a)3% slope, b) 6%slope, c) 9% slope. The dashed black lines are obtained by averaging the results of each pairs of tests.*

The same elaborations have been done for the two experiments with "low initial degree of saturation" over a 3% slope (test 1) and a 9% slope (test 15). The Figure 3.28 shows the results of these two tests which are characterized by a Minimum Discharge in input to the system.

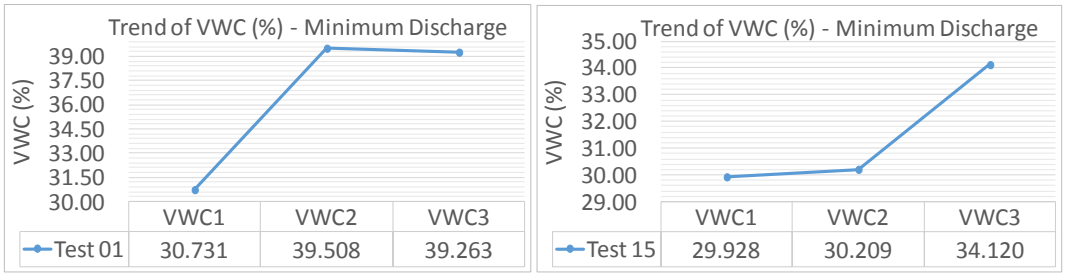

Figure 3.28.Overall Volumetric Water content for "low initial degree of saturation" (test 1 and 15)

Both the tests show a growth of soil moisture, which is more delay in the case of test 15. The test 1 shows a grater increase of soil moisture respect to the test 15; this fact could be related to lower slope considered in the experiment 1.

The same elaborations was conducted for the tests characterized by the grass cover in a 9% slope considering a maximum (test 24) and minimum (test 22) input discharge. TheFigure 3.29 shows that in case of grass cover the overall soil moisture increases more for minimum input discharges (+4.37%) than for the maximum ones (+0.51%). It is important to note that even starting from different initial soil moisture the 2 tests show the same value for the final soil moisure (36.25%). This fact that did not occur in the other tests could be due to the water retaining effect of the roots that beyond a certain limit does not allow to increase soil moisture.

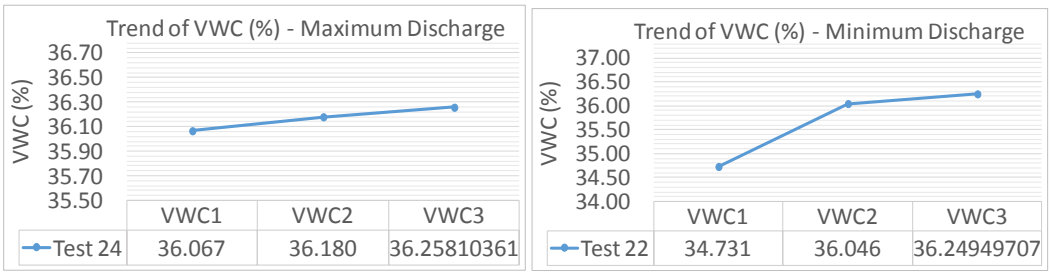

Figure 3.29. Overall Volumetric Water content in case of the grassy terrace(9% slope, max and min input discharges)

3.3.2.2 Hydrological analysis

Following the method described in section 3.2.3.2.1. for each test the hydrographs of the outflow discharges outflowing from the wall (runoff and groundwater) were obtained indirectly from the analysis of the recorded cumulative weight curves relative to the volume of water fallen into the buckets located at the bottom of the wall.

The Figure 3.30 shows an example of the filtering process related to the test 9 for the runoff component (Figure 3.30a) and for the groundwater component (Figure 3.30b). It is possible observing how the filtered lines (20 sec average discharge) for both components fit well the original data which are characterized by great variability due to the high frequency of data acquisition (1 second).

All the graphs of measurement results are reported in appendices.

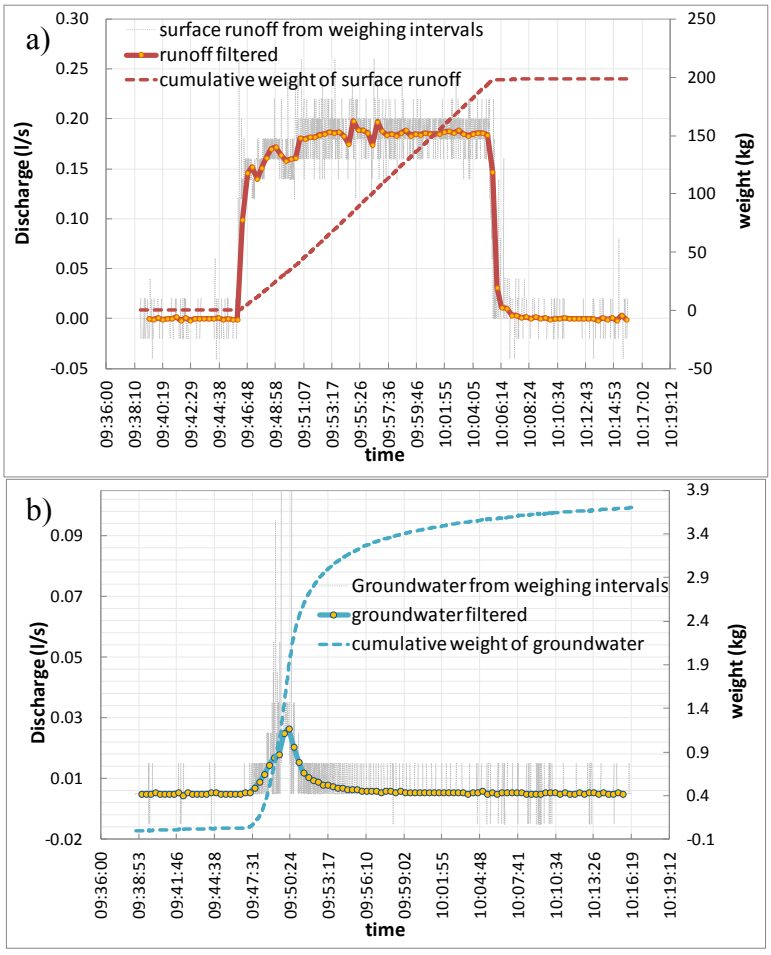

Figure 3.30. Example of filtering process related to the test 9 for runoff (a) and groundwater (b)

The Table 3.8 reports the results concerning the verification of the water balance between input and output for all the experimental tests. Each test is characterized by a water volume in

input, a surface runoff volume in output (*VtotRun*), a groundwater volume in output (*VtotGW*), and a water volume stored in the bottom of the plot; all these volumes were obtained from the recorded flow measurements.

The water balance error apply to each test is then given by:

$$WaterBalanceError = VtotInp - VtotRun - VtotGW - BottomWaterStorage - Terr.WaterStorage \quad (3.8)$$

The Table 3.8 shows the error values in terms of volumes (liters) and percentage (ratio between the error and volume in input). It is possible to notice that 70% of the tests are associated to a positive error lower than 5%; 26% of the tests show a positive error in a range 5-8% and only one test (n° 24) has a negative error (error highlighted in bold in Table 3.8).

Test n°	***Vol tot inp*** *(l)*	***Vol tot runoff*** *(l)*	***Vol tot gw*** *(l)*	***VWC1*** *(%)*	***VWC2*** *(%)*	***DH*** *(cm)*	***Bottom water storage*** *(l)*	***Terrace water storage*** *(l)*	***Water Balance error*** *(l)*	*%*
1	362.11	173.84	25.26	0.307	0.395	-3.68	43.72	99.86	19.43	5.37
2	39.78	19.62	8.49	0.397	0.398	-0.61	7.25	1.2	3.22	8.10
3	42.58	22.11	13.22	0.398	0.397	-0.02	0.24	6.91	0.10	0.24
4	198.19	195.18	2.97	0.396	0.395	0	0	0.04	0.000	0.00
5	82.51	59.84	4.25	0.382	0.394	-1	11.88	1.26	5.28	6.40
6	92.04	74.4	9.22	0.392	0.394	-0.3	3.57	3.27	1.59	1.72
7	188.97	182.1	4.53	0.393	0.395	0	0	2.34	0.000	0.00
8	256.48	184.62	1.33	0.316	0.317	-0.56	6.65	60.95	2.93	1.14
9	212.84	198.48	3.7	0.332	0.352	-0.06	0.71	9.63	0.32	0.15
10	231	186.22	35.57	0.342	0.347	-0.16	1.90	6.48	0.83	0.36
11	242.9	154.94	43.58	0.337	0.343	-1.61	19.13	16.7	8.55	3.52
12	209.3	181.3	4.4	0.339	0.352	-1.2	14.26	3.01	6.33	3.03
13	234.8	181.26	12.39	0.344	0.345	-2.3	27.32	1.68	12.14	5.17
14	251.9	154.16	79.14	-	-	-1	11.88	1.44	5.28	2.10
15	302.1	129.36	95.53	0.299	0.302	-2	23.76	42.89	10.56	3.5
16	197.7	155.2	7.02	0.341	0.356	-2	23.76	1.16	10.56	5.34
17	196.9	172.16	11.64	0.366	0.367	-0.7	8.32	1.09	3.69	1.88
18	235.1	207.38	16.3	0.371	0.372	-0.6	7.13	1.12	3.17	1.35
19	219	77.14	98.36	0.362	0.359	-2.5	29.7	0.6	13.20	6.03
20	216.9	163.14	17.29	0.366	0.365	-1.2	14.26	15.88	6.33	2.92
21	237.7	124.86	80.15	0.369	0.37	-1.9	22.57	0.09	10.03	4.22
22	203.49	86.04		0.347	0.36	-1.79	21.27	86.74	9.45	4.64
24	197.3	218		0.36	0.361	-3.47	41.22	0	-61.92	**-31.39**

Table 3.8. Water balance from measurement for the second configuration

In general, compared to the first configuration, the new setting has led to a good estimation of the different volume components and a consequent reduction of water balance errors.
In the last two tests (22 and 24) only the total output volume was measured (with a balance); it is important to note that, as shown Table 3.8, the test 24 had the volume in output greater than the volume in input; this is due to the fact that this test started too close to the previous experiments whose groundwater flow did not completed yet.
The Table 3.9 reports all the response times for all the tests whit bare soil for surface runoff and groundwater, obtained following the procedure described in section 3.2.3.2.2. In particular, the times have been identified by analyzing all the filtered runoff and groundwater hydrographs.

Test	$T1_{Runoff}$ *(min)*	$T2_{Runoff}$ *(min)*	$T3_{Runoff}$ *(min)*	$T4_{Runoff}$ *(min)*	$T1_{gw}$ *(min)*	$T2_{gw}$ *(min)*	$T3_{gw}$ *(min)*	$T4_{gw}$ *(min)*
1	17.17	17.75	62.57	65.72	6.20	9.20	14.25	20.55
2	1.19	2.55	5.67	8.67	4.77	7.77	8.88	17.82
3	1.07	1.77	7.45	10.33	1.48	2.90	7.17	18.27
4	0.38	1.13	10.07	12.67	4.83	5.95	5.95	13.37
5	0.82	1.92	7.05	9.62	1.90	3.88	8.13	15.57
6	0.52	1.25	7.52	10.10	1.97	4.43	5.65	10.10
7	0.50	0.87	10.38	12.95	4.13	6.35	11.10	17.07
8	2.98	7.82	46.55	48.37	30.70	39.68	49.85	59.20
9	0.37	1.12	19.52	22.12	8.38	11.03	11.03	17.62
10	0.17	2.57	12.73	14.83	2.83	5.18	5.18	16.73
11	4.70	5.82	39.83	43.98	1.33	3.68	6.10	10.55
12	1.52	2.90	19.33	21.48	4.15	4.30	4.30	12.38
13	0.12	0.48	15.95	17.35	1.20	2.60	2.60	4.70
14	0.52	1.18	12.83	13.85	1.57	3.68	6.10	10.55
15	4.25	12.75	46.75	53.92	7.95	11.62	43.37	54.27
16	5.83	10.38	37.37	40.12	11.58	14.78	23.88	8.77
17	1.95	6.08	20.35	21.85	1.98	3.35	4.05	18.90
18	0.62	3.97	12.22	13.73	0.95	2.43	3.07	6.93
19	3.13	3.50	19.77	21.83	3.18	8.47	20.87	23.15
20	4.02	7.78	41.63	44.43	6.07	7.45	10.18	17.37
21	0.63	1.73	12.63	14.37	0.98	5.08	12.63	22.23

Table 3.9. Response times identification

The analysis of the hydrological responses for the different tests shows some particular behaviours. A typical representation for "high initial degree of saturation" tests is described in Figure 3.31 (test 9), which shows the total filtered output discharge, the filtered runoff and groundwater and the time series recorded from the two piezometers.

After 0.37 minutes ($T1_r$) from the beginning of the forced flooding the surface runoff reaches the top of the dry stone wall; all the terrace area contributes to the outflow hydrogram at time $T2_r$ (1.12 minutes); the maximum peak runoff is recorded just before the end of the forced flooding at time $T3_r$ (19.52 minutes); then the surface runoff goes to zero at time $T4_r$ (22.12 minutes). At the time $T1_{gw}$ (8.38 minutes) the groundwater table, measured by the piezometers, reaches the reference quote of 18 cm and the groundwater starts to exit from the base of wall; the maximum peak of groundwater is recorded at time $T2_{gw=}$ $T3_{gw}$ (11.03 minutes); then the groundwater goes to zero at time $T4_{gw}$ (17.62 minutes). The analysis of the piezometer recored values shows, as expected, that the groundwater flow reflects the behaviour of the groundwater table.

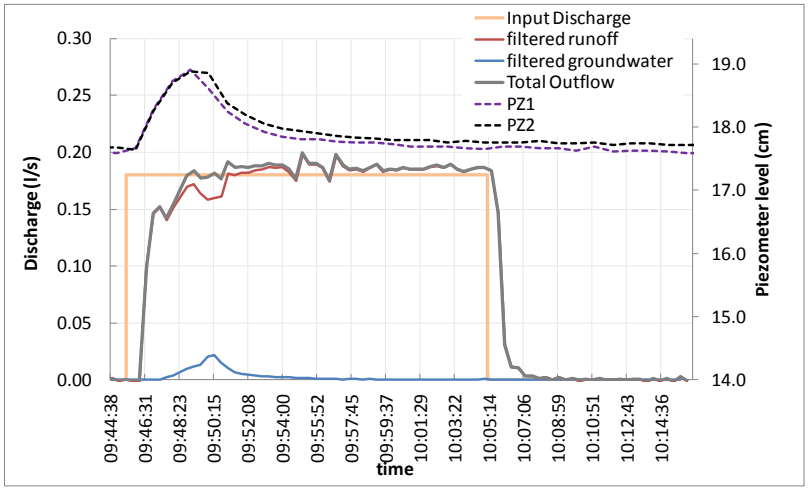

Figure 3.31. Example of hydrological response for test 9

Another particular case is represented by the "low initial degree of saturation" tests (Figure 3.32). The hydrological response is similar in the two cases. The test 1 with 3% slope shows a great infiltration at the beginning of the experiments with a delayed surface runoff production. Also the test 15 with 9% slope shows the anticipation of the groundwater production respect to the surface runoff component. This test is also characterized by a groundwater volume around 50% of the total output volume.

The analysis of the tests with grass cover in a 9% slope is reported in the Figure 3.33. It is important to note that in this case only the total output discharge is available. The visual

observations have showed that quite all the output volume is composed by the groundwater flow. Also the analysis of the Figure 3.33 seems to lead to this consideration; in fact its observation shows comparative trends for the outflow curves and the piezometric curves.

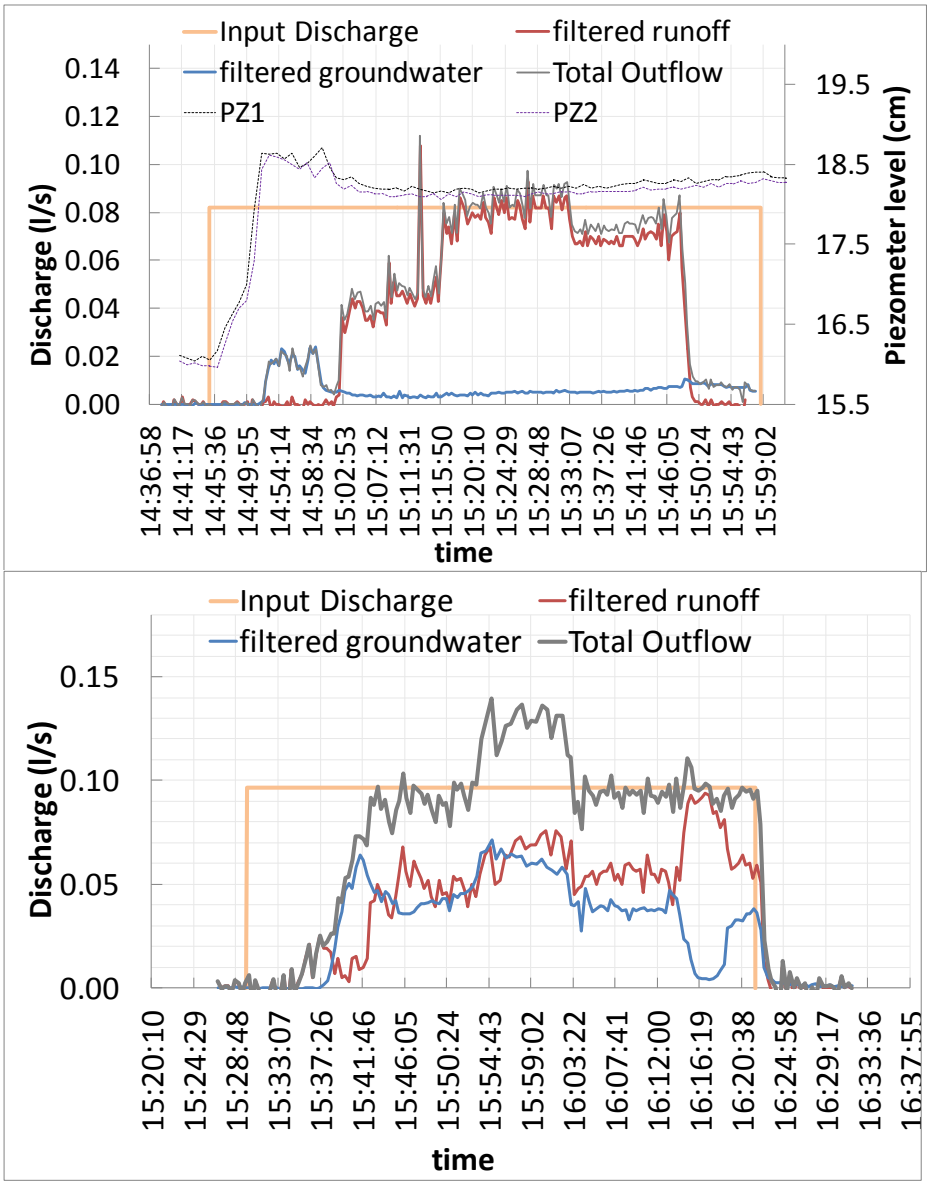

Figure 3.32. "low initial degree of saturation" tests: a) Test 1; b) Test 15

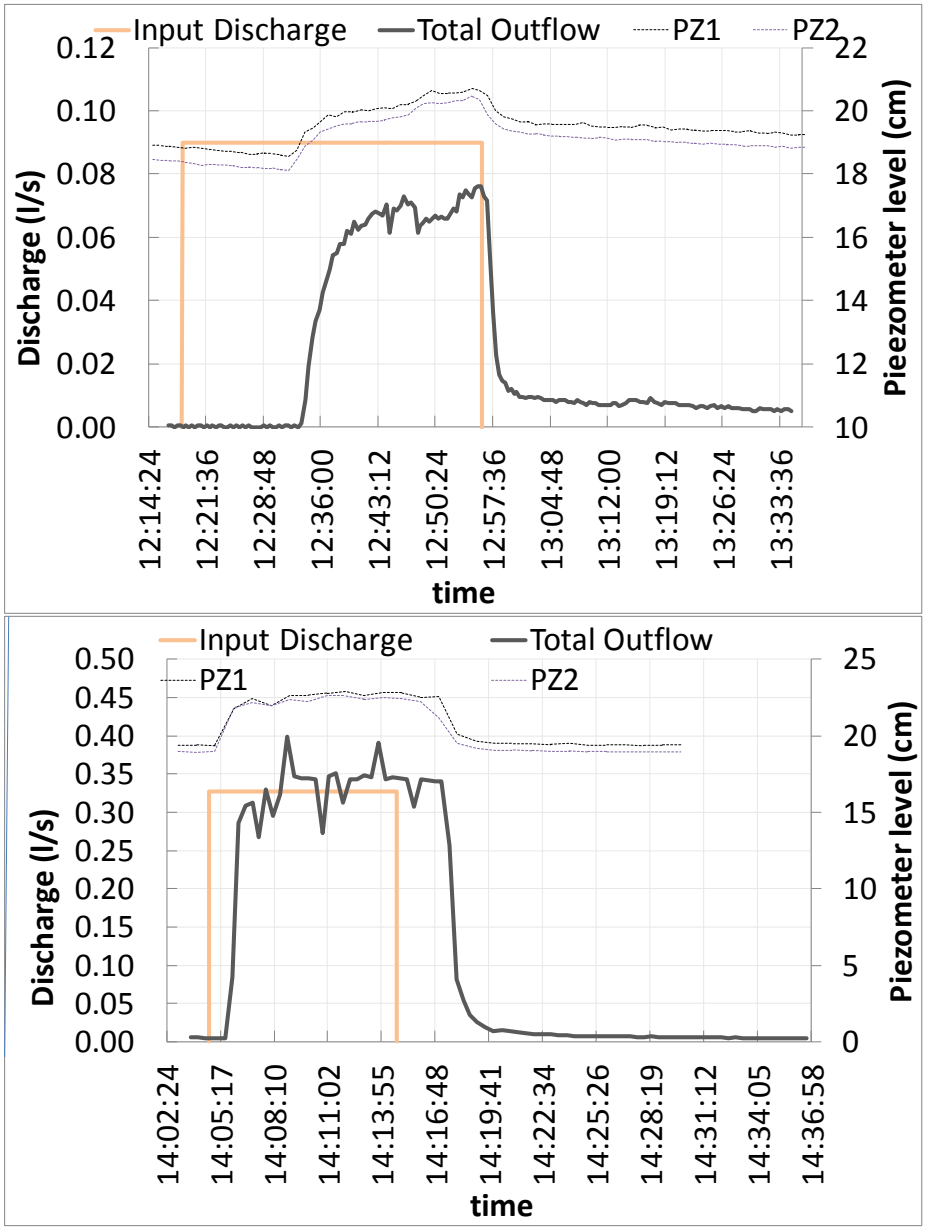

Figure 3.33. Tests with the plot covered with grass

Routing time *(s)*	***Discharge*** *(l/s)*
23	2.43
18	2.47
14	2.60
23	2.76
16	5.20
12	5.40
19	5.40

Routing time ***(s)***	***Discharge*** *(l/s)*
13	5.70
14	5.84
15	6.36
12	7.36
12	7.36
11	10.00
10	15.28
10	15.70
10	15.87
10	15.87
10	16.00
9	16.02
9	19.10
12	20.00

Table 3.10. Measured routing times

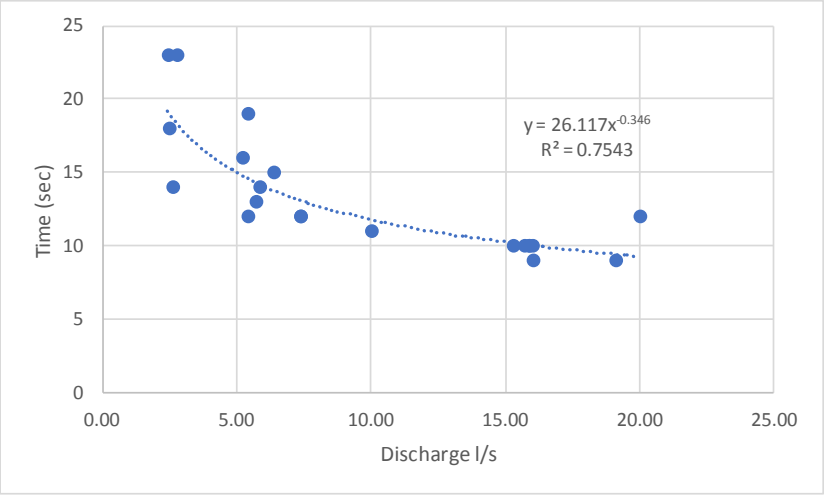

Figure 3.34. Measured times of routing along the wall as function of the input discharge.

3.3.2.3 Computation of the Curve Number

For the second configuration of the plot it was possible to calculate the Curve Number by applying the two methodologies described in 3.2.3.3 for the **terrace area** CN_{ta} and the **traditional** ***CN***.

The table Table 3.11 represents the computation of the special CN_{ta} (eq. 3.4) for all the tests (21 test with "high initial degree of saturation" and 2 with "low initial degree of saturation"). The total volume in output is the sum of the total runoff and groundwater volumes.
The value of the CN_{ta} ranges from 71.99 (test 8) to 99.99 (test 4) with an average value equal to 93.96.

Number test	***Total Vol Inp.*** *(l)*	***Total Vol Inp.*** *(mm)*	***Total Vol Out.*** *(l)*	***Total Vol Out.*** *(mm)*	S_{max} *(mm)*	***CN***
*1**	362.110	120.703	199.100	66.367	98.824	71.991
2	39.780	13.260	28.110	9.370	5.505	97.879
3	42.580	14.193	35.330	11.777	2.913	98.866
4	198.190	66.063	198.150	66.050	0.013	99.995
5	82.510	27.503	64.090	21.363	7.905	96.982
6	92.040	30.680	83.620	27.873	3.089	98.798
7	188.970	62.990	186.630	62.210	0.790	99.690
8	256.480	85.493	185.950	61.983	32.427	88.679
9	212.840	70.947	202.180	67.393	3.741	98.549
10	231.000	77.000	221.790	73.930	3.197	98.757
11	242.900	80.967	198.520	66.173	18.100	93.348
12	209.300	69.767	185.700	61.900	8.866	96.627
13	234.800	78.267	193.650	64.550	16.631	93.855
14	251.900	83.967	233.300	77.767	6.694	97.432
*15**	302.100	100.700	224.890	74.963	34.573	88.019
16	197.700	65.900	162.220	54.073	14.413	94.630
17	196.900	65.633	183.800	61.267	4.678	98.192
18	235.100	78.367	/223.680	74.560	4.001	98.449
19	219.000	73.000	175.500	58.500	18.094	93.350
20	216.900	72.300	180.430	60.143	14.614	94.560
21	237.700	79.233	205.010	68.337	12.634	95.262
22	203.490	67.830	86.040	28.680	92.592	73.285
24	197.300	65.768	218.000	72.667	-	-

*Table 3.11. Computation of the "terrace area CN". *As reported in 3.2.3.3., in the case of "initial low degree of saturation" (test 1 and 15) the calculated CN rapresents the "AMCII" conditions; for the rest of the tests the CN rapresents the "wet antecedent moisture content AMCIII" conditions.*

The curve number of test 24 has not been calculated since the total volume in output is greater than the total volume in input; in fact this test was executed too close to the previous which corresponding outflow did not finished.

The table Table 3.12 represents the computation of the traditional ***CN*** for all the tests characterized by bare soil (19 test with "high initial degree of saturation" and 2 with "low initial degree of saturation"). In this case (eq.3.3) the calculation takes into account only the contribution of the surface runoff. The value of the traditional ***CN*** ranges from 65.385 (test 19) to 99.60 (test 4) with an average value equal to 88.98.

As expected both the **traditional *CN*** and the **terrace area CN_{ta}** assume the lower values for the tests 1 and 15. In fact this tests are characterized by "low initial degree of saturation" and then they can be associated to the AMCII stantard conditions. The average CN_{ta} in case of "high initial degree of saturation" is greater than the one corresponding to "low initial degree of saturation".

Number test	***Total Vol Inp.*** *(l)*	***Total Vol Inp.*** *(mm)*	***Total Runoff Out.*** *(l)*	***Total Runoff Out.*** *(mm)*	S_{max} *(mm)*	***CN***
1*	362.110	120.703	173.84	57.947	130.723	66.022
2	39.780	13.260	19.620	6.540	13.625	94.909
3	42.580	14.193	22.110	7.370	13.141	95.081
4	198.190	66.063	195.180	65.060	1.019	99.600
5	82.510	27.503	59.840	19.947	10.419	96.059
6	92.040	30.680	74.400	24.800	7.274	97.216
7	188.970	62.990	182.100	60.700	2.376	99.073
8	256.480	85.493	184.620	61.540	33.277	88.416
9	212.840	70.947	198.480	66.160	5.133	98.019
10	231.000	77.000	186.220	62.073	18.516	93.206
11	242.900	80.967	154.940	51.647	45.965	84.677
12	209.300	69.767	181.300	60.433	10.775	95.931
13	234.800	78.267	181.260	60.420	23.118	91.658
14	251.900	83.967	154.160	51.387	53.236	82.673
15*	302.100	100.700	129.360	43.120	134.469	65.385
16	197.700	65.900	155.200	51.733	18.046	93.367
17	196.900	65.633	172.160	57.387	9.432	96.420
18	235.100	78.367	207.380	69.127	10.475	96.039
19	219.000	73.000	77.140	25.713	134.247	65.422
20	216.900	72.300	163.140	54.380	23.825	91.424
21	237.700	79.233	124.860	41.620	71.606	78.008

*Table 3.12. Computation of the "traditional CN". *As reported in 3.2.3.3., in the case of "initial low degree of saturation" (test 1 and 15) the calculated CN rapresents the "AMCII" conditions; for the rest of the tests the CN rapresents the "wet antecedent moisture content AMCIII" conditions.*

3.4 Hydrological modelling: The Hydro Terrace Model

In order to estimate the hydrological response of the terraced slope for different boundary conditions (slope, input discharge, soil characteristics) a new conceptual model, named HydroTerraceModel hereafter, has been proposed and implemented. After its implementation the model has been calibrated and validated based on the data recorded from the laboratory experiments described in 3.3.

The model is written in Matlab code and it is composed by the following submodules: 1) Infiltration module, 2) Surface runoff propagation module, 3) Groundwater module.

THE CALCULATION DOMAIN

The geometric domain of the model is described in the Figure 3.35. The terrace terrain is composed by several cells each one characterized by the following dimension: 1 meter wide, a height equal to H and a length equal to *dx*. The number of cells can vary depending on the length of the terrace and on the *dx* length selected by the user. The last cell is representative of the dry wall and at each cell is possible to associate different soil parameters and initial conditions. Before to run a simulation the user must indicate the calculation time step.

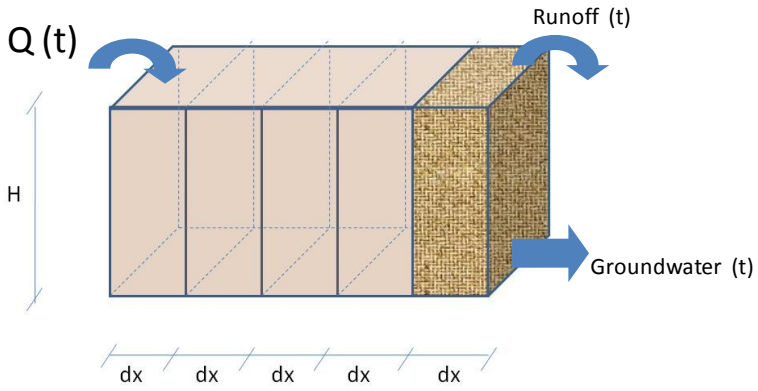

Figure 3.35. Conceptual scheme of the terrace

The program allows for the user to execute the following actions:

- Setting the model parameters
- Loading the input data (timeseries of input discharges and piezometers)
- Running in cascade the following 3 modules:
    - Infiltration module
    - Surface runoff propagation module
    - Groundwater module
- Saving the results in a txt file;

- Plotting automatically the modelled results compared with the corresponding measures

The free Matlab function[2] "Green Ampt Infiltration for Unsteady Rainfall Model" has been extended and incorporated as a subroutine in the HydroTerraceModel. In particular the Matlab script is based on the Fortran code of Parsons and Muñoz-Carpena[3] (2009). The code follows the method of Chu (1978), Mein and Larson (1971, 1973) and Skaggs and Kaheel (1982) to calculate infiltration for unsteady rainfall using the Green-Ampt equation applied to a portion of soil of 1 m^2.

THE INFILTRATION MODULE

Green Ampt Model: Background and Derivations

This discussion is a summary from Skaggs and Khaheel (1982). The Green Ampt model for infiltration was originally derived for infiltration from a ponded surface into a deep homogenous soil with a uniform initial water content (Green and Ampt 1911). Green and Ampt applied Darcy's Law by assuming that water enters the soil as slug flow. This assumption implies that there is a sharply defined wetting front which separates a zone that has been wetted from infiltration and a zone that is totally un-wetted (at the initial water content). In other words, as an approximation, they assumed that the transitions zone was very small. It follows the sketck of Figure 3.36.

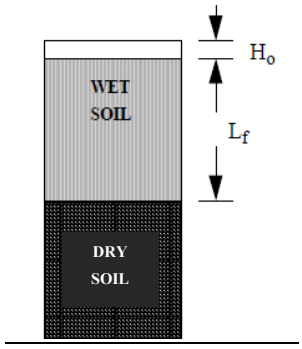

Figure 3.36. Scheme to illustrate the piston flow (Parsons and Muñoz-Carpena (2009))

From the Figure 3.36 we assume that the moisture content (Θ) is equal to the value under saturation (Θ_s) in the wet soil zone and a value Θ_i in the dry soil zone. Let K_s be the saturated hydraulic conductivity in the tranmission zone (saturated soil). Recall Darcy's Law, $Q =$

[2] http://www.mathworks.com/matlabcentral/fileexchange/49585-green-ampt-infiltration-for-unsteady-rainfall-model
[3] provided in: http://abe.ufl.edu/carpena/software/wingampt.shtml

$\mathrm{AK}\frac{\mathrm{dH}}{\mathrm{dz}}$ where Q is the flow (L/T), A is the Area (L^2), K is the saturated conductivity (L/T), H is the total hydraulic head (L), and z is the space coordinate (L). This is equivalent to $\mathrm{Q} = \mathrm{K}\frac{\mathrm{dH}}{\mathrm{dz}}$ where q is the flux (L/T) per unit area. Applying this form to the Figure 3.36,

$$f_p = K_s \frac{H_0 + L_f + S_f}{L_f} \tag{3.9}$$

where

f_p = infiltration rate (L/T)

K_s = hydraulic conductivity of the transmission zone (wetted zone) (L/T),

H_0 = depth of water ponded on the surface (L),

L_f = distance from the surface to the wetting front (L)

S_f = effective suction at the wetting front (L).

Note that the cumulative infiltration, F(L), is given by

$$F = L_f(\Theta_s - \Theta_i) = M\, L_f \tag{3.10}$$

where $M = (\Theta_s - \Theta_i)$

The effective suction at the wetting front, S_f, requires some knowledge of the development of the wetting front. This quantity is difficult to determine. This is often replaced by the average suction at the wetting front which is found from the soil water characteristic (Bouwer (1969), Mein and Larson (1973)). For the rest of our discussion we will use the average suction at the wetting front (*Sav*) as estimated by Mein and Larson (1973). If we assume that the surface has just ponded (that is, *Ho* ≈ 0), then 3.9 becomes

$$f_p = K_s + \frac{K_s\, Sav\, M}{F} \tag{3.11}$$

and M is called the fillable porosity. This is a direct measure of antecedent moisture conditions which is often estimated indirectly in other methods such as the SCS Curve Number method. Now substitute $f_p = \frac{\mathrm{dF}}{\mathrm{dt}}$ into 3.11. This yields:

$$\frac{dF}{dt} = K_s + \frac{K_s\, Sav\, M}{F} \tag{3.12}$$

Now we assume that F=0 at t=0, and integrating 3.12 with respect to t, we obtain:

$$\int_0^t \frac{dF}{dt} dt = \int_0^t K_s dt + \int_0^t \frac{K_s\, M\, Sav}{F} dt \qquad (3.13)$$

This yields the following equation for ponded conditions with steady rainfall:

$$\mathrm{K_s t} = \mathrm{F} - \mathrm{M\ Sav\ ln}\left(1 + \frac{\mathrm{F}}{\mathrm{M\ Sav}}\right) \qquad (3.14)$$

Now, we need to modify the Green Ampt approach to handle conditions non-ponded, unsteady rainfall. First, for the non-ponded condition, we know that all of the water must be infiltrating. Therefore $f_p = R$ where R is the rainfall intensity. The first step is to determine the cumulative infiltration at the time of ponding (call this F_p). This is found by setting f_p=R and using 3.11. The resulting equation is as follow:

$$R = K_s + \frac{K_s\, M\, Sav}{F_p} \qquad (3.15)$$

Solving for F_p we obtain

$$F_p = K_s + \frac{M\, Sav}{\frac{R}{K_s} - 1} \qquad (3.16)$$

Prior to ponding, f=R, so,

$$F_p = R\, t_p \qquad (3.17)$$

$$t_p = \frac{F_p}{R} \qquad (3.18)$$

where t_p is the time to ponding. So for steady rainfall, if t<t_p, then

$$f = R \qquad (3.19)$$

and for t>t_p ,

$$f = f_p = K_s + \frac{K_s\, Sav\, M}{F_p} \qquad (3.20)$$

Mein and Larson (1973) derived the following form of the Green Ampt equation,

$$K_s(t - t_p + t_p') = F - M\, Sav\ \ ln\left(1 + \frac{F}{M\, Sav}\right) \qquad (3.21)$$

where t_p' is the equivalent time to infiltrate the volume F_p under initially ponded conditions which can be calculated directly from 3.14.

Application of Green Ampt Model can be conducted by applying either 3.19 or 3.20 and 3.14 along with using 3.21.

For analyzing unsteady rainfall, it is helpful to utilize a water balance at the surface. Ignoring evaporation during the rainfall event, it follows:

$$\Delta P = \Delta F + \Delta s + RO \qquad (3.22)$$

where $\Delta P = R\,\Delta t$, the rainfall during the time period Δt, ΔF is the cumulative infiltration, Δs is change in surface storage, and RO is the surface runoff during the time period Δt . Chu (1978) offered a simplified systematic approach to using the Green Ampt model along with this water balance.

Integration of the Green Ampt routine to the HydroTerraceModel

The Green Ampt theory described above is applied to each cell of the terrace. In particular, the free available original script worked with only a single cell and for this thesis it was adapted to model a multiple cascade of cells. At a fixed time step Δt a generic cell receives in input a surface runoff volume from the upstream cell. This runoff is considered as spread uniformly in all the cell surface area and becomes the input for the Green Ampt routine. As described in Figure 3.37 the runoff produced as output of the infiltration module is then propagated to the adjacent downstream cell by means of the propagation module. At the same time, the infiltration amount produced by the infiltration module becomes the input of the Groundwater module.

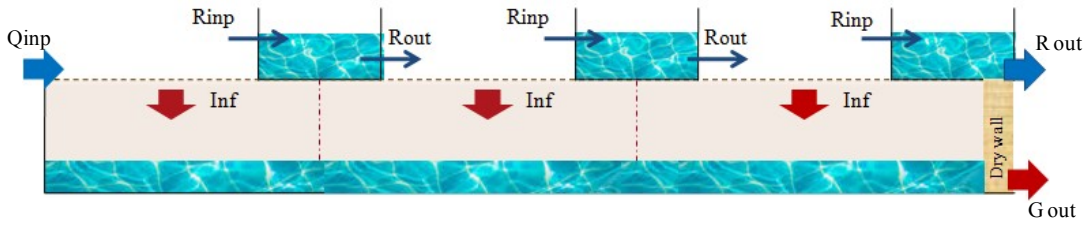

Figure 3.37. Conceptual schematization of the HydroTerraceModel

The initial condition of the infiltration module are:

- the initial soil water content in each cell: *wcini* (cm^3/cm^3);
- the time series of the discharges $Q(t)$ in input to the first upstream cell.

The soil parameters associated to each cell are the following:

- The satured hydraulic soil conductivity: K_{sat} (cm/hour);

- The average suction at the wetting front: *sav*(cm);
- The satured water content wc_{sat}: (cm^3/cm^3).

THE SURFACE RUNOFF PROPAGATION MODULE

The surface runoff is propagated following the linear transfer function theory (Beven, 2002) for which a linear store is a model element that considers the output Q [m^3s^{-1}] as directly proportional to the storage, S [m^3] (Figure 3.38). In detail the following mathematical procedure is solved for each cell of the model.

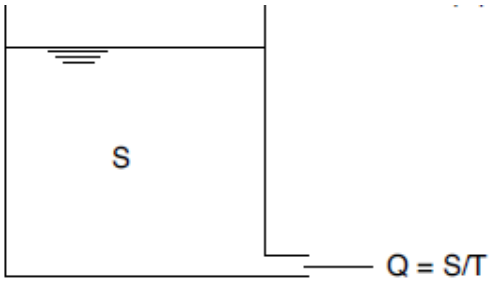

Figure 3.38. Conceptual schematization of a linear store.

Thus, we assume:

$$Q = S/T_s \qquad (3.23)$$

where T_s [T] is a parameter equivalent to the mean residence time of the store. For water, the linear store is physically equivalent to a straight-sided bucket with a hole in the bottom containing a porous material such that the outflow is laminar and proportional to the difference in head.

The mass balance equation for the linear store (or bucket) can be written as

$$\frac{dS}{dT} = u - Q \qquad (3.24)$$

where the differential $\frac{dS}{dT}$ is the rate of change of storage with time and u [m^3s^{-1}] is an input rate. To obtain an equation in the outflow Q, since $\frac{dS}{dT} = Q$ we can modify this equation to:

$$T_s \frac{dQ}{dT} = u - Q \qquad (3.25)$$

We assume here that the input sequence has already been suitably transformed to an effective input that can be related linearly to the outputs. For simple patterns of the effective input, this equation can be solved analytically. For example, for a sudden input rate u^* into an initially dry store at time t_o

$$Q_t = \frac{u^*}{T_s} e^{\{-(t-t_0)/T_s\}} \quad (3.26)$$

This is the impulse response or transfer function of the linear store expressed in continuous time. It has the form of an initial step rise followed by an exponential decline in the outflow. In hydrology and many other modelling applications, it is often usual to have measurements of inputs and outputs at discrete time increments (e.g., every hour) rather than in continuous time. Thus, using a simple explicit finite difference form of the mass balance equation of the linear store over a discrete time step of Δt, it can be formulated the equation:

$$\frac{Q_t - Q_{t-\Delta t}}{\Delta t} = \frac{u_t - Q_{t-\Delta t}}{T_s} \quad (3.27)$$

or

$$Q_t = \frac{\Delta t}{T_s} u_t + \left\{1 - \frac{\Delta t}{T_s}\right\} Q_{t-\Delta t} \quad (3.28)$$

or

$$Q_t = aQ_{t-\Delta t} + bu_t \quad (3.29)$$

where $a = 1 - \frac{\Delta t}{T_s}$; $b = \frac{\Delta t}{T_s}$; and to ensure mass balance between total inputs and total outputs, a + b = 1.

In the HydroTerraceModel at the end of each cell a virtual storage S is positioned. The input rate to this storage is the runoff produced by the infiltration module, which is transfered from the beginning of each cell up to the storage S by using the parameter surface velocity V_s [cm/s]. The output of each linear storage S is then the input of the infiltration module of the next cell. In correspondence of the last cell (the ones containing the dry stone wall) the output of the model has been then translated until the base of the wall by adding the time lapse of routing along the wall as reported in 3.3.2.2.

THE GROUNDWATER MODULE

A linear store model characterized by the mean residence time T_{gw}[s] has been used to predicted groundwater outflowing (exfiltrating) from the wall. The input rate to the groundwater linear storage in this case is the mean areal infiltration rate produced by the infiltration module at each time step which is transferred from the atmospheric surface level up to the groundwater table by using the parameter infiltration velocity V_{gw} [m/s].

The groundwater flow starts when the level of the groundwater table reaches the lower level of the metal drainpipe positioned at the base of the wall to collect the water during the experiments. This initial level depends on the amount of previous water losses from the

bottom of the metallic structure. This initial condition has been introduced in the groundwater module through a specification of the initial difference *dH* (cm) between the groundwater threshold level and the initial groundwater level measured from the piezometer positioned close to the outlet.

3.5 Application and verification of the model on the resuts of the terrace plot

Each experimental test has been simulated with the HydroTerraceModel to evaluate the capacity of the model to represent the physical processes which characterizes a terrace. The Table 3.13 reports the list of model parameters and its calibration range. The saturated hydraulic soil conductivity K_{sat} and the average suction at the wetting front Sav have been deducted from Rawsl et.al (1983) for a kind of soil which contains sandy, clay, loam and silt. The other parameter ranges are inside an acceptable range of phisycal value (Maidment, 1992).

Parameter name	Description	Parameter range
Ksat (cm/hour)	The satured hydraulic soil conductivity	0.1-6
sav (cm)	The average suction at the wetting front	10-30
Ts [s]	mean residence time for surface runoff	5-50
T_{gw}[s]	mean residence time for groundwater	30-1000
V_s [cm/s]	Surface velocity	2-15
V_{gw} [cm/s]	Infiltration velocity	0.1-30

Table 3.13.Parameter ranges

The process followed for the calibration of test 3 is reported in the following to understand the sensibility of model parameters. The process starts running the model with a initial set of parameters, reported in Table 3.14, selected inside the corresponding parameter range. The Figure 3.39(1) reports this initial result (it is the one characterized by a surface velocity V_s=5.5 cm/s) compared with a set of simulations obtained just changing the velocity V_s. The simulation with V_s =10 cm/s was selected as the better. The Figure 3.39 (2) reports the curve resulted from the analysis of the Figure 3.39 (1) (it is the one characterized by a surface

residence Time T_s=27.5 s) compared with a set of simulations obtained just changing the surface residence time T_s. The simulation with T_s=5 s was selected as the best. The Figure 3.39(3) reports the curve resulted from the analysis of the Figure 3.39(2) (it is the one characterized by a saturated hydraulic soil conductivity K_{sat} =0.6 cm/h) compared with a set of simulations obtained just changing the parameter K_{sat}. The simulation with K_{sat}=0.7 cm/h was selected as the best. The Figure 3.39(4) reports the curve resulted from the analysis of the Figure 3.39(3) (it is the one characterized by a average suction at the wetting front Sav =20 cm) compared with a set of simulations obtained changing the parameter Sav only. The simulation with *Sav*=18 cm was selected as the optimum. The final result of the runoff hydrograph is reported in the Figure 3.40(1). The Figure 3.40(2) shows the result of the calibration of the groundwater with following parameter selected from the Figure 3.39(5) and Figure 3.39(6): the mean residence time for groundwater T_{gw}=200 s and the infiltration velocity V_{gw}=2 cm/s.

Parameter	**Parameter range**	**Initial set of parameter**
V_s (cm/s)	1-15	5.5
T_s (s)	5-50	27.5
K_{sat} (cm/h)	0.1-6	0.6
Sav (cm)	10-30	20
T_{gw} (s)	30-1000	300
V_{gw} (cm/s)	0.1-30	1.45

Table 3.14. Initial set of parameters

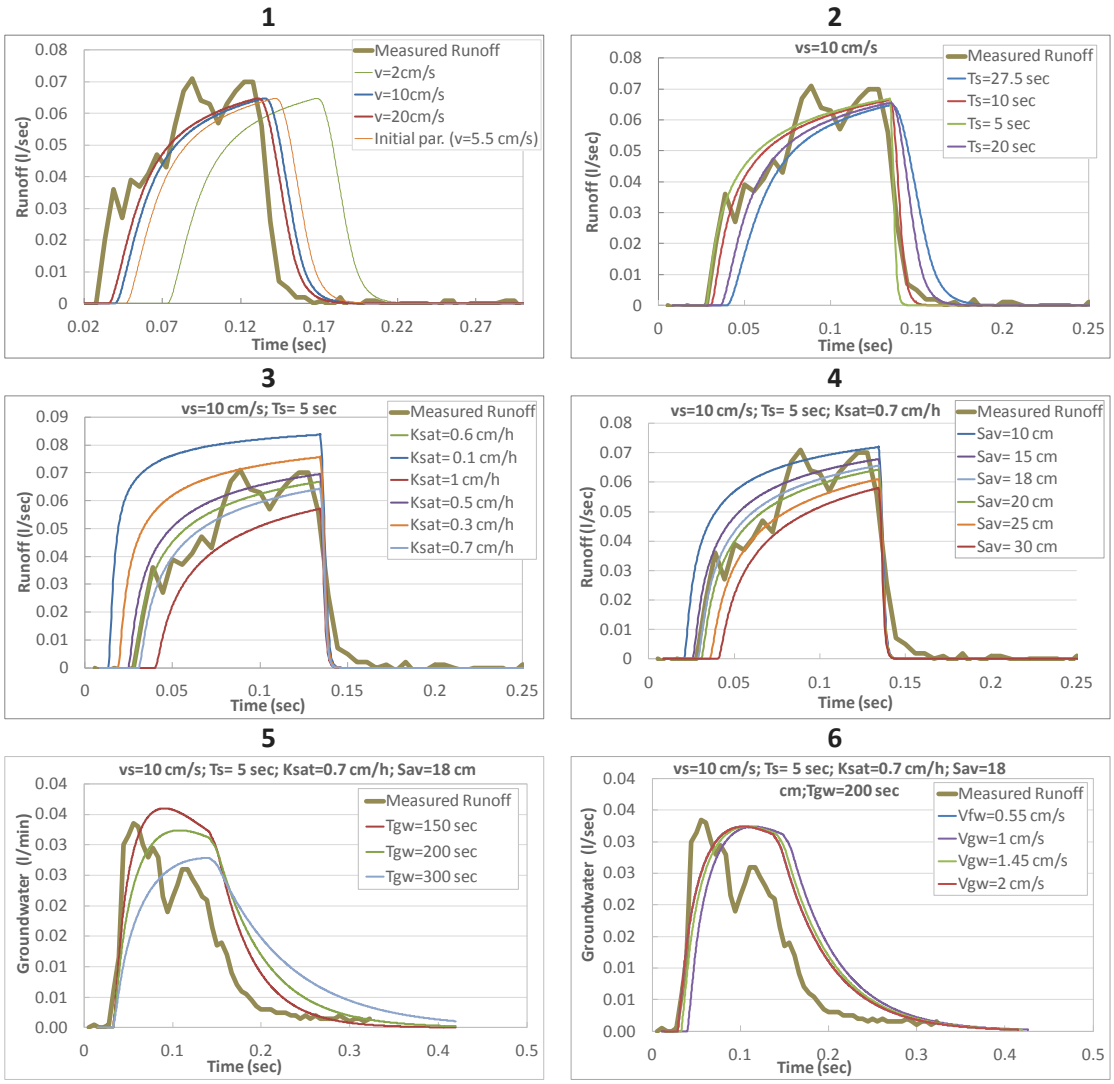

Figure 3.39. The sequence of the parameter calibration for the Test 3

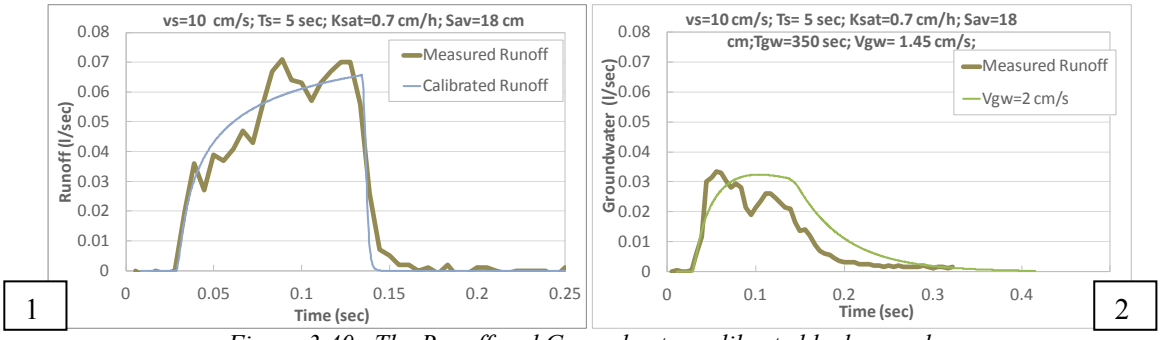

Figure 3.40. The Runoff and Groundwater calibrated hydrographs

The Figure 3.41 shows the result of the total calibrated output Discharge compared with the measured one. It is possible to evaluate a general good fit of the two curves even if there is an overestimation of the final part of simulated depletion curve of the hydrograph. In fact, it was not possible to reach a perfect calibration of the groundwater flow component as showed in Figure 3.40(2).

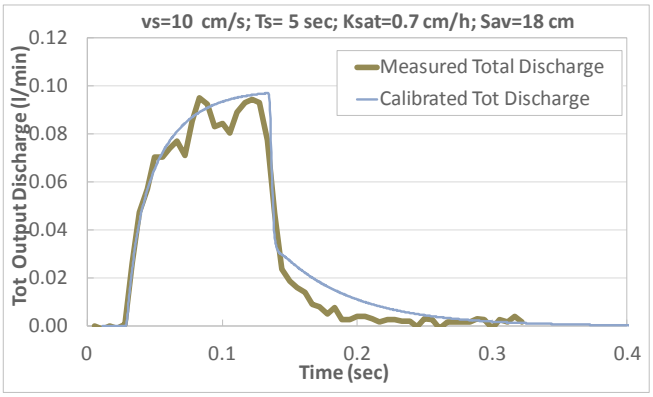

Figure 3.41. Total calibrated output discharge compared with the measured one

It is possible to notice that the simulated hydrogram fails to represent well the double peak present in the observed outflow. From a theoretical point of view in fact in the case of a constant rainfall, the hydrological behavior should be that described by the model. The double peak in the measurements can be explained by the observation of Figure 3.42. It is noted that in correspondence with the minimum in the runoff after the first peak, there is a peak of the groundwater outflow. On the basis of laboratory observations, it is believed that this behavior is due to the combination of two occurances:

- the excavation and the subsequent filling of temporary ponds of water distributed over the overall terrace area;
- the formation of sudden holes in the soil terrace upstream the dry stone wall which later are closed thank to the sediment transported from the incoming overlandflow.

It is clear that this kind of phenomenon can not be represented by the current model.

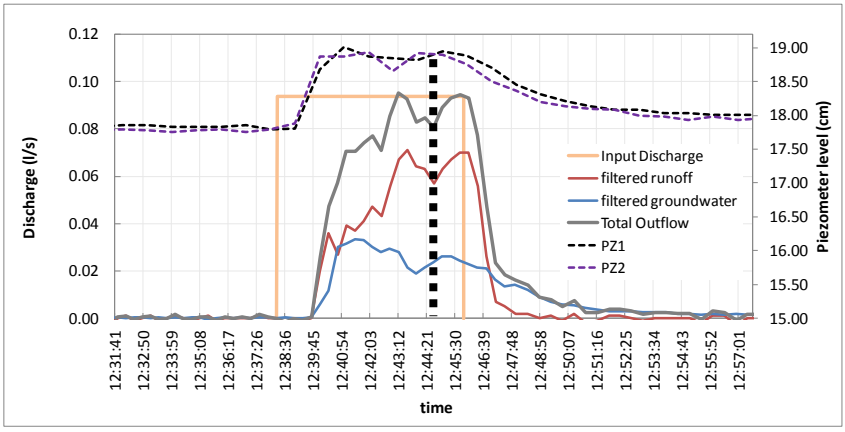

Figure 3.42. Explanation of the double peak in the observed runoff

The final calibrated parameter for the test 3 are reported in Table 3.15. This table contains the calibrated parameters for each one of the experimental tests characterized by a bare soil and the following statistical indices for the calibration evaluation:

$$I_{vol} = \frac{TotVol_{sim} - TotVol_{mis}}{TotVol_{mis}} \qquad (3.30)$$

$$I_{Qpeak} = \frac{Qpeak_{sim} - Qpeak_{mis}}{Qpeak_{mis}} \qquad (3.31)$$

where I_{vol} is the "volumetric index" obtained from the percentage difference between the simulated and measured water volume in output and I_{Qpeak} is the " peak discharge index" obtained from the percentage difference between the simulated maximum discharge and the measured maximum discharge in output.

The calibration results show that the 90% o tests have values of I_{vol} ranging between -25% and 25% and values of I_{Qpeak} ranging between -30% and 24%. The 61% of tests have and I_{vol} between -6% and 12% while the 57% of tests have an I_{Qpeak} between -15% and 15%. Only two tests have negative values of I_{vol}. This means that there is a general overestimation of simulated output volumes. This can be explained considering that the mathematical model does not take into account any water losses as well some additional water storage into the soil at the end of the experiment.

Test	V_s (cm/s)	T_s (s)	*Ksat* (cm/h)	*Sav* (cm)	T_{gw} (s)	V_{gw} (cm/s)	I_{vol}	I_{Qpeak}
1	15	5	2	18	1000	13.89	73.91%	23.26%
2	9	20	0.15	18	50	0.21	-32%	5%
3	10	5	0.7	18	350	1.45	8%	3%
4	6	5	0.08	18	300	2.78	-1%	-17%
5	8	10	0.4	18	80	2.78	22%	1%
6	5	5	0.3	18	300	2.78	1%	-9%
7	8	5	0.08	18	400	1.39	-6%	-6%
8	3	10	0.4	18	1000	0.14	21%	13%
9	10	5	0.08	18	50	1.39	3%	-9%
10	10	30	0.8	18	50	2.78	3%	-28%
11	8	30	0.8	18	80	0.56	9%	-31%
12	4	5	0.3	18	100	1.39	8%	-30%
13	15	50	3	18	80	27.78	25%	5%
14	10	10	5	18	100	2.78	9%	-31%
15	8	10	3	18	100	2.78	24%	-27%
16	3	30	0.2	18	1000	13.89	16%	-16%
17	6	20	0.4	18	80	1.39	8%	-20%
18	8	10	0.6	18	40	2.78	4%	-15%
19	6	10	6	18	60	0.56	20%	-4%
20	2	40	0.3	18	100	0.28	12%	-14%
21	8	10	6	18	150	2.78	9%	-2%

Table 3.15. Calibrated Parameter and performance indices

3.6 Discussion of sections 3.3 and 3.5

VOLUMETRIC WATER CONTENT ANALYSIS

The 9 TDR sensors has been installed in order to analyze the moisture of the soil during the different experiments. The probes have been set to record the data every minute.

The analysis of the data recorded has been developed in order to have a great view on the trend of volumetric water content during the tests and beyond, giving importance to the differences between the initial and final conditions. Moreover, a further analysis has been

focused on the analysis of an overall value of volumetric water content in the soil for every test. Thanks to the analysis features, same remarks can be formulated.

Based on the analysis of the data recorded for every test it is possible to note how the variations on VWC changes after the closing of the input discharge also. After the input discharge has been stopped, the moisture of the soil follows different contrasting behavior: raising, decreasing or remaining stable. This phenomenon is due to the movement of water which continues even after the stop of the release of the liquid in the system.

A comparison of the overall volumetric water content for the three discharges is reported in the Figure 3.43 for a 3% slope. The figure reports the results for the first and second configuration. It is possible to see that passing from the first to the second configuration, the volumetric water content increments tend to zero. This should be due to the greater compaction of the soil that characterizes the second set of tests.

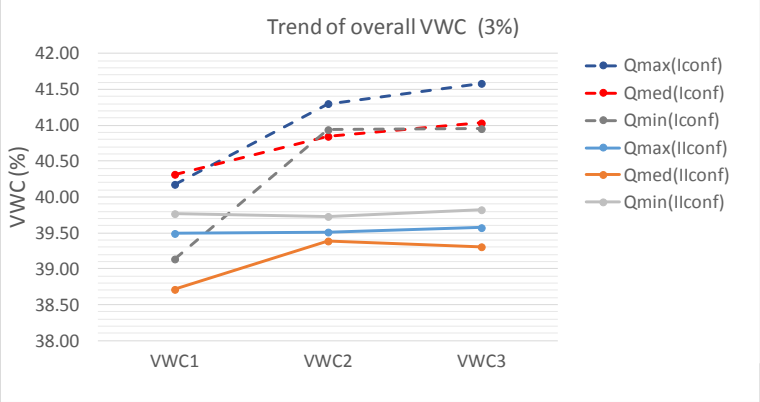

Figure 3.43. Trend of overall volumetric water content for the three different discharges at the 3% slope experiments. Comparison between the first and second configuration

The Figure 3.44 shows the globol results for the second configurations. The average volumetric water content trends have been reported for all the discharges and slopes.

The tests with 3% slopes show the lower increments of the humidity during the tests; the soil is very compacted, since several months passed from the first experiments; this leaded to a reduction of the infiltration rates.

Even in the test with 9% slope the soil moisture does not react since these tests were preceded by the test 15 (low initial degree of saturation), which lasts for more then 1 hour causing a large compaction of the soil.

The tests with a 6% slope reacts more in terms of humidity. In fact in this case the soil was reworked before the tests and the terrain is less compacted.

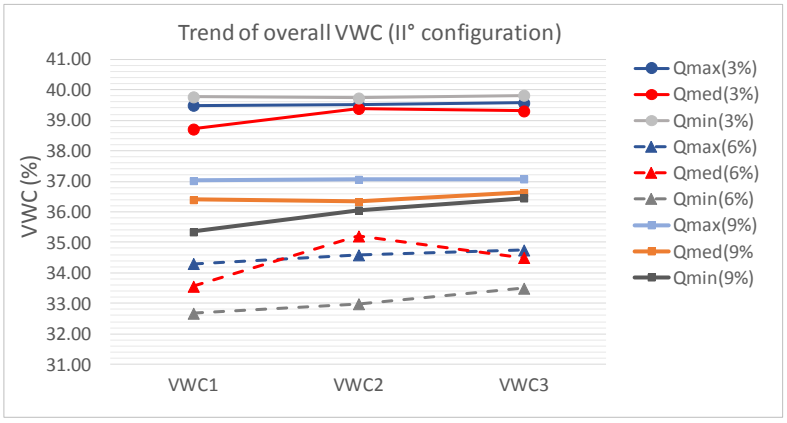

Figure 3.44. Trend of overall volumetric water content for the three different discharges, for all the slopes considered in the second configuration

HYDROLOGICAL ANALYSIS

In the previous part of this chapter, the results related with the hydrological analysis are reported in terms of characteristics response times.

It results necessary to match the different outcomes obtained and to analyze the response of the model even for other discharges.

When discrepancy it was found between the times from the first test and the replication, it results necessary to identify the cause of the different behavior. It has been carried on a comparison for the second configuration of the plot between the time 1 and the initial volumetric water content for the tests, in order to analyze whether the humidity of the soil can affect the response of the system.

In particular we expect that where the test takes more time is due lower humidity of the soil, that leads to a greater subtraction of the surface runoff.

In the Figure 3.45, the graphs related with this analysis has been reported for the minimum and maximum slopes. We expected greater values of volumetric water content are representative of the experiments that shows lower T1 due to the fact that a lower part of the initial input volume infiltrates and less time is needed to saturated the soil and consequently to trigger the surface runoff. This is evident for the % slope for the tests with the minimum discharge and for the 3% slope for the tests with the medium discharge; instead for the other cases the differences of initial volumetric water content is negligible and can not explain the difference of time T1 (which are in any case small). This analysis seems not to demonstrate clearly that for lower initial volumetric water content the runoff response is delayed.

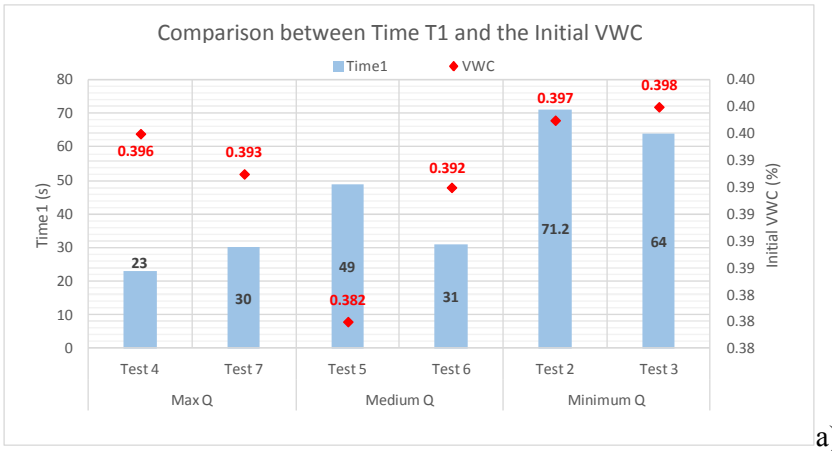

a)

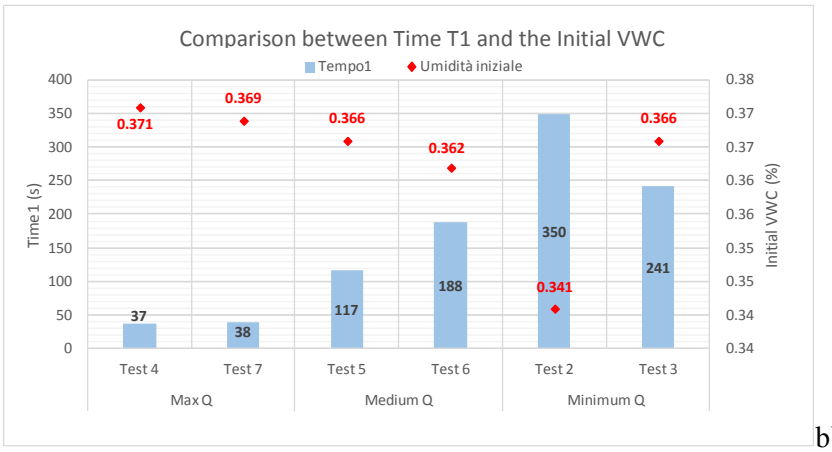

b)

Figure 3.45. Comparison between the recorded time 1 and the VWC at the beginning of the test; a)3%; c) 9%

The comparison between the discharges and the relative outcomes in terms of significative times (T1, T2, T3 and T4) has been processed for the surface runoff. In particular, the velocity of the surface water has been computed by dividing the space between the spillway and the toe of the wall for the time recorded. The velocity is so reported in cm/s and the space computed is equal to 380 cm, due to 300 cm of length of the slope and 80 cm related with the height of the dry-stone wall.

In the following graph (Figure 3.46) are reported the relationship of the different mean velocities computed for the time 1 and the discharges computed for all the slopes.

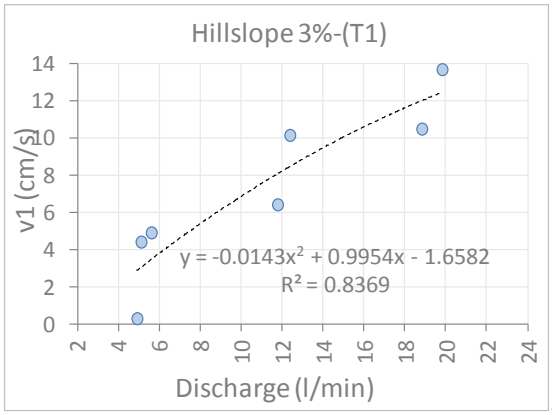

a)

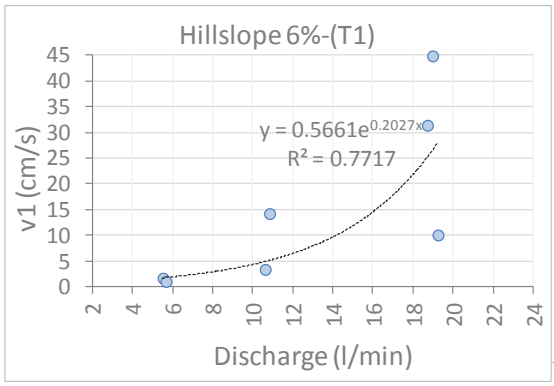

b)

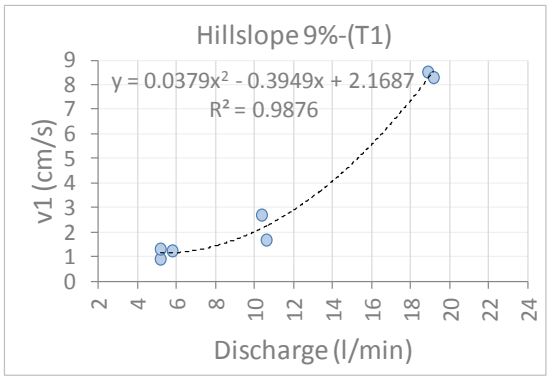

c)

Figure 3.46. Relationship between the time 1 recorded and the relative discharge; a)3%; b) 6%; c) 9%

For all the slopes, the time for the surface runoff to reach the base of the wall decreases with the increasing of the discharge. The Figure 3.47 reported the same results in terms of time. In particular, the relationship of the different times T1 analyzed and the discharges computed has been reported. It is possible to note that the variability ranges of time T1 decreases by increasing the input discharge; moreover the time values seem not be strictly dependent on the slopes in the case of maximum discharges.

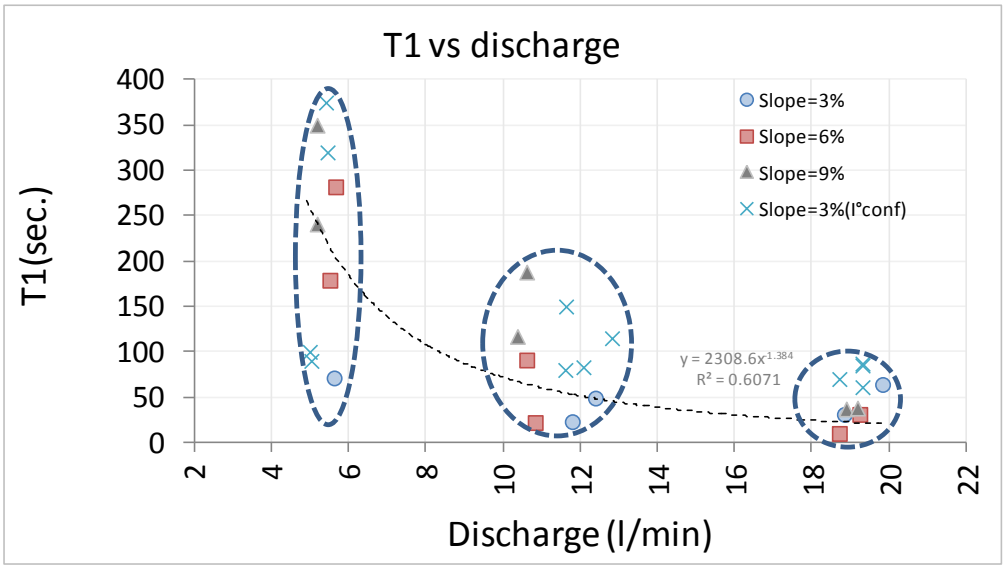

Figure 3.47. Response time T1 vs. discharge for all the slopes tested. For the 3% slope the first and second configurations results have been reported.

The same observation can be done by considering all the characteristic surface runoff response times (T1, T2, T3 and T4) as reported in Figure 3.48. In fact, the plot shows that the global hydrological response is faster in case of greater input discharges.

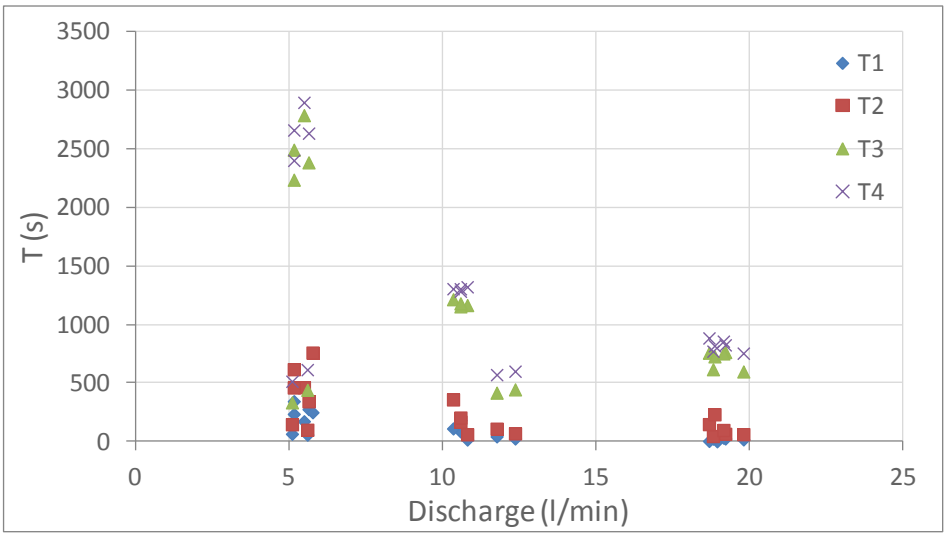

Figure 3.48. All characterists response times vs. input discharges

The concentration time of the terrace unit is represented by the Time T2. At this time, in fact, the entire area contributes to the formation of the outflow. The Figure 3.49 reports all the times T2 for the tests with "High initial degree of saturation" with different colours based on the respective slope. For the 3% slope the time T2 ranges from 0.86 and 2.55 minutes with an average value of 1.58 minutes; for the 6% slope the ranges is 0.48-5.81 minutes with an

average value of 2.34 minutes and for the 9% slope is 1.73-10.38 minutes with an average value of 5.5 minutes. In general it seems that by increasing the slopes the concentration time increases (that is routing velocity decreases in contrast) to what was expected. The casuses of this behavior have been studied by linking the Time T2 with all the boundary conditions (input discharge, initial soil moisture) and with the runoff coefficients. Considering the overall data togheter it was not possible to find useful evidences. One possible explanation derives from the observation that by increasing the slopes the relative roughness (depth/grain size) of the formed rills increased; this leaded to a delay of the response times.

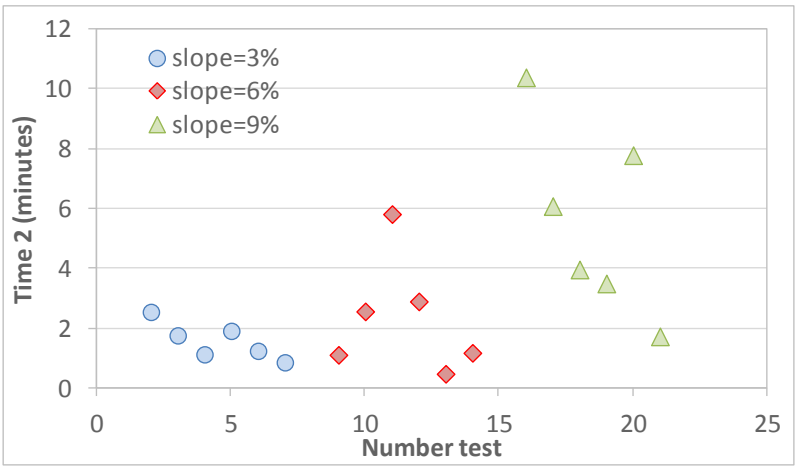

Figure 3.49. Concentration Time T2 for all the tests

Only for the 3% slope the relation between the time T2 and the input discharge shows a clear negative trends as shown in Figure 3.50. It means that, for this fixed slope, the response time decreases by increasing the input discharge which lead to an increases of surface runoff velocity. This fact is motivated by the absence of rill formation that instead characterize the greater slopes (6% and 9%). The wider variation for the 6% and 9% slope depends likely by the random formation of small rills differently affecting the overland flow propagation.

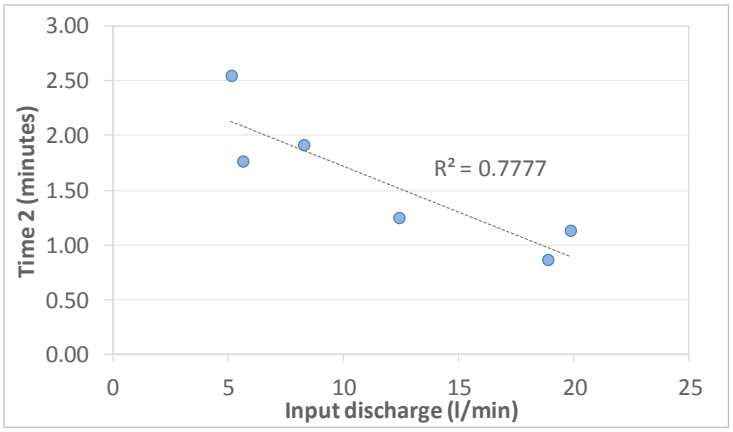

Figure 3.50. Concentration Time T2 in relation with the input discharge for the tests in the 3% slope

The depletion time of the terrace unit is represented by the difference between the Time T4 and the time T3. The Figure 3.51 reports all the depletion times for the tests with "High initial degree of saturation" with different colours based on the respective slope. For the 3% slope the depletaion time ranges from 2.56 and 3 minutes with an average value of 2.7 minutes; for the 6% slope the ranges is 1.01-4.15 minutes with an average value of 2.23 minutes and for the 9% slope is 1.5-2.8 minutes with an average value of 2.06 minutes. From these values it seems that time needed to drain the surface flow from the end of the irrigation decreases by increasing the slopes. It can also be observed in Figure 3.51 that for the 3% slope the range of variation of the depletion time remains very narrow for all modeled discharge.

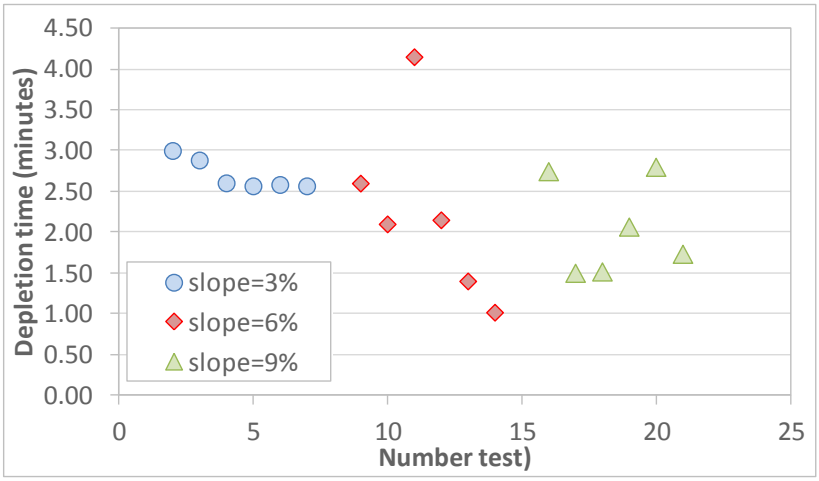

Figure 3.51. Depletion Time for the tests with "High initial degree of saturation"

An overall representation of the hydrological analysis in terms of total water volumes is reported in Figure 3.52 for the second configuration plot. It is possible to see that the runoff component is the main part of the output volume for every test.

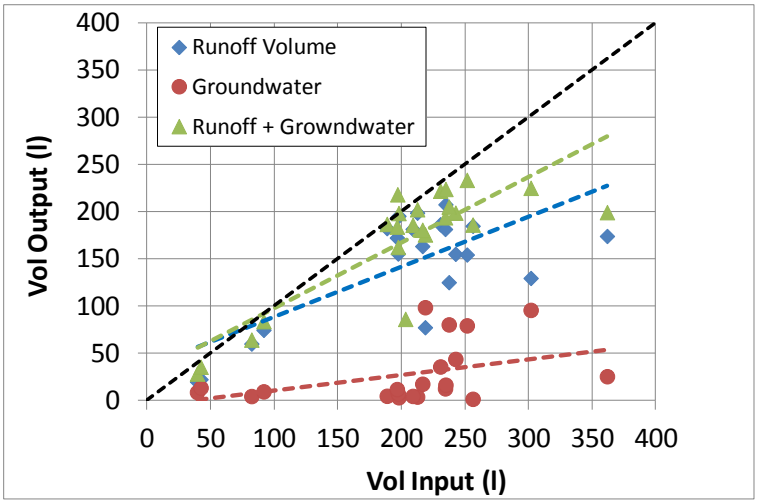

Figure 3.52. Input volumes vs. output volumes for the second configuration of the plot

COMPUTATION OF THE SPECIFIC CURVE NUMBER

The computation of the Curve Number has been applied in order to obtain a corrected value for the calculation of the runoff produced in a terraced area. The dry-stone wall represents break lines in the hillslope that can contributes to the surface runoff by the releasing of groundwater component. Therefore, the total superficial water generated by a terraced area is potentially greater than that of a normal hillslope. The computation of the Curve Number has been carried out by using the total amount of discharge recorded at the outlet, for the **terrace area** $\boldsymbol{CN_{ta}}$ and just the discharge produced by the runoff for a **traditional** ***CN***.

The computation gives back a similar range of values for what may concern the division according the two methods (Figure 3.53). Obviously, the *CN* related with the terrace system is greater due to the higher 'runoff' taken into consideration. In fact the average value of $\boldsymbol{CN_{ta}}$ is equal to 93.96 whereas the average value of ***CN*** is 88.98.

The points related with the computation of the curve number for the "low initial degree of saturation" tests are reported as separated series in the same plot; in case of the traditional *CN* they have low values as compared to the rest of the tests (with "high initial degree of saturation"). This fact can be explained considering that we can assume that "initial low water content" (test 1 and 15) represent medium antecedent moisture conditions *CN*(II) whereas "initial high water content" represent wet antecedent moisture conditions CN(III). The application of the following conversion equation

$$CN(III) = \frac{CN(II)}{0.43 - 0.0057(CN(II)} \qquad (3.32)$$

using as input the CN(II) of the tests 1 and 15 (72 and 88 respectively), returns CN(III) values equal to 85 and 95. These values are inside the variability ranges of the rests of the tests, which are associated to wet antecedent moisture content.

The high values of Curve Number reflect on high runoff coefficients. The Figure 3.54 reports the runoff coefficients derived directly from the observations and calculated as the ratio between the measured runoff volume and the total measured input volume. In particular, the range obtained in this research goes from 0.35 to 0.98 with an average value equal to 0.70.

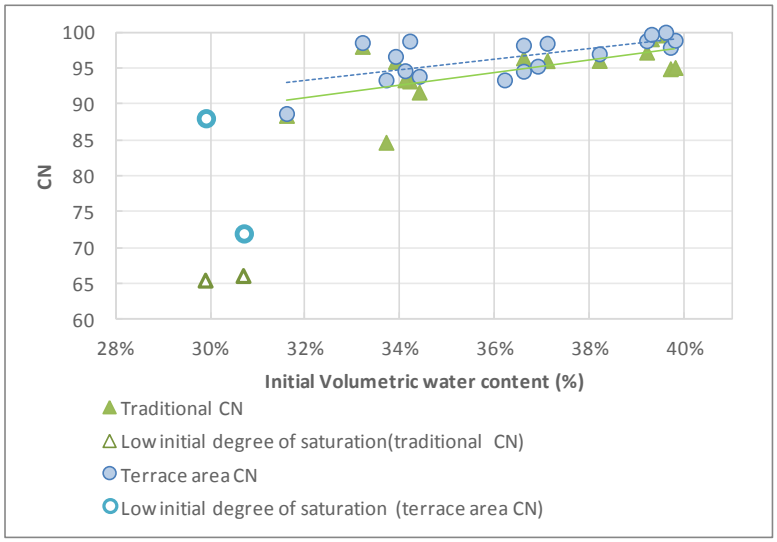

Figure 3.53. Traditional CN compared with the terrace area CN for all the experiments in the 2° conf. of the plot. The regression lines exclude the tests characterized by low initial degree of saturation.

The tests characterized by "low initial degree of saturation" (1 and 15), the one with lower initial groundwater table (19) and the tests with a grass cover (22) have runoff coefficients lower than 0.5. These values are lower respect to what is reported in the literature. For example Zhang et al. (2008) indicated that the runoff coefficient from sloping terraces with grasses and trees was only 3% in hilly areas of the Sichuan Basin (southern China). Gardner & Gerrard (2003), who measured runoff and soil erosion from plots on outward sloping agricultural terraces with slope angle approximately of 5° (8%), found Runoff coefficients (water running off the plot as a percentage of the total volume of water entering by rainfall) for individual rainfall events varied considerably from less than 5% to over 50%, depending on the nature of the event and the terrace. Van DiI Jk and Bruijnzeel (2004) found that runoff coefficients associated with terrace beds (16–26%) and that the runoff from terrace beds with appreciable vegetation cover was generally less than that from bare plots, especially under mixed cropping (0.1–24%).

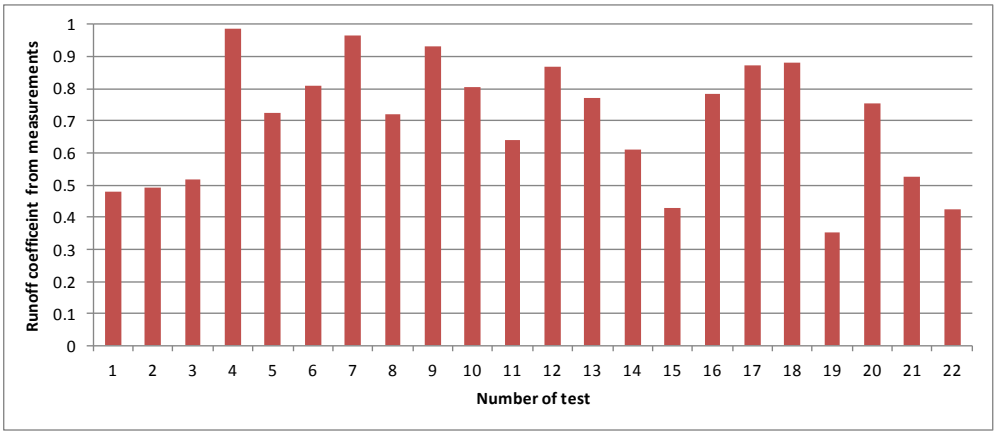

Figure 3.54. Runoff coefficients calculated from the measurements

The values obtained - both for CN and runoff coefficient - result rather elevated in respect of what is reported by the literature. This phenomenon is probably related with the following factors which can positive influence the production of runoff:

- The decided input discharges are non-representative of real precipitation events but they are more intense, considering their duration and continuity, if compared to real rain events;
- The physical model is contained on a metal box representing a closed system. Therefore, when the groundwater and the soil are totally saturated, the only path that the water can follow is toward the outlet of the model.
- The groundwater storage in the second configuration is very low since the initial groundwater table was set close to the threshold level that triggers the groundwater outflow.
- Compared to real field cases, no leakage losses to the deep layers of the soil are considered (e.g. water contribution to fractured rocky soil below the foundation level of the wall).

SURFACE AND SUBSURFACE WATER MOVEMENTS

The approach adopted during the laboratory experiments leads to gain new insight on surface and subsurface water movements in a terraced slope. In particular, some experimental evidences of the hydrological mechanisms responsible for water accumulation behind dry-stone walls that were missing in the specific literature.

In general, in all the tests it has been observed a particular phenomenon described in Preti et. al (2017). The flooding experiments performed showed the fast formation of infiltration excess overland flow, in agreement with previous studies (Gallart et. al, 2002; Gallart et al., 1994). Surface runoff moves downward with very high velocity (up to15 cm/s) following the surface topography and comes out from the top of the wall.

Part of the surface runoff encounters piping systems and local fractures, where water infiltrates very rapidly flowing in the subsurface until finding the upslope face of the wall, where it accumulates eventually emerging at the bottom and the downslope face of the dry-stone walls. Other pipes were probably created artificially during the excavation for the positioning of the probes.This fast subsurface flow (if existing) is added to the general small groundwater flow generated by the infiltration processes occurred in the part of soil not interested by piping. The overall subsurface flow exfiltrates from the base of the wall.

The piping system and local cracks arise and increase close to the wall, close to the lateral panels and just downstream the input spillway; the extension of the piping system varies test by test. This is in accordance to what is reported in Romero Diaz et al.(2007): “the heterogeneity and discontinuities of the subsurface leads to development of piping and localized zones of fast infiltration”. This, in turn, facilitates the formation of preferential flow pathways that, as often occurs also in natural hillslopes (e.g. Penna et al., 2015a, 2015b), sustains the development of subsurface hydrological connectivity within the slope.

Another behaviour that has been observed is the following: during the tests, the eroded soil produced and transported by the surface runoff progressively tended to close the underground pipelines close to the wall. During each test it has also been observed the excavation and the subsequent filling of temporary ponds of water distributed over the overall terrace area. These temporal storages led to an intermittend behaviour of the surface runoff outflows. The erosions processes are greater for larger slopes where the surface water tends to channelization in small rills with a rambling trend and this cause a modification of the response times (Figure 3.55). Moreover, in the case of dry initial conditions, some important cracks were observed in the soil and the surface water started only after their saturation.

Contrary to what is reported in the conceptual sketch of water flow pathways in a terracese bench proposed in Preti et al. (2017) in all the tests of this work a great part of the surface runoff (runoff coefficients always greater than 0.35) has been observed and recorded from coming out from the top of the wall. This is due to the fact that in the current physical model the surface layer of the soil, once wet, is very compact and the infiltration is very small

(especially for uncultivated soils) also upstream to the wall. In fact, the infiltration rates are mainly related to the pipying system and the preferential flow pathways.

Figure 3.55. Erosions processes and channelization in small rills

The Figure 3.56 shows a typical hydrological behavior in a test characterized by an important piping system. When the piping system is activated the runoff decreases and the groundwater depth increases. Then the piping is turned off thanks to the sediment feeding from the upper soil and the total outflow is represented only by the surface runoff component.

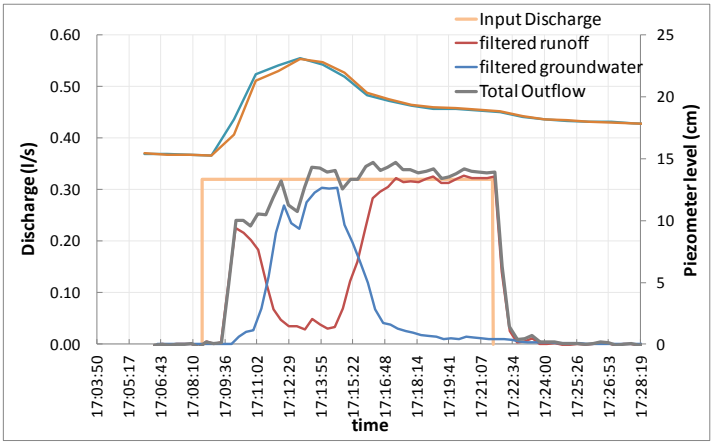

Figure 3.56. Hydrological response in case of piping (Test 14)

Finally it has been studied the maximum dry time interval between two consecutive tests for which it is possible to have favorable conditions to produce runoff. In the Table 3.16 all the tests are ordered on time. Here, is reported the percentage variation of **traditional *CN*** and the corresponding time interval from the previous test. A *CN*=85 has been chosen as threshold to characterize the tests with high satured conditions. Each test was marked in bold if it exceeded this threshold and also if its previous test respected this condition.This analysis shows that the maximum dry interval period to maintain high saturated conditions resulted to be equal to 24 hours.

Number of Test	*CN*	*CN variation from the previous test (%)*	*Time interval from the previous test (hour)*
1	66.02		
2	94.91	43.8%	241.5
3	**95.08**	0.2%	1
4	**99.60**	4.8%	3
5	**96.06**	-3.6%	19
6	**97.22**	1.2%	1
7	**99.07**	1.9%	1.5
8	88.42	-10.8%	285
9	**98.02**	10.9%	24
10	**93.21**	-4.9%	24
11	84.68	-9.2%	168
12	95.93	13.3%	96
13	**91.66**	-4.5%	24
14	82.67	-9.8%	48
15	65.39	-20.9%	120
16	93.37	42.8%	24
17	**96.42**	3.3%	2
18	**96.04**	-0.4%	22
19	65.42	-31.9%	120
20	91.42	39.7%	24
21	66.02	-14.7%	24

Table 3.16. Dry time interval between two consecutive tests

DISCUSSION ON THE MODEL RESULTS

The modeling results described in the section 3.5 were analyzed in order to evaluate the efficiency of the calibration and the parameters variability.

In order to extract the best simulations it is possible to calculate a global efficeny index I_{global} *using the following equation applied to the data reported in*

Table 3.15:

$$I_{global} = |I_{vol}| + |I_{Qpeak}| \qquad (3.33)$$

where I_{vol} is the volumetric index and I_{Qpeak} is the "peak discharge index" already defined in 3.5. The Table 3.17 reports the list of tests ordered in descending order of I_{global}.

Test	I_{vol}	I_{Qpeak}	I_{global}
6	**1%**	**-9.0%**	**10%**
21	**9%**	**-2.0%**	**11%**
3	**8%**	**3.0%**	**11%**
9	**3%**	**-9.0%**	**12%**
7	-6%	-6.0%	12%
4	-1%	-17.0%	18%
18	4%	-15.0%	19%
5	22%	1.0%	23%
19	20%	-4.0%	24%
20	12%	-14.0%	26%
17	8%	-20.0%	28%
13	25%	5.0%	30%
10	3%	-28.0%	31%
16	16%	-16.0%	32%
8	21%	13.0%	34%
2	-32%	5.0%	37%
12	8%	-30.0%	38%
11	9%	-31.0%	40%
14	9%	-31.0%	40%
15	24%	-27.0%	51%
1	74%	23%	97%

Table 3.17. Tests ordered in descending order of calibration efficiency

The Figure 3.57 shows the four best simulations which have a global index I_{global} ranging from 10% (test 6) and 12% (test 9). The worst simulations are the tests 15 and 1 that have a global index of 51% and 97.2%, respectively. This last two tests were characterized by "low initial degree of saturation" and are plotted in Figure 3.58. In this cases it is possible to note that the hydrological response is quite different from the theoretical one rapresented by the HydroTerraceModel. For example, the fact that the maximum output discharge is greater than the uniform input discharge is something not possible from the theoretical point of view. It means that during a real experiment the physical processes are more complicated than the

ones rapresented by a simple model, e.g. some unconsidered soil macroporosity/irregularity associated to certain experiments.

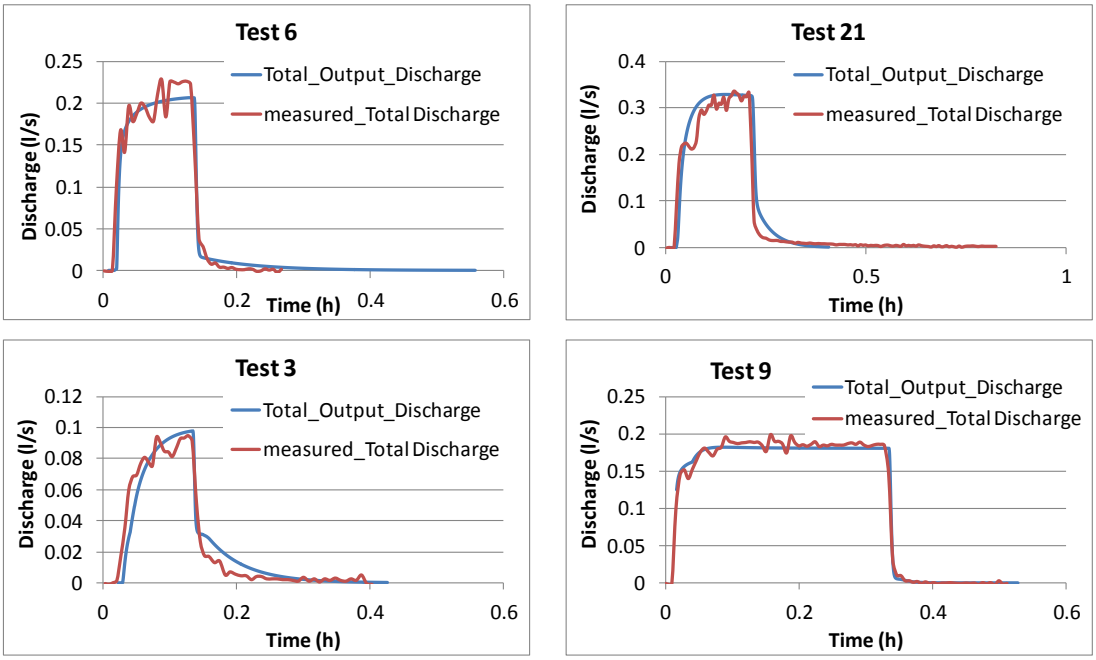

Figure 3.57. The forr best simulations a) test 6; b) test 21; c) test 3; d) test 9;

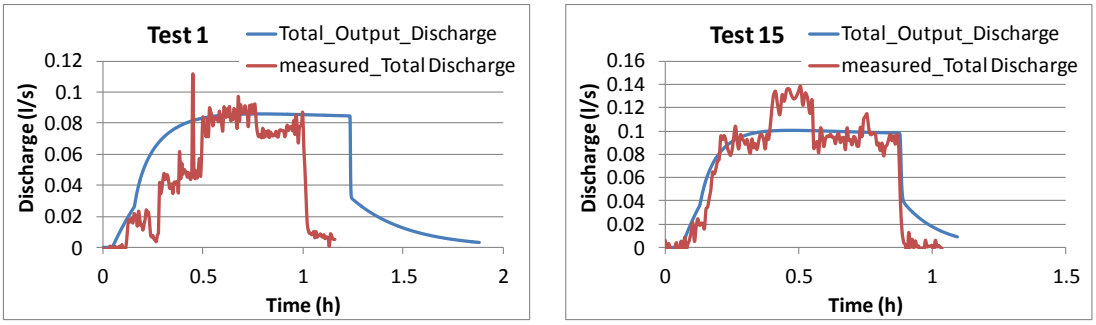

Figure 3.58. The two worst simulations a) test 1; b) test 15: in blue line the simulated values

For each kind of parameter, the calibrated values for each test have been visualized in Figure 3.59. The "Surface velocity" V_s ranges from 2 to 15 cm/s with an average value of 7.7 cm/s. The parameter "mean residence time for surface runoff " T_s ranges from 5 to 50 s with an average value of 15.48 s. The parameter "average suction at the wetting front" *Sav* is equal to 18 cm for all the tests. The parameter "satured hydraulic soil conductivity" *Ksat* ranges from 0.08 to 6 cm/h with an average value of 1.46 cm/h. The parameter "mean residence time for groundwater" T_{gw}" ranges from 40 to 1000 s with an average value of 260.47 s. The parameter "Infiltration velocity" V_{gw} ranges from 0.14 to 27.78 cm/s with an average value of 4.12 cm/s.

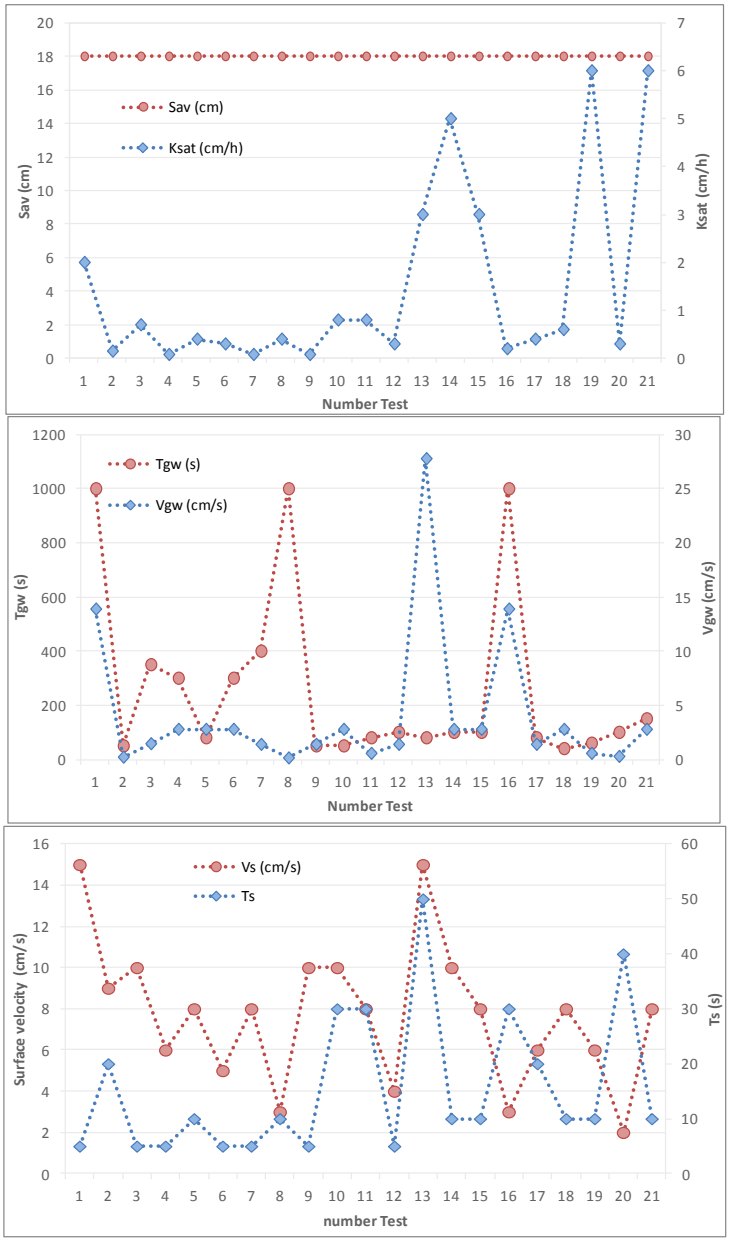

Figure 3.59. Trends of the calibrated parameters: a) V_s and T_s; b) Sav and K_{sat}; c) V_{gw} and T_g

The analysis of possible relations between the calibrated parameters and some of the boundary variables returns some additional evidences. The Figure 3.60 shows the surface velocity parameter V_s as very weakly correlated (R^2= 0.0634) to the input discharge; the plotted trend indicates how the surface velocity increases slowly with the discharge. This behavior is in accordance with the basics of hydraulics considering a low variability of the overland flow depth among all the tests; the significancy of the correlation is anyway extremely poor (R^2= 0.151).

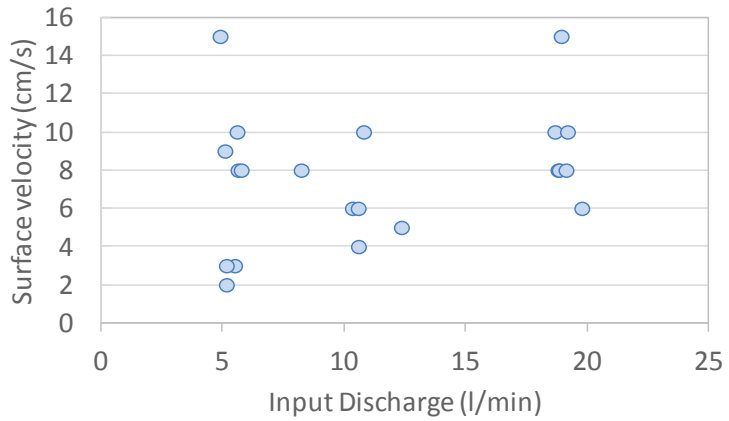

Figure 3.60. The relation between the parameter velocity vs the input discharge

The Figure 3.61 show the saturated conductivity parameter as function of the terrace slope; the results would seem demonstrating that the permeability increases if the terrace slope increases (the plotted correlation is only indicative being its significancy unsatisfactorily).

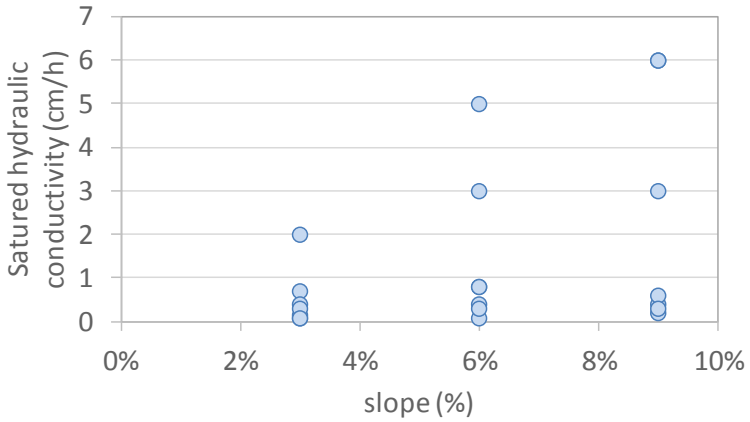

Figure 3.61. The relation between the slope and the saturated conductivity ksat

This last behavior can be explained by the observations made in laboratory. These have shown that the erosion processes increased if the terrace slope increased. So with the higher slope erosion is such as to form underground channels that increase the infiltration rates and can motivate the scatter of the calibrated values of the saturated hydraulic conductivity.

An analysis that was not addressed in this work but that would be interesting is to try to simulate the different tests using an average set of parameters. The evaluation of these results would be a useful in view of considering to use of this model in a real terrain context for which no calibration measures are available and for which boundary conditions may be very variable.

4 CONCLUSIONS

This work investigates the hydrological response of a bench terrace based on a mix of mathematical modelling and experimental research approaches.

- **On the Chapter 2**

A numerical modelling of a hypothetical pilot area resulted in a valuable approach to assessing the hydrological function of bench-terraces. Two indices were introduced to quantify the peak-discharge delay and reduction: the LTI and the PRI (symbol fully explained at pag. 28).

The first index consisted of a time-to-peak increment of the flood hydrograph scaled to a time-to-peak in a no terraces scenario. The second index indicated a peak discharge reduction scaled to a peak discharge prior to terrace building. The indices provided some simple relationships between the covered areas as expressed through a terrace-degree index (TDI) and flood hydrograph characteristics at a hillslope outlet. Via the simulation results, it was shown that the LTI increases with the TDI according to a parabolic function and the PRI follows a very distinct logarithmic dependence on the TDI.

Based on these estimations, and when overall conditions are not overly different from those of the pilot area, it can be concluded that a TDI of 15% is the lowest benchmark for minimum hydrological effects and that a TDI of 35% is a medium acceptable benchmark for warranting a significant hydrological benefit (PRI ≅ 60%). High flood peak delays (well suited to a runoff desynchronization at a basin scale) and reductions may also occur (LTI≅ 850%; PRI ≅ 90%) if the TDI is raised to 70%. All these hydrological benefits are mostly ascribable to the portion of the pilot area featured by a topographical outward-sloped stepped topography that delays the concentration time of the runoff.

An extension of this analysis to other topographical conditions and rainfall inputs could lead to a better understanding of bench-terrace efficiency for flood mitigation. This future investigation could test an alternative infiltration model accounting for throughflow within the soil layer and water exfiltration from terrace walls.

- **On the Chapter 3**

A long set of experimental tests were realized on a hillslope plot bounded by a dry-stone wall in order to understand the main hydrological processes which act in a terraced landscapes with dry-stone. This topic is of critical importance for correct strategies of water resource

management, agricultural practices and rural landscape maintenance. A conceptual model was then implemented to reproduce and explain the laboratory results.

This experimental research allowed to provide new laboratory evidences about the hydrological mechanisms that characterized a dry stone terrace and quantify the hydrological response in terms of response times and runoff production. Thanks to the physical model monitored by means of several hydrological devices, different hydrological analyses have been carried out; in particular, the outcomes obtained are related with three different analysis described as:

- Volumetric water content analysis: study of the variation of the humidity during different stages of the experiment;
- Hydrological analysis: study of the response in time of the water considering the surface and groundwater component;
- Computation of a specific curve number for a terraced area, relative comparison with the traditional curve number and values from literature.

The performance of the tests have been carried out by the release of a laminar sheet of water for a selected period of time. The tests are divided according to the initial humidity condition of the terrain, high/low degree of saturation, and three different decided discharges; maximum equal to 19.50 l/min, the medium of about 12 l/min and the minimum equal to 5 l/min. A total of 33 experiments have been performed with a bare soil and 2 tests where performed over the terrace cover with grass.

The pioneering experiences with the physical model have produced some significant results and discussion which represent useful information that helps to understand the hydrological behavior of the system. The volumetric water content analysis produced by the 9 TDR sensors installed was able to provide an overview of the trend of humidity in the soil during the experiments and important indications for a correct sensors setting.

The hydrological analysis gives back great results in terms of time of response of the different component of output discharge. In particular, it was possible to identify the different times needed for the surface runoff as the groundwater to reach the outlet.

The computation of a “terrace area curve number” and the relative comparison with the “traditional curve number” results in high values for both the methods. The first method results greater values since it is calculated assuming as output volume the sum of the surface runoff and the groundwater. In general the runoff coefficients from all the experiments are greater than the values reported in literature due to the specificity of the experiments (confined waterproof box, upstream input and no rain falling over the box, wet initial

conditions for the most part of the tests). The “terrace area curve number” is most representative than the “traditional curve number” in case of a sequence of terraces since the input discharge to a downstream terrace is given by the sum of the surface and groundwater runoff produced by the upstream terrace. However the experimental tests showed similar results for the two methods since the groundwater component is in general a small part of the total outflow volume.

Moreover the experimental observation showed that the soil and the subsurface structure of the terrace are highly spatially heterogeneous. This facilitates the formation of preferential flow pathways that lead to high vertical infiltration rates and the development of rapid subsurface flow. The heterogeneity of the terrace bench also includes piping systems where runoff immediately disappears.

The implemented conceptual hydrological model fits well the experimental data, especially it is able to reproduce the different water balance components with a good efficiency. Some tests characterized by a strong influence of piping were not well reproduced by the model in terms of peak discharges. This is due to the fact that the piping processes lead to a very impulse response of groundwater that the model is not able to simulate. In general the groundwater is not well simulated by the linear storage model implemented; a possible improvement could be the use of a physical 2D model to simulate the groundwater flow hypothesising a random location of the pipes.
Finally, it has been demonstrated that an integrated experimental approach involving physical and mathematical modelling is useful to understand the hydrological functioning related to a bench terrace system.

The results summarised above could be used in the future to merge in next investigations the findings from the mathematical model at a small-plot scale (simulation of one terrace unit with the developed HydroTerraceModel) with the propagation features that have emerged from modelling a bench terrace system at the hillslope scale. According to our outcomes, this merging is, in fact, essential, because the flood responses for very humid antecedent conditions and impermeable terrain below the base of the terraces might results in an unattended worst scenario of damage for hillslope and mountain territory.

5 REFERENCES

Agnoletti M, SantoroA, Emanueli F, Maggiari G, Preti F. 2012. Terracing and hydrogeological risk. A study of the environmental disaster of 25 October 2011 in Cinque Terre. In: Agnoletti, M., Carandini, A., Santagata, W. (Eds.), Florens 2012 Essays and researches. Bandecchi & Vivaldi Editori- Stampator, Pontedera 25–46.

Al Qudah K, Abdelal Q, Hamarneh C, Abu-Jaber N. 2016. Taming the torrents: the hydrological impacts of ancient terracing practices in Jordan. Journal of Hydrology 542: 913–922. https://doi.org/10.1016/j. jhydrol.2016.09.061.

Arnáez J, Lana-Renault N, Lasanta T, Ruiz-Flaño P, Castroviejo J. 2015. Effects of farming terraces on hydrological and geomorphological processes. A review. CATENA 128: 122–134. https://doi.org/10.1016/j.catena.2015.01.021.

Arnáez J, Lasanta T, Errea M.P, Ortigosa L. 2011. Land abandonment, landscape evolution, and soil erosion in a Spanish Mediterranean mountain region: the case of Camero Viejo. Land Degrad. Dev. 22, 537–550.

Beach T, Dunning N.P. 1995. Ancient Maya terracing and modern conservation in the Petin Rain Forest of Guatemala. J. Soil Water Conserv. 50, 138–145.

Beach T, Luzzadder-Beach S, Dunning N, Hageman J, Lohse J. 2002. Upland agriculture in the Maya Lowlands: ancient Maya soil conservation in Northwestern Belize. Geogr. Rev. 92, 372–397.

Bertolo P, Wieczorek GF. 2005. Calibration of numerical models for small debris flows in Yosemite Valley, California, USA. Natural Hazards and Earth System Sciences 5: 993-1001.

Beven, K.J.Rainfall-Runoff modeling: the primer, 2002, John Wiley & Sons, LTD.

Bouwer, H. 1969. Infiltration of water into nonuniform soil. J. Irrigation and Drainage Division of ASCE 95:451-462

Brandolini P, Cevasco A, Capolongo D, Pepe G, Lovergine F, Del Monte M. 2016. Response of terraced slopes to a very intense rainfall event and relationships with land abandonment: a case study from Cinque Terre (Italy). Land Degradation and Development. https://doi.org/10.1002/ ldr.2672.

Branduini P. 2009. Il ruolo dei muri a secco nella salvaguardia del paesaggio. In: Accademia dei Georgofili. 2009. Muri di sostegno a secco: aspetti agronomici, paesaggistici, costruttivi e di recupero. Polistampa Ed.

Buzzanca G. 2016. Analysis of the hydrological behavior of a terrace system: pioneering experiments of physical modeling. Master degree thesis. Department Tesaf, University of Padova.

Camera C, Apuani T, Masetti M. 2011. Parametrization of a dry retaining wall on a terraced slope in Valtellina (Northern Italy) and stability analysis. Procedings of the 8th international symposium on Field Measurments in GeoMechanics, Berlin.

Camera C, Masetti M, Apuani T. 2012. Rainfall, infiltration, and groundwater flow in a terraced slope of Valtellina (Northern Italy): field data and modeling. Environmental Earth Sciences 65: 1191-1202. DOI:10.1007/s12665-011-1367-3.

Camera C, Apuani T, Masetti M. 2014. Mechanisms of failure on terraced slopes: the Valtellina case (northern Italy). Landslides 11: 43–54. https://doi.org/10.1007/s10346-012-0371-3.

Cammeraat, L.H. 2004. Scale dependent thresholds in hydrological and erosion response of a semi-arid catchment in southeast Spain. Agric. Ecosyst. Environ. 104, 317–332.

Chow VT, Maidment DR, Mays LW. 1988. Applied Hydrology. McGrawHill Book Company, NY.

Chu, ST. 1978. Infiltration during unsteady rain. Water Resources Research. 14(3):461-466.

Cots-Folch R, Martı`nez-Casasnovas J.A, Ramos M.C. 2006. Land terracing for new vineyard plantations in the north-eastern Spanish Mediterranean region: landscape effects of the EU Council Regulation policy for vineyards' restructuring. Agric. Ecosyst. Environ. 115, 88–96.

Critchley,W.R.S. and Bruijnzeel, L.A. 1995. Terrace risers:erosion control or sediment source? In Singh, R.B. and Haigh, M.J. (eds), Sustainable reconstruction of highland and headwater regions. Oxford and IBH Publishing, New Delhi: 529–41.

Critchley,W.R.S., Sombatpanit, S. and Medina, S.M. 2001.Uncertain steps? Terraces in the tropics. In Bridges, E.M., Hannam, I.D., Oldeman, L.R., Penning de Vries, F.W.T., Scherr, S.J. and Sombatpanit, S. (eds), Response to land degradation. Science Publishers, Enfield, NH: 325–38.

Crosta GB, Dal Negro P, Frattini P. 2003. Soil slips and debris flows on terraced slopes. Natural Hazards and Earth System Sciences 3: 31–42. https://doi.org/10.5194/nhess-3-31-2003.

D'Agostino V, Bettella F, Pozza E. 2012. Rheological assessment of a debris flow from the laboratory experiments to the real scale modeling.Proceedings of the 12th Congress INTERPRAEVENT 2012, Grenoble.

Dipartimento della Protezione Civile. 2008. Analisi regionalizzata delle precipitazioni per l'individuazione di curve segnalatrici di possibilità pluviometrica di riferimento. Relazione del Commissario Delegato per l'Emergenza concernente gli eccezionali eventi meteorologici del 26 settembre 2007 che hanno colpito parte del territorio della Regione Veneto. OPCM n. 3621 del 18/10/2007.(in Italian).

Douglas T.D, Critchley D, Park G.J. 1996. The deintensification of terraced agricultural land near Treve´ lez, Sierra Nevada, Spain. Global Ecol. Biogeogr. Lett. 5, 258–270.

Douglas, T.D, Kirkby S.J, Critchley R.W, Park G.J. 1994. Agricultural terrace abandonment in the Alpujarra, Andalucı´a, Spain. Land Degrad. Rehabil. 5, 281–291.

Dunjo´ G, Pardini G, Gispert M. 2003. Land use change effects on abandoned terraced soils in a Mediterranean catchment, NE Spain. Catena 52, 23–37.

Donkin, R.A. 1979. Agricultural Terracing in the Aboriginal New World Viking Fund Publications in Anthropology, vol. 56. University of Arizona Press, Tucson.

Dunning N.P, Beach T, Farrell P, Luzzadder-Beach S. 1998. Prehispanic agricultural and adaptive regions in the Maya Lowlands. Cult. Agric. 20, 87–101.

Fang, Z.S, Zhou P.H, Liu Q.D, Liu B.H, Ren L.T. and Zhang H.X. 1981. Terraces in the loess plateau of China. In Morgan, R.P.C. (ed.), Soil conservation: problems and prospects. Wiley, Chichester: 481–513.

Fathi-Moghadam M, Kashefipour M, Ebrahimi N, Emamgholizadeh S. 2011. Physical and Numerical Modeling of Submerged Vegetation Roughness in Rivers and Flood Plains. Journal of Hydrologic Engineering16: 858–864.

Flo-2D, 2009. Flo-2D Basic References Manual (www.flo-2d.com).

Gachene, C.K.K., Jarvis, N.J., Linner, H., Mbuvi, J.P. 1997. Soil erosion effects on soil properties in a highland area of central Kenya. Soil Sci. Soc. Am. J. 61, 559–564.

Gallart F, Llorens P, Latron J. 1994.Studying the role of old agricultural terraces on runoff generation in a small Mediterranean mountainous basin. Journal of Hydrology159: 291-303.DOI:10.1016/0022-1694(94)90262-3.

Gallart F, Latron J, Llorens P. 2005, Catchment dynamics in a Mediterranean mountain environment: the Vallcebre research basins (South Eastern Pyrenees). I: Hydrology, in: C.

Garcia and R. Batalla (editors), Catchment Dynamics and River Processes: Mediterranean and other climate regions. Elsevier, Amsterdam, pp 1-16.

Gallart F, Latron J, Llorens P, Martínez-Carreras. N. 2009. Hydrology in a Mediterranean mountain environment, the Vallcebre Research Basins (North Eastern Spain). IV. Testing

hydrological and erosion models. Proceedings of the Congreso Internacional sobre Desertificación, Congresos Científicos de la Universidad de Murcia, 16 septiembre, 2009 – 18 septiembre, 2009. http://congresos.um.es/icod/icod2009/paper/viewFile/4061/4001

Gallart F, Llorens P, Latron J, Regüés D. 2002. Hydrological processes and their seasonal controls in a small Mediterranean mountain catchment in the Pyrenees. Hydrology and Earth System Sciences 6: 527–537.

Gardner RAM, Gerrard AJ. 2003. Runoff and soil erosion on cultivated rainfed terraces in the Middle Hills of Nepal. Applied Geography23: 23-45.

Green WH, Ampt G. 1911. Studies in soil physics, part I - the flow of air and water through soils. Journal of Agricultural Science4:1-24.

Greppi C. 2007. Ciglionamenti e terrazzamenti nella Toscana centrale: dal passato al futuro, Paesaggi terrazzati: culture e esperienze a confronto. Venezia.

Grove AT, Rackham O. 2003. The nature of Mediterranean Europe: an ecological history. Yale University Press: New Haven

Healy P.F, Lambert J.D, Arnason J.T, Hebna R.J. 1983. Caracol, Belize: evidence of ancient Maya Agricultural Terraces. J. Field Archaeol. 10, 397–410.

Hudson, N.W. 1981. Soil conservation, 2nd edn. Batsford, London.

Jiao JY, Wang WJ, Li J. 1999. Analysis on soil and water conservation benefit of level terrace under different rainfall condition in loess hilly region. Journal of Soil Erosion and Soil and Water Conservation5: 59–63.

Lasanta T, Arnaez J, Oserin M, Ortigosa LM. 2001. Marginal lands and erosion in terraced fields in the Mediterranean mountains. A case study in the Camero Viejo (Northwestern Iberian System, Spain).Journal ofMountain Research and Development21: 69-76.

Latron J, Llorens P, Soler M, Poyatos R, Rubio C, Muzylo A, Martínez-Carreras N, Delgado J, Regüés D, Catari G, Nord G, Gallart F. 2009. Hidrología de un ambiente Mediterráneo de montaña. Las cuencas de Vallcebre (Pirineo Oriental) I. 20 años de investigaciones hidrológicas. This volume.

Laureano P. 2004. Il sistema dei terrazzamenti nel paesaggio euromediterraneo. In: La cultura dei terrazzamenti per la salvaguardia del paesaggio. Acts of the international convention, Vietri sul Mare, May 2004, Menabò Edizioni, Salerno.

Li MH, Yang MJ, Soong R, Huang HL. 2005. Simulation typhoon floods with gauge data and mesoscale-modeled rainfall in a mountainous watershed. Journal of Hydrometeorology6:306-323. DOI: 10.1175/JHM423.1.

Li, X.H, Yang J, Zhao C.Y, Wang B. 2012. Runoff and sediment from orchard terraces in southeastern China. Land Degrad. Dev., http://dx.doi.org/10.1002/ ldr.1160.

Li XH, Yang J, Zhao CY, Wang B. 2014. Runoff and sediment from orchard terraces in southeastern China. Land Degradetion and Development25: 184-192. DOI: 10.1002/ldr.1160.

Li XH, Zhang ZY, Yang J, Zhang GH, Wang B. 2011. Effects of Bahia grass cover and mulch on runoff and sediment yield of sloping red soil in southern China.Pedosphere21: 238–243. DOI: 10.1016/S1002-0160(11)60123-9.

Londoño, A.C., 2008. Pattern and rate of erosion inferred from Inca agricultural terraces in arid southern Peru. Geomorphology 99, 13–25.

López-Vicente M, Poesen J, Navas A, Gaspar L. 2013. Predicting runoff and sediment connectivity and soil erosion by water for different land use scenarios in the Spanish Pre-Pyrenees. Catena 102: 62–73. https:// doi.org/10.1016/j.catena.2011.01.001.

Louwagie G, Gay S, Sammeth F, Ratinger T. 2011. The potential of european union policies to address soil degradation in agriculture. Land Degradation & Development 22, 5–17

Lu HS, Zhu YH, Skaggs TH, Yu ZB. 2009. Comparison of measured and simulated water storage in dryland terraces of the Loess Plateau, China. Agricultural Water Management 96: 299–306.

Maidment D.R. (Editor in Chief) 1993, Handbook of Hydrology, McGraw-Hill, 1424 pages. (Translated into Chinese in 2002, and distributed there by www.sciencep.com)

Marcadella A. 2014. Analisi idro – meteorologica dell'evento di piena improvvisa del 2 – 3 agosto 2014 sul bacino del Rio Lierza nel comune di Refrontolo (TV). Bachelor thesis, University of Padova (in Italian).

Marshall R.G. and Ruban T.F. 1983. Geotechnical aspects of pipeline construction in Alberta. Canadian Geotechnical Journal 20: 1–10.

Meerkerk AL, van Wesemael B, Bellin N. 2009. Application of connectivity theory to model the impact of terrace failure on runoff in semi-arid catchments. Hydrological Processes 23:2792-2803.

Mein R.G. and C.L. Larson. 1971. Modelling the infiltration component of the rainfall-runoff process. Bulletin 43. University of Minnesota, MN, Water Resources Research Center.

Mein R.G. and C.L. Larson. 1973. Modeling infiltration during a steady rain. Water Resourc. Res. 9(2):384-394.

Mirtskhoulava Ts.E. 2001. Soil erosion: forecasting, risk, conservation. Georgian Institute of Water Management and Engineering Ecology, Tbilisi.

Morgan R.P.C. and Hann M.J. 2003. Design of diverter berms for erosion control and biorestoration along pipeline rights-of-way. Poster paper presented to Land Reclamation 2003, Runcorn.

Morgan RPC.2005. Soil Erosion and Conservation. 3rdEdition. Blackwell Publishing Ltd, Oxford, UK.

Ore G, Bruins H.J. 2012. Design features of ancient agricultural terrace walls in the Negev desert: human-made geodiversity. Land Degrad. Dev. 23, 409–418.

Parsons J.E, Muñoz-Carpena R.: WinGAmpt. A Windows based teaching tool for Green-Ampt Infiltration for Unsteady Rainfall Model. Version 0.3 – 2009. Biol. & Agricultural Engineering Agricultural & Biol. Engineering North Carolina State University University of Florida.

Penna D, Mantese N, Hopp L, Dalla Fontana G, Borga M. 2015a. Spatiotemporal variability of piezometric response on two steep alpine hillslopes. Hydrological Processes 29: 198–211. https://doi.org/10.1002/hyp.10140.

Penna D, van Meerveld HJ, Oliviero O, Zuecco G, Assendelft RS, Dalla Fontana G, Borga M. 2015b. Seasonal changes in runoff generation in a small forested mountain catchment. Hydrological Processes 29: 2,027–2,042 https://doi.org/10.1002/hyp.10347.

Perlotto C. and D'Agostino V. 2016. Performance assessment of bench terraces through 2-d modelling. Land Degradation & Development land degradation & development (2016) DOI: 10.1002/ldr.2653

Post B. 2005. Dry stone walls of the United Kingdom. State University of New York College of Environmental Science and Foresty.

Preti et. al. 2017. Conceptualization of water flow pathways in agricultural terraced landscapes. Land Degradation & Development land degradation & development (2017). DOI: 10.1002/ldr.2764

Preti F, Bresci E, Ravenna V. 2001. Field measurements for hydrologic mapping in old terraced land. Int. Conf. on Sustainable soil management for environmental protection. Soil physical aspects. Firenze, July.

Preti F. 2002. Evoluzione degli effetti delle sistemazioni idraulico agrarie e forestali sui deflussi di piena, Atti 28° Convegno Nazionale di Idraulica e Costruzioni Idrauliche, Potenza.

Preti F, Forzieri G, Chirico G.B. 2011. Forest cover influence on regional flood frequency assessment in Mediterranean catchments, Hydrol. Earth Syst. Sci., 15, 3077–3090, 2011 www.hydrol-earth-syst-sci.net/15/3077/2011/doi:10.5194/hess-15-3077-2011.

Preti F, Settesoldi D, Paris E, Mazzanti B. 1996. Criteri e procedure per la valutazione delle piene nel territorio toscano. Atti del XXV Convegno di Idraulica e Costruzioni Idrauliche, Torino, settembre 1996, CNR-GNDCI, pp. 317-328.

Preti F, Tarolli P, Dani A, Calligaro S, Prosdocimi M. 2013. LiDAR derived high resolution topography: the next challenge for the analysis of terraces stability and vineyard soil erosion. Journal of Agricultural Engineering 44: 85–89. https://doi.org/10.4081/jae.2013.258.

Ravenna V. 2001. Effetti sul rischio idraulico dell'evoluzione dell'uso del suolo e delle sistemazioni di versante in un piccolo bacino delle Alpi Apuane. Laurea degree thesis. Università di Firenze, Dipartimento di Ingegneria Agraria e Forestale.

Romero Diaz A, Marin Sanleandro P, Sanchez Soriano A, Belmonte Serrato F, Faulkner H. 2007. The causes of piping in a set of abandoned agricultural terraces in southeast Spain. Catena 69: 282–293. https://doi.org/10.1016/j.catena.2006.07.008.

Sereni E. 1961. Storia del paesaggio agrario italiano. Edizioni Laterza, Bari.

Spencer J.E, Hale S.A. 1961. The origin, nature and distribution of agricultural terracing. Pacific Viewpoint 2, 1–40.

Skaggs R. W. and R. Khaheel. 1982. Chapter 4: Infiltration. In Hydrologic modeling of small watersheds.Ed. by C. T. Haan, H. P. Johnson and D. L. Brakensiek, 139-149, St. Joseph, MI, ASAE. pp. 121-168.

Tarolli P, Preti F, Romano N. 2014. Terraced landscapes: from an old best practice to a potential hazard for soil degradation due to land abandonment.Anthropocene6:10-25. DOI:10.1016/j.ancene.2014.03.002.

Tarolli P, Sofia G, Calligaro S, Prosdocimi M, Preti F, Dalla Fontana G. 2015. Vineyards in terraced landscapes: new opportunities from lidar data.Land Degradation and Development26:92–102. DOI: 10.1002/ldr.2311.

Trischitta D. 2005. Il paesaggio dei terrazzamenti: tra cultura e natura. In: Il paesaggio terrazzato, Un patrimonio geografico, antropologico, architettonico, agrario, ambientale. Atti del seminario di Studi Taormina.

U.S. SCS. 1986: Urban Hydrology for small watershade. Technical release 55, U.S Department of agriculture.

Wakindiki I.I.C, Ben-Hur M. 2002. Indigenous soil and water conservation techniques: effect on runoff, erosion, and crop yields under semiarid conditions. Aust. J. Soil Res. 40, 367–379.

Van Dijk A.I.J.M. 2002. Water and sediment dynamics in benchterraced agricultural steeplands in West Java, Indonesia. PhD thesis, Vrije Universiteit, Amsterdam (available at http://www.geo.vu.nl/geomil/ad.html).

Van Dijk AIJ, Bruijnzeel LA. 2004. Runoff and soil loss from bench terraces. 1. An event-based model of rainfall infiltration and surface runoff. European Journal of Soil Science55:299–316. DOI: 10.1111/j.1365-2389.2004.00604.x.

Van Wesemael B, Poesen J, Sole´ Benet L, Cara Barrionuevo L, Puigdefa´ bregas J. 1998. Collection and storage of runoff from hillslopes in a semi-arid environ-ment: geomorphic and hydrologic aspects of the aljibe system inAlmeria Province, Spain. J. Arid Environ. 40, 1–14.

Varotto M. 2008. Towards the rediscovery of the middle landscapes. Terraced landscapes of the Alps. Atlas. In: Scaramellini, G., Varotto, M. (Eds.), ALPTER Project. Marsilio, Venezia, In: http://www.alpter.net.

Vieri R, Bresci E, Preti F. 2015.Historical terraces influence on peak runoff and Hydraulic Hazard at watershed scale. Quadermi di Idronomia Montana32/1: 333-344.

Villi V, Bacchi B. 2001.Valutazione delle piene nel triveneto.Publication of C.N.R. G.N.D.C.I.2511 (in Italian).

VSS. 1999. Swiss Standard SN 670 010b Soil parameters. Association of Swiss Road and Traffic Engineers, Zurich.

Wakindiki I.I.C, Ben-Hur M. 2002. Indigenous soil and water conservation techniques: effect on runoff, erosion, and crop yields under semiarid conditions. Aust. J. Soil Res. 40, 367–379.

Wischmeier WH, Smith DD. 1978. Predicting rainfall erosion losses. Agr. Handbook, U.S. Dept. of Agr, Science and Education Administration537.

Williams P. 2002. Rethinking disaster-induced collapse in the demise of the Andean highland states: Wari and Tiwanaku. World Archaeol. 33, 361–374.

Yu B, Rose CW, Coughlan, KJ & Fentie B. 1997. Plot-scale rainfall-runoff characteristics and modeling at six sites in Australia and Southeast Asia. Transactions of the American Society of Agricultural Engineers40: 1295–1303.

Yuan T, Fengmin L, Puhai L. 2003. Economic analysis of rainwater harvesting and irrigation methods, with an example from China. Agric. Water Manage. 60, 217– 226.

Zhang JH, Su ZA, Liu GC. 2008. Effects of terracing and agroforestry on soil and water loss in hilly areas of the Sichuan Basin, China.Journal of Mountain Science5:241–248. DOI: 10.1007/s11629-008-0189-6.

Index of Tables

Index of Figures

APPENDICES: MEASUREMENTS RESULTS

2° CONFIGURATION : TEST 01

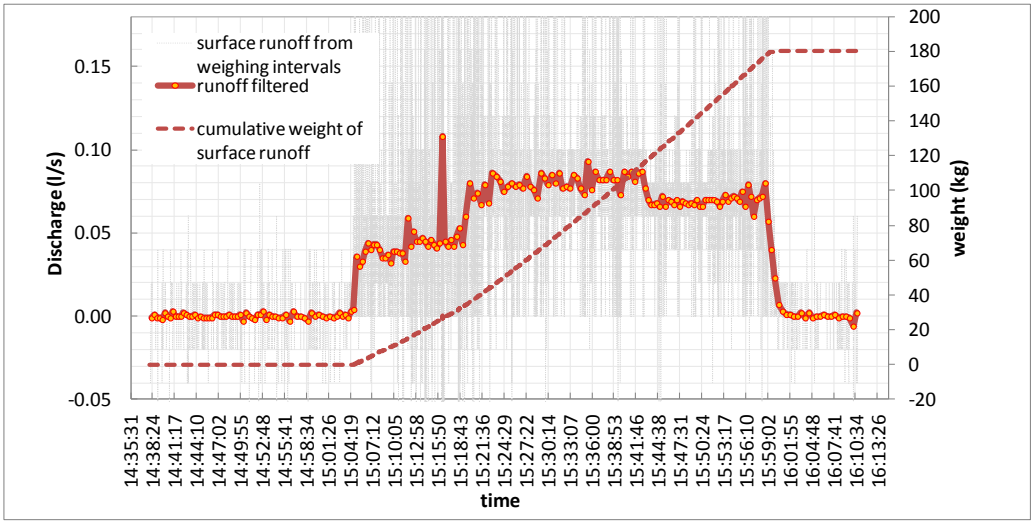

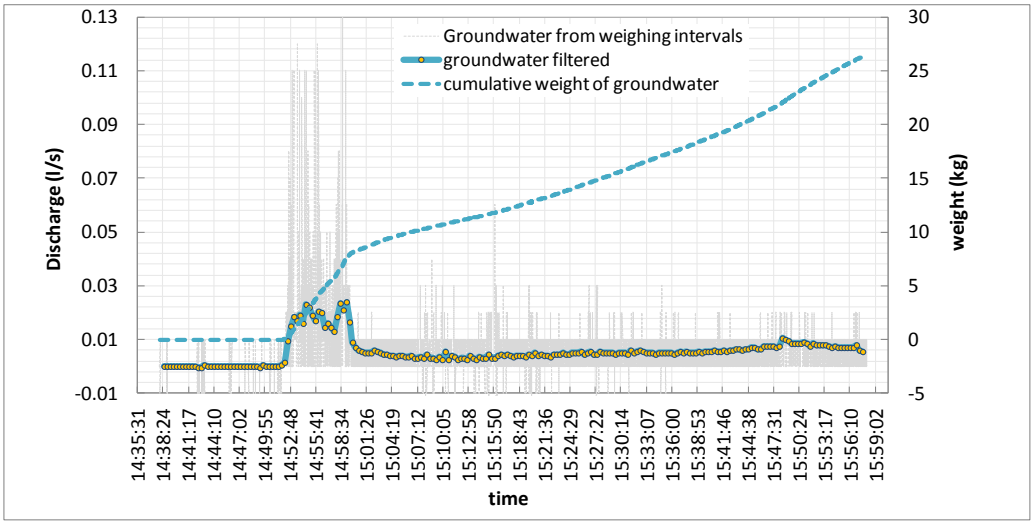

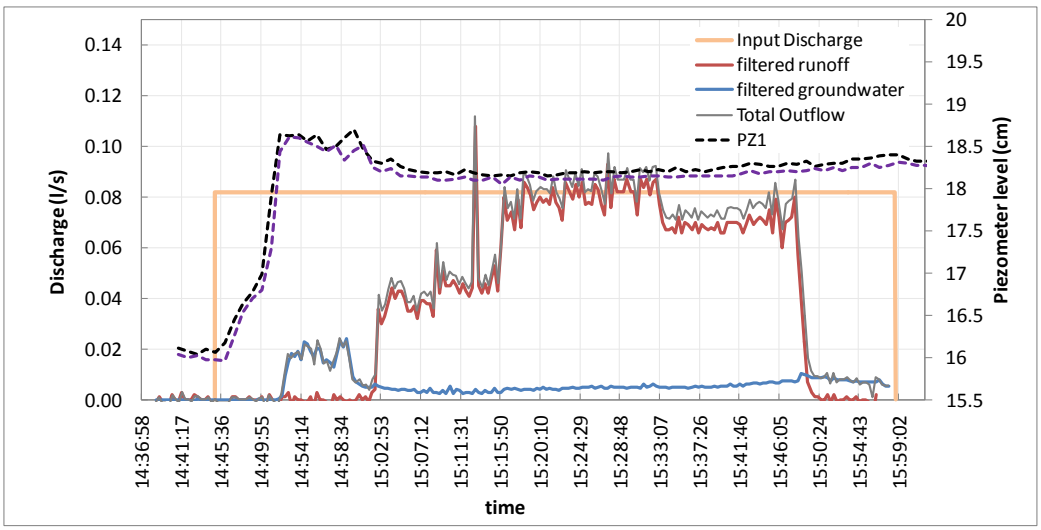

2° CONFIGURATION : TEST 02

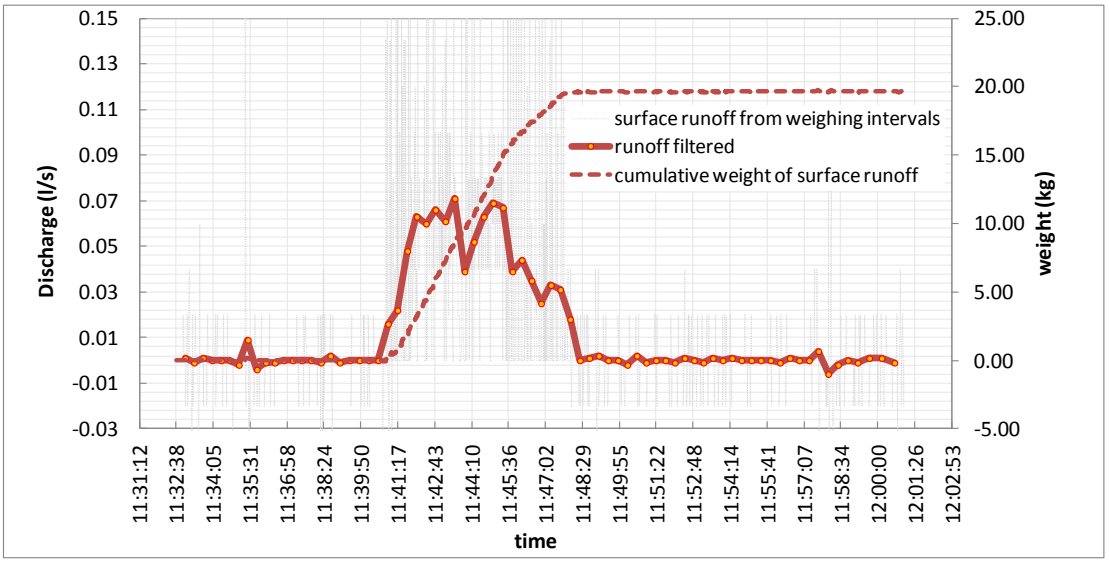

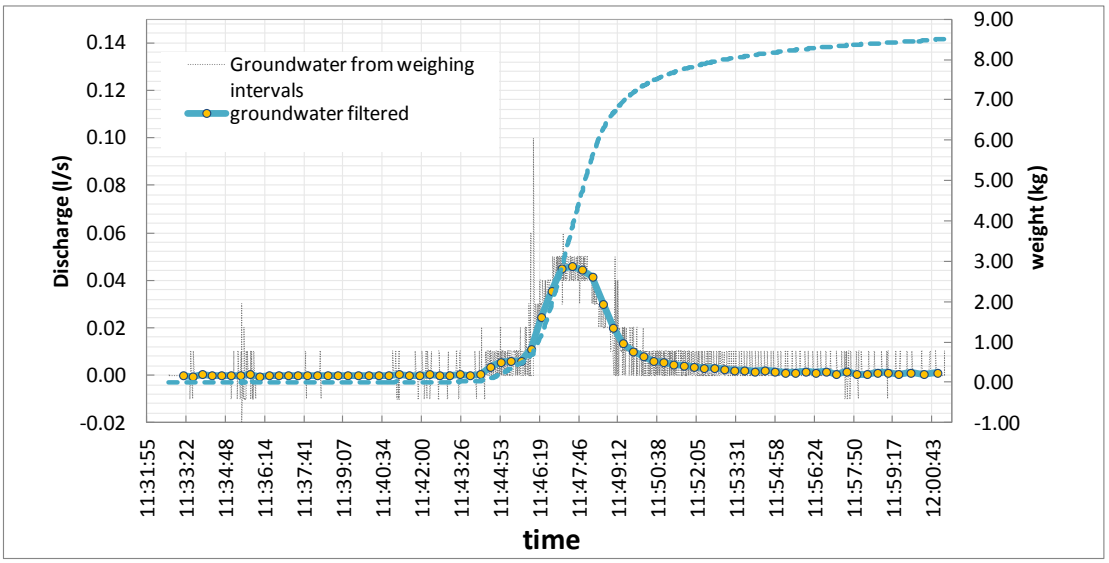

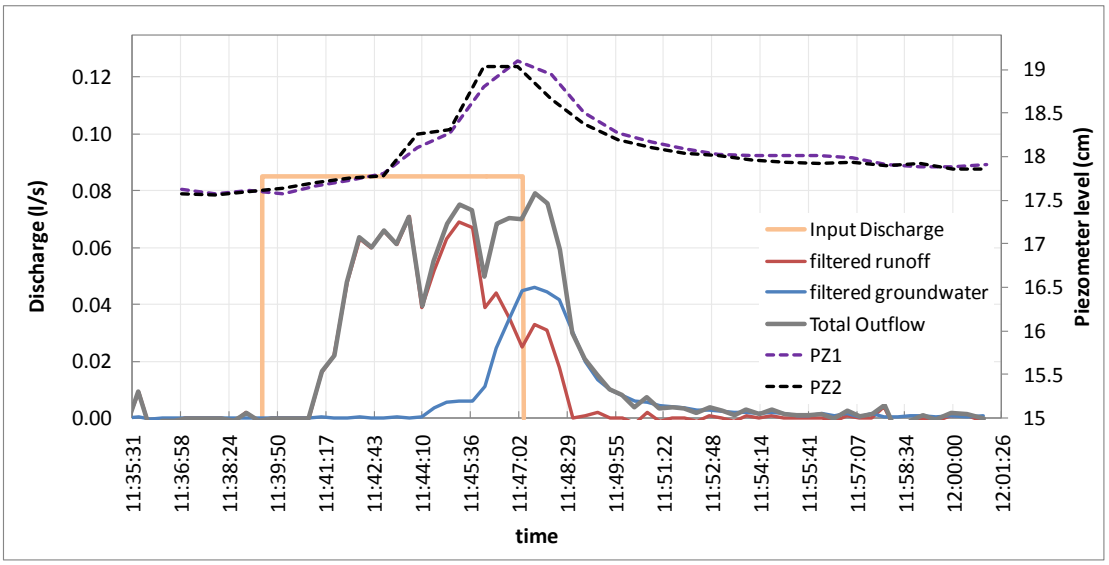

2° CONFIGURATION : TEST 03

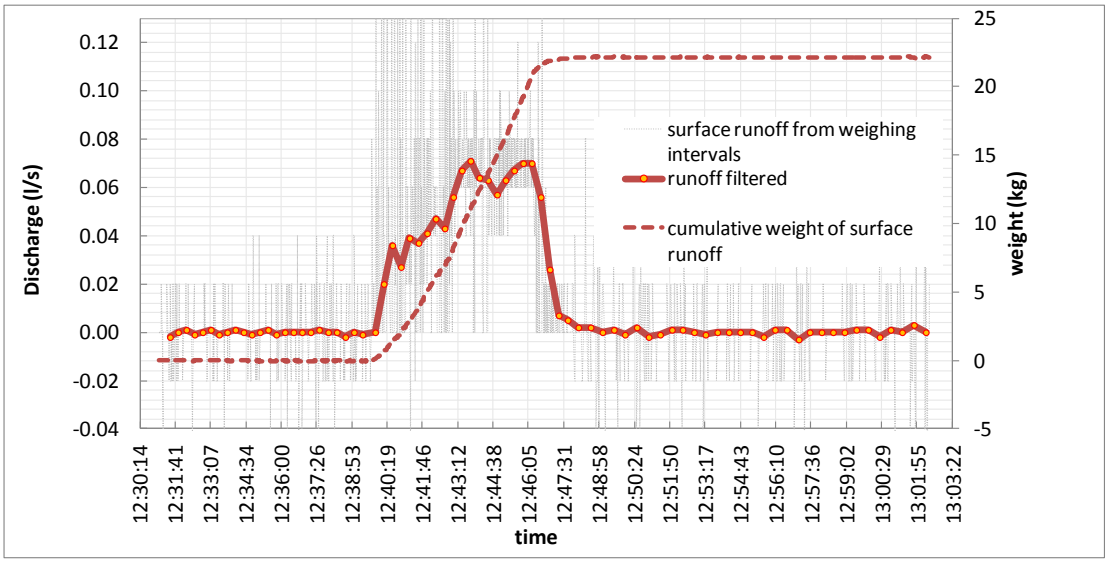

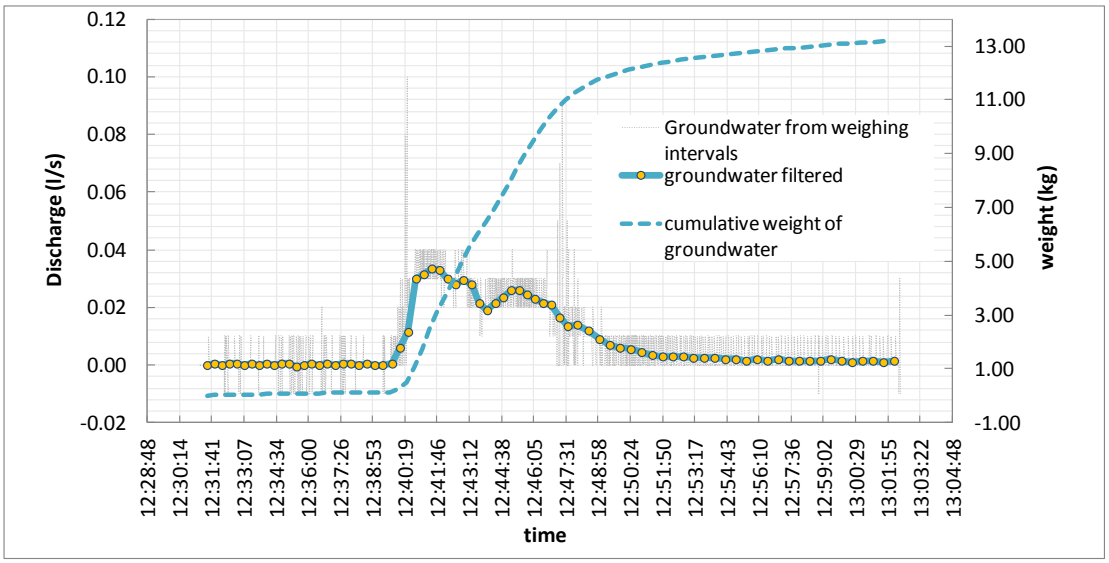

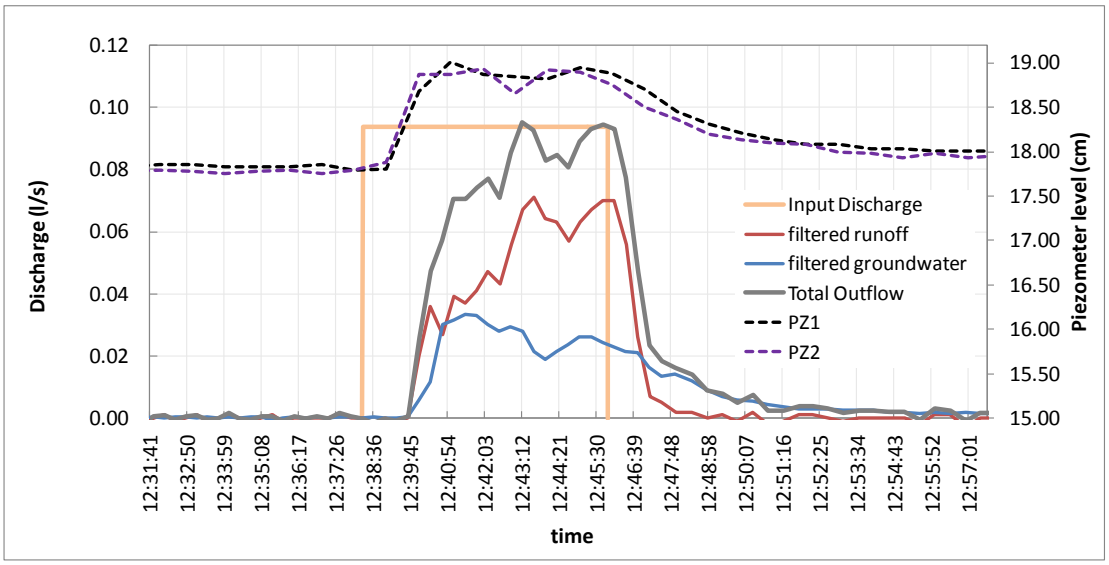

2° CONFIGURATION : TEST 04

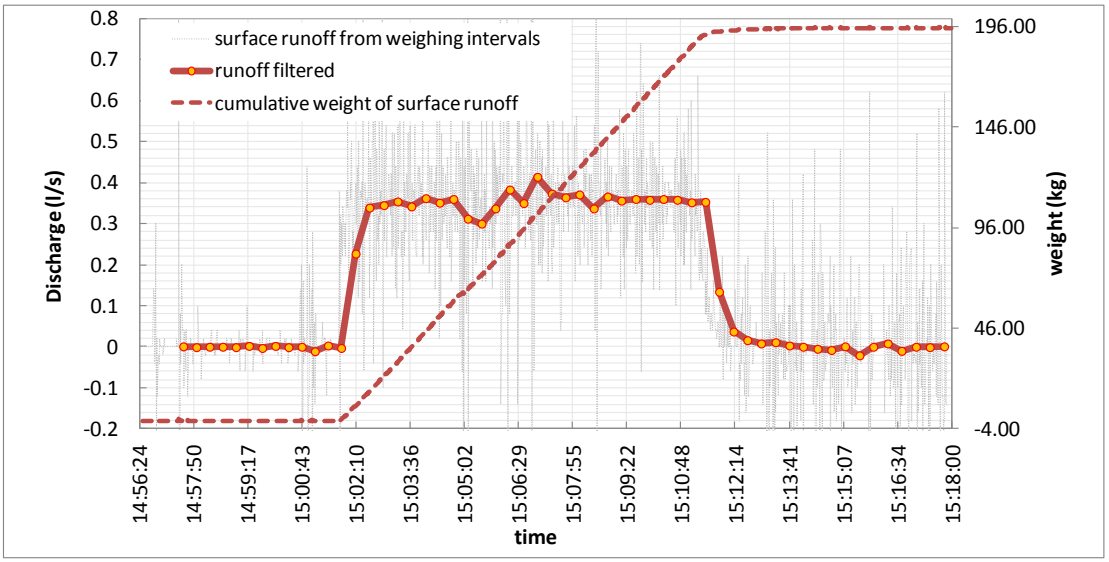

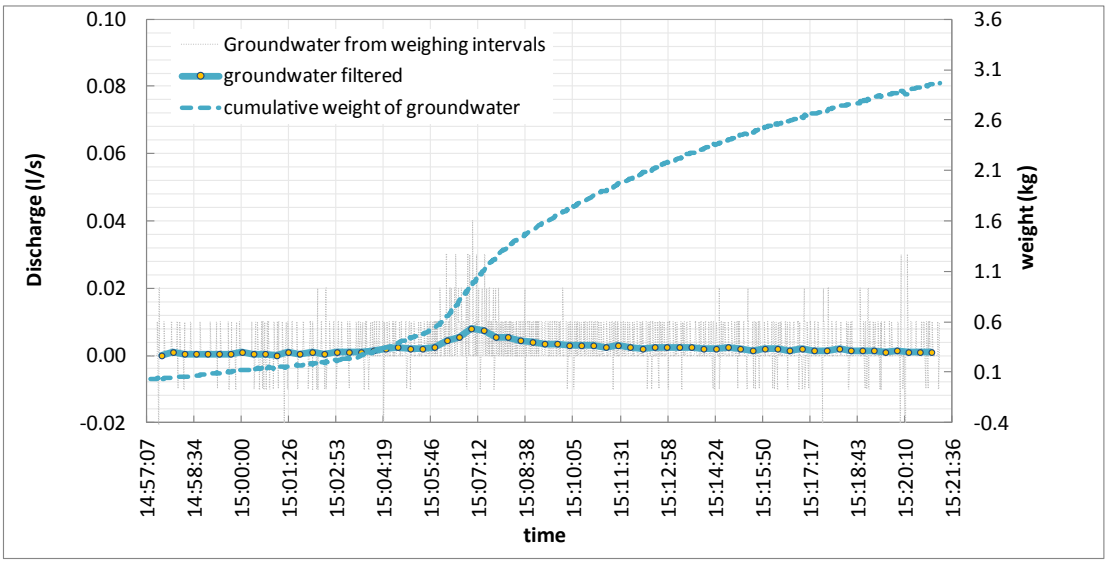

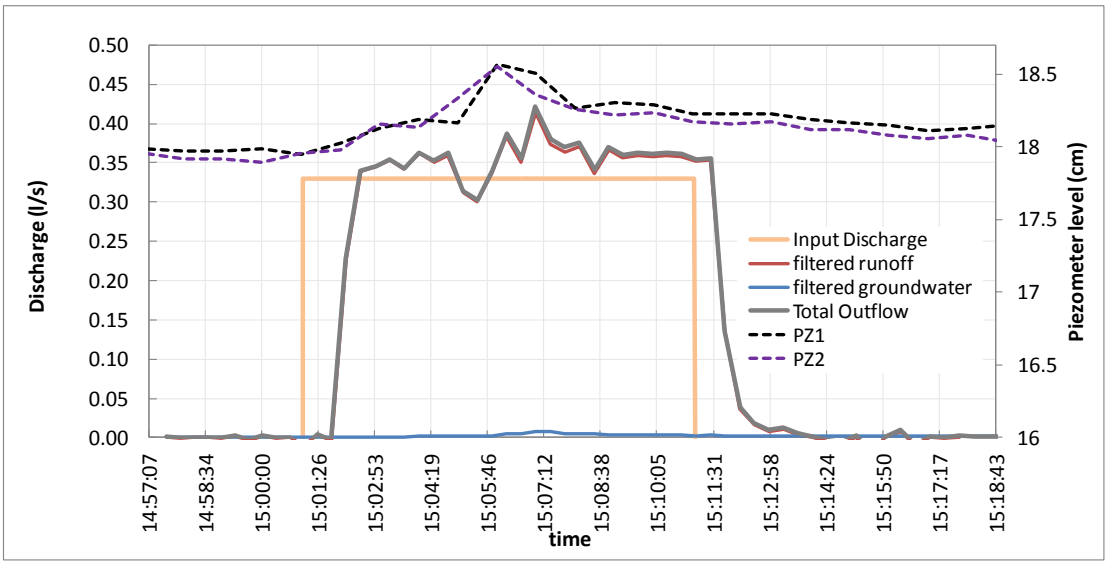

2° CONFIGURATION : TEST 05

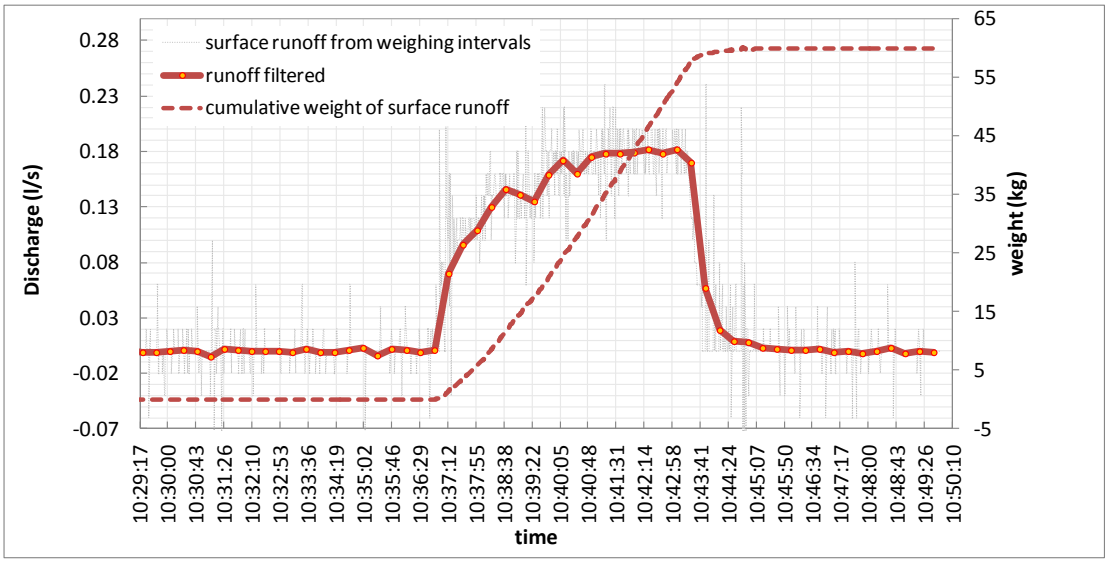

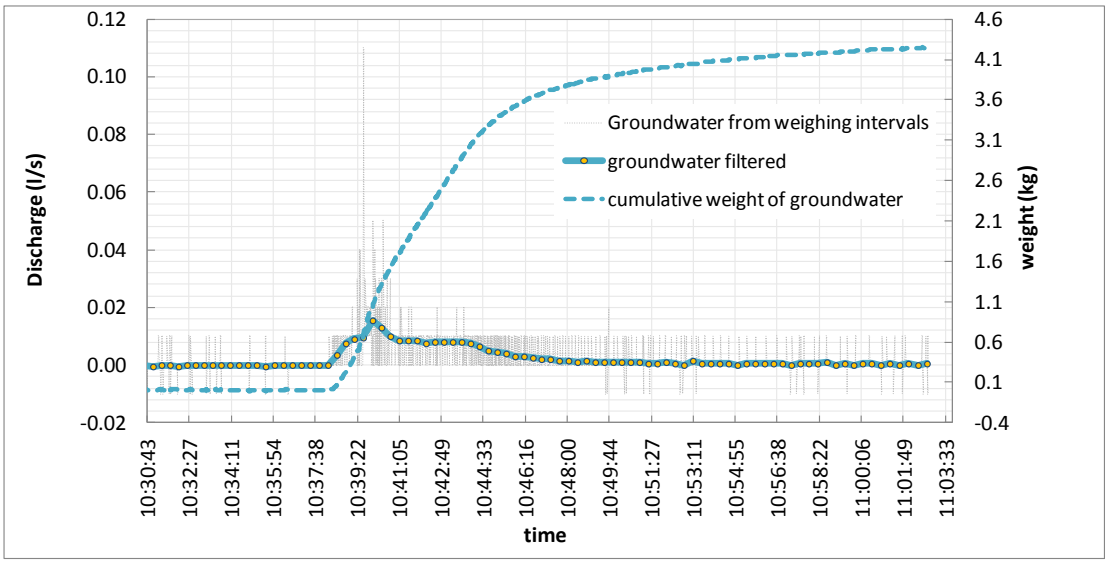

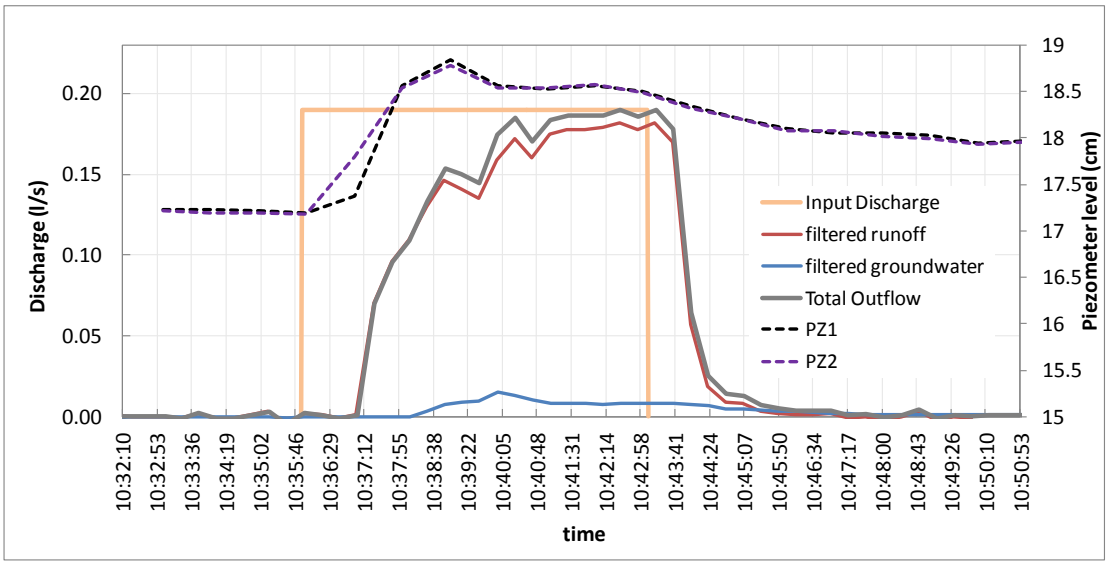

2° CONFIGURATION : TEST 06

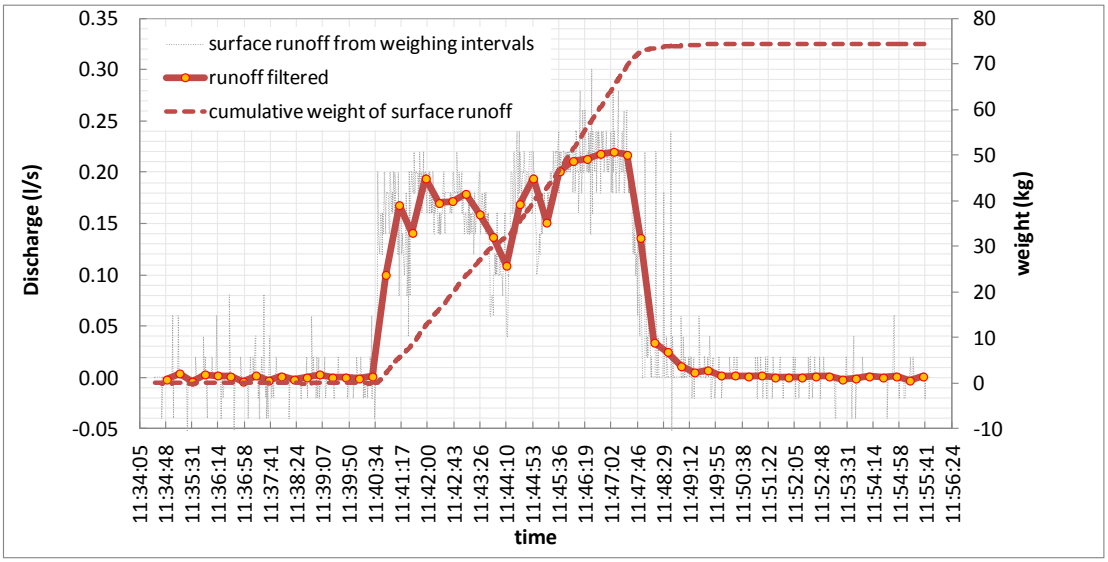

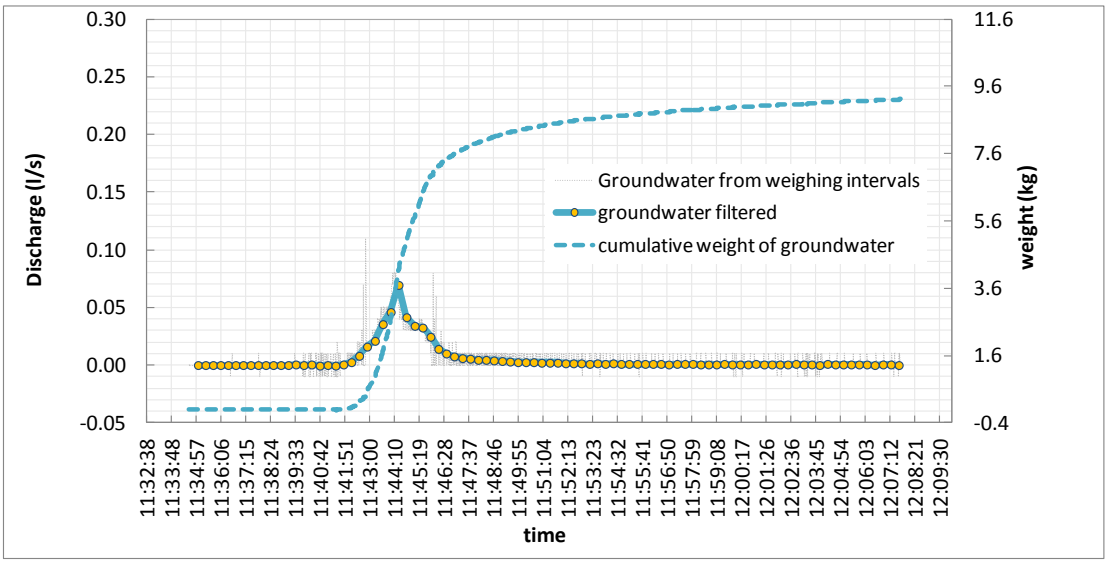

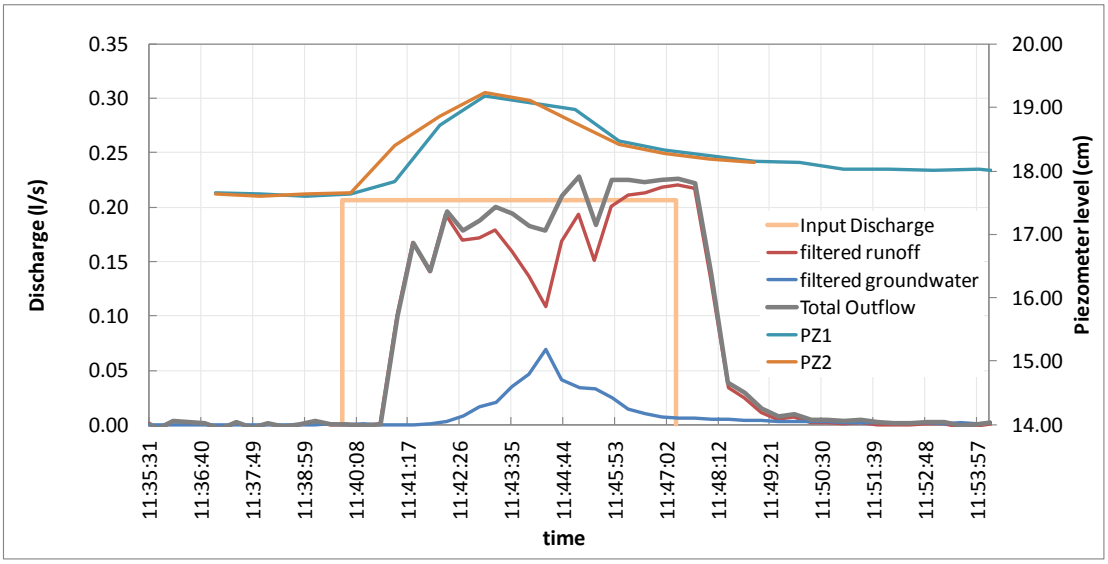

2° CONFIGURATION : TEST 07

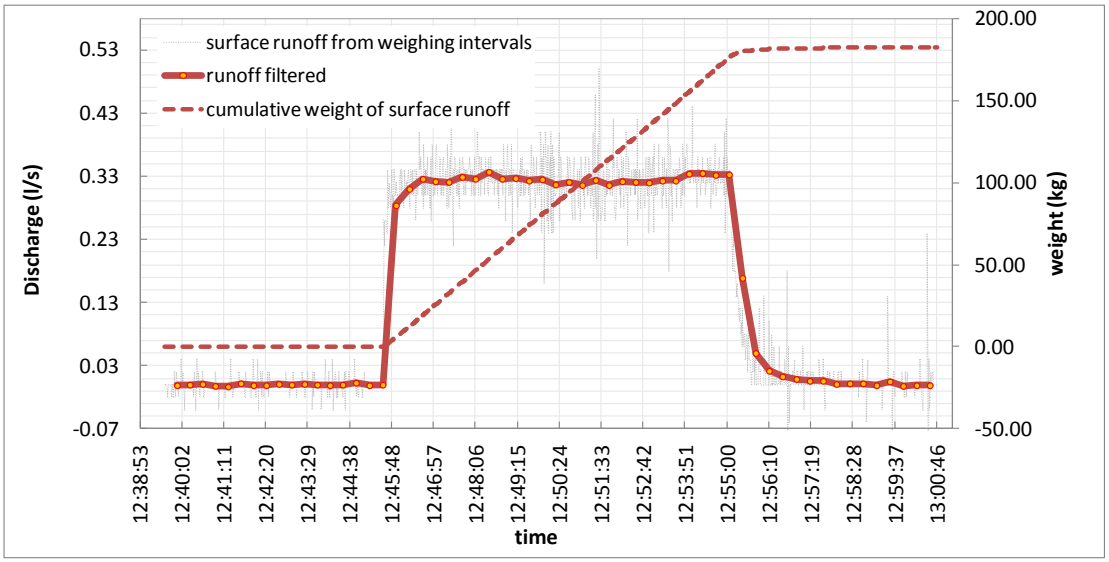

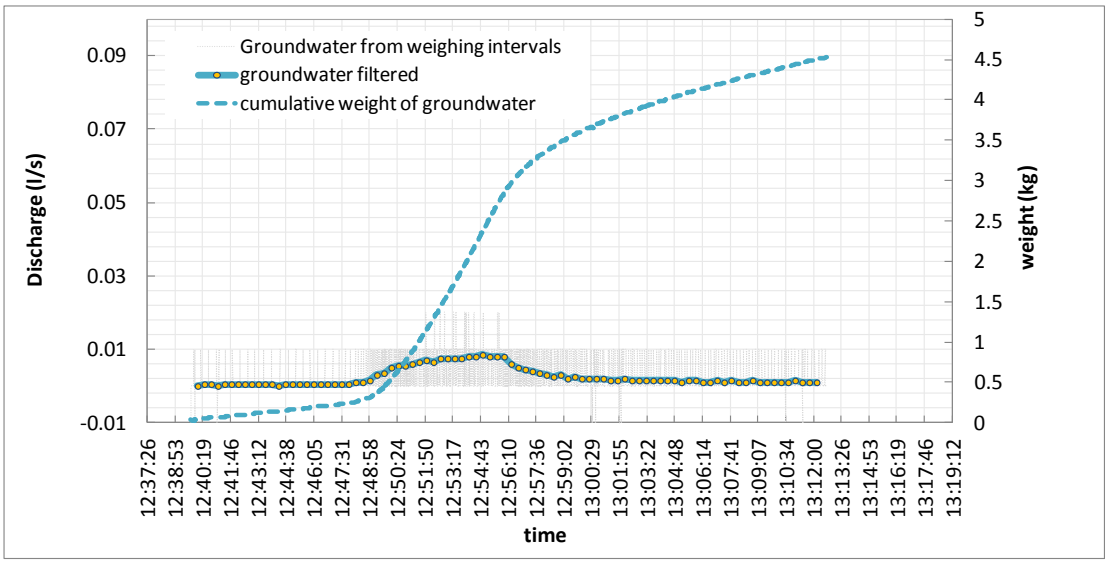

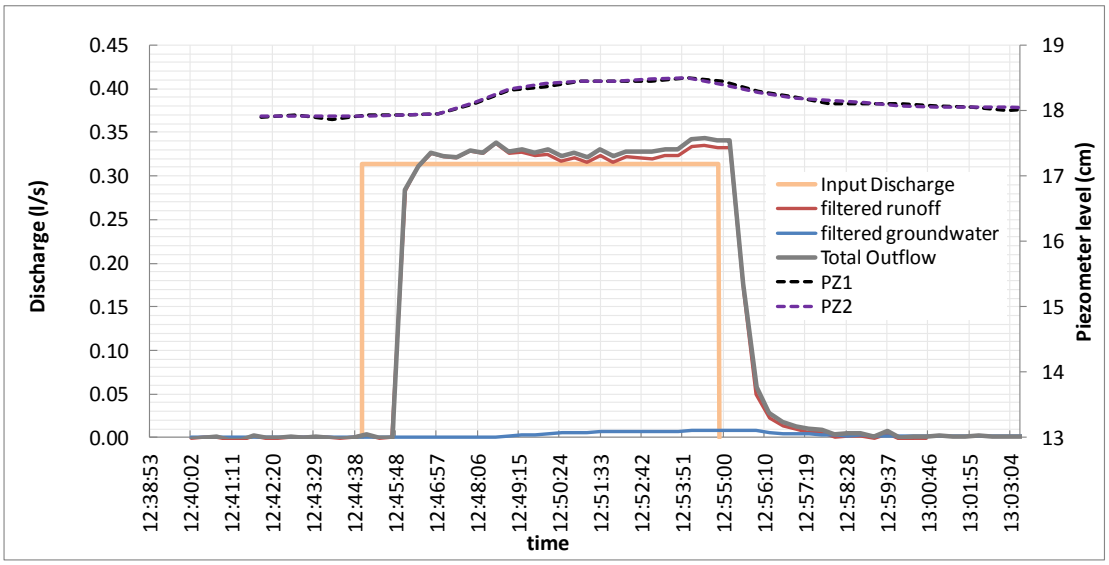

2° CONFIGURATION : TEST 08

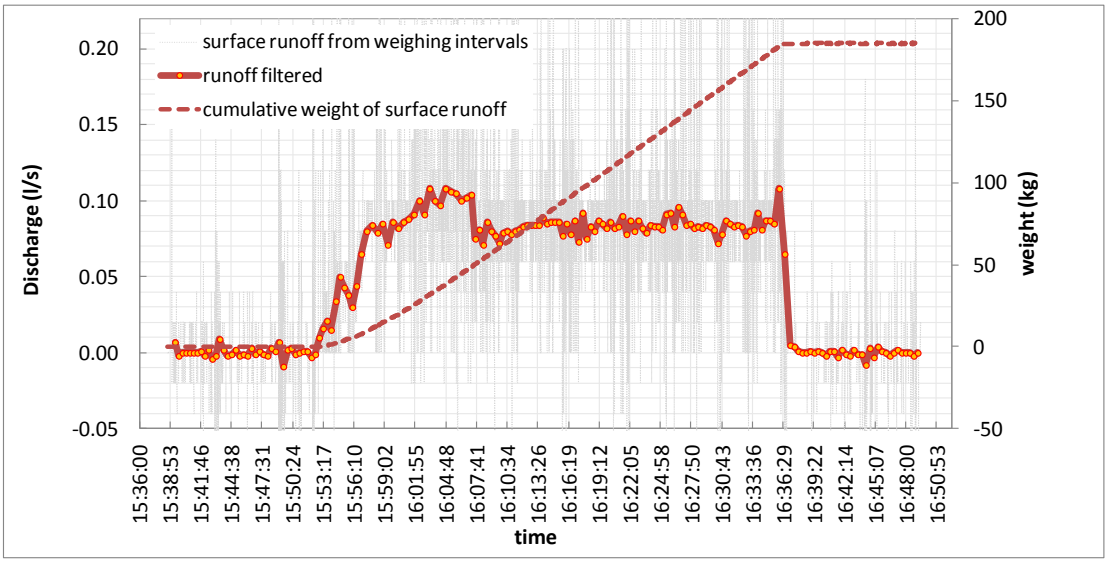

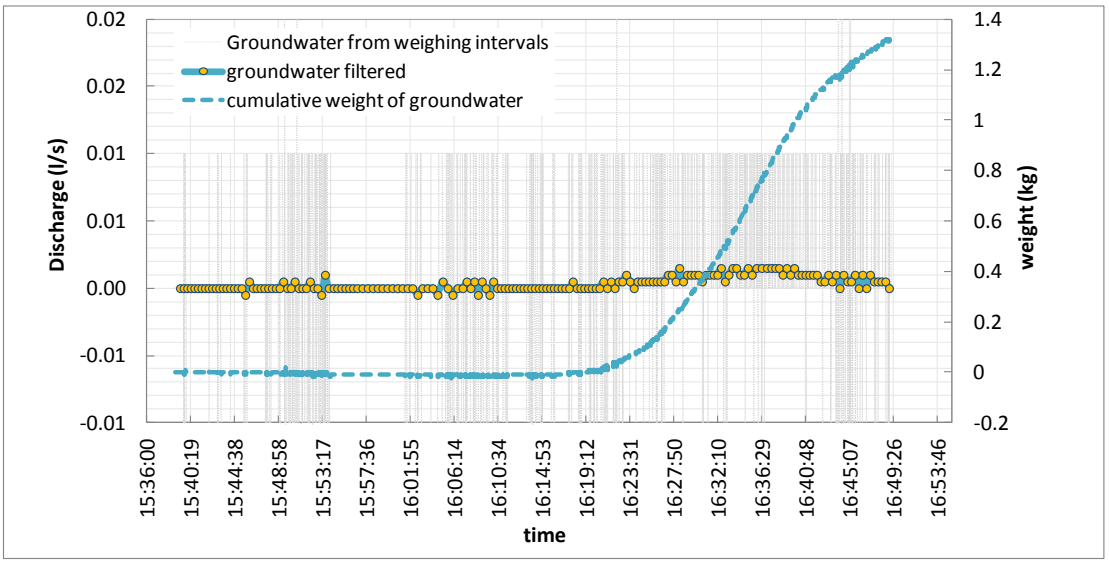

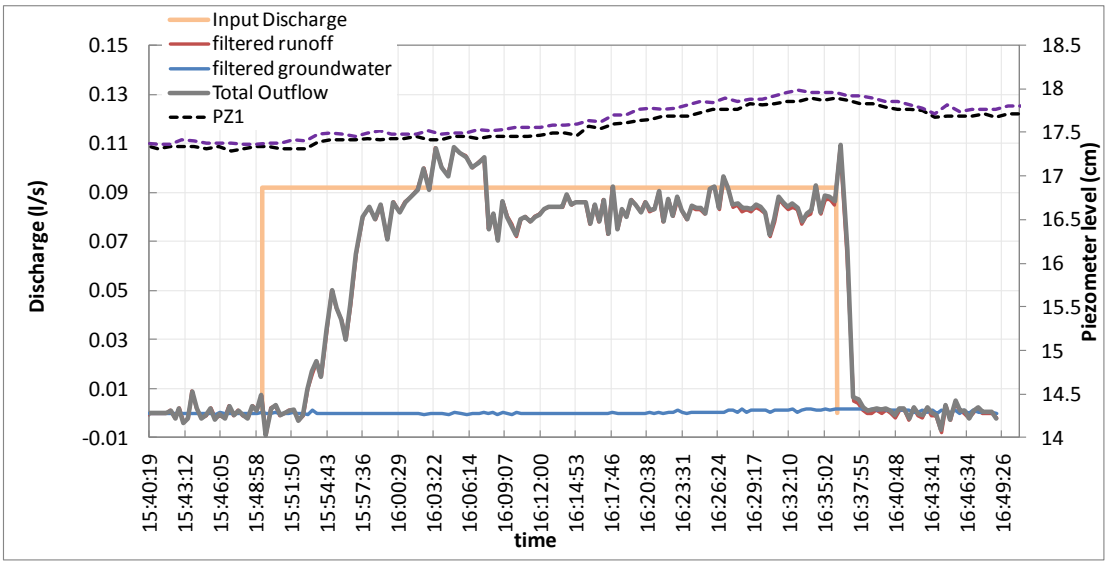

2° CONFIGURATION : TEST 09

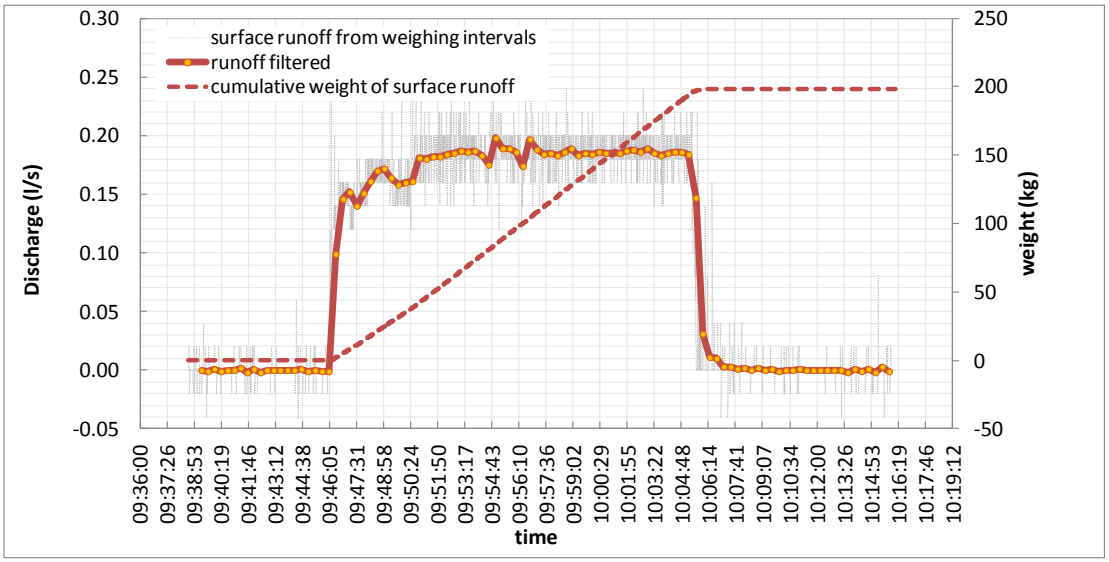

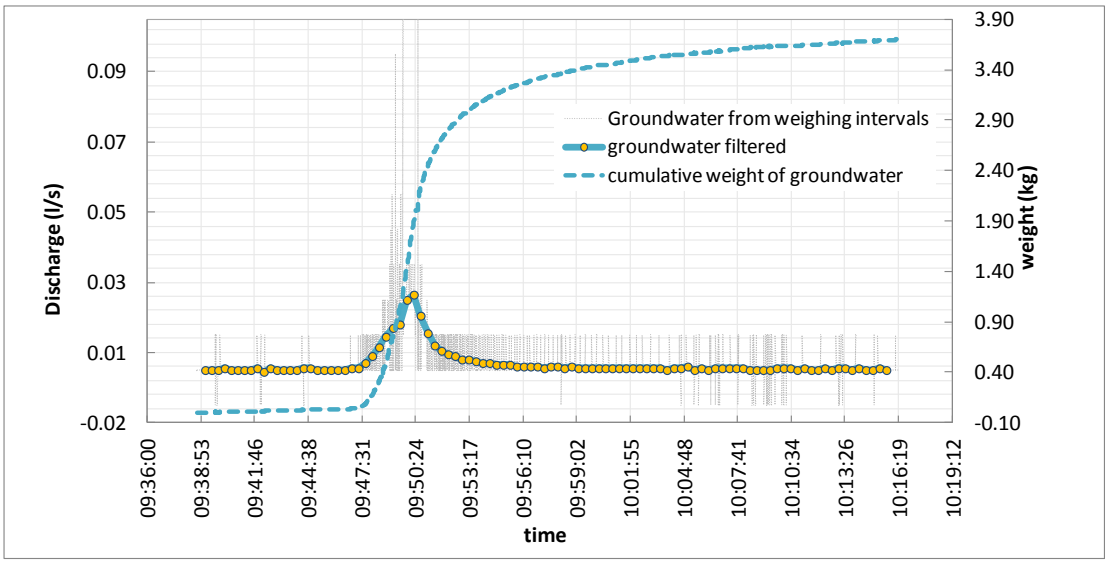

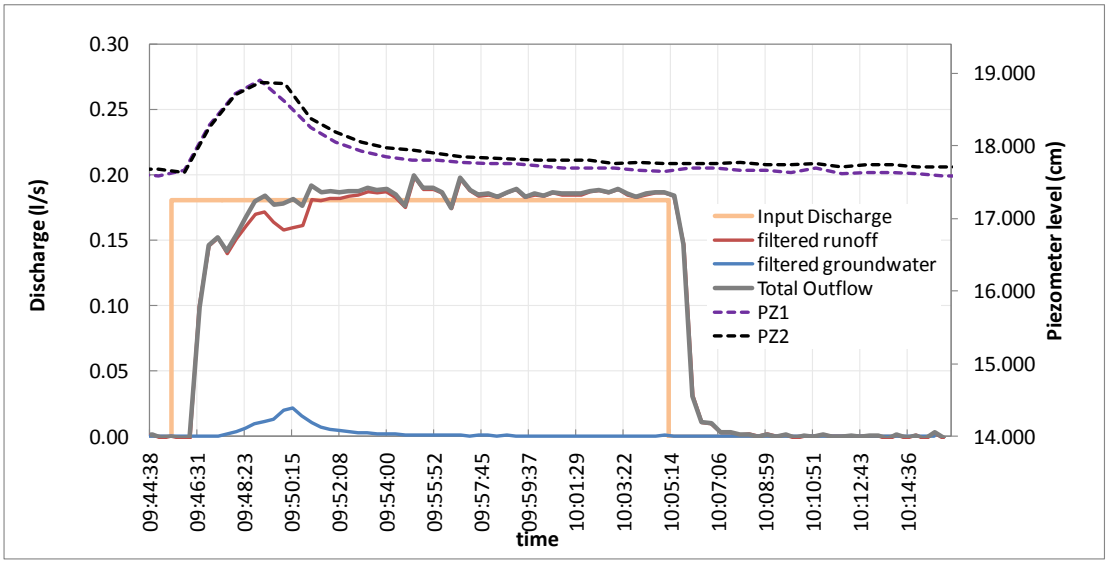

2° CONFIGURATION : TEST 10

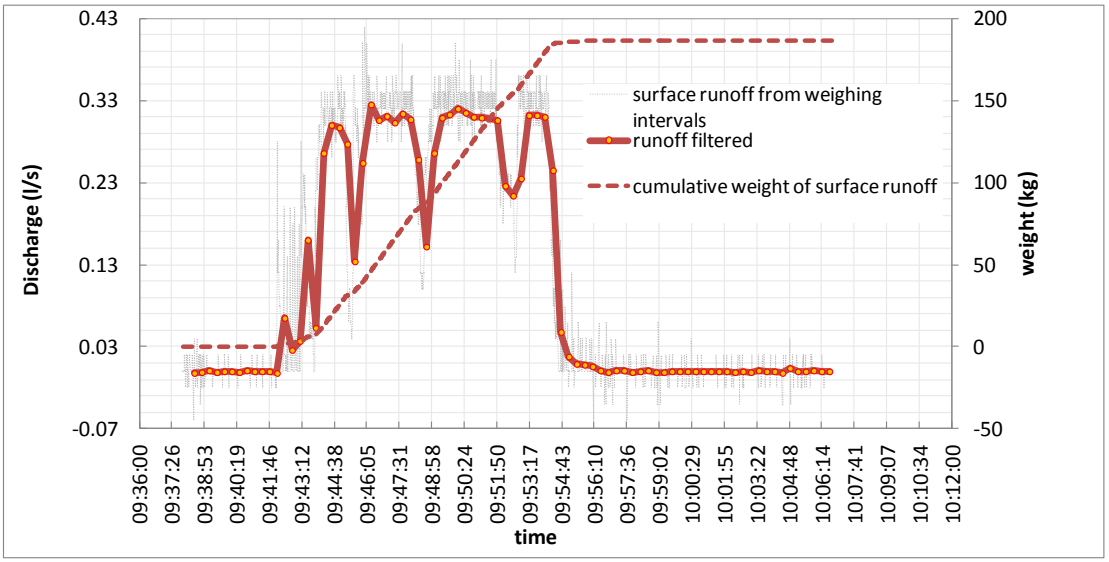

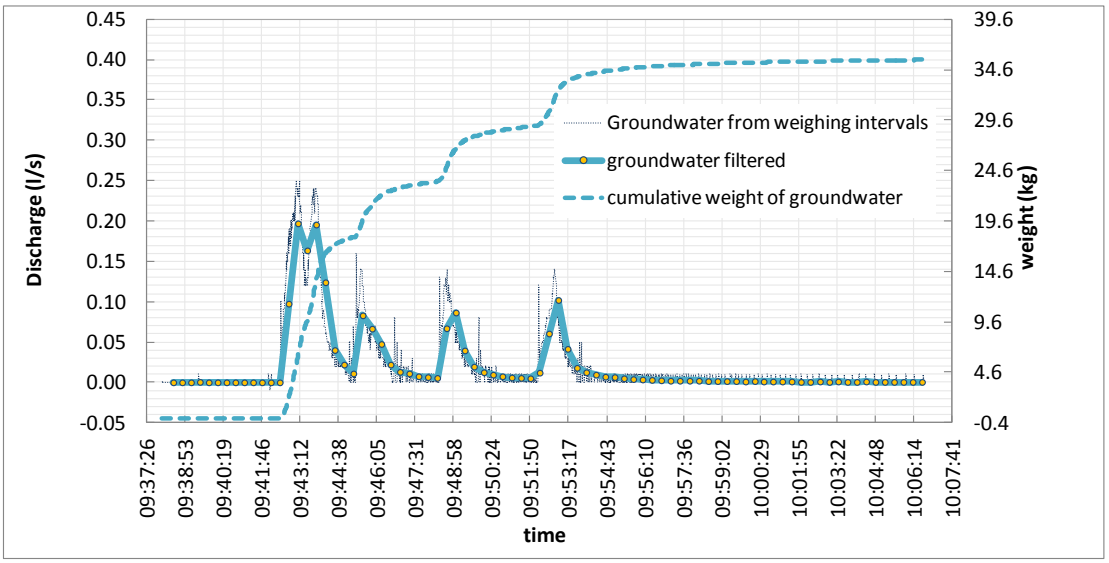

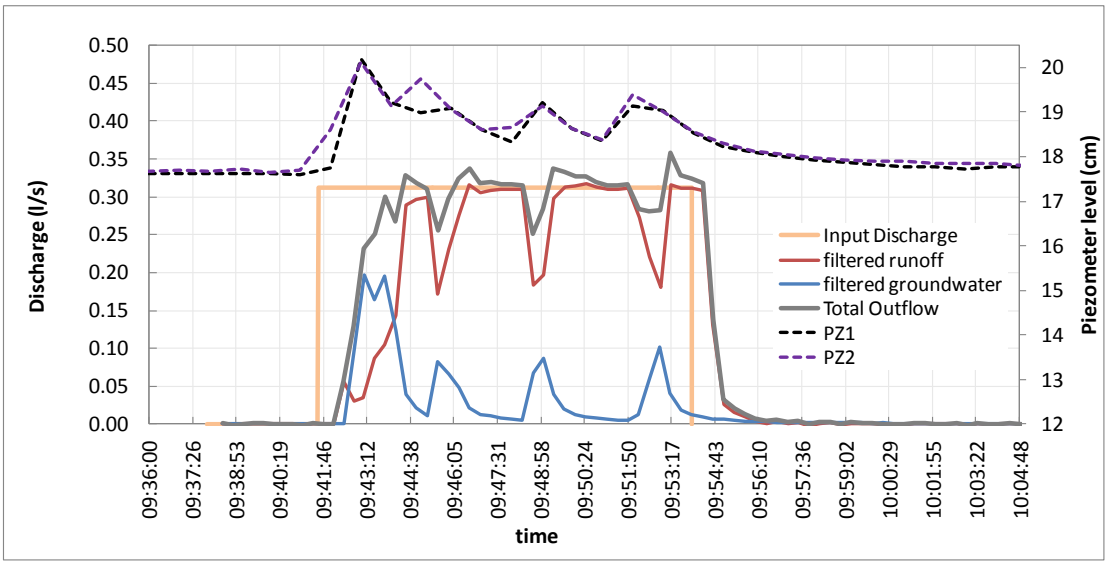

2° CONFIGURATION : TEST 11

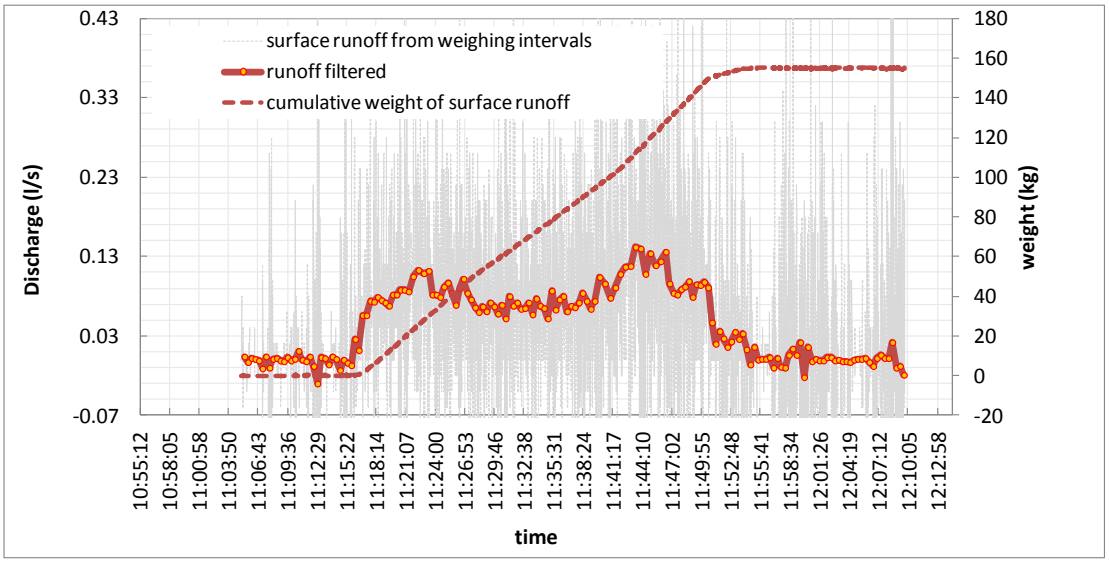

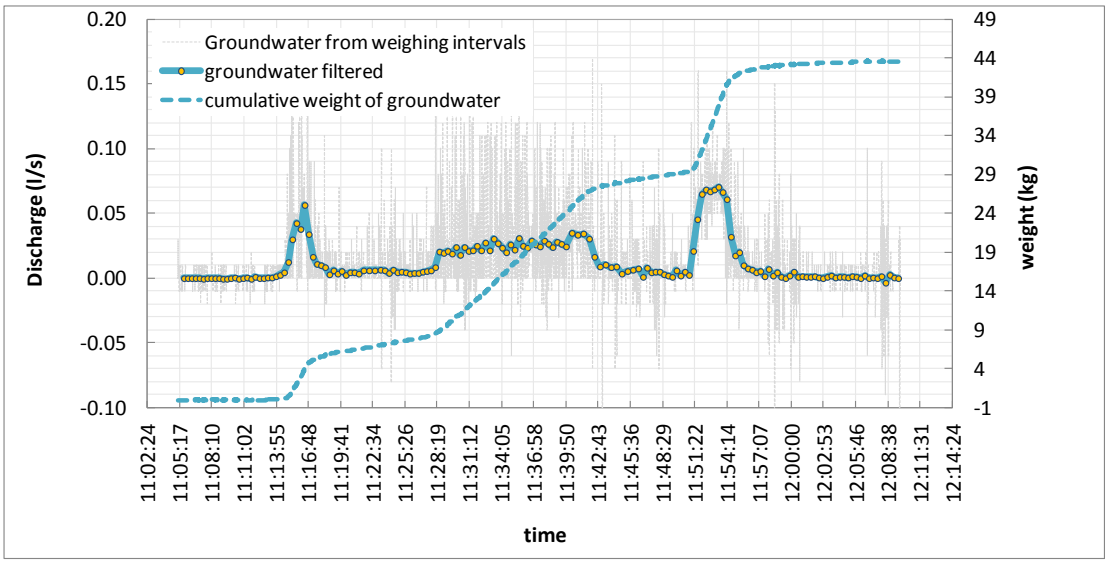

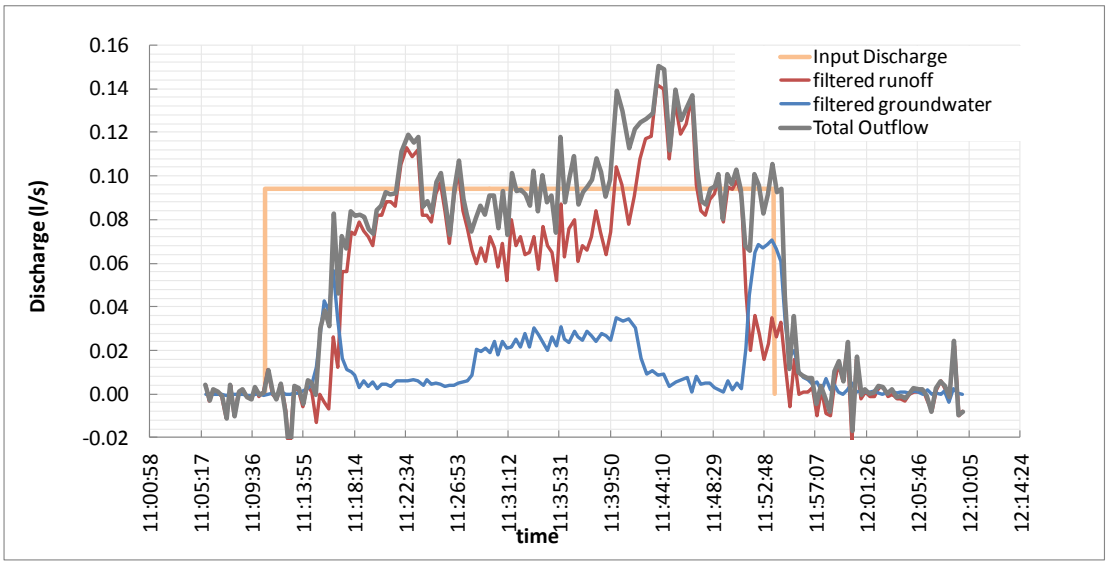

2° CONFIGURATION : TEST 12

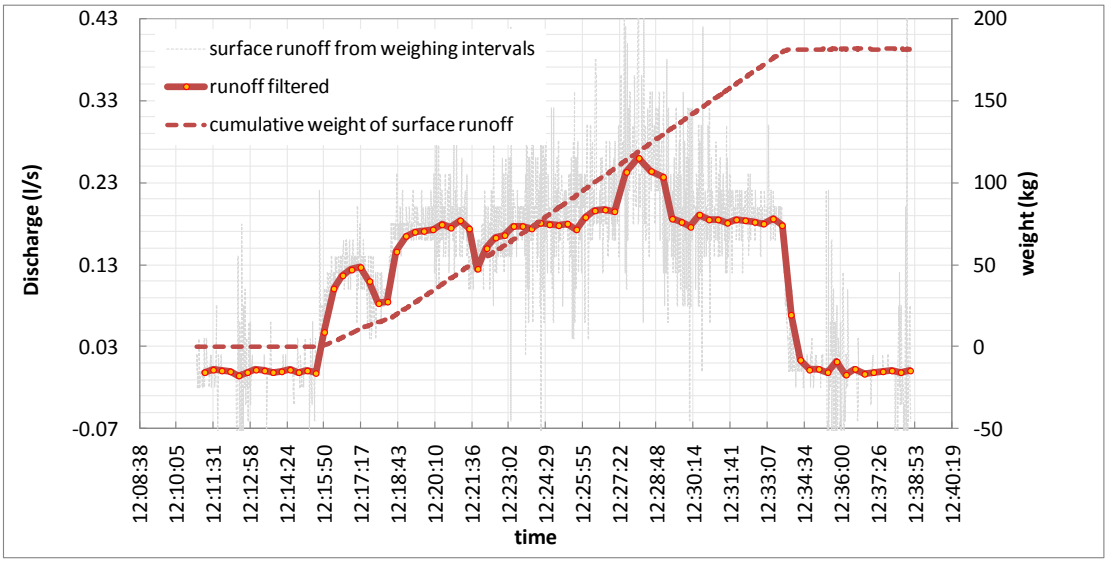

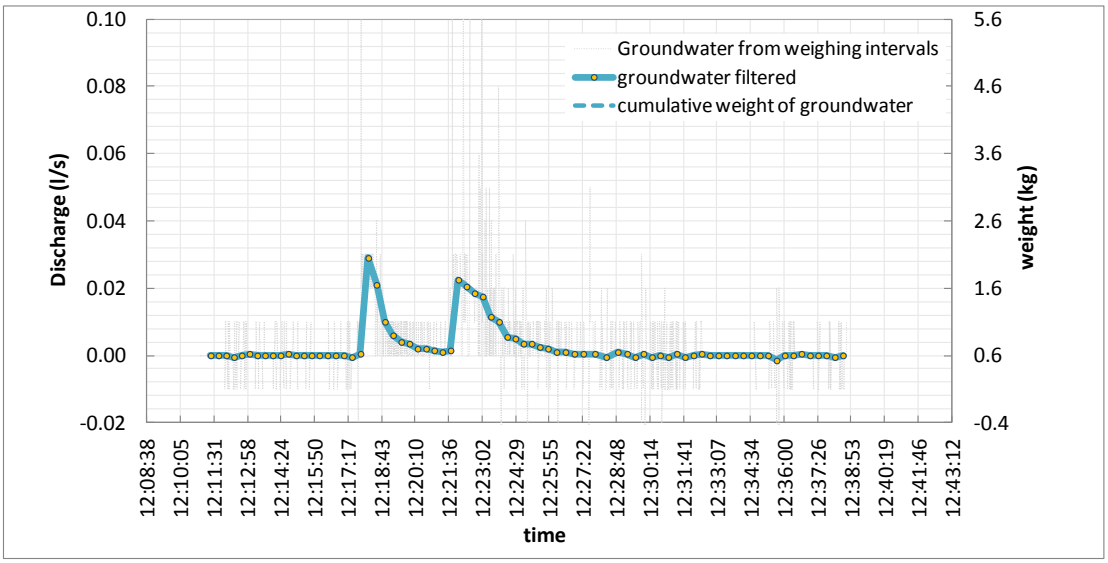

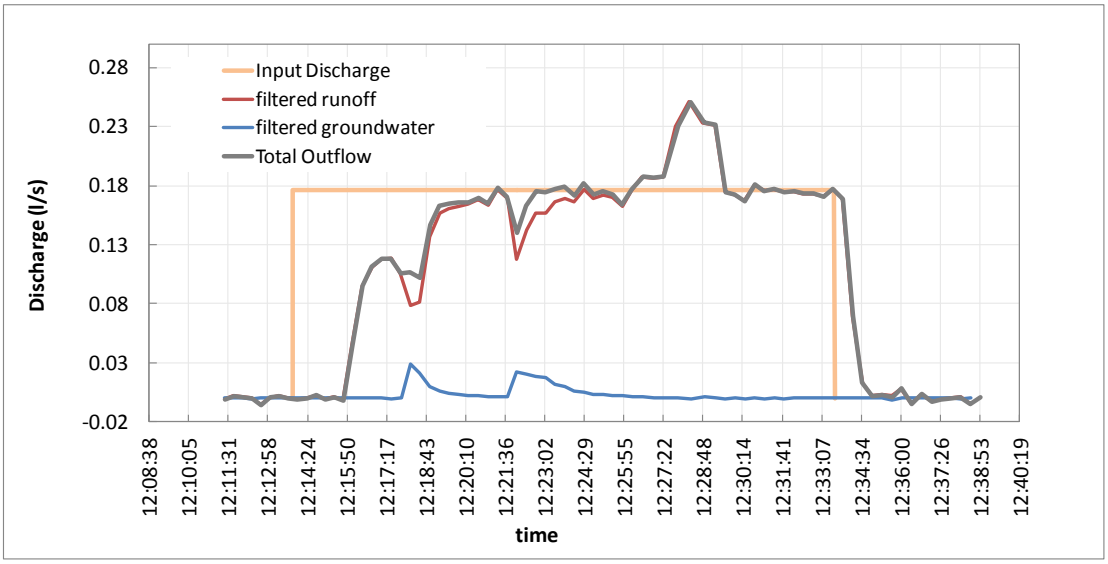

2° CONFIGURATION : TEST 13

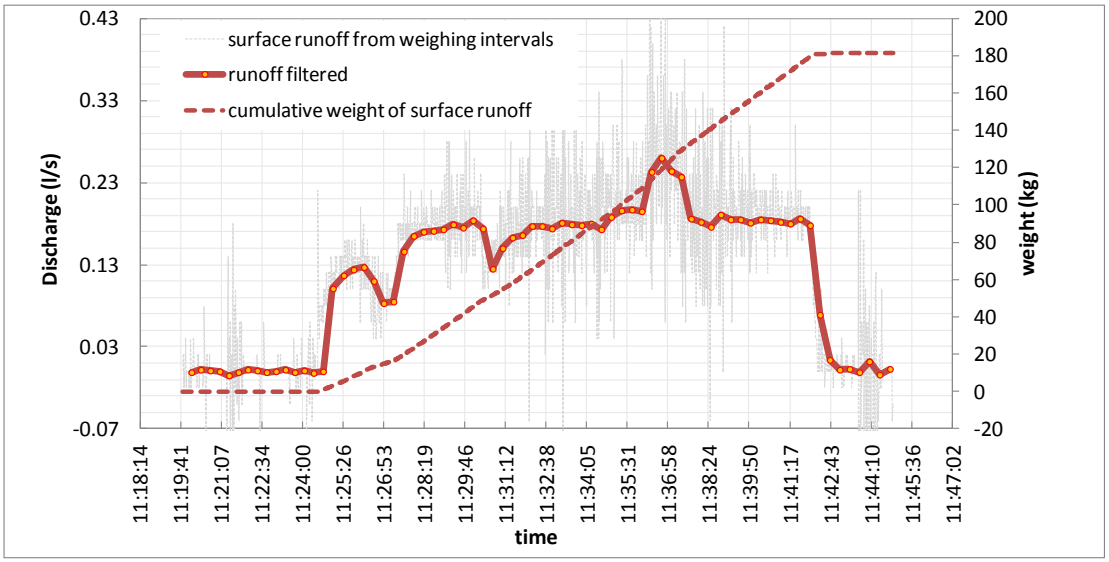

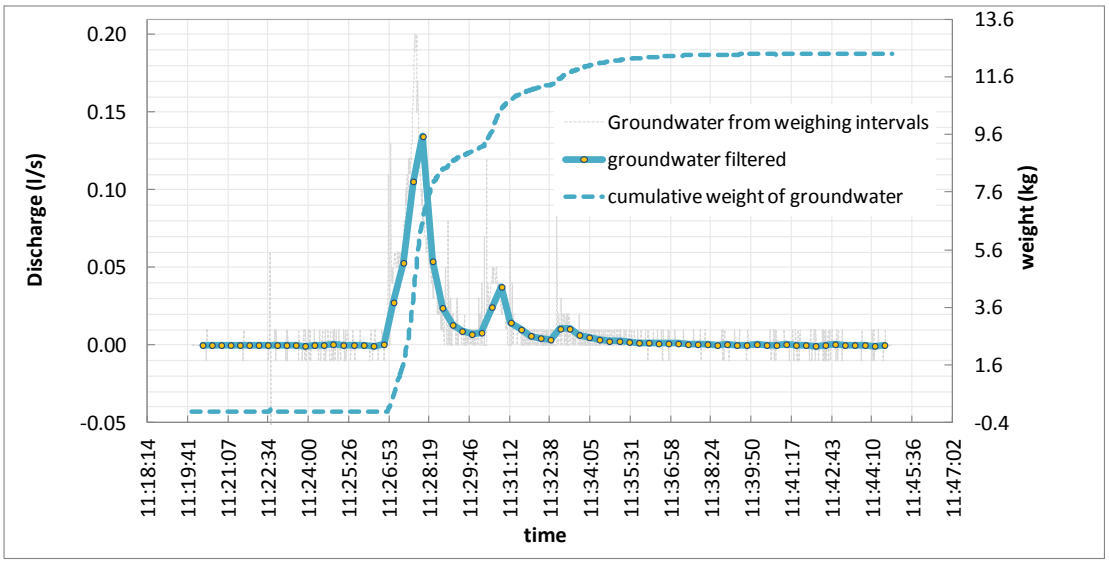

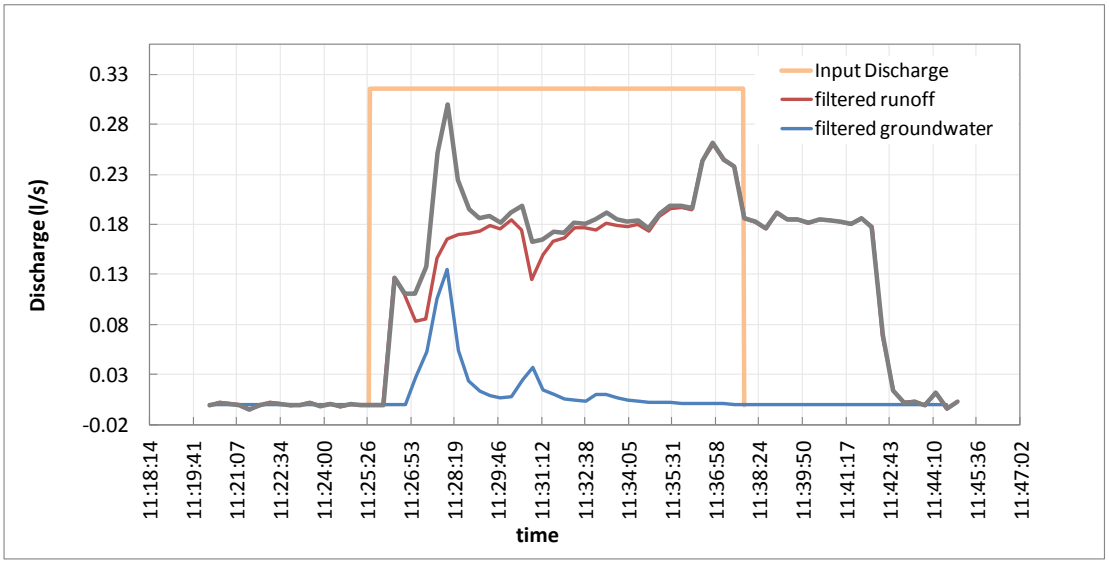

2° CONFIGURATION : TEST 14

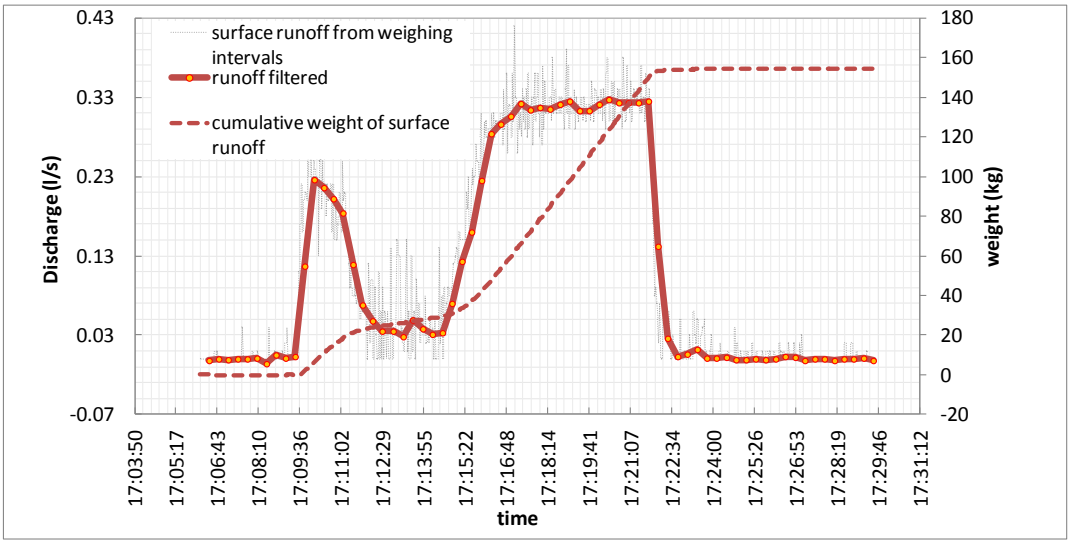

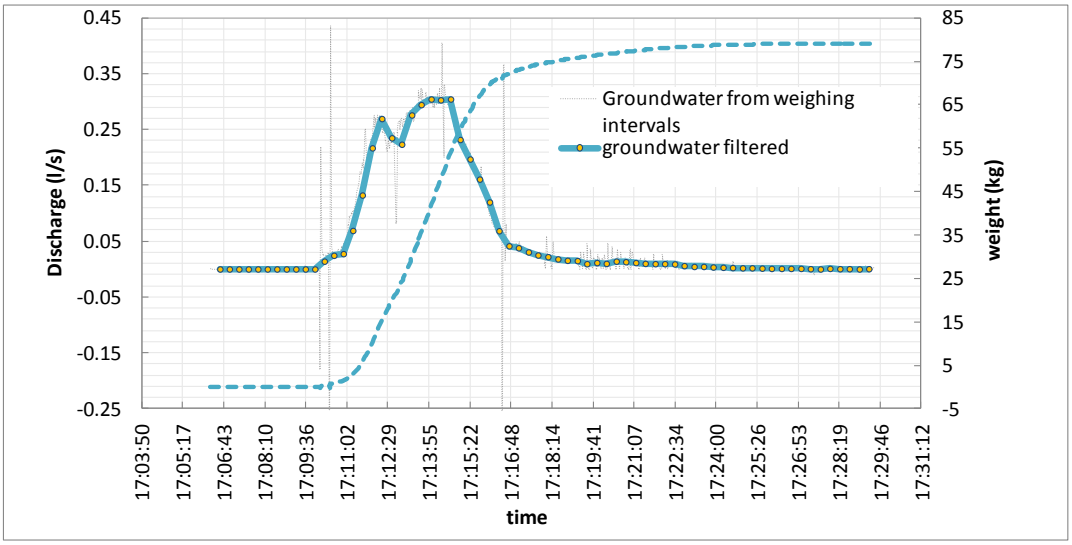

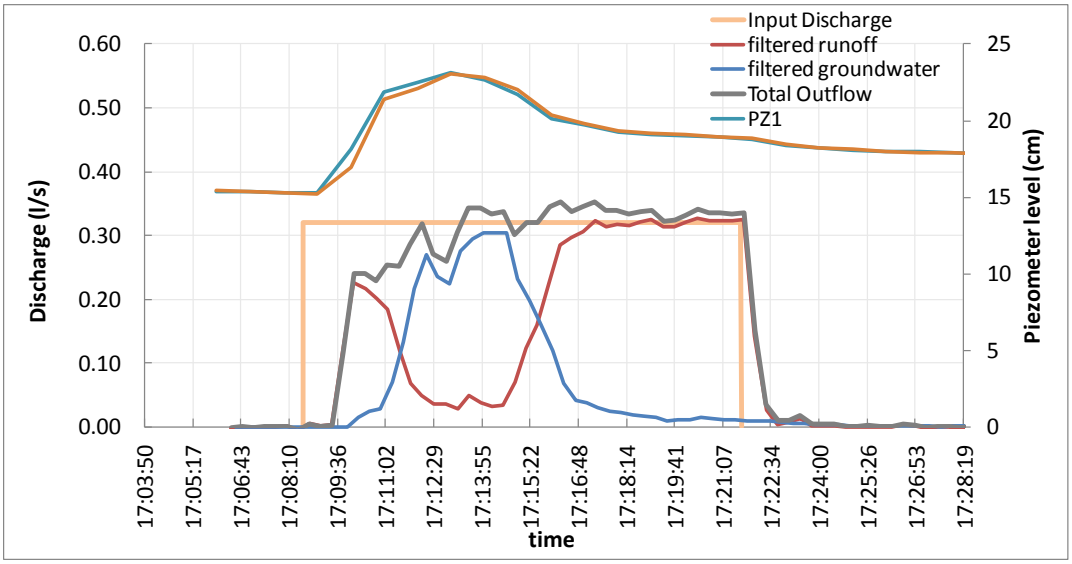

2° CONFIGURATION : TEST 15

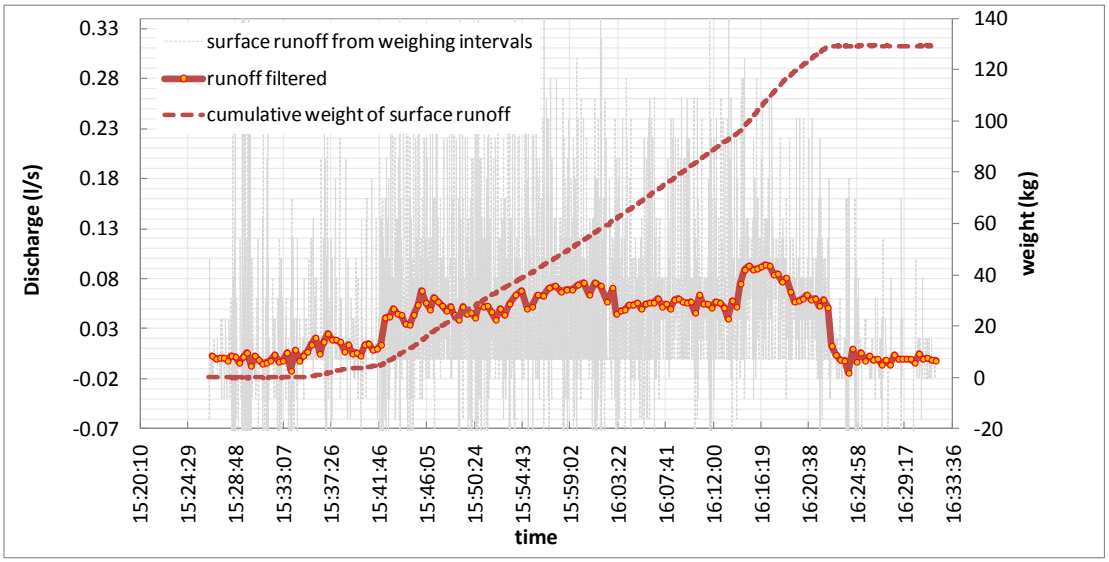

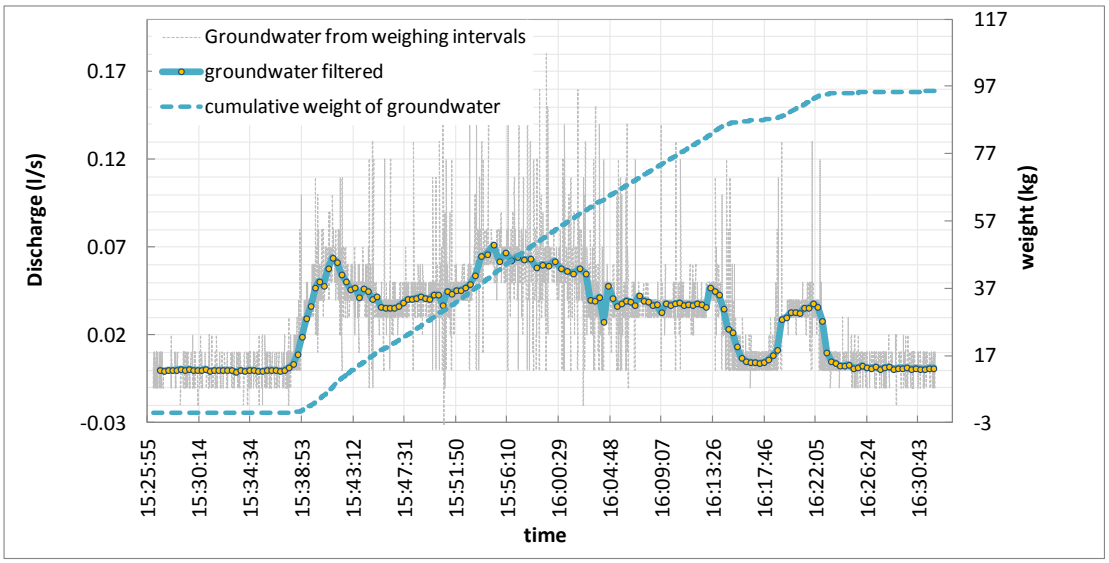

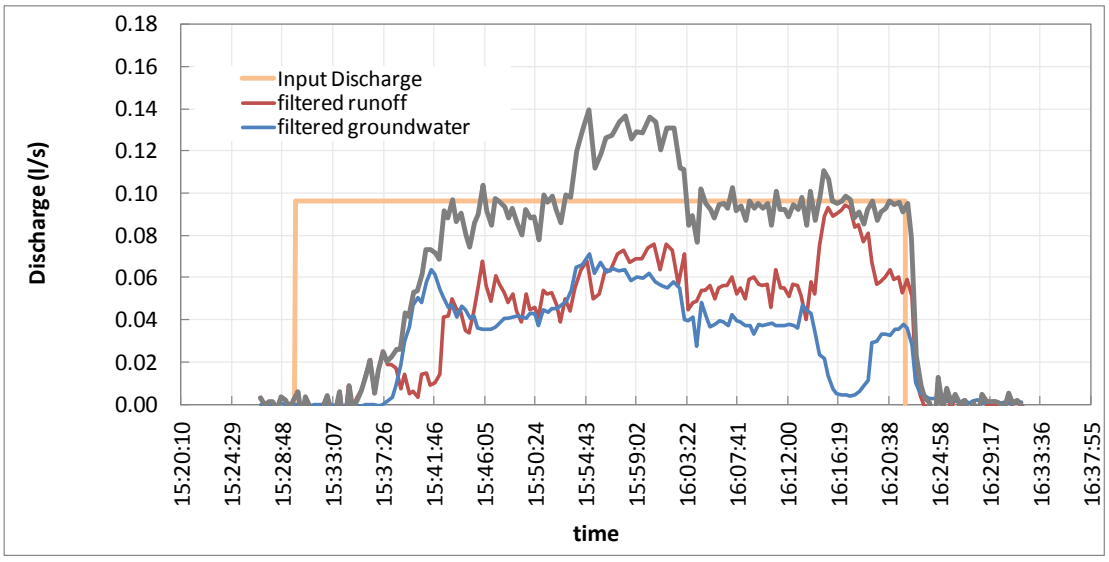

2° CONFIGURATION : TEST 16

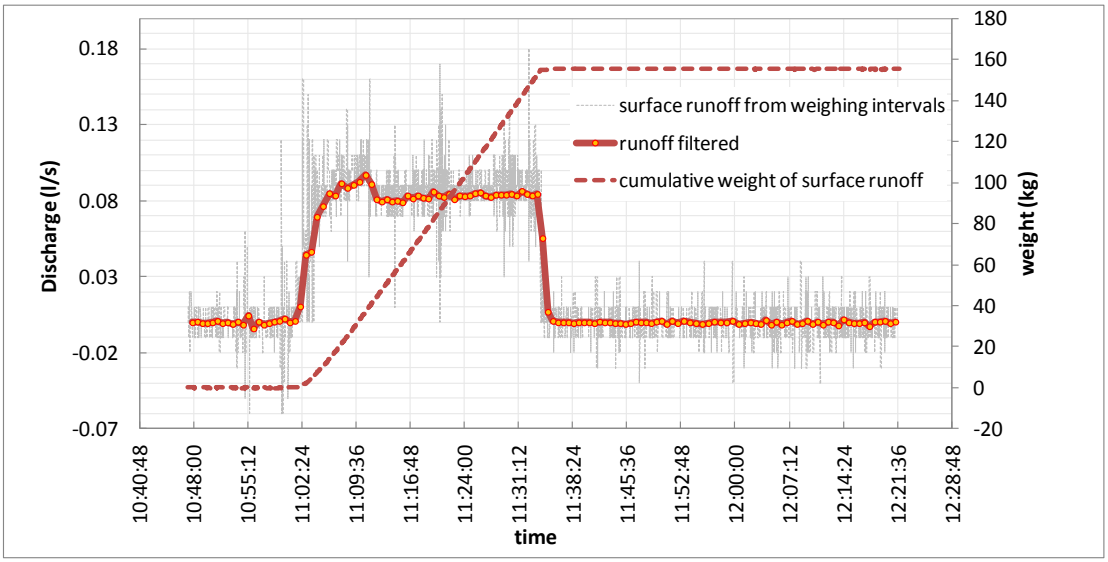

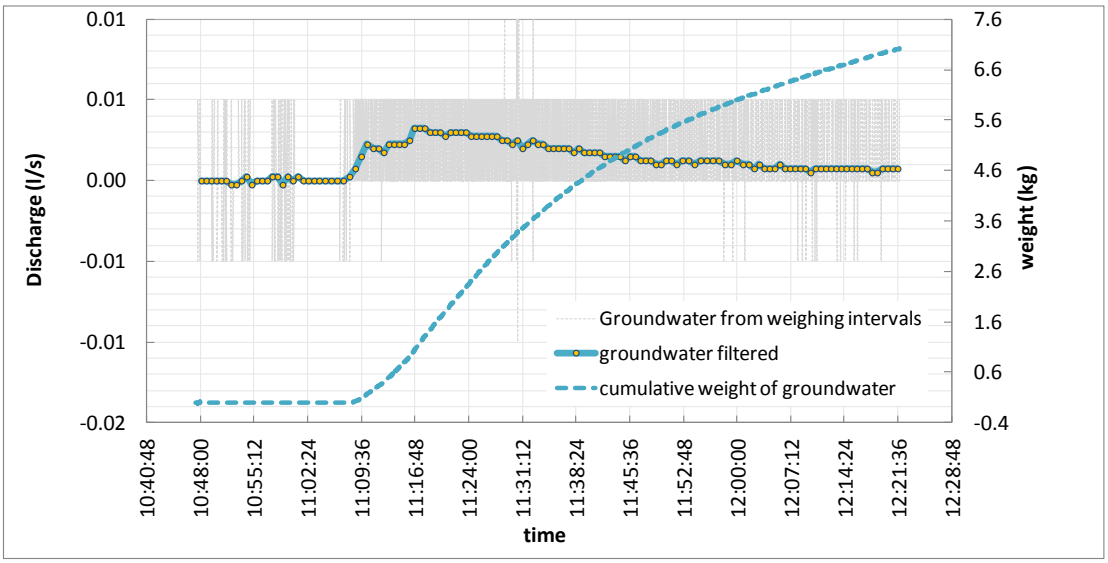

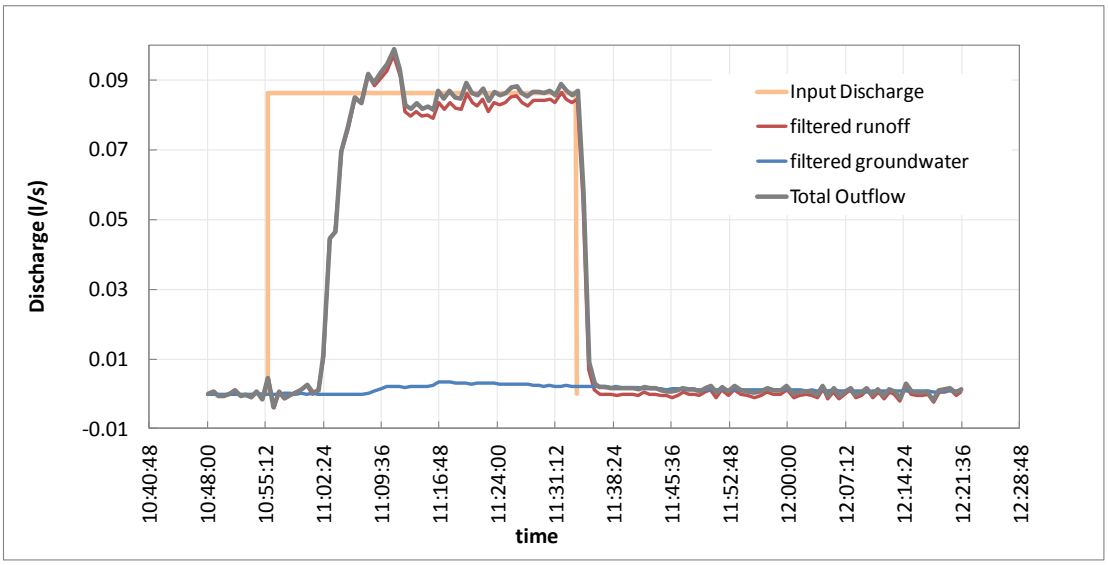

2° CONFIGURATION : TEST 17

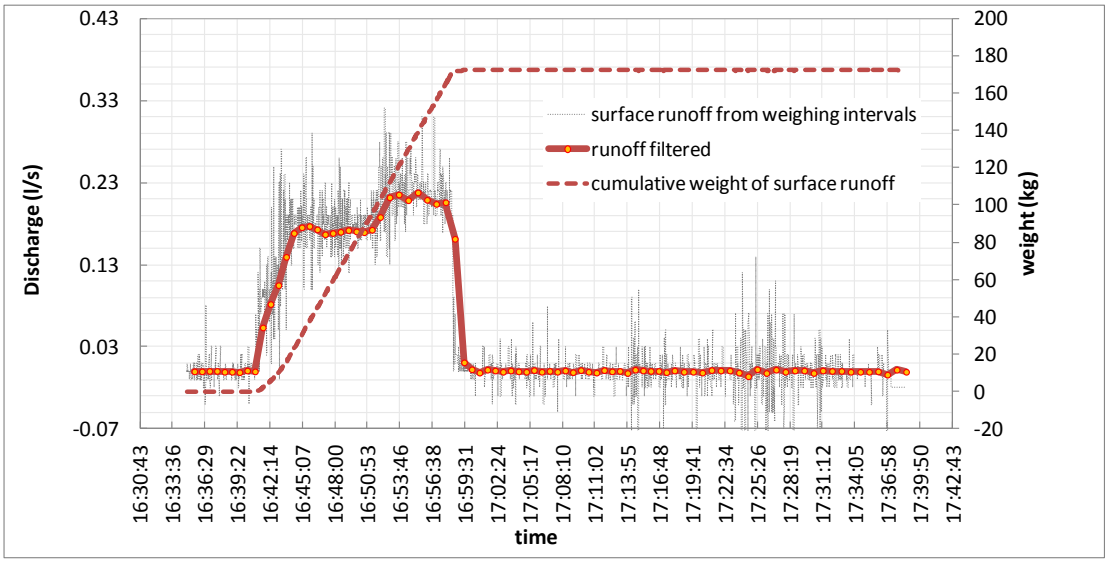

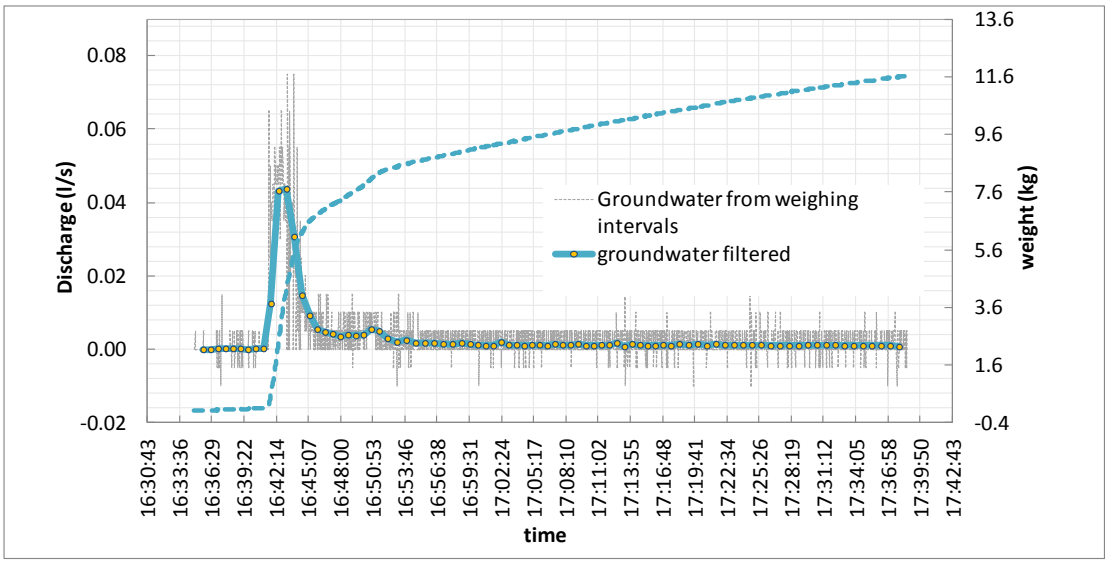

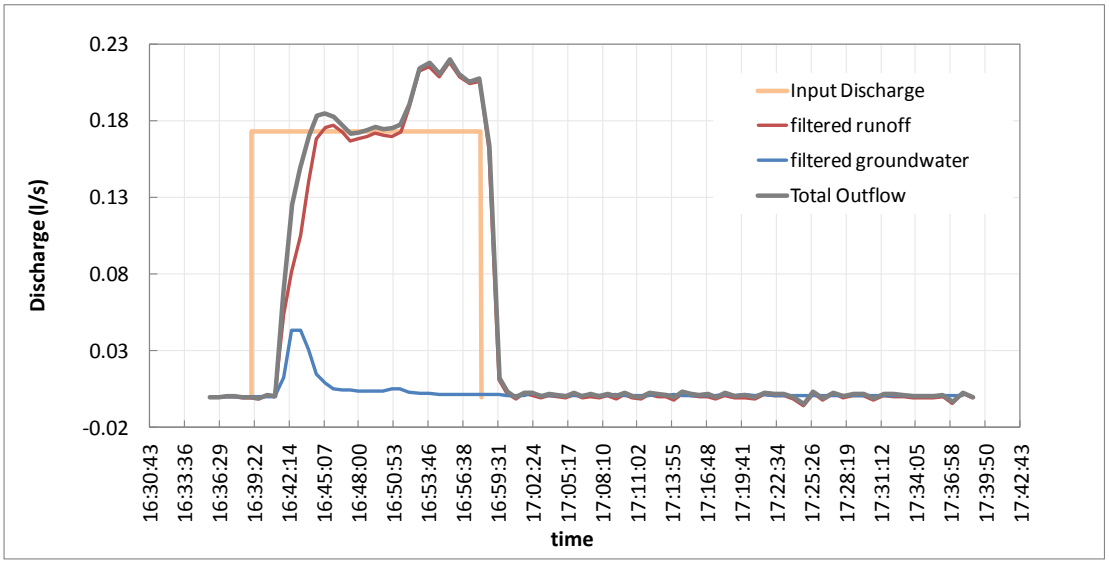

2° CONFIGURATION : TEST 18

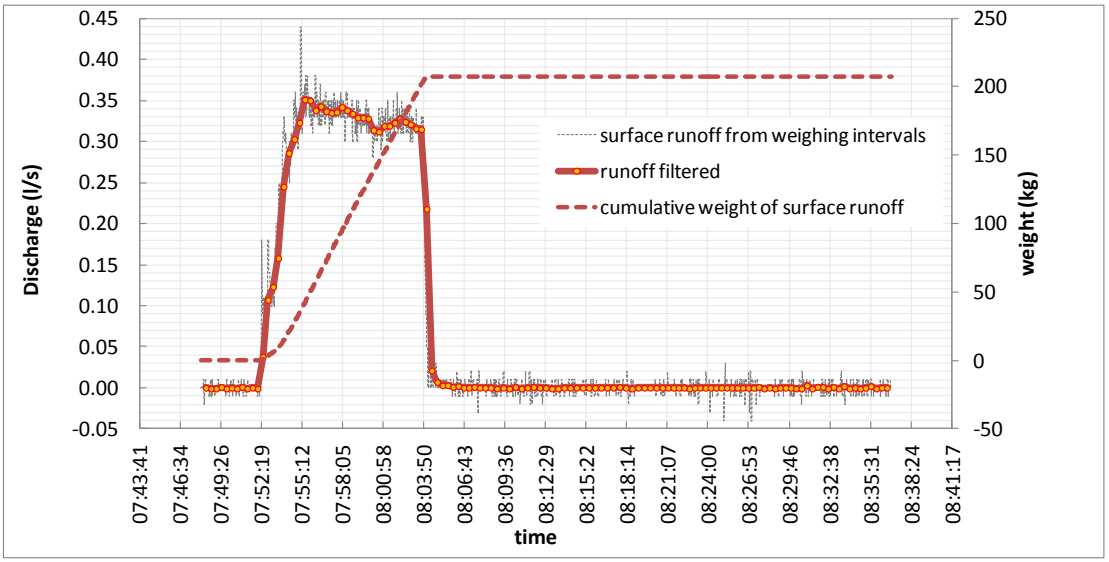

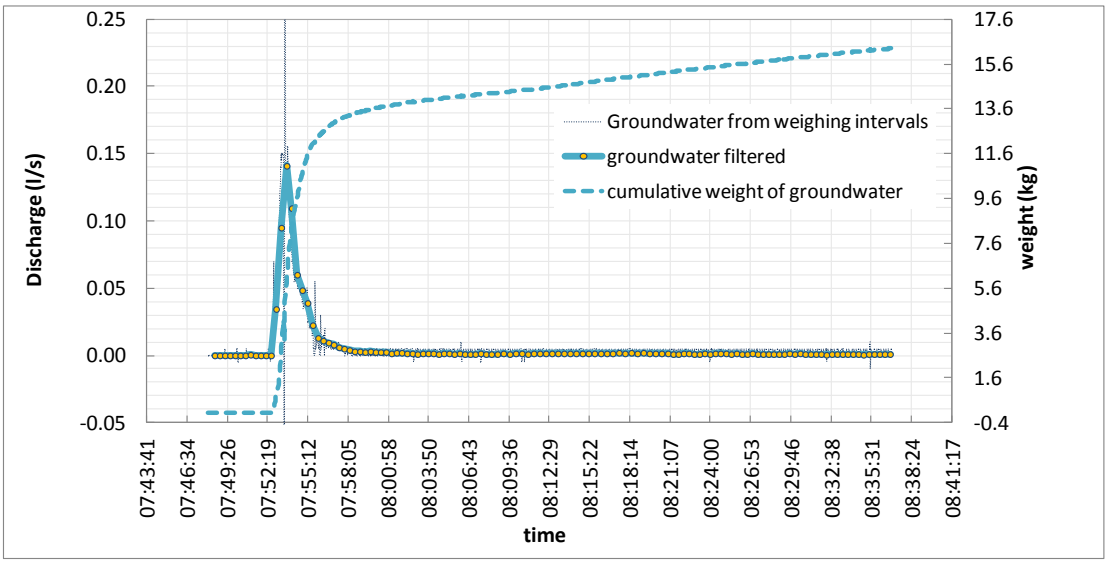

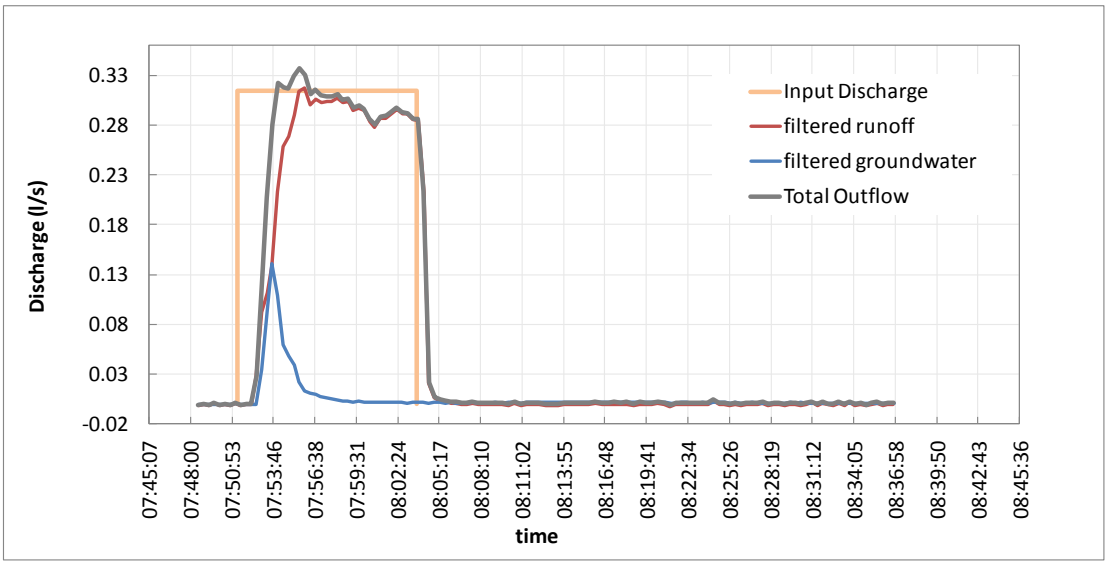

2° CONFIGURATION : TEST 19

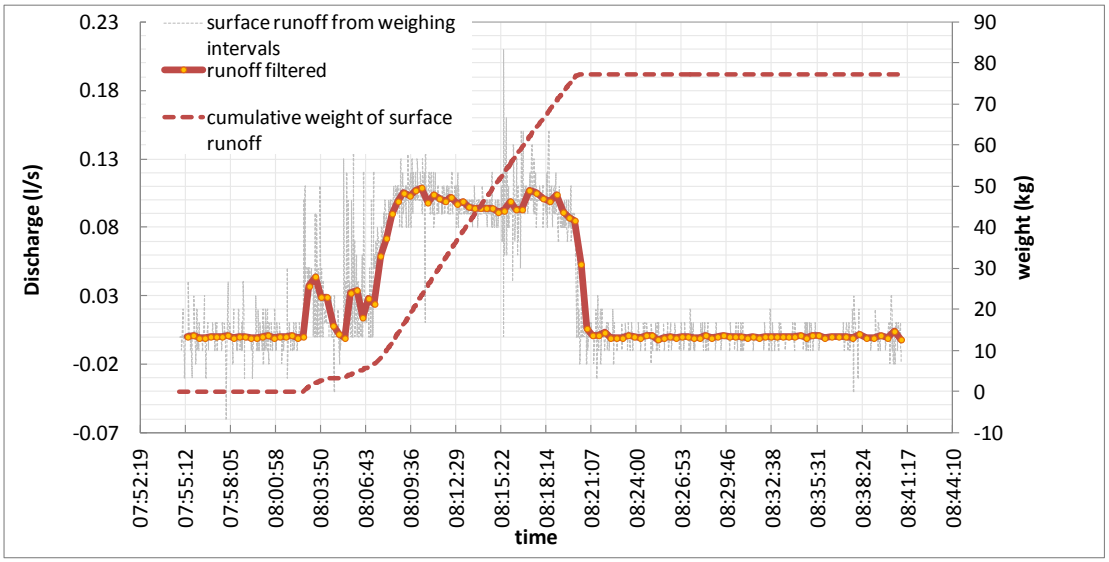

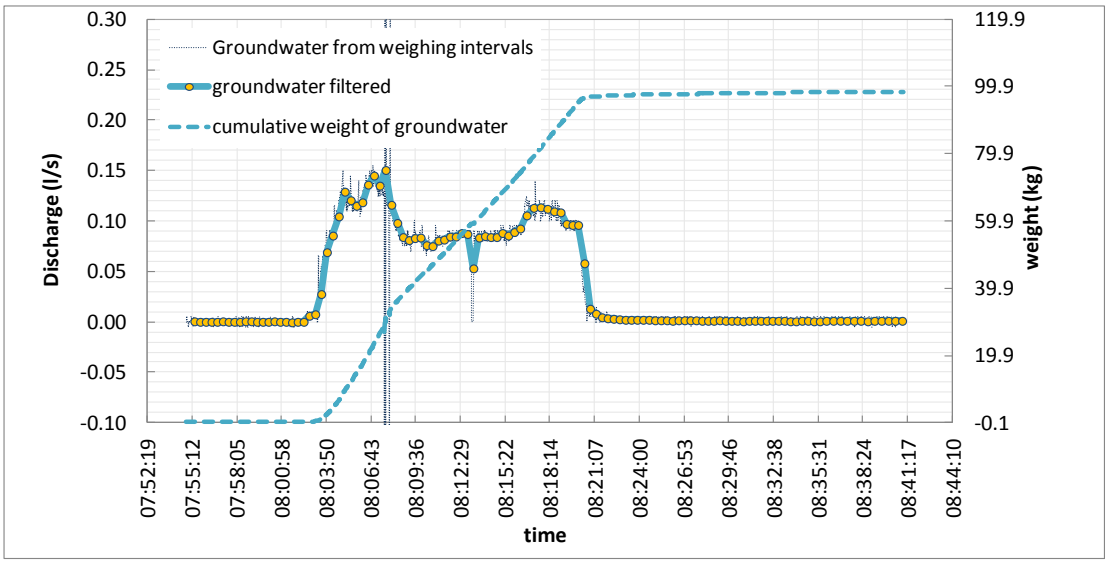

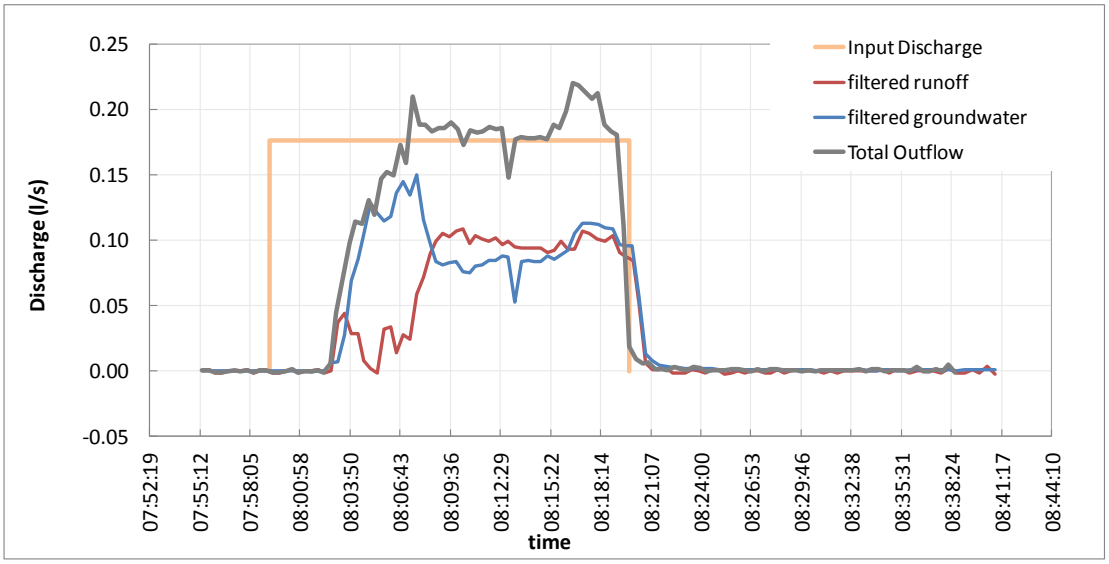

2° CONFIGURATION : TEST 20

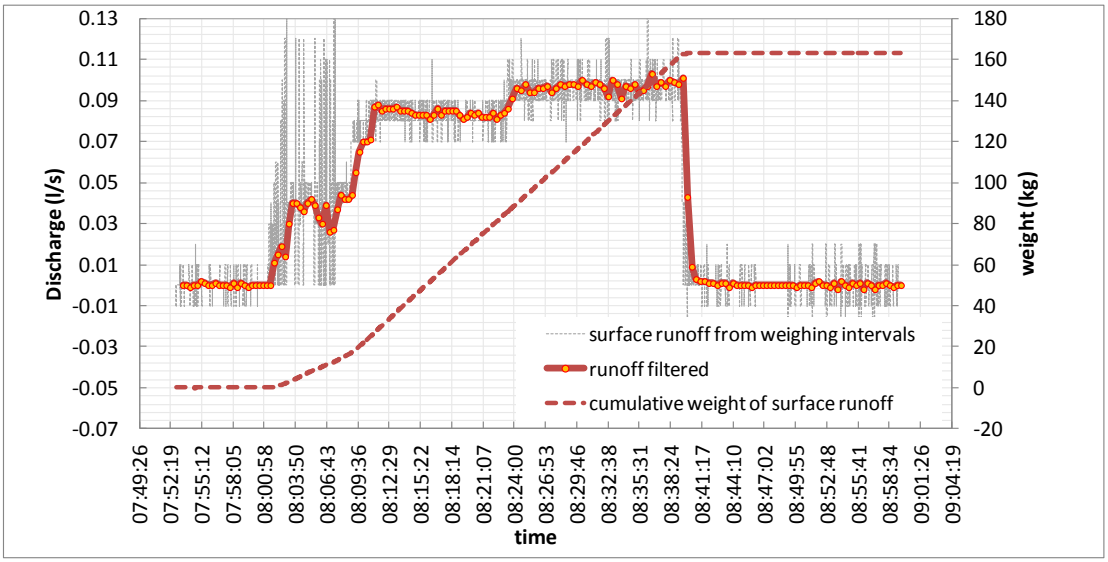

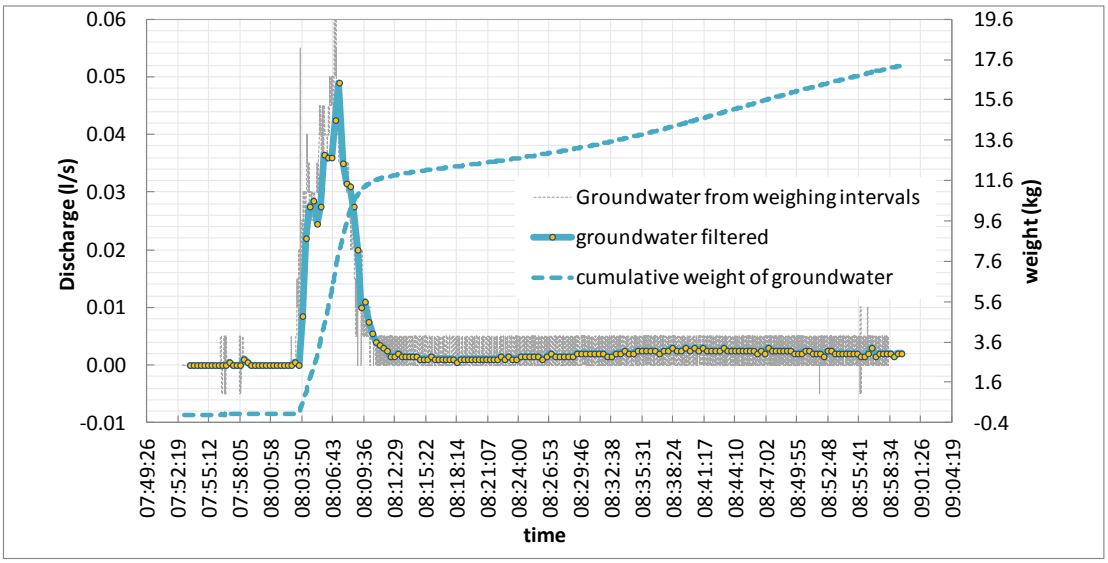

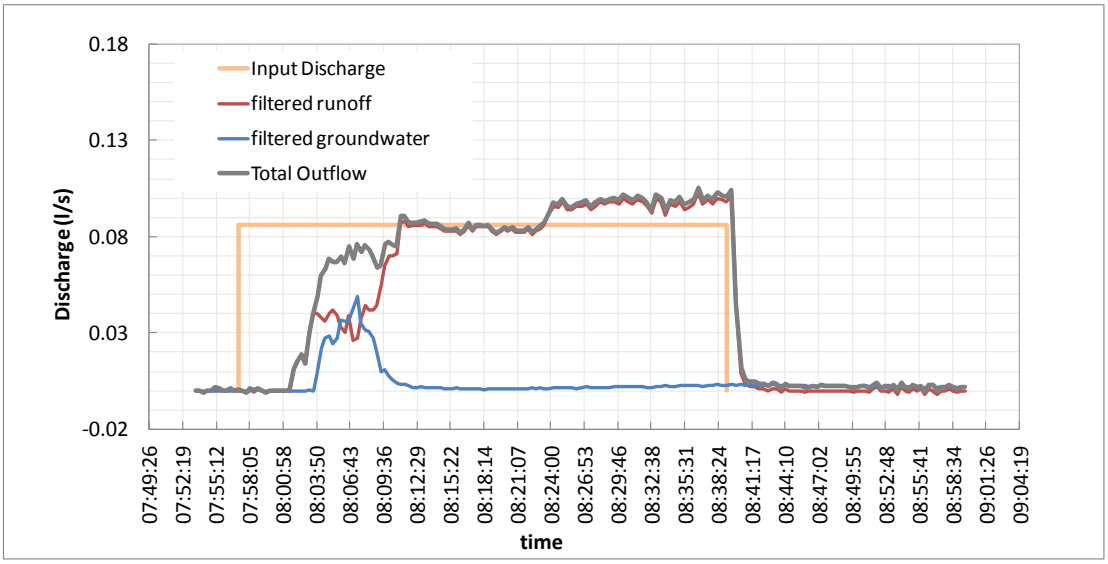

2° CONFIGURATION : TEST 21

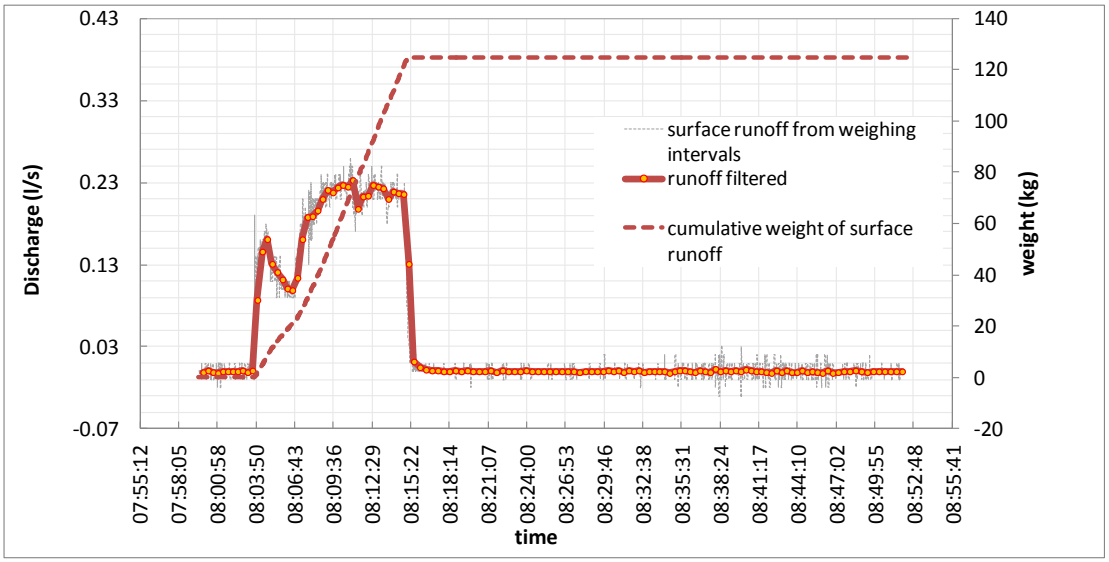

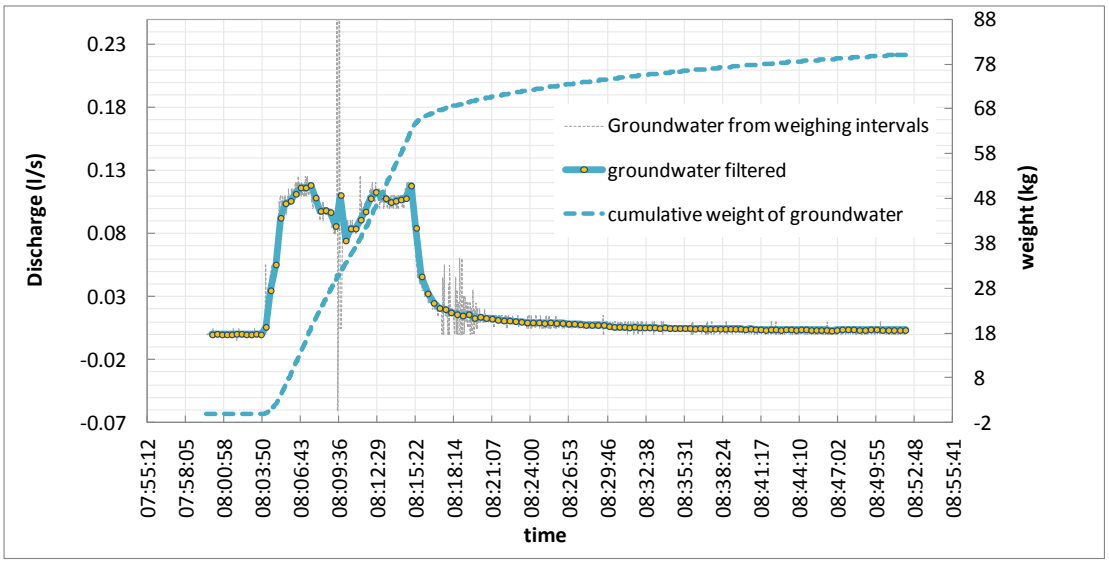

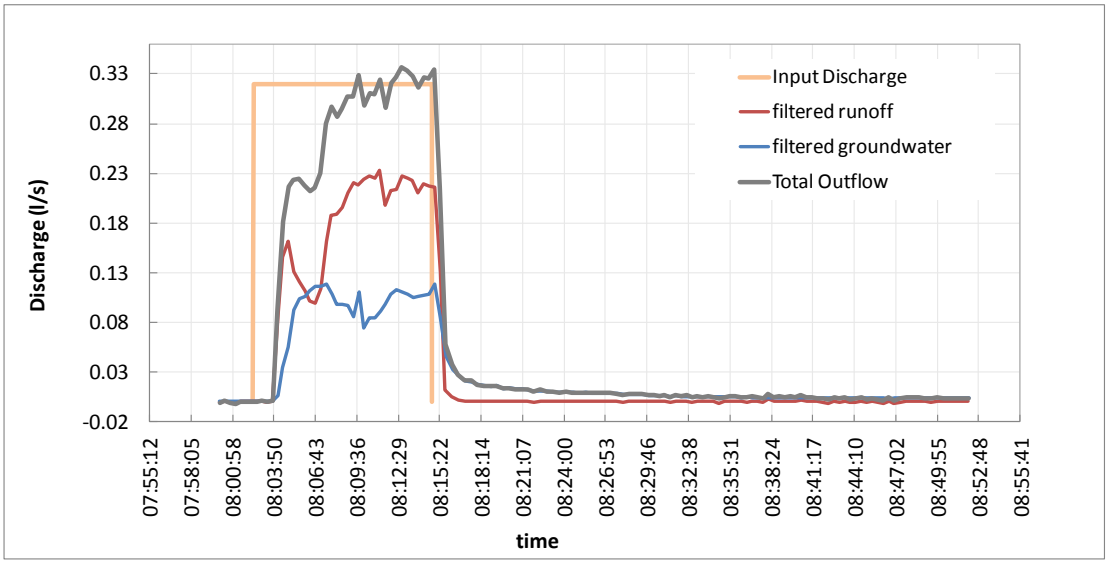

ACKNOWLEDGEMENT

Firstly, I would like to express my sincere gratitude to my supervisor Professor Vincenzo D'Agostino for the continuous support of my Ph.D study and related research, for his patience, motivation, and immense knowledge. His guidance helped me in all the time of research and writing of this thesis.

I thank the Professor Davide Matteo Pettenella and all the Professors of the Doctoral School for the lessons and discussions that I benefit during my three years of study and research.

I am also very grateful to the reviewers of this thesis, Professor Daniele Penna and Professor Gian Battista Bischetti; their comments and suggestions helped to improve this work.

I would like to thank the Prof. Francesco Morari and his collaborators, especially the Dr. Carlo Camarotto for their suggestions and for having provided me the instruments for monitoring the soil moisture.

I would like to thank the Prof. Michele Scotton for his advices on the choice of the grass type to cultivate on the terrace.

I would like to thank the Dr. Anna Paola Perazzolo of the Veneto Region (Unità Organizzativa Forestale Ovest -Verona Province) thanks to which it was possible to realize the dry stone wall.

I thank my colleagues Francesco and Roberta with whom I shared the office for three years.

I would like to thank my friend Luisa for the support we did each other and for our relaxing breaks that lightened my working days.

I would like to thank the funny technicians of the University Farm, in particular Roberto and Franco, for their availability and help during the experimental laboratory tests.

I would like to thank my mother for supporting me spiritually throughout writing this thesis and my life in general.

Finally, the most important thank goes to my husband Daniele, who is my life and he helped me to face the most difficult times during this long period of study, and he supported me to achieve this important goal.